Copyright is owned by the Author of the thesis. Permission is given for a copy to be downloaded by an individual for the purpose of research and private study only. The thesis may not be reproduced elsewhere without the permission of the Author.

STUDIES TOWARDS THE DEVELOPMENT OF A MULTI-PURPOSE HOME SELF-TEST KIT FOR THE DETECTION OF URINARY TETRAHYDROCORTISONE AND TESTOSTERONE METABOLITES

A thesis submitted in partial fulfilment of the requirements for the degree of Master of Science in Chemistry at Massey University

Claire Margaret Nielsen

2003

Abstract

The development of homogeneous enzyme immunoassays (HEIA) for testosterone glucuronide (TG) and tetrahydrocortisone glucuronide (THEG) in urine are described. The proposed test system is based on the Ovarian Monitor homogeneous immunoassay system, established by J.B Brown and L.F. Blackwell *et al.*[1] as a simple, laboratory accurate, monitoring device for the measurement of estrone glucuronide (E1G) and pregnanediol glucuronide (PdG) as markers of the fertile phase during a womans menstrual cycle. This information can be used readily by women to identify their cyclical periods of fertility and infertility.

The major testosterone metabolite in the urine of males, testosterone β-glucuronide, was synthesised by firstly preparing the glycosyl donor α-bromosugar and conjugating this with testosterone under standard Koenigs-Knorr conditions. ^{1}H nmr studies confirmed that the synthetic steroid glucuronide had the same stereochemistry as the naturally occurring urinary testosterone glucuronide.

Testosterone glucuronide and tetrahydrocortisone glucuronide conjugates of hen egg white lysozyme were prepared using the active ester coupling method in good yield. Unreacted lysozyme was successfully removed from the reaction mixture by a combination of cation-exchange chromatography in 7 M urea and hydrophobic-interaction chromatography. S-Sepharose chromatography allowed two of the major conjugation products in each steroid-glucuronide reaction mixture to be isolated and characterised by MALDI mass spectrometry. All of the selected conjugates were found to be mono-acylated species, with the exception of one of the testosterone glucuronide conjugates, which was found to contain a mixture of mono- and di-substituted hen egg white lysozyme conjugates. Conjugates prepared in this way were tested for their suitability as signal generators in a homogenous immunoassay system for measurement of testosterone glucuronide and tetrahydrocortisone glucuronide in urine samples based on the already established Ovarian Monitor home fertility assay.

Immunogens required for raising anti-steroid antibodies were also prepared using the active ester method to conjugate testosterone glucuronide and tetrahydrocortisone glucuronide to the carrier protein, bovine thyroglobulin. These immunogens were then used to raise anti-testosterone glucuronide and anti-tetrahydrocortisone glucuronide antibodies in four New Zealand White rabbits. The antisera obtained over a number of months from each rabbit were screened for their ability to inhibit the lytic activity of the corresponding steroid glucuronide-lysozyme conjugate. Although all the antisera showed the immunogens had stimulated the

---

[1] Brown JB, Blackwell LF, Cox RI, Holmes JM and Smith MA (1988). Chemical and homogenous enzyme immunoassay methods for the measurement of estrogens and pregnanediol and their glucuronides in urine. *Progress in Clinical and Biological Research* **285**:119-38.

production of anti-steroid glucuronide antibodies, the antiserum titre was low, and meant that the volume of antiserum required to inhibit the lytic activity was high. Nevertheless, despite the low antiserum titres, the selected antisera could be used to produce good standard curves for testosterone with sensitivity close to that required for TG and an excellent standard curve for THEG.

Potential applications of home assays for urinary testosterone glucuronide are in self-monitoring of testosterone levels in men undergoing long term testosterone supplementation for a diagnosed androgen deficiency or steroidogenic abnormality. Tetrahydrocortisone glucuronide is a major metabolite of cortisol, the main glucocorticoid produced by the body in response to stress and disease, and has potential as a biomarker for assessing therapies designed to reduce stress and for individuals suffering from stress related conditions such as hypertension and heart disease.

Acknowledgements

I am especially grateful to my supervisor Associate Professor Len Blackwell for his tremendous support, guidance and advice throughout the study presented, and for his willingness to read the drafts in record time - without sparing the red pen.

Others who helped along the way that I would like to thank include;

My laboratory co-workers; Dr Delwyn Cooke for her invaluable advice and expertise in numerous areas and Dr Krishanthi Jayasundera for her guidance with the organic synthesis and passing on her MALDI expertise.

Associate Professor Dave Harding for the use of the FPLC equipment and to Dick Poll for his assistance and many discussions on separation procedures.

Debbie Chesterfield from the Massey University Small Animal Production Unit for organising the rabbits and the generous discount in fees which helped make the project possible.

Dr Gavin Collis for his organic synthesis advice, unique sense of humour and the chocolate puddings (fuel) while flatting at Te Awe Awe Street.

I also gratefully acknowledge the PhD theses as sources of reference by Mark Smales, Yinqiu Wu and particularly Delwyn Cooke on the Ovarian Monitor and related topics.

A final thanks goes to my partner Mitchell, for all the support, patience, dinners, wine and allowing me to monopolise his computer for writing this thesis.

Table of Contents

Chapter Two: Synthesis and purification of biomaterials required for the immunoassay of testosterone glucuronide (TG) and tetrahydrocortisone glucuronide (THEG)

List of Figures

List of Schemes

List of Tables

Abbreviations

A_{280}	Absorbance at 280 nm
A_{595}	Absorbance at 595 nm
Ab	Antibody
Ag	Antigen
BSA	Bovine serum albumin
DCC	*N',N'*-dicyclohexylcarbodiimide
DMF	Dimethylformamide
E1G	Estrone glucuronide
EC_{50}	Analyte midpoint of Ovarian Monitor standard curve
ELISA	Enzyme linked immunosorbent assay
ESMS	Electrospray mass spectroscopy
Fab	Antigen binding fragment
FPLC	Fast protein liquid chromatography
GC	Gas chromatography
HEIA	Homogenous enzyme immunoassay
HEWL	Hen egg white lysozyme
HPLC	High performance liquid chromatography
IgG	Immunoglobulin type G
KLH	Keyhole Limpet Hemocyanin
m.p.	Melting point
MALDI	Matrix assisted laser desorption and ionisation spectroscopy
MW	Molecular weight (molar mass)
MWCO	Molecular weight cut-off
NHS	*N*-hydroxysuccinimide
NMR	Nuclear magnetic resonance
PdG	Pregnanediol glucuronide
RIA	Radioimmunoassay
SDS	Sodium dodecyl sulphate
ΔT	Change in transmission
TG	Testosterone-17β-glucuronide
THEG	Tetrahydrocortisone-3α-glucuronide
THY	Thyroglobulin
TLC	Thin layer chromatography
TNBS	2,4,6-trinitrobenzene 1-sulphonic acid
tris	Tris(hydroxymethyl)aminomethane
WHO	World Health Organisation

CHAPTER ONE

Measurement of steroid hormones and the development of a multi-purpose home or on-site assay system based on the Ovarian Monitor

1.1 Background to the study

There is a growing realisation that non-invasive home, or point-of-care (for example at the patients medical centre), devices capable of delivering laboratory-accurate data for biomarkers of health and disease to lay individuals and health professionals will revolutionise medical and health practices. A biomarker can be defined as "any substance or process that could be monitored in tissues or body fluids that predicts or influences health or assesses the incidence or biological behaviour of disease" [1]. The best known biomarker is probably blood glucose for which there are already many semi-quantitative devices available used by diabetics to determine their blood glucose levels as a measure of control and immediate insulin requirements. Numerous other important biomarkers of health and disease states are also known and many of these are small molecule intermediates in biosynthetic pathways essential for maintaining homeostasis. During metabolism detoxification of such compounds occurs in the liver, often by hydroxylation reactions involving cytochrome P450 enzymes and subsequent conjugation to glucuronic acid, and to a lesser extent sulphuric acid, in preparation for excretion via the renal system. This detoxification pathway also applies to many xenobiotic compounds such as ingested drugs. Thus, many of the important biomarkers are products of metabolism and are excreted in urine as glucuronide or sulphate conjugates. In principle the relatively high levels of urinary glucuronide metabolites constitute a battery of biomarkers that can be incorporated into non-invasive home or point-of-care urine tests if suitable methodology can be developed.

All glucuronides have the same sugar structure that contains a reactive carboxyl functional group (shown in Figure 1.1) which can be conjugated with various reagents or proteins in

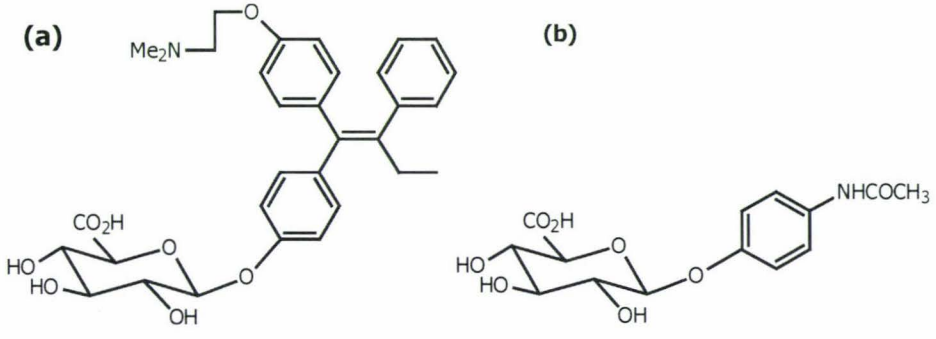

Figure 1.1 Examples of glucuronide metabolites: (a) tamoxifen-4-glucuronide [2], a major urinary metabolite of the potent antiestrogen tamoxifen which is routinely used in the treatment of breast cancer and; (b) paracetamol glucuronide [3].

chemical reactions to produce biomaterials for assays. Clearly, reactions developed for one glucuronide will be applicable to all glucuronides albeit with some modifications, thus success with one system opens the way for a wide range of tests. This thesis is concerned therefore with developing a multi-purpose assay system based on biomarkers containing the generic glucuronide structure.

1.2 Steroids as biomarkers of health and disease

Apart from the monitoring of blood glucose to monitor insulin requirements by diabetics one of the most widely used class of biomarkers has been the steroids, particularly those that function as indicators of the key events in the human menstrual cycle. As well as their role in determining gender and fertility, there is increasing evidence that steroids have other important roles in health and disease. For example it has long been known that the human response to fear, stress and anxiety is also mediated by steroid hormones, and evidence of the potentially deleterious effects of chronic stress on our long term health is increasing. Individual susceptibility to disease may also be monitored using steroid biomarkers since many diseases may result in an overproduction, or underproduction of steroid hormones.

Much interest also exists in developing new approaches to the identification of patients at high risk of disease recurrence particularly by using point-of-care or home testing. For instance, it has been established that androgens play a role in the pathogenesis of breast cancer [4,5]. In a large study of women with operable breast cancer (n = 113), urinary total testosterone levels in 24 hour samples were measured before surgery using gas chromatography to determine the "normal" excretion rate [6]. Further 24 hour samples were taken 40 days after surgery and thereafter once every six months at a specific time during the menstrual cycle for five years. In these women recurrence of breast cancer was associated with supra-normal urinary testosterone secretion. Thus, testosterone is a likely target as an important biomarker and monitoring of testosterone levels in women postmastecomy is especially important in the first five years following surgery since this has been identified as an important time frame during which relapse may occur [6].

A second interesting possibility is the major glucocorticoid hormone cortisol. The concentration of cortisol in the blood plasma is widely used as an indicator of stress [7,8,9], and cortisol metabolites in the urine have been used as a measure of stress in the workplace. In a recent example the level of hypothalamic-pituitary axis (HPA) activation in doctors working the night shift at a hospital who typically experienced stress, fatigue and sleep deprivation was measured [10]. When off-duty, the excretion of the major cortisol urinary metabolites (tetrahydrocortisone + allotetrahydrocortisone + tetrahydrocortisol + allotetrahydrocortisol) in physicians was approximately the same as the non-physician controls. However, while on-duty

the sum of the major cortisol metabolites excreted in the urine increased by a factor of two compared to the off-duty excretion levels as shown in table 1.1 [10].

Table 1.1 Excretion rates (mg 24 hr^{-1}) of cortisol metabolites in on- and off-duty male physicians and in healthy men (controls)

	Physicians (n=8)			Controls (n= 16)	
Glucocorticoid	**Off-Duty**	**On-Duty**	***P* Value***		***P* Value‡**
	Mean ± SD			**Mean ± SD**	
Tetrahydrocortisone	1.8 ± 0.7	4.0 ± 0.9	0.0005	1.4 ± 0.6	0.05
Tetrahydrocortisol	0.9 ± 0.3	2.0 ± 0.5	0.0005	0.8 ± 0.3	0.30
Allotetrahydrocortisol	0.4 ± 0.3	0.7 ± 0.4	0.001	0.5 ± 0.3	0.15
Allotetrahydrocortisone	0.1 ± 0.6	0.1 ± 0.7	0.002	0.2 ± 0.3	0.30
Main glucocorticoid metabolites§	3.1 ± 1.2	6.8 ± 1.6	0.0005	2.9 ± 1.1	0.30
Ratio of cortisone/cortisol metabolites	1.5 ± 0.2	1.6 ± 0.2	0.10	1.3 ± 0.4	0.05

*Comparing on- with off-duty physicians
‡Comparing off-duty physicians with controls
§ Tetrahydrocortisone + allotetrahydrocortisone + tetrahydrocortisol + allotetrahydrocortisol

Cortisol metabolites may also be excreted and quantified in the feces of animals [8]. Recently this has been used as a more practical non-invasive alternative to urine testing as an indicator of stress in animal welfare studies and wildlife breeding programs [11,12].

1.3 General pathway for the biosynthesis of steroid hormones

For the development of non-invasive techniques to monitor steroid production, basic knowledge of the biosynthetic and metabolic pathways by which they are formed and excreted into biological fluids is necessary to aid in the choice of specific biomarkers. For example, many steroids are released from biosynthetic tissues in a pulsatile fashion, and the plasma concentration may increase by as much as 50 to 100% depending on the time of sampling. Steroids circulating in the plasma may be either quickly cleared from the circulation and appear in the urine in the form of glucuronide and sulphate conjugates or metabolised into more potent forms by the target tissue. For example, cortisone may be metabolised to cortisol in the liver; testosterone may be metabolised to dihydrotestosterone in the prostate, or metabolised further to estrogens in reproductive tissues.

The naturally occurring steroid hormones are all based on a fused tetracyclic hydrocarbon ring structure. Substituents, (e.g. carbonyl, hydroxy, methyl) located at specific positions within the steroid skeleton allow the steroids to be classified into three main chemical categories based on androstane, pregnane or oestrane ring structures (Figure 1.2). However the steroid hormones are more commonly classified by their biological activities into androgens, oestrogens, progestogens, corticosteroids and mineralocorticoids [13].

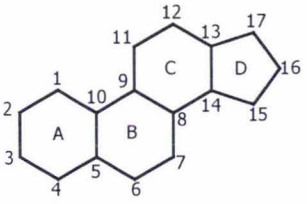

Tetracyclic steroid ring structure

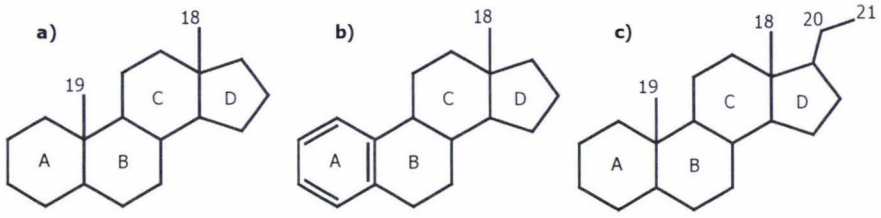

Figure 1.2 Structures of (a) androstane, (b) oestrane and (c) pregnane ring systems.

The major sites of steroidogenesis are the gonads (estrogens and androgens) and adrenal gland (corticosteroids, mineralocorticoids and androgens), although other organs such as the brain, liver and adipose tissue also play a significant role [14]. Recent experiments also suggest the nervous system produces steroid hormones [15]. The overall pathway for the synthesis of all steroid hormones is similar and tissue specific, cell-specific and even subcellular compartment specific differences in the expression of particular steroidogenic enzymes regulate the types and relative amounts of particular steroid hormones synthesised. All steroids are derived from pregnenolone which is itself synthesised from the precursor steroid cholesterol, as shown in Scheme 1.1. Cholesterol may be synthesised from acetate or derived from pools of cholesterol esters in steroidogenic tissues, but the preferred route for around 80% of the cholesterol used for steroid hormone production is via absorption of low density lipoprotein (LDL) cholesterol from the diet [15].

The first step in steroid biosynthesis involves the transfer of cholesterol to the inner mitochondrial membrane where it undergoes side chain cleavage of the $C_{20\text{-}22}$ carbon bond by the cytochrome (CYP) P450 enzyme CYP11A (cholesterol desmolase) to form the 21 carbon steroid pregnenolone [16]. Delivery of cholesterol to the inner mitchondrial membrane is mediated by steroidogenic acute regulatory (StAR) protein, and forms the rate-limiting step of the reaction.

The second subsequent side-chain cleavage of pregnenolone to form testosterone can occur by two distinct pathways. In the Δ^5 pathway, CYP17 catalysed hydoxylation of C_{17} and cleavage of the C_{17}-C_{20} bond occurs before reduction of the C_{17} ketone group by 17β-hydroxysteroid dehydrogenase (17β-HSD) and oxidation of the A-ring by 3β-hydroxysteroid dehydrogenase Δ^5-Δ^4 isomerase (3β-HSD Δ^5-Δ^4 isomerase). In the Δ^4 pathway this sequence is reversed; A-ring oxidation occurs before side chain cleavage and reduction of the C_{17} ketone group. The point in the pathway at which A-ring oxidation occurs depends upon the relative amounts of the

enzymes for the various substrates present and their compartmentalisation within the cell [17]. The predominant pathway in the testes and ovarian follicles, appears to be the Δ^5 pathway (pregnenolone, dehydroepiandrosterone, androstenediol) whereas as the Δ^4 pathway (pregnenolone, progesterone, androstenedione) is dominant in the corpus luteum [18].

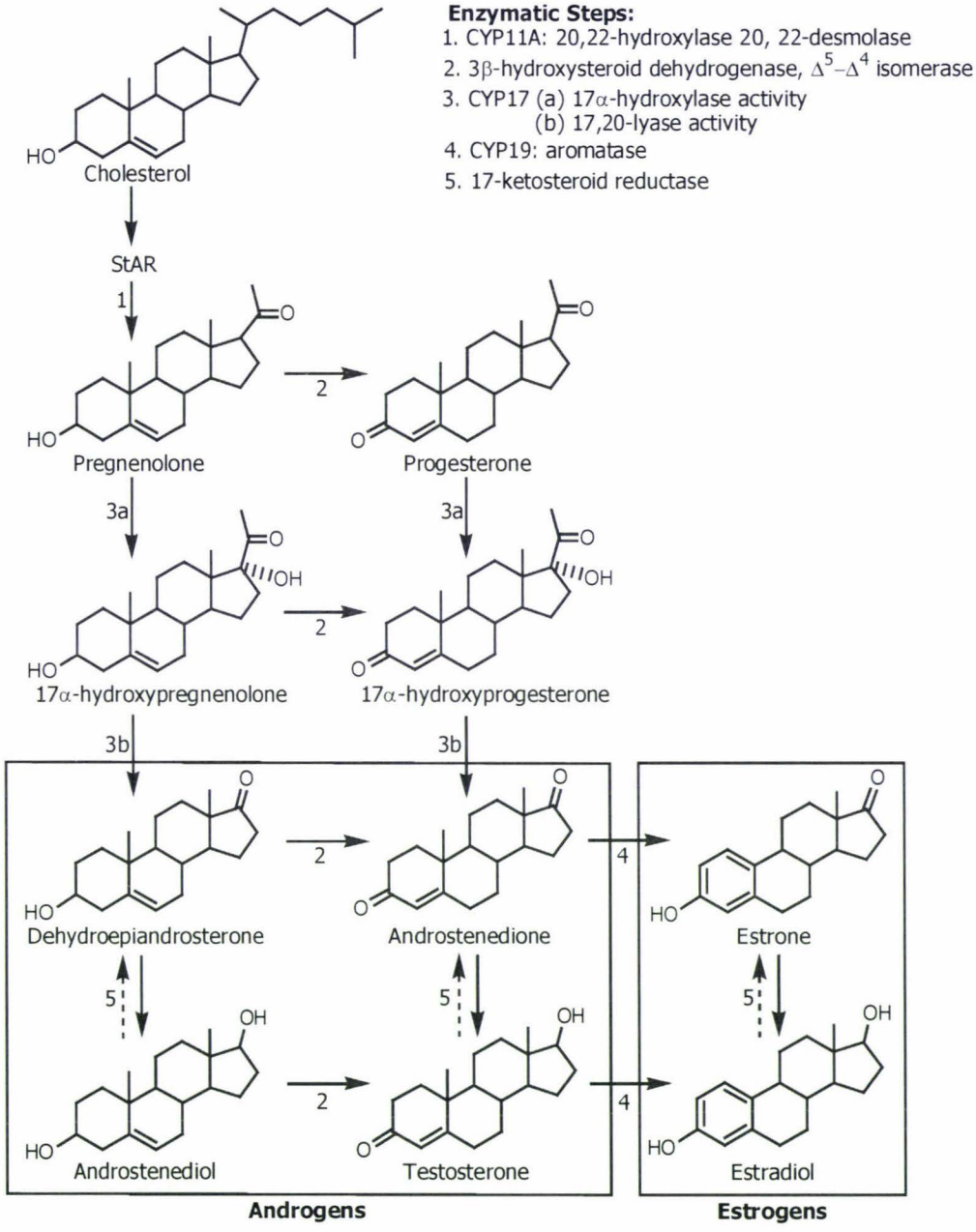

Scheme 1.1 Biosynthesis of androgens and estrogens from cholesterol [19]

Androstenedione and testosterone can be converted to their respective estrogens, estrone and estradiol by the cytochrome P450 aromatase enzymes in testes, ovary and extraglandular tissues of both sexes [17]. These conversions are irreversible and require the reduction of the C_3 ketone functional group, removal of the C_{19} methyl group and aromatisation of the A-ring [20]. Although there is more androstenedione produced by the ovary than testosterone the

equilibrium of the 17β-hydroxysteroid dehydrogenase catalysed reaction ensures that most of the resulting ovarian estrogen is converted to estradiol [21].

1.4 Steroids as markers of the fertile window in the human menstrual cycle

The central problem of fertility detection in humans, who lack an estrus symptom, is to identify the fertile window in a menstrual cycle. This is a variable period of days surrounding ovulation when an act of coitus may result in a pregnancy. Since the position of the day of ovulation is usually quite variable even within cycles from the same woman the fertile window will vary from cycle to cycle and from woman to woman. The length of the fertile window will also vary from cycle to cycle and from woman to woman. It is generally agreed that the ovum only survives for 8 - 12 hours after ovulation [22] but sperm survival in the female genital tract extends the fertile window by an amount determined by the sperm survival time. This is generally believed to average about 3 days [22] however pregnancies have been documented that seem to require a rare survival time of up to 6 or 7 days. Hence the maximum length of the fertile window can be 7 - 8 days (Brown *et al* personal communication). What is needed to detect and monitor the fertile window is a biochemical marker for the beginning and end of this time.

To achieve this goal it is first necessary to review the basic physiology of the human menstrual cycle. The menstrual cycle is controlled by a coordinated flow of chemical information between the ovary and the pituitary gland as shown in Figure 1.3.

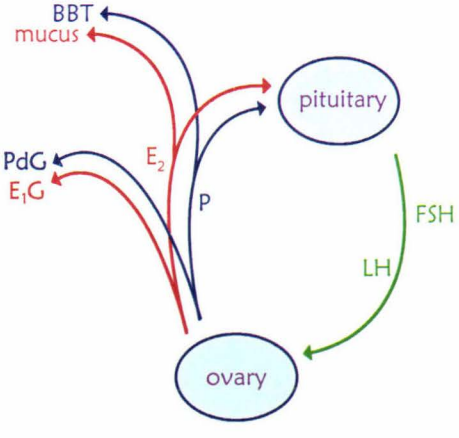

Figure 1.3 Schematic diagram of pituitary-ovary communication. Abbreviations: BBT, basal body temperature; P, progesterone; PdG, pregnanediol glucuronide; E2, estradiol; E1G, estrone glucuronide; LH, luteinising hormone; FSH, follicle stimulating hormone.

The major chemicals which carry the information are the pituitary hormones, follicle stimulating hormone (FSH) and luteinising hormone (LH) which carry information to the ovary and the ovarian hormones, estradiol (E2) and progesterone (P) which signal ovarian responses to the pituitary. Progesterone secreted from the ovary is rapidly cleared from the circulation by conversion to various metabolites. The major conjugated metabolite of progesterone excreted

in the urine is pregnanediol glucuronide (PdG) (about 20%) [23] which may be used as an index of ovarian progesterone production [24]. Once estradiol leaves the ovarian environment, it is oxidised by hydroxysteroid dehydrogenase enzymes in the liver to the less bioactive estrone. Estrone may either then re-enter the circulation or be rapidly metabolised further to estriol or conjugated in the liver to estrone glucuronide (E1G), which is excreted in large amounts in the urine. As well as being present in high quantities, estrone glucuronide is excreted rapidly and levels of E1G appear to be directly correlated to circulating levels of estradiol. This orchestrated chemical communication flow provides a means for "eavesdropping" non-invasively on the ovary to ascertain the state of follicular and corpus luteum development (and hence the state of fertility) at any time throughout the menstrual cycle.

Although the best biochemical markers for the beginning and end of the fertile window are serum estradiol and progesterone their analysis requires several blood samples to be taken during the menstrual cycle which is generally considered an uncomfortable and invasive procedure. As noted above the urinary metabolites estrone glucuronide (E1G) and pregnanediol glucuronide (PdG) (shown in Figure 1.4) are widely accepted as alternative biomarkers of ovarian estradiol and progesterone production respectively. The measurement of urinary metabolites over serum analyses has the advantage that frequent specimen collection is easier and non-invasive with less stress to the subject [25]. In addition the urinary excretion rates are more closely related to ovarian secretion rates and integrate the pulsatile secretion of these hormones [25].

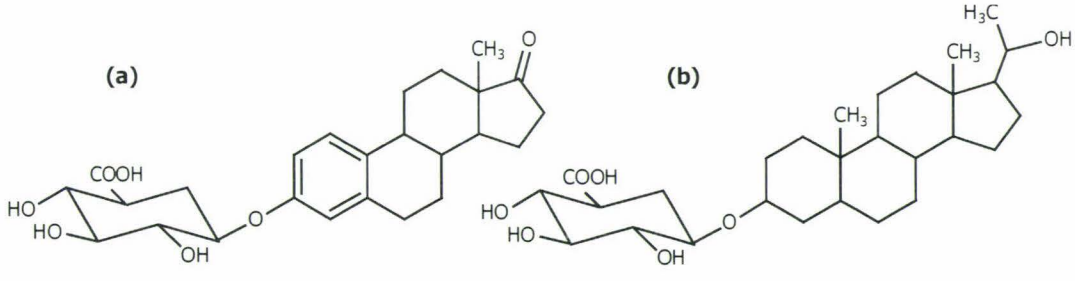

Figure 1.4 Structure of **(a)** estrone glucuronide (E1G) and **(b)** pregnanediol glucuronide (PdG).

All of the available or foreseeable methods of detecting and predicting fertility depend on access to a procedure that detects one or more of the signals shown in Figure 1.3. It should be noted that no matter which method is being used the meaning of the underlying information remains the same.

1.5 Analysis of steroids and their glucuronides

Although some hormones may be measured directly in biological fluids by a readily available assay, some information can be obtained only by measuring the ratio of biosynthetic precursors or hormone metabolites. Information of this type is necessary for the diagnosis of endocrinological diseases which result from disruption of the normal pathways of steroid biosynthesis (e.g. adrenal hyperplasia [26]) or metabolism (e.g. polycystic ovaries [27] and apparent mineralocorticoid excess [28]). Blocks in biosynthesis or metabolism brought about by enzyme deficiencies or enzyme mutations can be readily identified by increased levels of steroids intermediate in the biosynthetic pathway which would normally be present at low levels. Many assays used currently for the identification and quantification of steroid hormones are based on either binding assays or chromatographic methods. Typically immunoassays are used for the analysis of single steroids, measured routinely in a clinical setting and allow rapid, high-throughput, simple analyses. Assays for multiple or unusual steroids normally rely on chromatography methods. While affording high specificity and comparable sensitivity these techniques are often more time consuming, labour intensive and often require specialised technicians to operate.

1.5.1 Chromatography techniques

Chromatography based methods used for the analysis of urinary steroids can be divided into several categories, the most common being paper, thin layer (TLC), high performance liquid (HPLC) and gas chromatography (GC). HPLC and GC are the most common methods applied in routine assays, whereas paper and thin layer chromatography, although popular in the past are now only used in research and organic synthesis laboratories. The preferred detection system for steroid profiling by GC is a mass spectrometer, which allows highly sensitive detection with excellent specificity. Recent reports also suggest that super-critical fluid (SCF) chromatography may have potential for the separation of steroids [29]. This method is based in the fact that some compounds, for example carbon dioxide, have a "critical" temperature and pressure above which their gaseous and liquid phases are no longer distinguishable. The fluids formed under these conditions have enhanced separating capacity by allowing a greater degree of interaction between stationary and mobile phases. However the instrumentation for SCF analysis is not yet widely available for routine analyses.

While intact steroids and steroid conjugates can be assayed directly by GC using high temperature programmes, samples often require lengthy pre-treatment prior to analysis. For example, some steroids particularly corticosteroids, are thermolabile and must be chemically derivatised to prevent losses prior to analysis by GC. Steroid conjugates and columns are also subject to degradation under the high temperatures (350 °C) required to elute the steroid glucuronides [13]. As a result steroid conjugates are often hydrolysed using enzymes such as β-glucuronidase, to yield the free steroid which is then derivatised prior to analysis and the total

levels of steroid are reported [30]. This was the basis of the total estrogen method of Brown *et al.* which revolutionised our understanding of the human menstrual cycle in the second half of last century [31]. HPLC-MS systems can also be applied to the direct analysis of steroids in urine and plasma. The speed of analysis is often much faster since no derivatisation is required and the technique can be performed at room temperature allowing analysis of thermally unstable molecules, for example intact glucuronide and sulphate conjugates [32,33]. However HPLC-MS systems may not be as sensitive as GC-MS and radioimmunoassay (RIA) systems (discussed in section 1.5.2.1) and some buffered mobile phases may be incompatible with the mass spectrometer. Buffer salts may precipitate out around the interface, resulting in increased noise and necessitate frequent cleaning of the ionisation cone.

1.5.2 Immunoassay techniques

The binding of antibodies to specifically labeled antigens forms the basis of a range of assay techniques known collectively as immunoassays. The antigen may be attached to various labels including radioactive isotopes, as in radioimmunoassay (RIA), fluorescent compounds (in fluorescence polarization assays, FPIA) chemiluminescent molecules (CLIA) or rely on enzymes which form the basis of a battery of tests known as enzyme immunoassays or enzyme-linked immunosorbent assays (ELISA).

1.5.2.1 Radioimmunoassay

A large number of journal reviews and texts have been published on the development of immunoassay techniques [34,35,36]. The basic principle of all immunoassays is that a labeled antigen (i.e. the compound of interest) competes with unlabeled antigen present in the sample (e.g. serum or urine) for a limited number of binding sites on an antibody. Radioimmunoassay (RIA) was the first immunoassay approach developed in the late 1950's [37] and employs radioactive isotopes, usually iodine or tritium, as the antigen label. The principal reactions involved in typical RIA systems are illustrated in Scheme 1.2.

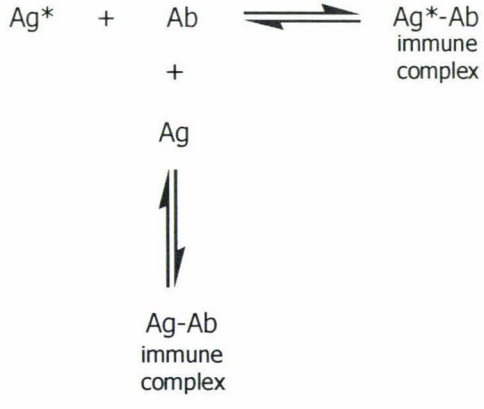

Scheme 1.2 The principle reactions involved in radioimmunoassay (RIA). Abbreviations: Ag*, labeled antigen; Ab, antibody specific for the antigen; Ag, unlabeled antigen in the sample or standard.

Appropriate volumes of antibody (Ab, which is specific for the antigen of interest), radiolabeled antigen (Ag*) and sample containing free antigen (Ag) are incubated together. Because the antibody concentration is limited, the antigen in the test sample must compete with the labeled antigen for the limited number of binding sites provided by the antibody molecules. Hence when equilibrium is reached, the greater the concentration of antigen present in the sample, the less labeled antigen that will be bound by the antibody. The next step in the assay involves separation of the antibody bound labeled antigen from the free labeled antigen. This is necessary since it is not possible to distinguish between free and bound radioactive label by the usual counting techniques. Separation is normally achieved by using procedures which separate the antigen-antibody complex while leaving the unbound antigen, both labeled and unlabeled, in solution. In practice, precipitation of the antigen-antibody complex from solution is most often achieved by adding a second antibody (which has been raised against the first antigen-binding antibody) to the reaction mixture. After separation, the radioactivity in either the free or antibody bound fraction of antigen is measured by radioactive counting. The amount of radioactivity observed is then compared to a standard curve constructed by assaying several samples containing known concentrations of unlabeled antigen.

The major advantage of RIA is the high sensitivity and specificity obtainable with radiolabeled compounds. Since the radioactive label provides a distinct signal that shows little interference from other compounds in a biological fluid, radioimmunoassays have the capacity to detect compounds at levels of picomoles per litre or less. Although these systems are still in use for the detection of low levels of testosterone and cortisol in plasma [38], urine [39] and saliva [40] there are a number of disadvantages associated with the use of radiolabeled antigens. These include the disposal of the radioactive waste material, the limited half life and stability of some labeled antigens and the need for a specially equipped laboratory and expensive counting equipment to measure radioactivity at the assay end point. In addition the need to physically separate the bound and free labeled antigen makes the automation of RIA systems difficult and increases the cost of RIA analysis. However, radioimmunoassays can be established for any analyte providing a suitable specific antibody can be raised against the analyte. Many examples of radioimmunoassays for steroids and in particular estrone glucuronide and pregnanediol glucuronide have been reported [42,43,44].

1.5.2.2 Non-isotopic immunoassay techniques

Since the introduction of RIA a variety of immunoassay systems using non-isotopic labels have been developed for the measurement of steroids and other small analytes in biological fluids. The most successful non-isotopic systems applied to the analysis of steroids include chemiluminescence and fluorescence immunoassay systems which employ either a luminescent or fluorescent tag (e.g. fluorescein or isoluminol) to label and measure the amount of bound and free antigen present in the sample. Both these methods have been applied to the

measurement of steroid and drug metabolites in body fluid [45,46,47]. The main advantages of chemiluminescent and fluorogenic substrates are their low cost, high sensitivity, long shelf-life of the lyophilised conjugates and the absence of radiation hazards [48]. The main disadvantages are associated with high background (signal to noise ratio) interference from endogenous substances in the sample matrix and light scattering, the need to use maximally purified water, and problems with temperature and pH variations which can affect the wavelength and intensity of the emitted light [49].

1.5.2.3 Enzyme immunoassays

The development of immunoassay systems employing enzymes as the non-isotopic signal generating substances has proven to be a particularly popular alternative to RIA. Enzyme immunoassays (EIA's) utilise a) an enzyme labeled with antigen (called an enzyme conjugate), b) the ability of antibodies to discriminate between structurally similar antigens and c) the specificity and catalytic nature of the enzyme towards its substrate which facilitates signal amplification. Direct comparisons have shown that EIA's can be as sensitive or even more so than the corresponding RIA's, without most of the disadvantages associated with radiolabeled antigens [48,50].

Enzyme immunoassays can be divided into two broad groups, heterogeneous immunoassays and homogeneous immunoassays. Heterogeneous enzyme immunoassays (which include the enzyme linked immunosorbent assays or ELISA) are those in which the enzyme labeled with antigen is equally active in the antibody-bound and free state and therefore must be separated before any measurements can be made - as is the case with standard RIA. In homogeneous enzyme immunoassay systems the activity of the enzyme conjugate is extensively inhibited when antibody binds to the antigen. Thus, the amount of antibody bound enzyme label (which depends on the concentration of free antigen present) can be easily measured in solution by a simple kinetic measurement without the need for time consuming separation procedures.

The first homogeneous enzyme immunoassay (HEIA) was performed by Rubenstein and co-workers in 1972 [51] as an alternative to RIA and other heterogeneous immunoassays of the time. Rubenstein demonstrated that polyclonal antibodies specific to morphine could bind to a hen egg white lysozyme (HEWL) – carboxy methylmorphine conjugate and inhibit the enzyme activity by up to 98%. Lysozyme is one of the few enzymes that exhibits such extensive inhibition after binding to an anti-analyte antibody but enzymes such as malate dehydrogenase have been used in commercial EMIT (enzyme-multiplied immunoassay technique) by the SYVA company in California. Other homogeneous assay techniques exist which make use of a change in some property of the system, such as a change in fluorescence polarisation on binding to an antibody, and assays for estrone glucuronide and pregnanediol glucuronide have been described using these techniques [52,53].

1.5.3 Immunoassays for home monitoring – The Ovarian Monitor for estrone glucuronide and pregnanediol glucuronide

It is clear that for home monitoring of any analyte, classical chromatographic assays and radioimmunoassays, and most non-isotopic assays are completely unsuitable. Most reported home assay systems for monitoring fertility have involved either lateral flow membrane assays (or immunochromatography assays) and the Ovarian Monitor which is based on Rubenstein's HEIA technique [51]. For the Ovarian Monitor, a lysozyme-E1G or lysozyme-PdG conjugate must be prepared by combining hen egg white lysozyme (HEWL) with an appropriate activated carboxyl group reagent derived from the steroid glucuronide and isobutyl chloroformate (mixed anhydride method [51,54]) or dicycohexyl carbodiimide (active ester method [55]). The lysozyme conjugate is prepared by coupling of E1G or PdG (*via* the carboxyl groups of the glucuronide moiety) with the amino groups of lysine residues on the surface of the enzyme. The lytic activity of the resulting conjugates in the immunoassay is determined by changes in light transmission of a suspension of the bacterial substrate *Micrococcus lysodeikticus* (*M. lysodeikticus*).

The synthetic steroid glucuronides are also used to prepare immunogens to raise the appropriate antibodies by coupling them (separately) to a protein carrier such as bovine serum albumin or thyroglobulin before injection into sheep or rabbits. A minimum of six months is usually required for the generation of high titre antibodies.

The Ovarian Monitor home fertility system consists of two parts; the assay monitor and a specially designed plastic assay tube (Figure 1.5). The monitor itself consists of a cell holder maintained at 40 °C by a built-in thermostat, an automated timer, a 650 nm light source (a light emitting diode, LED) and a detector. The assay tube is placed inside the cell holder and maintained at 40 °C during the assay. The LED transmits light through the sample to a detector on the opposite side, which then displays the transmission result on the screen as a digital readout. The built-in timer is triggered by a magnetic switch activated by closing the cell holder lid and indicates the completion of each incubation step by a series of beeps.

The plastic assay tube contains the assay components freeze dried at different levels on the tube wall. The antiserum and buffer salts are freeze dried at the bottom of the tube with a small glass bead to facilitate mixing, the lysozyme-hapten conjugate is immobilised near the centre of the tube and the *Micrococcus lysodeikticus* is immobilised near the top. This allows the assay components to be mixed in the appropriate order when sequential additions of urine and water are made. Separate assay tubes are required when assaying for E1G and PdG; E1G tubes contain anti-E1G antibodies and E1G-HEWL conjugate, while the PdG tubes contain anti-PdG antibodies and PdG-HEWL conjugate.

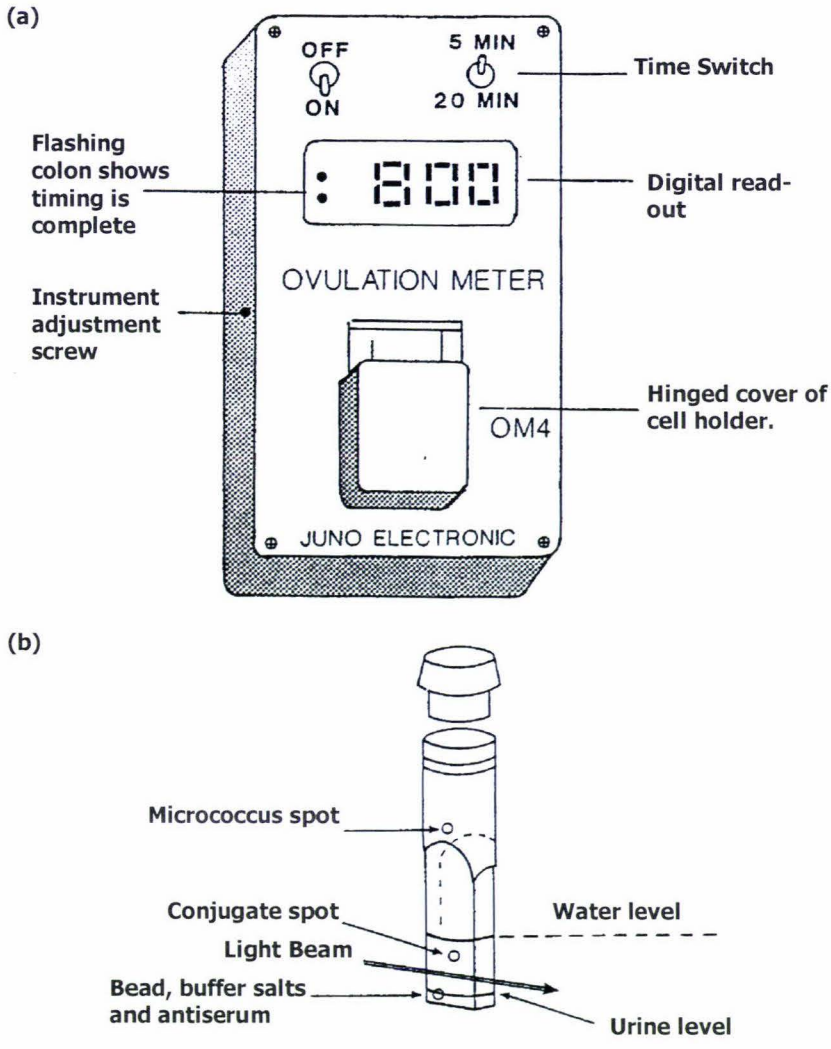

Figure 1.5 The Ovarian Monitor **(a)** and an Ovarian Monitor assay tube **(b)**, showing the position of the assay components freeze-dried to the tube.

The Ovarian Monitor assay is based on the classic enzyme-multiplied immunoassay technique (EMIT) and takes place in three discrete steps as shown in Scheme 1.3.

Step one: The antigen antibody reaction

In the first step, 50 μL of time diluted urine is carefully added (via syringe) to the bottom of the assay tube. The tube is then placed inside the cell holder and allowed to incubate for five minutes to allow time for the buffer salts and antibody (Ab) freeze-dried on the bottom of the tube to completely dissolve. The Monitor signals the end of the incubation period by a series of beeps, after which the tube is removed and gently shaken horizontally for a count of twenty seconds to allow the steroid antigen (Ag, i.e urinary estrone glucuronide or pregnanediol glucuronide) to mix freely with the corresponding anti-steroid antibody (Ab).

Binding of the steroid to the antibody is rapid and effectively irreversible within the time frame of the assay [56]. Thus the level of antibody neutralisation, and hence the amount of free antibodies remaining at the end of the first step is directly proportional to the level of steroid in the urine.

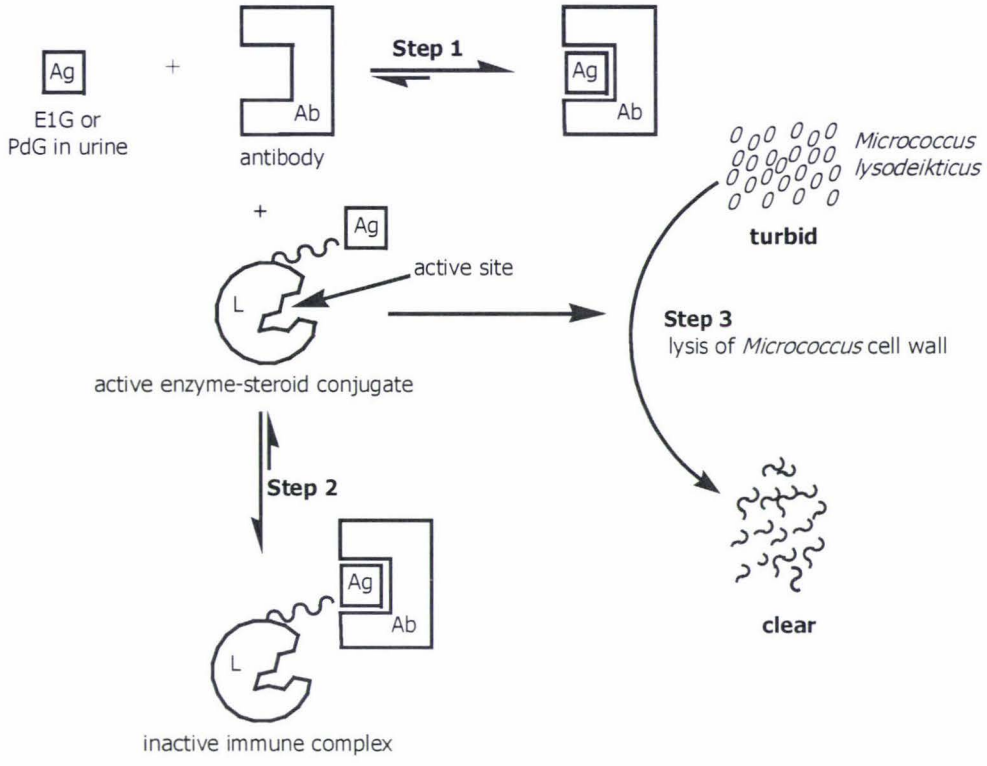

Scheme 1.3 Principle reactions in the Ovarian Monitor homogeneous enzyme immunoassay. Abbreviations used: Ag, antigen i.e urinary estrone glucuronide (E1G) or pregnanediol glucuronide (PdG); L, hen egg white lysozyme; Ab, anti-E1G or anti-PdG antibody.

Step 2: The antibody steroid glucuronide-lysozyme conjugate reaction

In the second step, the lysozyme conjugate spot is dissolved by careful addition of 300 μL of distilled water by syringe to the assay tube. The tube is then gently shaken horizontally for another count of twenty seconds and returned to the Ovarian Monitor cell holder to incubate for a further period (PdG, 5 min; E1G, 20 min).

During the incubation step, the excess antibody which was not bound by urinary steroid in the first step is allowed to bind (again effectively irreversibly on the time scale of the assay) to the steroid-lysozyme conjugate. Binding of the steroid-lysozyme conjugate to its corresponding antibody inactivates the enzyme due to the antibody sterically blocking the access of the bacterial substrate to the active site and also partly by steric restriction of access to the transition state [57]. In this step the level of antibody binding is directly proportional to the amount of free antibody left at the end of the first step. Thus, the level of free enzyme conjugate remaining at the end of step two is proportional to the level of steroid glucuronide in the original sample of urine.

Step 3: The Micrococcus lysodeikticus reaction

In the third and final step, the free conjugate remaining after the end of step two is given access to its natural substrate, the gram positive bacterium *Micrococcus lysodeikticus*. At the end of the incubation period in step 2 (signaled by a second series of beeps) the tube is removed from the cell holder and vigorously shaken for a count of twenty seconds to uniformly suspend the freeze dried *M. lysodeikticus* cells and returned to the cell holder. Closing the cell holder signals the start of the enzyme assay and triggers the Monitor to record the initial transmission value, $T_{0\ min}$. In solution the suspended *M. lysodeikticus* cells are large enough to scatter light and the solution appears opaque. However as the conjugate proceeds to lyse the *Micrococcus* cells by breaking the glycosidic bonds between sugar units in the polysaccharide component of the cell wall, the initially turbid solution begins to clear as the strength of the cell wall decreases and the cell collapses.

At the end of the assay period (PdG, 5 mins; E1G, 20 mins), the timer sounds and the difference between the final and initial transmission values (E1G, $\Delta T\ 5\ min^{-1}$; PdG, $\Delta T\ 20\ min^{-1}$) is left permanently flashing on the LED screen. This change in transmission is a measure of the rate of lysis over the predefined assay period. Because only the free enzyme conjugate retains its lysis activity, the change in transmission (or the rate of clearing) is directly proportional to the amount of unbound conjugate remaining at the end of step two, which is in turn determined by the amount of steroid in the initial urine sample.

Thus when the level of steroid glucuronide in the urine is low, most of the antibody is available for binding and inactivating the enzyme conjugate, resulting in a low rate of clearing of the turbid *Micrococcus lysodeikticus* suspension. However as the concentration of steroid in the urine increases and becomes antibody bound, the proportion of antibody available for inhibiting the conjugate activity decreases resulting in increased rates of lysis activity and higher rates of clearing. Thus, low levels of urinary steroid are associated with only small changes in light transmission (ΔT), whereas a high level of steroid generates a large change in transmission. Using a set of known concentrations a standard curve can be generated which relates the steroid glucuronide concentration to the observed change in transmission. A typical example of an optimised estrone glucuronide (E1G) curve relating the 24 hr molar excretion rates to the change in transmission over a twenty minute assay period ($\Delta T\ 20\ min^{-1}$) is illustrated in Figure 1.6. The curve shows the direct relationship between the lysis rate and the urinary steroid levels. The working range, i.e. the range of E1G excretion rates over which the curve is steepest and thus best able to discriminate between small changes in concentration is 25 – 410 nmol E1G $24\ hr^{-1}$ (as indicated by the arrows). This range includes the physiological range of E1G concentrations expected in the urine of normally cycling women. The midpoint or point of

inflection (EC_{50}) of the curve corresponds to the steroid concentration in the middle of the physiological range at ~140 nmol E1G 24 hr^{-1}.

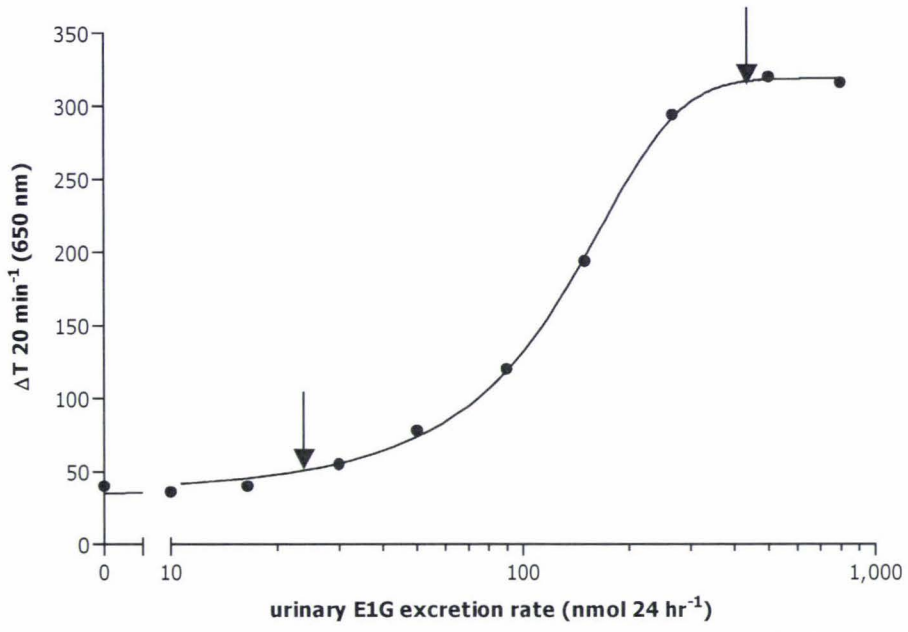

Figure 1.6 A standard curve for estrone glucuronide (E1G) generated using the Ovarian Monitor. The steepest section and thus most sensitive region of the curve corresponds to the range of E1G concentrations expected in the female urine during a normal menstrual cycle.

The standard curve generated with the pre-dried assay tubes for any batch of antiserum and lysozyme steroid conjugate is extremely reproducible and eliminates the need to establish a new standard curve for each new analysis (unlike radioimmunoassay where a new standard curve must be generated for each new batch of samples analysed). Since the standard curve is programmed into the Monitor, the tubes are colour coded to the match the standard curve to which they belong. Using such a curve, the Ovarian Monitor (Mark IV) can convert the change in transmission value to a 24 hour molar excretion rate. Conversion to the twenty-four hour molar excretion rate is not absolutely necessary for home use (unless quantitative data is required) as it is the pattern of hormone excretion that is important for the determination of fertility status. For example each batch of PdG tubes is labeled with the ΔT 5 min^{-1} value equivalent to a threshold value of 6.3 μmol PdG 24 hr^{-1}. Thus the woman need only check if she has exceeded this change in transmission to know she has reached the late infertile days of the menstrual cycle.

To monitor the changes in fertility status over the menstrual cycle the women can also plot their data as a change in transmission ΔT vs. cycle day (Figure 1.7). Hence a simple rate measurement gives a direct measure of the concentration of steroid glucuronide in the urine which allows couples either trying for, or trying to avoid pregnancy to determine what stage in the fertility cycle the women is. For example, Figure 1.7 shows that the beginning of fertility is

most likely on day 4 (6 days prior to the peak E1G day) as judged by the first rise in E1G above the preceding baseline [58]. The most fertile day is on day 11 (following the mid-cycle E1G peak day) and the end of her fertility for this cycle is given by the PdG rise on day 14 when the PdG threshold value is exceeded [25].

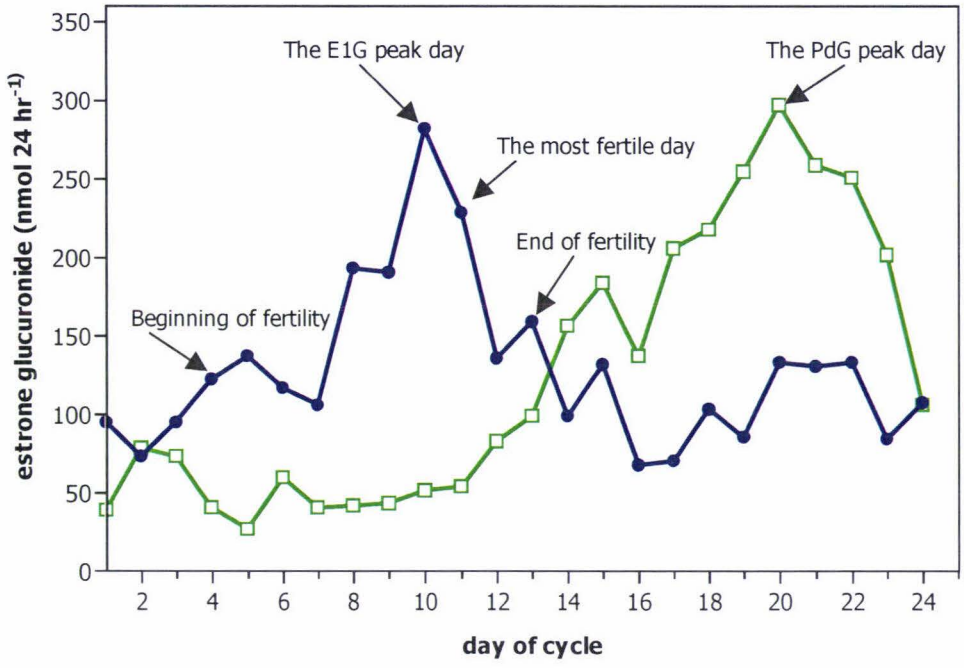

Figure 1.7 Normal menstrual cycle obtained by a women using the Ovarian Monitor.

Timed-diluted specimens of urine are essential for the assay to correct for fluctuations in urine volume which degrade the information and may render it uninterpretable in extreme cases. The urine may be collected overnight or during the day, provided that the period of collection is at least three hours [56]. The urine is diluted with tap water in a specifically graduated jug, such that the final dilution corresponds to the voiding of 150 mL hr^{-1}. This value is chose to represent the mean urine volume excreted of 3600 mL excreted in a 24 hour period. A portion of the diluted urine is then placed in a plastic tube and stored frozen if the test is not to be done immediately.

The validity of the Ovarian Monitor home test system has been verified by numerous trials, including a World Health Organisation trial (WHO) [59], and has been accredited by the Australian National Association of Technical Authorities (NATA) for routine monitoring of the gonadotrophin treatment of infertile women [60] at the Royal Woman's Hospital, and the Mercy Hospital in Melbourne. The E1G assay has also been used since 1987 for monitoring estrogen responses during hyperstimulation on a large IVF program.

1.6 A multi-purpose self monitor for other urinary hormone metabolites

It is obvious that the work carried out with the Ovarian Monitor should be applicable to a whole range of alternative steroid glucuronides providing that the required conjugates and antibodies can be synthesised. A range of assay tubes could then be developed using exactly the same techniques for other analytes of clinical or commercial interest. If the Monitor system were adapted so that it could recognise any assay tube introduced into it by appropriate coding then the same Monitor could measure a range of analytes in a home environment or in a point-of-care setting. For testing the multi-Monitor proposal, the major difficulty is to select an analyte for which there is likely to be a sufficient interest and demand for the test.

1.6.1 Testosterone as a biomarker

Male hypogonadism may be defined as a failure of the testes to produce testosterone, spermatozoa or both. The most common causes of hypogonadism are associated with failure of the anterior pituitary gland, deficiencies in enzymes responsible for testosterone biosynthesis, and chromosomal abnormalities such as Kleinfelter's syndrome (47,XXY karyotype) which affects ~1 in 400 males [61]. Chemotherapy or radiation therapy may also result in long term testicular damage and reduced production of testosterone. Other conditions associated with a low testosterone in men include acute stress, alcoholism, obesity and chronic or acute illness including HIV, leukemia and cirrhosis of the liver [47,62]. Plasma levels of free testosterone also show a steady decline with age, by approximately 1.2% per year starting at around age 40 [63]. Age related testosterone decline may result in the loss of the diurnal rhythm of plasma testosterone secretion and cause a range of physical symptoms including a progressive decrease in muscle mass, loss of libido, erectile dysfunction, reduced sperm count and osteoporosis [61]. In adult females the opposite occurs; an excess of testosterone production is indicative of a large number of abnormalities including polycystic ovaries, (as a result of defects in the enzymes that metabolise testosterone and cortisol) and ovarian tumours [64,65]. Increased levels of testosterone in women are also associated with hirsutism, and adrenal hyperplasia [47].

Over 4 million men in the USA diagnosed with a testosterone deficiency undergo replacement therapy, mostly by self-injection of testosterone every one to three weeks [66]. One of the major problems with this method of self-administration is that it is difficult to mimic the bodies production and management of testosterone levels. Injection introduces a high dose of testosterone, maintained for only the first few days after injection, returning to basal levels at the end of the treatment period. Testosterone administered by mouth is absorbed into the portal blood stream and promptly degraded by the liver so that only a small portion reaches the systemic circulation. More effective alternatives to androgen therapy involve administration of testosterone in a slowly absorbed form (dermal patches or a micronised oral preparation) or the administration of chemically modified analogs [67]. Recently a gel based formula containing

testosterone known as Androgel has become available in the USA [68]. To be administered once or twice a day, Androgel is thought to produce a more even plateau of testosterone concentration, thus avoiding the fluctuation in plasma levels resulting from injection.

The safe use of testosterone replacement therapy relies on the monitoring of testosterone levels in biological fluid to assess the response to treatment, requiring multiple visits to the hospital or specialist. Such frequent visits may involve major disruption to family and working life, and may cost a considerable amount in travel and time away from work. In a clinical setting, testosterone is most frequently measured in the plasma. However since it is released from the testes in episodic spikes during the day, and is 25% higher in the morning than at night, at least 3 blood samples, taken at 20- to 40-minute intervals during the morning are required for measurement [69].

Home monitoring of testosterone production, performed by the patient, has the potential to overcome may of these problems by limiting the number of trips to a specialist clinic but still allow their dose regimes to be monitored safely.

1.6.1.1 Testosterone biosynthesis

In men, over 95 % of the testosterone is produced by the Leydig or interstitial cells of the testes and is mainly controlled in adulthood by lutenising hormone produced by the pituitary gland [47]. In normal females, approximately half the testosterone produced is made by the ovaries; the remainder originates from the adrenal glands and conversion from estrogen in the periphery [70]. The pathway of testosterone biosynthesis from cholesterol has been illustrated already in Scheme 1.1.

In normal males an average of 5 - 6 mg of testosterone is secreted into the plasma per day [71]. For females this level is much lower at around 1.5 mg day [72]. In the blood, only 1 - 2% of the total testosterone circulates in the free state (unbound), the rest is bound to plasma binding proteins. Approximately 45% is bound with high affinity to a β-globulin called sex hormone-binding globulin (SHBG), 50% is loosely bound to albumin, and other 1 - 2% is bound to an α_2-globulin called corticosteroid binding globulin (CBG) [73]. SHBG has about a 1000 fold higher affinity for testosterone than albumin, but the concentration of albumin is so much higher that the binding capacities of both proteins is considered to be similar [17]. For many years, only the free testosterone fraction was regarded as the biologically active portion available for entry into cells and binding to androgen receptors. It is now widely accepted that protein-bound testosterone can dissociate in the capillary bed and nearly all the albumin bound testosterone is available for tissue uptake *in vivo* so that the bioavailable testosterone in men is about half the total (equal to the free plus albumin bound fraction) [74,75].

In adult males testosterone production shows diurnal variation, with the highest levels in the early morning, followed by a progressive fall throughout the day, reaching the lowest levels in the evening and during the first few hours of sleep (Figure 1.8). Peak and lowest values may differ by approximately 15%, although more pronounced differences are sometimes observed [76].

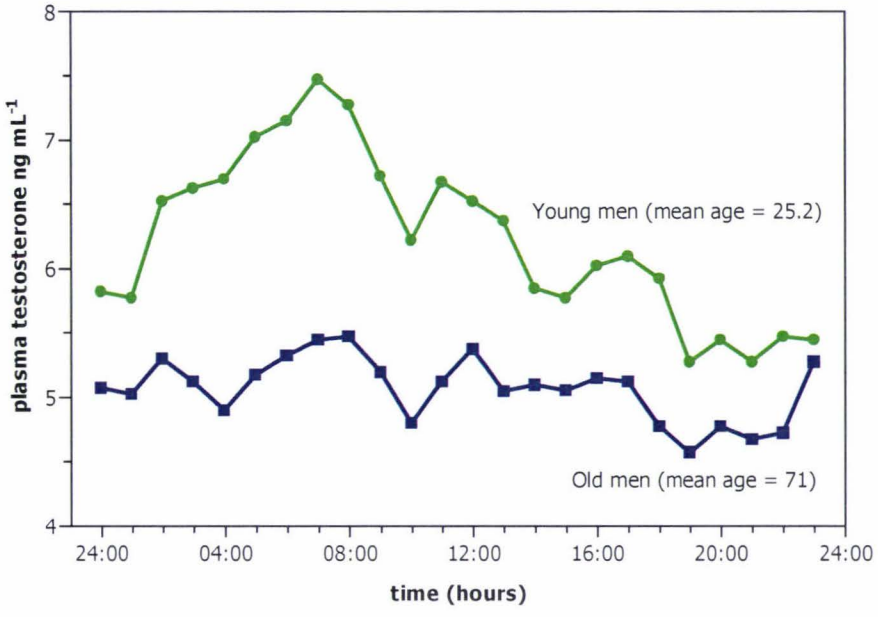

Figure 1.8 Diurnal pattern of testosterone levels in plasma [77].

1.6.1.2 Biological activity of testosterone

Testosterone that is not bound to plasma proteins diffuses out of capillaries and into target as well as non-target cells. Despite being the major steroid hormone produced by the testes, testosterone has few direct actions; instead, it serves as a circulating precursor (or pro-hormone) for formation of the more potent 5α-reduced metabolite dihydrotestosterone (DHT). In the target cells testosterone and DHT bind to the same high-affinity androgen receptor, and the hormone-receptor complexes attach to DNA response elements to initiate biologic responses (shown schematically in Figure 1.9). These include the regulation of gonadotropin secretion by the hypothalamic-pituitary system, initiation and maintenance of spermatogenesis, and control of the male sex-drive [17].

Alternatively, a variety of tissues including the testes, brain, breast and adipose tissue can metabolise testosterone and its immediate precursor androstenedione into estrogens. Estrogen formation is catalysed by the cytochrome P450 enzyme CYP19 (aromatase), which converts testosterone into estradiol and androstenedione into estrone (see Scheme 1.1). These metabolites, particularly estradiol, are biologically active and may act locally by binding to estrogen receptors in the tissues in which they are formed or re-enter the plasma.

The role of estrogens in male physiology is complex and not completely understood, but is thought to include acceleration of the pubertal growth spurt, accrual and maintenance of bone density, a role in male sexual drive, and an influence on gonadotropin secretion [17]. In addition, estrogens may enhance androgen activity by increasing the number of androgen receptors in the prostate. In turn androgens appear to act as weak antiestrogens by preventing the binding of estrogen to the estrogen receptor [17].

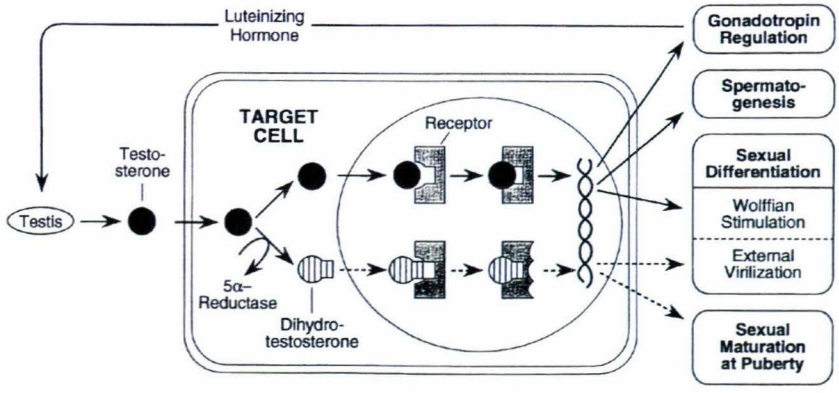

Figure 1.9 Schematic diagram of androgen action. Testosterone, secreted by the testis, binds to the androgen receptor in a target cell either directly or after conversion to dihydrotestosterone (DHT). DHT binds more tightly than testosterone. The major actions of androgens (shown on the right of the diagram) are either mediated by testosterone (solid lines) or by DHT (broken lines) [17].

1.6.1.3 Hepatic metabolism of testosterone

As for estradiol and progesterone, inactivation and excretion of testosterone and DHT occurs primarily in the liver, although metabolic enzymes are also present in other organs including the gut and kidneys [13]. Hepatic metabolism of testosterone also serves to increase the water solubility of the steroids by conjugation to glucuronic acid or sulphates, which facilitates their excretion in the urine as explained for E2 and P4 (section 1.4). Unconjugated steroids that are filtered by the kidney are largely reabsorbed [19].

The enzymatic reactions involved in hepatic metabolism are the same for androgens and corticosteroids, all containing a conjugated Δ4,3-keto moiety on the A-ring [13]. Oestrogens on the other hand, have an aromatic A-ring and are not substrates for the enzymes in these pathways [78]. The major reactions involved in the hepatic metabolism of testosterone include: (a) irreversible reduction of the A-ring across the 4-5 double bond from either the α (catalysed by 5α-reductase) or β (catalysed by 5β-reductase) side of the A-ring. This step yields two isomers which differ in the orientation of the C_5 hydrogen between the fused A and B rings. The 5α-metabolites have *trans* fused rings, which are essentially planar and similar to the parent steroids whereas the *cis* 5β fused rings are more skewed. (b) The 3α,5α/β reduced steroids are substrates for 3α-hydroxysteroid dehydrogenases which catalyse reduction of the

3-keto group to form 3α,5α- and 3α,5β-tetrahydrosteroid metabolites which are then (c) rapidly conjugated to sulphates or glucuronic acid and excreted. The conjugates are more soluble in water and have a much lower affinity for plasma binding proteins than did the parent steroid, with glucuronides having the lowest affinity of all [13]. The 3α,5β-reduced products of androstenedione are also substrates for 17β-hydroxsteroid dehydrogenase (17β-HSD) enzymes as shown in Scheme 1.4.

In principle any of the range of testosterone metabolites present in the urine as glucuronides could serve as a urinary biomarker for serum testosterone production in humans. However, the stereospecific reductions which occur *in vivo*, while not impossible *in vitro,* nevertheless require a significant amount of synthetic effort. In the absence of information on the relative levels of these possible biomarkers in urine it seems sensible, at least at this stage of development, to focus on testosterone glucuronide as the urinary marker. It is relatively easy to synthesise and is expected to be excreted into the urine of males in significant amounts.

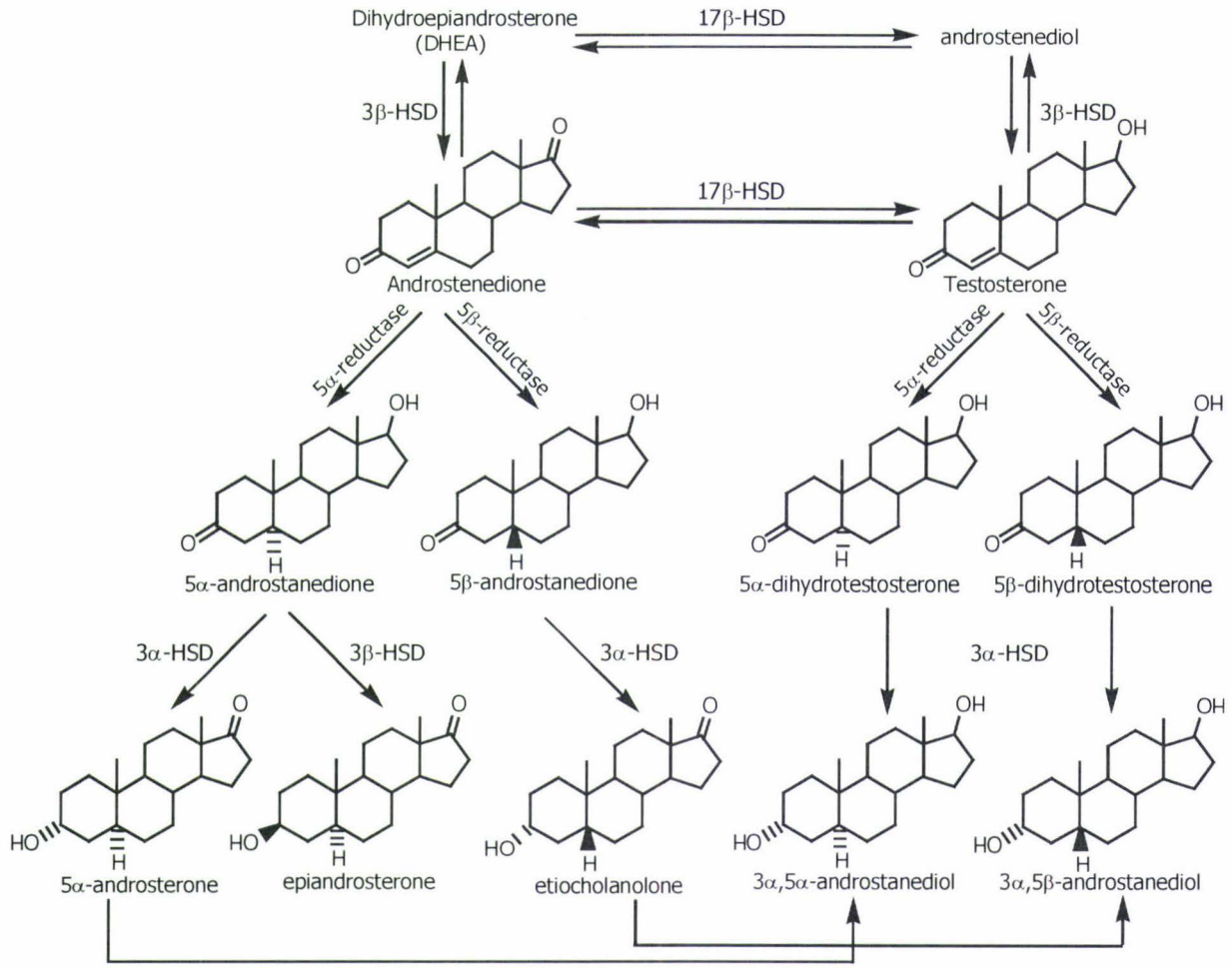

Scheme 1.4 Metabolism of androgens [13]

1.6.2 Cortisol and its metabolites as biomarkers of stress and disease

Although there is some variation in the way that "stress" is defined, common among these definitions is that stress is a process in which environmental demands tax or exceed individuals' adaptive capacities, contributing to biological and psychological changes that may place them at risk for illness [79].

While cortisol activation in response to stress is protective in the short term, the chronic or extreme activation may have long-term negative consequences. Cortisol stimulates the immune system and counteracts inflammatory and allergic reactions at normal levels but can suppress the immune system at excessive levels or when prescribed therapeutically in a synthetic drug form [80]. Whereas hypercorticolism is associated with diseases characterised by immunosuppression and reduced ability to fight infections, including HIV [81,82,83] it may also increase susceptibility of developing chronic inflammatory disease, autoimmune disease and other diseases characterised by inflammation [80]. Hypercortisolism has also been associated with arthritis, multiple sclerosis and all types of cancer [83] and is the primary symptom of Cushing's disease [84]. Cortisol excess may also lead to insulin resistance, hypercholesterolemia and hypertriglyceridemia, thereby contributing to the development of adult onset diabetes, hypertension and heart disease [85,86].

Recently, the suggestion has been that elevated cortisol levels are in fact the causative agent of disease and the results have been presented at an International Conference [83]. For example, it has been proposed that HIV stimulation induces the adrenal gland to produce elevated levels of cortisol and that elevated cortisol is, by itself, capable of inducing all of the symptoms and opportunistic infections encountered in AIDS [87]. Also, evidence has been presented which suggests that high levels of cortisol play a role in Alzheimer's disease, memory loss, shrinking of the brain and aging [88]. The more conventional view is that the elevated cortisol levels are associated with other underlying mechanisms and are indicative rather than causative. For the purposes of this discussion it does not matter which view is correct since the high levels of cortisol can be used as a diagnostic tool in either case and appropriate strategies taken to alleviate the underlying conditions. There is also evidence that cortisol levels are of diagnostic importance for athletes; in particular elite women athletes who may face menstrual cycle disturbances [89].

1.6.2.1 Cortisol biosynthesis

The synthesis of cortisol from cholesterol shown in Scheme 1.5 occurs exclusively in the adrenal cortex via a series of reactions catalysed by cytochrome P450 (CYP) and various short chain dehydrogenase enzymes. These enzymes are located in either the lipophillic membranes of the smooth endoplasmic reticulum (ER) or the inner mitochondrial membrane. As the series of enzymatic reactions to convert cholesterol into cortisol proceeds, the steroid intermediates shuttle between the membranes of the two organelles [19]. In humans, the necessary transformations from cholesterol to cortisol proceed as follows; cholesterol is imported into mitochondria and converted to pregnenolone by the cytochrome P450 enzyme, CYP11A as described for E1G and PdG in section 1.3. Pregnenolone is then transferred to the ER, where a 17α-hydroxylase (CYP17) converts it to 17-hydroxypregnenolone. This is then a substrate for 3β-hydroxysteroid dehydrogenase Δ^5-Δ^4 isomerase which catalyses oxidation at C3, resulting in a ketone functional group, and isomerisation of the double bond to form 17-hydroxyprogesterone. A further hydroxylation in the smooth ER by a 21-hydroxylase (CYP21) converts 17-hydroxyprogesterone to 11-deoxycortisol. The latter is transferred back to the mitochondria and is converted to cortisol by an 11β-hydroxylase (CYP11B1). The final step is highly efficient, resulting in 98% conversion of 11-deoxycortisol to cortisol, which diffuses rapidly into the circulation without significant storage in the adrenal cortex [19]. An alternative pathway for cortisol biosynthesis exists in the mitochondria whereby oxidation of pregnenolone at C3 followed by isomerisation of the double bond forming progesterone occurs before the series of hydroxylations at C17 (17-OH progesterone), C21 (11-deoxycortisol) and finally at C11 in the ER terminating in cortisol [90].

Cortisol secretion under basal (i.e. non-stressed) conditions ranges from 8 mg/day to 25 mg/day (22 - 69 μmol/day) with a mean of ~9.2 mg/day (25 μmol/day) [91]. In the plasma only 3 - 10% of circulating cortisol is in the free state. Approximately 80 - 90% is bound with high affinity to corticosteroid binding protein (CBG) and the remaining 5 to 10% is bound to albumin [19]. As for testosterone (see section 1.6.1.1) albumin has a much lower affinity for cortisol than CBG, but a much higher capacity. The dissociation of cortisol from albumin is more rapid, thus the albumin bound steroid is thought to be more readily available to the tissues than that bound by CBG. A third binding protein, α_1-acid glycoprotein can also bind cortisol, but appears to be only of minor importance to cortisol transport since it preferentially binds progesterone [19].

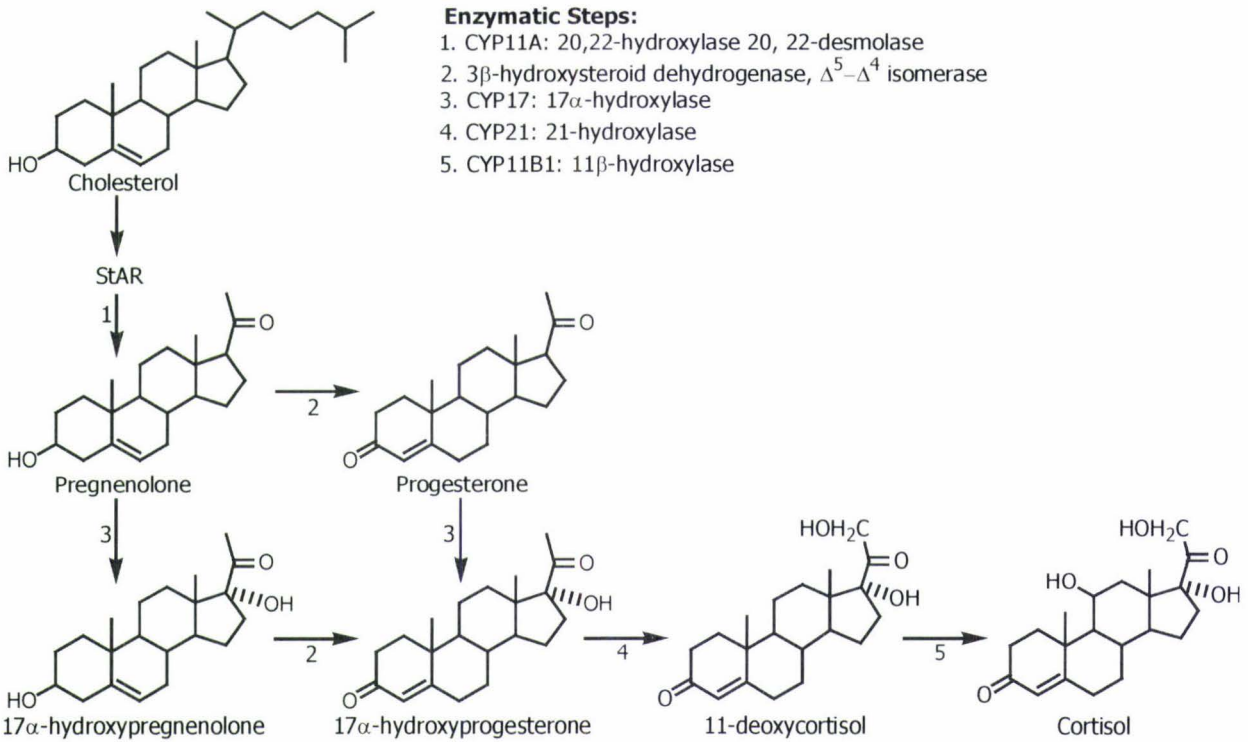

Scheme 1.5 Biosynthesis of cortisol from cholesterol [19].

Normally about 10 - 15 pulsatile bursts of cortisol are secreted into the plasma in a 24 hour period in adults [19,92]. Like testosterone, cortisol levels in the blood show a clear diurnal rhythm. The levels are lowest around midnight and peak about half an hour after awakening as shown in Figure 1.10 [93]. Peak levels on awakening may be 50 – 100% higher than the lowest levels. Hence this factor must be taken into account when designing assay protocols for cortisol or its metabolites.

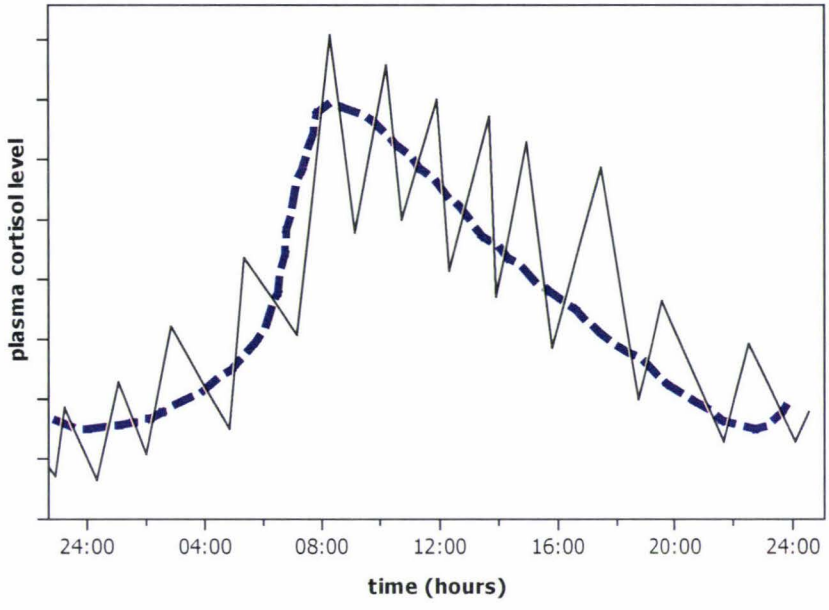

Figure 1.10 Diurnal pattern of cortisol levels in plasma [78].

1.6.2.2 Biological activity of cortisol

Under basal conditions, cortisol interacts mostly with high affinity mineralocorticoid receptors, which are important for normal homeostatic control of metabolic processes and fluid balance. However, when the hypothalamic-pituitary-adrenal (HPA) axis (those glands responsible for integrating the central nervous system and endocrine system) is activated during a stressful experience, cortisol levels can increase ten-fold and at these levels cortisol may bind to lower affinity glucocorticoid receptors in target tissues [94].

Through its interaction with glucocorticoid receptors cortisol is hypothesised to promote short term survival in an acutely stressful event by: (1) increasing glucose and oxygen supply to skeletal muscles and heart and brain to facilitate flight and sharpen cognition to allow an appropriate behavioural response; 2) suppressing reproductive, immune and digestive functions to conserve energy; 3) promoting analgeisa and 4) activating the autonomic nervous system [95].

Increasing levels of cortisol also act as a negative feedback signal to suppress further release of the hormones which stimulate cortisol production; corticotropin-releasing hormone (CRH) released from the hypothalamus and adrenocorticotropin-releasing hormone (ACTH) released from the pituitary (as shown in Figure 1.11).

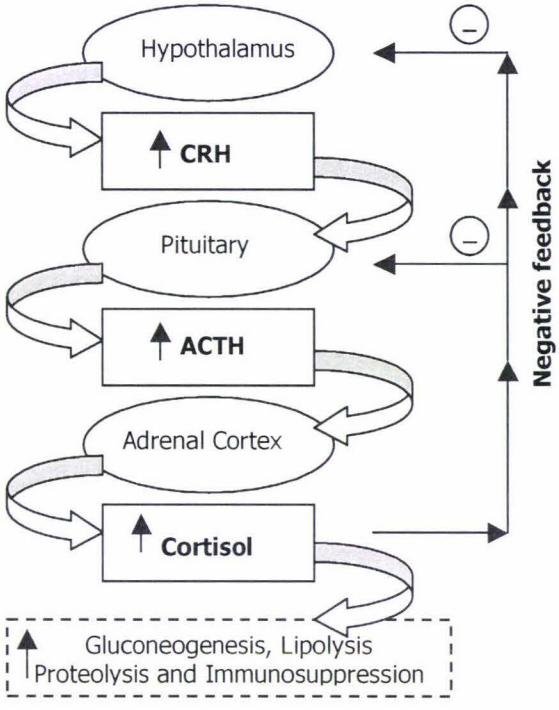

Figure 1.11. Hypothalamic-pituitary axis (HPA) activation. When activated the HPA leads to the sequential release of hormones at each level of the axis, culminating in the release of cortisol. Through negative feedback inhibition, increasing levels of cortisol supress further CRH and ACTH release at the level of the hypothalamus and pituitary. Abbreviations: HPA, hypothalamic-pituitary-adrenal; ACTH, adrenocorticotropin-releasing hormone; CRH, corticotropin-releasing hormone [78].

1.6.2.3 Hepatic metabolism of cortisol

As noted earlier, the androgens and corticosteroids both contain a conjugated Δ4,3-keto moiety on the A-ring and are metabolised by common pathways in the liver. The metabolic steps a), b) and c) described for hepatic metabolism of testosterone in section 1.6.1.3 also apply to cortisol, and the resulting cortisol metabolites are illustrated in Scheme 1.6.

In addition, cortisol is a substrate for the enzyme 11β-hydroxysteroid dehydrogenase type 2 (11β-HSD2) which catalyses the oxidation of the 11β-hydroxy group to form the inactive metabolite cortisone. Inactivation of cortisol by 11β-HSD2 occurs in the kidneys and other mineralocorticoid sensitive tissues [96] to protect mineralocorticoid receptors from illicit occupation by cortisol, which is present in concentrations in excess of the preferred ligand,

aldosterone [97]. Cortisone may then be metabolised by steps a), b) and c) as outlined for cortisol or reactivated back to cortisol by 11β-HSD1 in several metabolic tissues including the liver, muscles, adipose tissue and brain [98,99]. Further reduction at the C_{20} position in the side-chain of 3α,5β-tetrahydro corticosteroids, by 20-dehydroxysteroid dehydrogenases can give rise to the corresponding 20α and 20β isomers, namely cortols by reduction of cortisol and cortolones by reduction of cortisone [13]. Finally cleavage of the C_{17} side chain may take place, producing 19 carbon metabolites that have a ketone group at the C_{17} position, such as 11β-hydroxyandrostenedione and 11-ketoetiocholanolone [19].

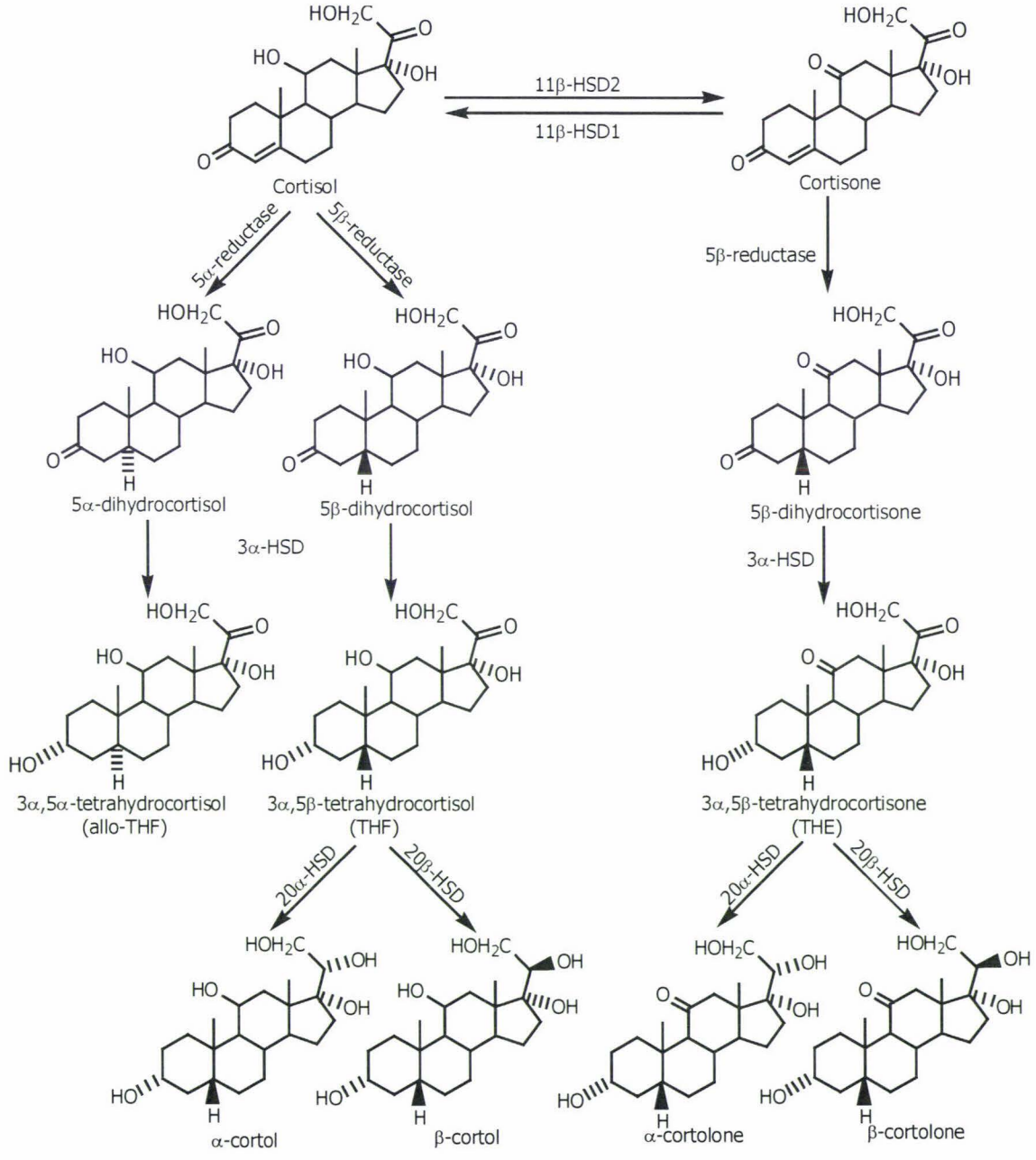

Scheme 1.6 Metabolism of cortisol and cortisone [13].

In the urine of normal subjects the 5β metabolites predominate (5β:5α-tetrahydrocortisol 2:1). Approximately 50% of the secreted cortisol appears in the urine as tetrahydrocortisol (THF), allo-THF and tetrahydrocortisone (THE); 25 % as cortols and cortolones; 10% as 19 carbon steroids and 10% as cortolic and cortolonic acids. The remaining metabolites exist in the urine as unconjugated steroids; cortisol, cortisone, 6β- and 20α/β-metabolites of THF and THE [100,101]. Marked differences in the amount of total urinary cortisol metabolites excreted by age-matched males and females also exist. The reason for the difference is thought to reflect differences in the hypothalamic-pituitary adrenocorticol axis or primary differences in adrenal function [102]. Normally less than 1% of cortisol is excreted unchanged in the urine of humans. Although this can be measured using RIA the levels are only of the order of 50 μg per day [15].

In a recent study by Yergey *et al.* [103], the metabolites of cortisol in urine were examined by a novel mass spectrometric procedure known as chemical reaction interface mass spectrometry or CRIMS. In this procedure the hydrolysed urinary metabolites of radiolabeled cortisol (9,12,12-$^{2}H_{3}$ cortisol) were measured in six human subjects and it was found that 5β-tetrahydrocortisone (THE) was the major metabolite constituting 42% of the total cortisol metabolites. Tetrahydrocortisone has three available hydroxy groups and hence this compound may appear in urine as a variety of glucuronides, sulphates or mixed sulphates and glucuronides. The 3α-glucuronide is the major metabolite and is excreted in amounts corresponding to about 5 mg per day [103] similar to pregnanediol-3α-glucuronide [25]. These levels are sufficient to make it possible to produce a rapid (5 minute) home and laboratory test for tetrahydrocortisone-3α-glucuronide, as a measure of total free cortisol by adaptation of our presently existing home test for the steroidal markers of the fertile phase of the human menstrual cycle [56,60].

1.7 Aims of the present study

In summary the aims of the present study are:

1. To expand the range of urinary steroid metabolites that can be measured using the Ovarian Monitor homogeneous immunoassay format currently used as a home monitoring device for determining the fertile period during a women's menstrual cycle.

2. To prepare biomaterials for a testosterone glucuronide assay that can be used as a device for application to the urine of males as a biomarker of testosterone in men undergoing androgen replacement therapy.

3. To prepare biomaterials for a tetrahydrocortisone glucuronide assay that could be used in a device for measuring stress.

4. To establish standard curves for the two urinary metabolites which are capable of measuring the physiological ranges of testosterone glucuronide and tetrahydrocortisone glucuronide.

CHAPTER TWO

Synthesis and purification of biomaterials required for the immunoassay of testosterone glucuronide and tetrahydrocortisone glucuronide

2.1 Introduction

In order to adapt the Ovarian Monitor assay system to the measurement of testosterone glucuronide (TG) and tetrahydrocortisone glucuronide (THEG) in urine, it is first necessary to synthesise the biomaterials required to perform the immunoassay. These include a ready supply of purified steroid glucuronide (hapten), suitable hapten-hen egg white lysozyme (HEWL) conjugates to be used as the immunoassay signal generators, and immunogenic complexes (hapten coupled to a suitable carrier protein) required for raising anti-hapten antibodies in animals. In this chapter the synthesis, purification and characterisation of these assay biomaterials will be discussed.

2.1.1 Synthesis of naturally occurring steroid glucuronide metabolites

For the synthesis of steroid glucuronides used in the production of immunoassay biomaterials the correct stereochemistry is essential since the naturally occurring glucuronide metabolites of testosterone and tetrahydrocortisone excreted in urine all have the β-configuration at the anomeric carbon (Figure 2.1). If the glucuronide bond between the sugar and the steroid moiety were in the α-orientation, the anti-steroid antibodies raised in rabbits by injection of the steroid α-glucuronide immunogen conjugates would probably be non-specific for the naturally occurring isomer. The synthetic hapten-HEWL conjugates used as signal generators for the immunoassay must also have the steroid hapten in the correct configuration if they are to compete with the endogenous steroid for the antibody binding sites.

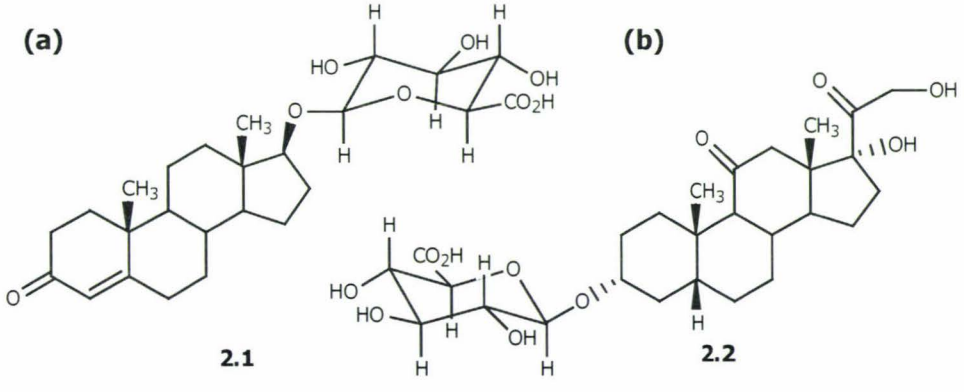

Figure 2.1 Structures of the naturally occurring β-glucuronide isomers (a) testosterone-17β-glucuronide (TG) and (b) tetrahydrocortisone-3α-glucuronide (THEG).

The most widely used method for the synthesis of β-glucuronides involves coupling an acetate protected glycosyl halide with the alcoholic or phenolic group of the acceptor under anhydrous conditions in the presence of a halide ion acceptor or promoter (often incorrectly termed the catalyst) typically a heavy-metal salt, for example Ag_2CO_3, Ag_2O, $Hg(CN)_2$, or $CdCO_3$ [104]. This general procedure is known as the Koenigs-Knorr reaction, named after its creators W. Koenig and E. Knorr who prepared the alkyl tetra-*O*-acetyl-β-D-glucopyranoside **2.4** from the corresponding α-bromosugar **2.3** in 1901 [105] (Scheme 2.1).

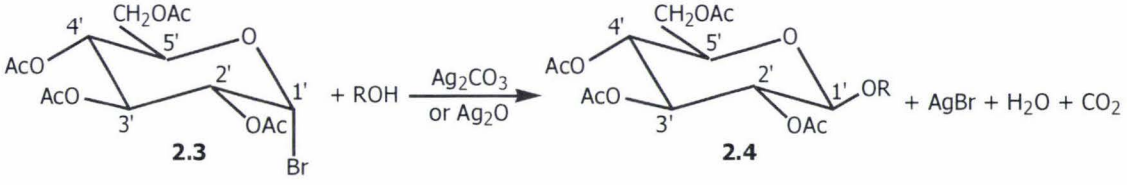

Scheme 2.1 Koenigs-Knorr synthesis of an alkyl tetra-*O*-acetyl-β-D-glucopyranoside [106].

The common solvents used for glucuronidation by Koenigs-Knorr conditions have included benzene, toluene and quinoline [3]; whichever solvent medium is employed, the water formed during the reaction can react with the α-bromosugar, and therefore must be removed (typically by using molecular sieves or azeotropic distillation) to achieve a good yield. Additional base may also be needed to react with the hydrogen bromide formed during the reaction [3]. Both cadmium carbonate, silver carbonate and more recently silver triflate (AgOTf), have been used as acid acceptors and promoters for the synthesis of steroid glucuronides. Commercially available $CdCO_3$ is often the preferred promoter since it typically gives superior yields compared to silver carbonate which must be prepared fresh each time and is more difficult to dry. The acyl protected glycosyl bromides remain the glycosyl donors of choice for the synthesis of β-linked steroid glucuronides since they are relatively stable (if kept under desiccation at –20 °C or dissolved in absolute methanol) and may be easily prepared in good yield from readily available starting materials.

2.2.2 Synthesis of steroid glucuronide–lysozyme conjugates as signal generators

Hen egg white lysozyme is a relatively small (MW 14,300 Da), highly basic protein, roughly ellipsoidal in shape (dimensions 45 x 30 x 30 Å) with a well-defined enzymatic cleft on one side, which divides the enzyme into two lobes [107]. The entire protein consists of a single polypeptide chain of 129 residues cross-linked by four disulphide bridges which are in part, responsible for the unusually high stability of the enzyme [108]. The highly basic nature of HEWL (pI = 10.5) [109] is due to the high proportion of lysine and arginine residues on the proteins surface. These positively charged residues are essential for maintaining the specific activity of the enzyme, since substrate binding is highly dependant upon the electrostatic attraction between the positively charged enzyme and the negatively charged cell wall of the *Micrococcus lysodeikticus* cell membrane [110].

The Ovarian Monitor hapten-HEWL conjugates are formed by attaching the steroid glucuronide via the carboxylic acid group of the sugar moiety to the ε-amino groups of lysine resides (or the N-terminal amino group) on the surface of lysozyme. Lysozyme has six lysine residues on its surface at positions 1 (N-terminal α-amino group), 13, 33, 96, 97 and 116 within the amino acid sequence and all six residues theoretically can be acylated by a variety of coupling reagents. The most commonly used procedures to activate the steroid glucuronide carboxylic acid group for coupling to HEWL are the mixed anhydride procedure of Rubenstein *et al.* [51] and Leute *et al.* [54] and the active ester method of Rajkowski *et al.* [55].

For an assay based on the steric inhibition of lysozyme activity by binding of anti-hapten antibodies it follows that the steroid moieties attached to the enzyme must be located close to the active site region. For lysozyme, only three of its six lysine residues are readily conjugated by steroid glucuronides by the active ester and mixed anhydride reactions at close to stoichiometric ratios of the reagent. However all three positions (lysines 33, 97 and 116) are located close to the active site of the enzyme. The distribution of lysine residues around the active site of HEWL is shown in Figure 2.2.

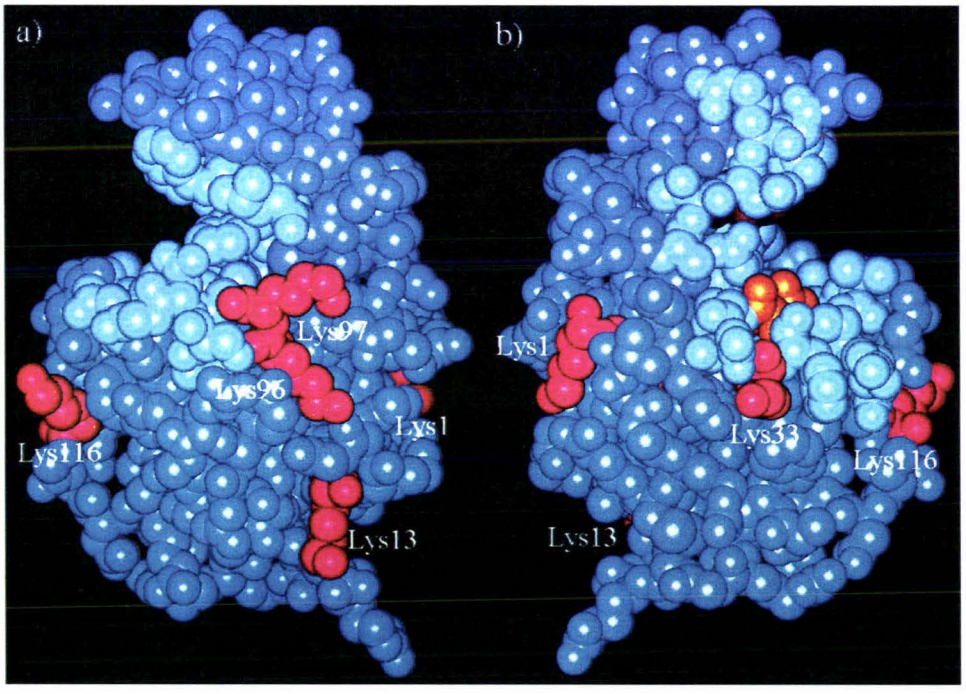

Figure 2.2 Computer generated space-filling model representing hen egg white lysozyme viewed from opposing sites of the molecule showing the location of the six lysine residues with respect to the active site cleft. Colour Key: medium blue - general protein, pale blue – binding site cleft, orange – Glu 35 active site residue, brown – Asp 52 active site residue, red – lysine residues [111]

Lysine 116 is positioned under the mouth of the active site cleft, lysine residues 96 and 97 are found at one corner of the mouth with lysine 33 at the other corner. In comparison the lysine residues 1 and 13 are located well away from the active site cleft on the opposite side of the molecule.

Although lysines 33, 97 and 116 are readily acylated [112], because each acylation event results in the removal of a unit of positive charge, the specific activity of highly substituted enzyme conjugates (> 2 haptens per molecule) is reduced such that their lysis rate in the presence of substrate is too low for rapid signal generation during the Ovarian Monitor assay. Conjugation of a non-polar molecule with HEWL also makes the individual conjugate families more hydrophobic than native lysozyme which may also contribute to the reduced specific activity of highly acylated conjugates. Thus to maximise the yield of active conjugates it is necessary to choose the acylation conditions which produce a low number of substitutions per HEWL [113]. For example, the standard active ester coupling protocol used in this thesis to prepare steroid-glucuronide-HEWL conjugates uses a molar ratio of 1.5:1 steroid-glucuronide:HEWL.

Since the location and number of haptens per lysozyme is impossible to control via the active ester reaction and mixed anhydride reactions, a low hapten:HEWL coupling ratio inevitably means that significant amounts of unreacted HEWL will remain after the conjugation reaction. A potential problem thus arises since any unreacted enzyme in the conjugate material used in the immunoassay will also show lytic activity. This background lysis rate will be constant for a given level of free lysozyme contamination, but unlike the hapten-HEWL conjugates, the activity of the unconjugated HEWL will not be inhibited by anti-hapten antibody.

Because the ability of the assay to discriminate between similar hormone concentrations in urine is determined by the difference in enzyme activity between the bound and free conjugate, the presence of any uninhibitable lysozyme will reduce the sensitivity of the assay by an amount proportional to the level of contamination [114]. Thus, one of the most important considerations in the preparation and purification of hapten-HEWL conjugates for use in the immunoassay is the complete removal of unreacted lysozyme. Furthermore, the binding strength between the hapten-HEWL conjugates and the corresponding anti-hapten antibodies in the immune complex is highly dependent on the position of the hapten on the enzyme surface [115]. Since this feature will also affect the sensitivity and working range of the standard curve, the purification method used must also be able to separate the individual conjugate families from each other as well as unreacted HEWL.

At present, a two-step isolation and purification procedure developed by Cooke [115] is the preferred method for the large-scale preparation of pure (lysozyme free), steroid glucuronide-HEWL conjugate isomers. That procedure, as adapted in this chapter, utilizes the differences in charge and hydrophobicity of the different conjugates and lysozyme to isolate the main TG-HEWL and THEG-HEWL conjugate fractions for use as signal generators in the homogenous enzyme immunoassays for TG and THEG, and will be described in detail in Chapter Three.

2.2.3 Synthesis of immunogens for antibody production

In general, small molecules (MW < 1000 Da) are non antigenic since their structural simplicity and low molecular weight fail to stimulate the host animal's immune system. However, it is possible to elicit an immune response to such haptens by conjugating them to a carrier protein, thus forming an immunogen [47]. Proteins such as bovine serum albumin (BSA, MW 66,430 Da), thyroglobulin (THY, MW 660,000 Da) and keyhole limpet hemocyanin (KLH, MW 450 kDa – 13,000 kDa) are a few of the carrier molecules commonly used in the preparation of steroid glucuronide immunogens [47,116-118]. BSA and thyroglobulin are well suited as carrier proteins, due to their low cost, good solubility in various aqueous buffers and high content of available ε-amino lysine residues (59 in BSA [119] and 177 in bovine thyroglobulin [120]). BSA is also highly soluble in water miscible solvents, which are required for the synthesis of immunogens containing hydrophobic drugs [121]. Immunogens prepared using KLH as the carrier protein have also been used for the production of anti-steroid antibodies [122]. However the KLH immunogens are notoriously difficult to characterise due to their poor solubility and variable mass of the protein.

Usually only a fraction of the total lysine residues present in a carrier protein are accessible for conjugation with a hapten. For example of the 59 lysine residues in BSA, a maximum of between 30 and 35 lysine residues can be coupled [119]. In general, the hapten:carrier ratio recommended for immunogen production is one to three haptenic groups per 10,000 Da of carrier (i.e. 6 - 18 hapten moieties per BSA molecule). A higher ratio is thought to decrease the quality (specificity) of the antibodies. It is possible that under these conditions the animal's immune system becomes indifferent towards the immunogen [123]. However, coupling ratios as high as 15 - 30 haptens per molecule of BSA have been reported as being "optimal" for the production of highly specific antiserum [119,121]. The ideal ratio to produce antibodies having both high affinity and specificity is likely to dependant on the size and chemical nature of the hapten. Numerous other factors such as the species of animal, animal handling protocols and immunisation procedures such as the number and spacing of the immunisations, the adjuvant and injection site will also have a marked effect on the success of antibody production.

Following the successful production of highly specific antibodies to estrone glucuronide (E1G) using E1G-thyroglobulin immunogen conjugates [124] thyroglobulin was also used as the carrier protein to prepare TG and THEG immunogens in the following chapter. The active ester approach used to prepare the hapten-HEWL conjugates was also used to prepare the immunogens, since the high acylating character of the active ester reagent allows a high number of haptens to be covalently attached to the surface of the carrier protein.

2.2.4 Estimation of the hapten:carrier coupling ratio

The molar ratio of hapten to carrier in the immunogen can be determined by a number of methods, including measurement of radioactivity labeled hapten [117], lysine titration using trinitrobenzene sulfonic acid (TNBS) [125,126], UV difference spectroscopy and amino acid analysis [119,127,128]. Determination of the number of haptens covalently attached to the immunogen is an important factor when assessing the quality and titre of the resulting antibodies. In order to characterise the thyroglobulin immunogens prepared in this chapter using the available equipment, two relatively straightforward spectroscopic methods were chosen. Namely, determination of the number of unacylated ε-amino groups in the immunogens by trinitrobenzene sulfonic acid assay [126] and the UV difference method [129] which is based on the absorption spectrum of the immunogen compared to those of the hapten molecule and the carrier.

Thus in summary, the goals of the project to be addressed in this chapter are:

1. To synthesise and characterise testosterone-17β-glucuronide under Koenigs-Knorr conditions, (due to time constraints, and the more complex synthetic strategy required for its synthesis, THEG was purchased from a commercial supplier).

2. To prepare and purify stable, TG-HEWL and THEG-HEWL conjugates for use as the immunoassay signal generators, and

3. To synthesise and characterise TG and THEG thyroglobulin conjugates to be used as immunogens for raising anti-TG and anti-THEG antibodies in rabbits.

2.2 Experimental

2.2.1 Apparatus

All protein chromatography methods were performed on a Pharmacia fast protein liquid chromatography system (FPLC), generously supplied by Associate Professor Dave Harding, Separation Science Unit, Massey University. The system consisted of two P-500 pumps, a Pharmacia mixer, an LCC-500 liquid chromatography controller, an MV-7 motor valve injector for manual injection of small aliquots (~100 μL) and a P-1 peristaltic pump for loading samples on a preparative scale. Analysis of the conjugate mixtures was performed on a prepacked Pharmacia Mono-S HR 5/5 strong cation-exchange column (50 x 5 mm I.D.). Large scale purification was carried out with a Pharmacia HR 16/50 (500 x 16 mm I.D.) column packed with Pharmacia S-Sepharose (fast-flow) cation exchange resin and a 150 x 16 mm I.D. column which was prepacked with Pharmacia hydrophobic-exchange Butyl-Sepharose resin. All chromatography procedures were carried out at room temperature and the elution gradient and buffers specific to each column are described in the figure legends. All buffers were prepared fresh and filtered and degassed using 0.22 μm type GV filter membranes (Millipore Corporation, Ireland) before use. Prior to injection or loading, each sample was also filtered using 0.22 μm type GV type filter membranes. The sample elution profile was recorded using a 280 nm single path UV-1 monitor coupled to a two-channel Pharmacia chart recorder. Fractions of column eluent were collected from the S-Sepharose and Butyl Sepharose separations using a Pharmacia Frac-100 fraction collector and the absorbance of individual fractions (where required) at 280 nm was recorded using a Hewlett Packard 8452A diode array spectrophotometer in quartz cuvettes.

Flash column chromatography was carried out using Silica gel 60 (230 - 400 mesh ASTM) (Scharlau Chemie, Spain). Disposable Sep-Pak Plus C-18 columns used in the preparation of testosterone-17β-glucuronide were purchased from Waters Corporation (Massachusetts, USA). Thin layer chromatography (TLC) was performed using precoated, aluminium backed silica gel-60 (0.2 mm) sheets with fluorescent indicator UV_{254} (Alugram). Melting points were determined on a Reichert (Austria) microscope hot plate apparatus, and are uncorrected.

Hen egg white lysozyme conjugates were concentrated on a large scale using Macrosep centrifugal concentrators, molecular weight cut-off (MWCO) 10 K (Filtron Technology Corporation Massachusetts, USA). Small aliquots of the conjugates were concentrated and dialysed for mass spectral analysis using Centricon centrifugal filter devices, Millipore Corporation (Bedford, USA). Immunogen conjugates were partially purified using Pharmacia PD-10 columns (5 cm, 9.1 mL capacity) pre-packed with Sephadex G-25 M. Centrifugation of large sample volumes was carried out using a Sorval Dupont RC-5B refrigerated centrifuge.

Smaller samples were centrifuged with a Heraeus Biofuge Pico bench-top centrifuge in microcentrifuge tubes. Small diameter dialysis tubing (MWCO 10 K) was obtained from USB (Chicago, Illinois), and large diameter dialysis tubing (MWCO 10 K) was obtained from the Scientific Institute Centre (London, England).

Electrospray mass spectral (ESMS) data were obtained using a Micromass ZMDESMS Quadrupole Spectrometer. Matrix assisted laser desorption mass spectra of the lysozyme conjugates were obtained on a Micromass MALDI-LR spectrophotometer in linear mode. ^{1}H nuclear magnetic resonance (^{1}H NMR) data were measured using a 400 MHz Bruker Advance spectrophotometer using deuterated methanol (CD_3OD) as the internal standard and a 270 MHz JEOL GX-270 spectrometer using deuterated chloroform ($CDCl_3$) as internal standard. Chemical shift values (δ_H) are expressed in ppm relative to the internal standard. The notation used is s = singlet, d = doublet, dd = double doublet, t = triplet and m = multiplet. Coupling constants (J) are recorded in Hertz (Hz).

2.2.2 Reagents

D-glucurono-6,3-lactone, deuterated methanol (CD_3OD) and deuterated chloroform ($CDCl_3$) were obtained from Merck-Schuchardt (Darmstadt, Germany). Hydrogen bromide (hydrobromic acid) 33 wt% solution in glacial acetic acid was obtained from Acros Organics (New Jersey, USA). Urea and acetic anhydride were obtained from BDH Laboratory Supplies (Poole, England). Sodium (laboratory grade) was obtained from Hopkins and Williams (Essex, England) and the perchloric acid (70% w/w) from AJAX chemicals (Auburn, NSW, Australia). L-lysine monohydrochloride, L-glutamic acid, sodium dodecyl sulphate (SDS), 2,4,6-trinitrobenzene 1-sulfonic acid (TNBS), Tween-80, thyroglobulin (from bovine thyroid), cadmium carbonate, testosterone, testosterone-17β-glucuronide, tetrahydrocortisone-3α-glucuronide and hen egg white lysozyme (grade VI), three times recyrstallised, dialysed and lyophilised) were obtained from Sigma Chemical Company (St. Louis, MO, USA). Coomassie Brilliant Blue G-250 and maleic acid were purchased from USB (Cleveland Ohio). Sodium hydrogen carbonate ($NaHCO_3$), sodium hydroxide (NaOH) and ammonium sulphate ($(NH_4)_2SO_4$, minimum assay 99.5%) were obtained from Scharlau Chemie (Barcelona, Spain). Sodium chloride (NaCl) was obtained from Prolabo (France). Tris(hydroxymethyl)-aminomethane (Tris), was obtained from Serva (New York).

N-hydroxysuccinimide (NHS) was obtained from United States Biochemical Corporation (USB) and subsequently purified via recrystallisation from ethanol/ethyl acetate (1:1), and dried *in vacuo* [130]. *N,N'*-Dicyclohexylcarbodiimide (DCC) was originally purchased from Merck (München, Germany) and purified as follows: Solid DCC was liquefied by gently heating a round bottom flask containing the DCC in a warm water bath. The dense liquid was then dissolved in CH_2Cl_2 and dried over powdered $MgSO_4$ for 4 hours. The solution was filtered and the CH_2Cl_2

removed on rotary evaporator, followed by vacuum distillation at ~0.6 mm, oil bath temperature 145 °C. *N,N*-Dimethylformamide (DMF) was dried for 24 hr over anhydrous calcium sulphate, distilled under reduced pressure (20 torr, collected at 56 °C) and stored over 4 Å molecular sieves. Anhydrous methanol was prepared as follows: Dry magnesium turnings (5 g) and iodine (0.5 g) were gently heated with 50 – 75 mL of methanol in a flask until the iodine was no longer visible and the magnesium turnings had dissolved, thus forming the methoxide. Additional methanol was added to bring the total volume in the flask to 1 L, and allowed to reflux for three hours before distillation.

All other chemicals and reagents were of analytical grade or higher and used without further purification. All water used was of Milli-Q grade.

Stock tris-maleate buffer (1 M) was prepared by mixing maleic acid (19.32 g), Tris (52.8 g), NaCl (34 g), Tween-80 (53.2 mL of a 1/100 dilution in Milli-Q water), and HCl (7.48 mL of concentrated acid) in approximately 900 mL of Milli-Q water. The pH was adjusted to pH 7.0 with 0.1 M NaOH as required and the total volume made up to 1 L. All tris-maleate buffers required were diluted from this stock accordingly.

2.2.3 Methodology

2.2.3.1 Synthesis of methyl 1,2,3,4 tetra-*O*-acetyl glucopyranuronate

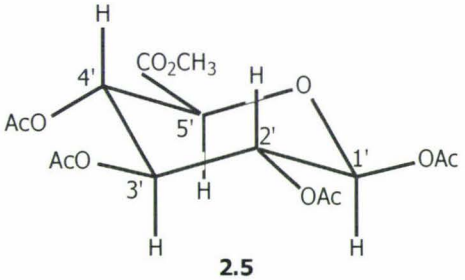

2.5

The title compound **2.5** was prepared from D-glucurono-6,3-lactone (commonly referred to as glucuronolactone in this thesis) according to the method of Bollenback *et al.* [131] with minor modifications. A solution of sodium methoxide was freshly prepared by dissolving sodium metal (0.27 g, 11.7 mmol) in anhydrous methanol (200 mL) on ice. Glucuronolactone (35.7 g, 0.2 mol) was added slowly to the sodium methoxide solution with continuous stirring until all the lactone had dissolved. The methanol was then removed from the resulting bright yellow solution by rotary evaporation (10 - 12 mm, water bath temperature ≤ 40 °C) affording the crude methyl glucopyranuronate as a yellow foam and a residual orange syrup. Acetic anhydride (138 mL, 1.46 mol) was added dropwise to the crude product over a period of one hour with regular shaking of the flask to redissolve the solid. A solution of perchloric acid (0.6 mL, 70% w/w, 7.11 mmol) was diluted with acetic anhydride (20 mL) and added to the crude product via a pressure equalizing funnel over approximately half an hour. The reaction mixture

was then stirred gently for ~16 hrs at 4 °C. A further 0.2 mL of perchloric acid (70% w/w 2.37 mmol) was then added and the reaction mixture was allowed to stand overnight at 4 °C. The resulting crude crystals of acetylated sugar were filtered from the orange/brown mother liquor using a sintered glass funnel and washed with diethyl ether (~20 mL). Recyrstallisation from absolute ethanol afforded methyl 1,2,3,4-tetra-*O*-acetyl glucopyranuronate crystals as colourless needles (29.5 g, 78.4 mmol, 39%), mpt 175 - 177 °C, literature mpt 176.5 – 178 °C [131]; ^{1}H NMR (270 MHz, $CDCl_3$): δ_H 2.07 (s, 3H, $OCOCH_3$), 3.69 (s, 3H, $COOCH_3$), 4.13 (d, 1H, J = 9.45 Hz, H-5'), 5.30 - 5.06 (m, 3H, H2', H3', H4'), 5.72 (d, 1H, J = 7.69 Hz, H1').

2.2.3.2 Synthesis of methyl-1-bromo-1-deoxy-2,3,4-tri-*O*-acetyl-α-D-glucopyranuronate

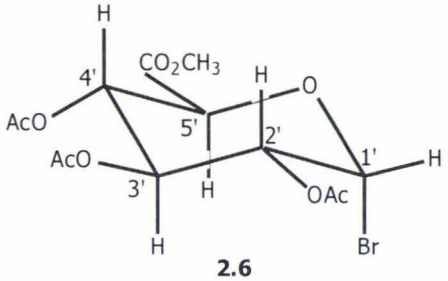

2.6

Methyl tetra-*O*-acetyl α-glucopyranuronate **2.5** (7.05 g, 18.7 mmol) was dissolved in hydrogen bromide solution (33% w/v in acetic acid, 28mL) and stirred gently at 35 - 40 °C (water bath) for 15 minutes, followed by overnight stirring at 4 °C. The acetic acid and unreacted HBr were removed under reduced pressure (10 - 12 mm, water bath ≤ 50 °C), giving a brown syrup which was redissolved in chloroform (35 mL) and washed with aqueous saturated sodium bicarbonate (2 x 35 mL), water (1 x 35 mL) and brine (1 x 28 mL). The chloroform layer containing the bromosugar was collected and dried over sodium sulphate for several hours before the chloroform was removed by rotary evaporation to give the crude bromosugar as a thick syrup. The crude product was recrystallised twice from absolute ethanol to afford methyl 1-bromo-1-deoxy-2,3,4-tri-*O*-acetyl-α-D-glucopyranuronate **2.6** as a white crystalline solid (5.19 g, 70%, 13.1 mmol), mpt 104 - 106 °C, literature mpt 106 – 107 °C [131]. ^{1}H NMR (270 MHz, $CDCl_3$): δ_H 2.06 (s, 3H, $OCOCH_3$), 2.07 (s, 3H, $OCOCH_3$), 2.12 (s, 3H, $OCOCH_3$), 3.78 (s, 3H, $COOCH_3$), 4.58 (d, 1H, J = 10.31 Hz, H5'), 4.86 (dd, 1H, J = 9.99, 4.05 Hz, H2'), 5.23 (t, 1H, J = 9.73 Hz, H3'), 5.62 (t, 1H, J = 9.75 Hz, H4'), 6.65 (d, 1H, J = 3.97 Hz, H1').

2.2.3.3 Synthesis of methyl 3-oxoandrost-4-en-17-yl, 2',3',4'-tri-*O*-acetyl-β-D-glucopyranosiduronate.

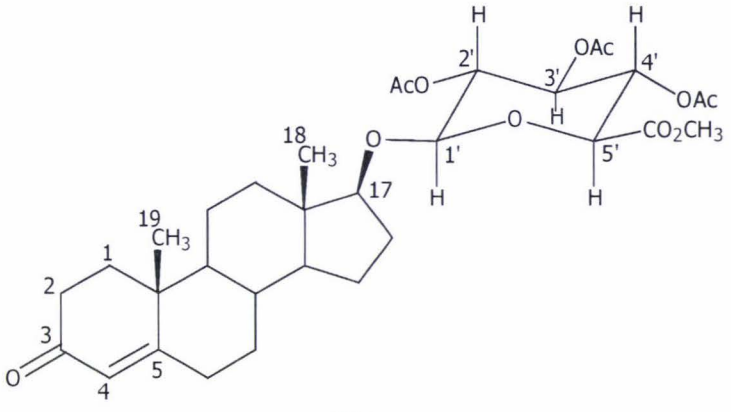

2.7

The title compound **2.7** was synthesised by coupling commercially available testosterone with methyl 1-bromo-1-deoxy-2,3,4-tri-*O*-acetyl-α-D-glucopyranuronate **2.6** (molar ratio of testosterone:bromosugar 1:2.9) as follows: Dried cadmium carbonate (1.47 g, 8.43 mmol) was added to a solution of testosterone (730.6 mg, 2.53 mmol) in anhydrous toluene (146 mL), and the suspension was concentrated to approximately 94 mL by distillation to remove residual moisture. After distillation, a solution of bromosugar (2.94 g, 7.41 mmol), in anhydrous toluene (50 mL) was added using a pressure equalising funnel, keeping the addition rate the same as the distillation rate. The solution was then refluxed for 24 hours, during which time the solution colour changed from tan to bright turquoise and finally pale bottle green. The reaction progress was monitored by thin layer chromatography (TLC) against a sample of known testosterone glucuronide triacetate methyl ester dissolved in acetone. The TLC plate was run using a 3:7 mixture of acetone:hexane and developed by immersing the plate in Kober reagent (90% ethanol, 10% concentrated H_2SO_4) followed by heating at 120 °C for 10 minutes. When the TLC plate of the reaction mixture showed that free testosterone was no longer present, the $CdCO_3$ was removed by filtration through a celite pad which was then washed with dichloromethane. The combined filtrate and washings were washed with water (30 mL), dried over anhydrous sodium sulphate and concentrated under reduced pressure (water bath temperature ≤ 40 °C). The crude sample was then redissolved in hexane and loaded onto a Silica gel 60 (230 - 400 mesh) flash column (dimensions 17 cm x 2 cm I.D.). The product was eluted using a step-wise gradient of 100 mL of 20%, 30%, 40%, 50% and finally 55% ethyl acetate in hexane pumped through the column using a hand-operated air pump. Multiple fractions (each 10 - 12 mL) of the eluent were collected and those fractions containing the product (identified by TLC as fractions containing 50 – 55% ethyl acetate in hexane; TLC mobile phase acetone:hexane 3:7, developed using Kober reagent as described above) were pooled and concentrated under reduced pressure (10 - 12 mm, water bath ≤ 40 °C) to afford a pale yellow syrup. The product was then purified further by firstly dissolving it in acetone (10 mL), and pouring it into water (40 mL) followed by stirring the resulting solution rapidly on ice

for one hour. The solution was then left to stand at 4 °C overnight resulting in a white amorphous solid, which was filtered and washed with a small amount of water. The crude product was recrystallised in $MeOH/H_2O$, by firstly redissolving the solid in a small amount of methanol by gentle heating and allowing the solvent to cool to room temperature before adding water (20 mL) to precipitate methyl-3-oxoandrost-4-en-17yl, 2',3',4'-tri-*O*-acetyl-β-D-glucopyranosiduronate **2.7** as a white solid in 39% yield (602.7 mg). ^1H NMR (270 MHz, $CDCl_3$): δ_H 0.74 (s, 3H, CH_3-18), 1.17 (s, 3H, CH_3-19), 2.00 and 2.03 (s, 3H, H2', 3', 4' – $OCOCH_3$), 3.57 (t, 1H, H17α), 3.74 (s, 3H, CO_2CH_3), 3.98 (d, J = 8.79 Hz, 1H, H5'), 4.59 (d, J = 7.69 Hz, 1H, H1'), 4.99 (t, 1H, H2'), 5.15 - 5.27 (m, 2H, H3' and H4'), 5.71 (s, 1H, H4). ES/MS m/z: found 605.5 (MH^+), MH^+ for $C_{32}H_{45}O_{11}$ requires 605.7; found 627.4 (MNa^+), MNa^+ for $C_{32}H_{45}O_{11}Na$ requires 627.7.

2.2.3.4 Synthesis of 3-oxoandrost-4-en-17-yl, β-D-glucopyranosiduronic acid

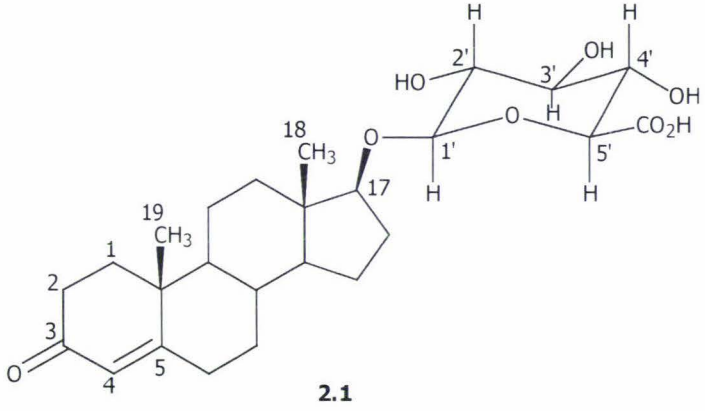

2.1

In the next step of the synthesis, sodium hydroxide (3.77 mL, 0.5 M), was added dropwise to a solution of compound **2.7** (227.3 mg, 0.38 mmol) dissolved in methanol (25 mL) at room temperature (molar ratio of ester:NaOH, 1:5). When TLC (solvent system 1:1 ethyl acetate:hexane, developed using Kober reagent as described in section 2.2.3.3) indicated that the starting material was no longer present, the solution was titrated to pH 8 with 0.5 M HCl and rotary evaporated to dryness to afford a large amount of a creamy white solid. The solid was then redissolved in water (25 mL) and titrated to pH 2.5 with 0.25 M HCl to give the free acid form of the glucuronide.

The product was then partially purified by passing the glucuronide solution (~26 mL) through a disposable C-18 Sep-pak cartridge, which had been pre-equilibrated by sequential washing with methanol (2 mL), 50% aqueous methanol (5 mL) and water (5 mL). The sample was passed through the column by gravity filtration, after which the residual sodium chloride was removed by washing the cartridge with water (2 mL). The product was then eluted with 70% aqueous methanol (6 mL) and taken to dryness on a rotary evaporator to give a pale yellow oil. The product was then precipitated by addition of diethyl ether (10 mL) to the flask, and the solid

isolated by filtration and washed with a small amount of cold methanol. Recystallisation of the crude product from 50% aqueous methanol afforded 3-oxoandrost-4-en-17-yl, β-D-glucopyranosiduronic acid **2.1** as a white crystalline solid (62.1 mg, 35.6%) mpt = 170 – 172 °C (literature mpt 182.0 - 183.5 °C [132]). ^{1}H NMR (400 MHz, CD_3OD): δ_H 0.80 (s, 3H, CH_3-18), 1.14 (s, 3H, CH_3-19), 3.11 (t, 1H, H2'), 3.37 - 3.39 (m, 2H, H3' and H4'), 3.42 (d, J = 9.01 Hz, 1H, H5'), 3.62 (t, 1H, H17α), 4.27 (d, J = 7.80 Hz, 1H, H1'), 5.61 (s, 1H, H4). ES/MS m/z: found 465.27 (MH^+), MH^+ for $C_{25}H_{37}O_8$ requires 465.56.

2.2.3.5 Active ester conjugation of testosterone glucuronide and tetrahydrocortisone glucuronide with hen egg white lysozyme

a) Preparation of tetrahydrocortisone glucuronide-hen egg white lysozyme conjugates

Tetrahydrocortisone-3α-glucuronide (23.0 mg, 42.55 μmol) was dissolved in anhydrous DMF (150 μL) in a small vial to give a clear yellow solution. Fresh standard solutions of NHS and DCC were prepared by dissolving 30 - 35 mg of each reagent in the required amount of anhydrous DMF to give a 0.6 M solution. To the solution of THEG was added NHS (92.2 μL of the 0.6 M stock solution, 55.3 μmol), followed by DCC (92.2 μL of 0.6 M stock solution, 55.3 μmol). The resulting solution was mixed by gently shaking the vial sideways and left to stand at room temperature for 2 hours. After one hour, crystals of dicyclohexyl urea (DCU) were observed indicating the active ester of THEG had formed. The solution containing the *N*-hydroxysuccinimide ester of THEG was then slowly added drop-wise with constant stirring to a solution of HEWL (0.405 g, 28.32 μmol) in 1% $NaHCO_3$ (10.1 mL, pH 9) on ice (THEG:HEWL molar ratio 1.5:1). The mixture was stirred gently overnight at 4 °C, and dialysed against Milli-Q water (5 x 1 L) at 4 °C. A small aliquot (100 μL) of the conjugate mixture was then removed for ion exchange analysis (see section 2.2.3.6) and the remainder was stored at –20 °C.

b) Preparation of testosterone glucuronide-hen egg white lysozyme conjugates

TG-HEWL conjugates were prepared in the same manner described for the THEG-HEWL conjugates above using the following quantities of reagents and solutions: TG (15.1 mg, 32.5 μmol) was dissolved in anhydrous DMF (150 μL) to give a slightly opaque solution. NHS (70.4 μL of 0.6 M stock, 42.2 μmol) followed by DCC (70.4 μL of 0.6 M stock, 42.2 μmol) was added to the TG solution vial with gentle mixing and left to stand for two hours. After one hour, crystals of DCU could be observed indicating that formation of the TG active ester had been successful. The solution of TG active ester was then added slowly dropwise to a solution of HEWL (0.31 g, 21.7 μmol in 7.75 mL of 1% $NaHCO_3$, pH 9) on ice with constant stirring (TG:HEWL molar ratio 1.5:1). The resulting conjugate solution was then dialysed and stored as described for the THEG-HEWL conjugates above.

2.2.3.6 Mono-S cation-exchange chromatography of TG-HEWL and THEG-HEWL conjugates

The success of each steroid glucuronide–lysozyme coupling reaction was checked by cation-exchange chromatography on a Mono-S HR 5/5 column in 7 M urea [113]. To prepare the samples for analysis, an aliquot (100 μL) of dialysed conjugate mixture was diluted with 800 μL of the equilibrating buffer (buffer A) and filtered through a 0.2 μm PVDF Phenomenex membrane. An aliquot (100 μL) of the filtered solution was then manually injected onto the Mono-S column pre-equilibrated with buffer A. The chromatographic conditions used were: flow rate 0.5 mL/min; chart recorder speed 0.2 cm/min; UV absorption of eluent monitored at 280 nm. Mobile phase buffer A; 420.42 g urea/L (7 M), 7.8 g $NaH_2PO_4.2H_20$/L (50 mM) adjusted to pH 6 with 1 M NaOH. Buffer B; buffer A + 58.5 g/L NaCl (1 M) adjusted to pH 6 with 1 M NaOH. Elution of the sample was affected by increasing the relative percentage of sodium chloride elution buffer (buffer B) as follows: 0% B for 5 mins, 0 - 30% B in 40 min, 30 - 100% B in 5 min. Between injections the column was washed with 100% B for 15 - 20 mins, then 0% B for 10 mins to re-equilibrate the column.

2.2.3.7 S-Sepharose fast-flow purification of TG and THEG-HEWL conjugates

Selected THEG-HEWL and TG-HEWL conjugates were purified from the dialysed conjugate mixture by cation-exchange chromatography on a preparative scale using a Pharmacia S-Sepharose (fast-flow) column. The chromatographic conditions used were as follows: flow rate 1.5 mL/min; chart speed 0.2 cm/min; UV absorption of eluent monitored at 280 nm. Mobile phase buffer A; 420.42 g urea/L (7 M), 7.8 g $NaH_2PO_4.2H_20$/L (50 mM) adjusted to pH 6 with 1 M NaOH. Buffer B; buffer A + 58.5 g/L NaCl (1 M) adjusted to pH 6 with 1 M NaOH.

Before loading the conjugate mixture, sufficient solid urea and sodium dihydrogen phosphate dihydrate were added to give a 7 M urea, 50 mM phosphate solution. The pH of each solution was adjusted to 6.0 with 1 M NaOH, filtered through a 0.22 μM (Millipore) type GV filter and loaded onto the S-Sepharose column (pre-equilibrated with buffer A) using a peristaltic pump. The sample was eluted using a linear salt gradient from 0 M to 1 M NaCl in 810 minutes as follows: 0 - 21% B in 693 min, 21% B for 90 min, 21 - 100% B in 27 min, 100% B for 90 min, 100 - 0% B in 20 min. Fractions of eluent (6 mL) were collected every 4 minutes, and the absorbance at 280 nm of each fraction recorded using a Shimadzu UV spectrophotometer. The required peak fractions were pooled and dialysed against MQ water (5 x 2 L changes) and stored at -20 °C until required.

2.2.3.8 Butyl Sepharose hydrophobic interaction chromatography of the TG-HEWL and THEG-HEWL conjugate fractions

The final step in the purification of the TG-HEWL and THEG-HEWL conjugates involved passing the pooled S-Sepharose (fast-flow) fractions down a Butyl Sepharose hydrophobic-interaction column. To prepare the conjugate samples for loading, sufficient solid ammonium sulphate and sodium dihydrogen phosphate dihydrate were added to give a 1.4 M $(NH_4)_2SO_4$, 50 mM NaH_2PO_4 solution. Each conjugate solution (sample size 15 - 40 mL) was adjusted to pH 6.6 with 1 M NaOH and filtered using a 0.22 μM (Millipore) type GV filter membrane before loading it onto the column pre-equilibrated with buffer A using a peristaltic pump. The gradient conditions used to elute the different conjugate samples varied slightly and are recorded in the figure legends of the individual traces. The chromatographic conditions common to each separation were as follows: flow rate 1.4 mL/min, chart speed 0.1 cm/min. Buffer A: 50 mM sodium dihydrogen phosphate dihydrate, 1.4 M ammonium sulphate adjusted to pH 6.6 with 1 M NaOH; buffer B: 50 mM sodium dihydrogen phosphate dihydrate titrated to pH 6.6 with 1 M NaOH.

The absorbance at 280 nm of each fraction (collected every 4 minutes), was recorded using a Shimadzu UV spectrophotometer. Selected peak fractions were then pooled and dialysed against MQ water (6 x 1 L changes at 4 °C) and concentrated by Macrosep centrifugal concentrators (MWCO 10 K membrane). An aliquot of each dialysed conjugate (150 μL) was removed for Mono-S analysis to check each conjugate for the presence of HEWL as described in section 2.2.3.6. The remaining volume of each conjugate was then diluted 1:1 with 0.7 M tris-maleate buffer (pH 7.0) to adjust the final buffer concentration to 0.35 M tris-maleate pH 7.0, and stored at –20 °C until required.

2.2.3.9 MALDI mass spectrometry of TG-HEWL and THEG-HEWL conjugates

In order to obtain MALDI mass spectra of the conjugates and native lysozyme it was first necessary to concentrate the samples and remove the buffer salts (0.35 M tris maleate) in which they were stored. Prior to analysis, aliquots (400 - 700 μL) of each purified HEWL conjugate were dialysed against MQ water (2 mL x 8 changes) and concentrated (final volume ~ 45 - 95 μL) using Centricon YM-10 filter tubes centrifuged at 5000 rpm for 40 - 60 mins at 5 °C. An aliquot of the dialysed sample was also used for determination of the protein concentration of each conjugate by Coomassie assay in section 2.2.3.10.

2.2.3.10 Coomassie protein assay for determination of lysozyme concentration of the TG-HEWL and THEG-HEWL conjugate solutions.

The dialysed samples used to obtain a mass spectrum of the conjugates were also used to estimate the concentration of HEWL in each conjugate solution by Coomassie assay. Dialysis of the conjugates before protein determination was necessary since the 0.35 M tris-maleate buffer the conjugates were stored in reacted with the protein reagent to give a high background absorbance (i.e. very high blank readings).

The Coomassie Blue protein reagent was prepared according to the method of Bradford [133] by dissolving Coomassie Blue G250 (100 mg) in 95% ethanol (50 mL). To this solution was added 85% phosphoric acid (100 mL) and distilled water to make the total volume up to 1 L. After thoroughly mixing, the solution was transferred to an amber bottle for storage at 4 °C. Immediately before use the solution was filtered through Whatman no. 1 filter paper to remove any precipitated dye.

The standard samples for generation of the standard curve were prepared by pipetting 0 - 20 μL of a HEWL stock solution (200 μg mL^{-1} in MQ water) into three separate wells of an ELISA plate and making the total volume in each well up to 20 μL with Milli-Q water. Samples of the conjugates were diluted between 1/15 and 1/60 with water and 5 μL of each were added to three separate wells and diluted to 20 μL with water alongside the standards. Protein reagent (200 μL) was then added to each well and mixed using the ELISA plate reader medium intensity "shake" function (2 x 5 seconds). After standing at room temperature for 15 minutes the absorbance of each solution was recorded at 595 nm and plotted as a function of the HEWL concentration (μM) using GraphPad Prism (version 2.00) software. The standard curve was generated from the data points using non-linear regression analysis and the HEWL concentration in each sample was obtained from the curve by the fitting program.

2.2.3.11 Preparation of TG-thyroglobulin and THEG-thyroglobulin immunogen conjugates

Testosterone glucuronide (TG) and tetrahydrocortisone glucuronide (THEG) were conjugated to the lysine groups of the carrier protein thyroglobulin (THY) using the *N*-hydroxysuccinimide (NHS)/dicyclohexylcarbodiimide (DCC) coupling method [55] for use as immunogens to raise anti-TG and anti-THEG antibodies in New Zealand white rabbits. All reagents and glassware used to prepare the *N*-hydroxysuccinimide steroid esters were thoroughly dried before use, and the stock solutions of DCC and NHS (each 0.6 M) were prepared as for the previous active ester TG-HEWL and THEG-HEWL couplings described in section 2.2.3.5.

(a) Preparation of testosterone glucuronide-thyroglobulin immunogen conjugates

Testosterone glucuronide (6.9 mg, 14.85 μmol) was dissolved in anhydrous DMF (70 μL) in a small vial to give a slightly opaque solution. To this solution was added NHS (32.2 μL of 0.6 M stock solution, 19.32 μmol), followed by DCC (32.2 μL of 0.6 M stock solution, 19.32 μmol). The resulting solution was mixed by gently shaking the vial sideways and left to stand at room temperature for 2 hours. After one hour, crystals of dicyclohexyl urea (DCU) were observed indicating the active ester of TG had formed. The solution containing the *N*-hydroxysuccinimide ester of TG was then added slowly drop-wise with constant stirring to a solution of thyroglobulin (100 mg, 151.5 nmol) in 1% $NaHCO_3$ (2.5 mL, pH 9.3) on ice (TG:THY molar ratio 98:1). The addition of each drop of active ester solution was associated with the formation of a small amount of white precipitate. Once all the active ester solution had been added, the mixture was stirred for a further 40 minutes and dialysed at 4 °C against Milli-Q water (4 x 1 L), followed by 0.01 M NaCl (2 x 1 L). After dialysis the immunogen solution was centrifuged (6000 rpm for 90 minutes at 4 °C) in order to remove the precipitated protein from the previous stage. As a final purification step to remove unreacted reagents, the dialysed immunogen solution was passed through a Pharmacia PD-10 column (prepacked with Sephadex G-25 M) which had been pre-equilibrated with 25 mL of 0.01 M NaCl. Each sample was eluted from the PD-10 column with 3.5 mL of 0.01 M NaCl and divided into 0.5 mL aliquots for storage at –20 °C.

(b) Preparation of tetrahydrocortisone glucuronide-thyroglobulin immunogen conjugates

THEG-THY conjugates were prepared in the same manner as described for the TG-THY conjugates using the following quantities of reagents and solutions: Tetrahydrocortisone glucuronide (8.0 mg, 14.80 μmol) was dissolved in anhydrous DMF (50 μL) in a small vial to give a clear yellow solution. To this solution was added NHS (32.1 μL of 0.6 M stock solution, 19.26 μmol), followed by DCC (32.1 μL of 0.6 M stock solution, 19.26 μmol). The remaining procedure was then carried out as described for testosterone glucuronide above (THEG:THY molar ratio 98:1)

2.2.3.12 Coomassie protein assay for determination of thyroglobulin concentration in TG-thyroglobulin and THEG-thyroglobulin immunogen solutions.

The thyroglobulin concentration in each immunogen solution was determined by Coomassie assay based on the method of Bradford [133] essentially as described in section 2.2.3.10 with the following exceptions: The thyroglobulin standards were prepared by pippetting 0 - 200 μL of a 100 μg mL^{-1} thyroglobulin solution in 0.01 M NaCl into duplicate microcentrifuge tubes, and making the total volume up to 200 μL with 0.01 M NaCl. Aliquots of each immunogen (60, 100 and 200 μL) were also prepared in duplicate and made up to 200 μL with 0.01 M NaCl

alongside the standards. Protein reagent (1 mL) was then added to the samples and standards and mixed with the protein solution by gentle inversion of each tube. After standing at room temperature for 15 minutes, 200 μL of each standard and sample was autopipetted into the wells of an ELISA plate and the absorbance of each solution at 595 nm was obtained as described in section 2.2.3.10.

2.2.3.13 Characterisation of TG-thyroglobulin and THEG-thyroglobulin immunogen conjugates

(a) UV difference spectroscopy to determine the hapten:carrier ratio.

Solutions of TG-THY, THEG-THY conjugates and free THY (each containing 123.5 nM thyroglobulin according to the Coomassie protein assay in section 2.2.3.12) were prepared by dilution with 0.01 M NaCl. Reference solutions of tetrahydrocortisone glucuronide (197.31 μM in 0.01 M NaCl) and testosterone glucuronide (50.23 μM in 0.01 NaCl containing 2% MeOH) were also prepared to determine the extinction coefficients of each steroid at selected wavelengths. The ultraviolet spectrum of each sample was recorded using a Hewlett Packard UV spectrophotometer, and the difference spectrum attributed to the steroid moiety was obtained by subtracting the spectrum of unconjugated THY from that of each steroid glucuronide-thyroglobulin conjugate. In each case the spectrophotometer was zeroed using the buffer in which the protein was dissolved as a blank.

(b) Trinitrophenylation procedure to determine the hapten:carrier ratio

The number of steroid residues coupled to thyroglobulin was estimated by the method of Shashidar *et al.* [126] with some modifications. Aliquots of L-lysine hydrochloride, L-glutamic acid (containing 0 - 8 μg amino acid), thyroglobulin and thyroglobulin conjugate (both 128.7 μg thyroglobulin) in 4% $NaHCO_3$ (pH 8.5) were diluted with additional 4% $NaHCO_3$ solution to a total volume of 1 mL. Freshly prepared TNBS (0.5 mL, 0.1%) was added to each sample with vortex mixing and the reaction was carried out by incubating the tubes in a water bath at 42.5 °C for 3 hours. Following incubation 10% aqueous SDS (0.5 mL) and HCl (0.25 mL, 0.1 N) were added with vortex mixing, and the absorbance of each solution was recorded at 336 nm using a Hewlett Packard UV spectrophotometer after appropriate blank corrections. The number of free ε-amino groups present in the carrier protein and hapten-protein conjugates was directly determined from a standard curve generated from the difference in the absorbance at 336 nm for TNP-L-lysine and TNP-L-glutamic acid standards (0 – 24.4 μM). The percent conjugation of hapten to protein was calculated using the Equation 2.1.

$$\% \text{ conjugation} = \frac{\text{conc. of } \varepsilon\text{-amino group in carrier protein} - \text{conc of } \varepsilon\text{-amino group in hapten protein conjugate)}}{\text{conc. of } \varepsilon\text{-amino group in carrier protein}} \times 100$$

Equation 2.1

2.3 Results and discussion

2.3.1 Synthesis of the glycosyl donor α-bromosugar

The glycosyl halide donor α-bromosugar (methyl 1–bromo-1-deoxy-2,3,4-tri-*O*-acetyl-α-D-glucopyranuronate) **2.6** was synthesised from glucuronolactone **2.8** in three steps as outlined in Scheme 2.2.

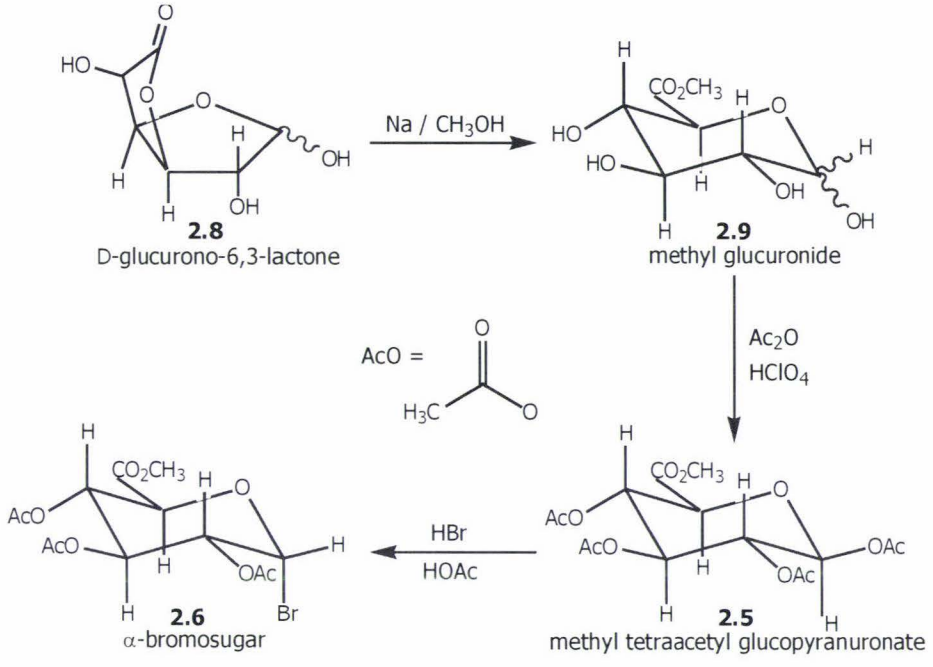

Scheme 2.2 Synthesis of methyl 1,2,3,4-tetra-*O*-acetyl glucopyranuronate (acetylated sugar) and 1-bromo-1-deoxy-2,3,4-tri-*O*-acetyl-α-D-glucopyranuronate (bromosugar) from D-glucurono-6,3-lactone.

The first step involves the opening of the lactone ring of **2.8** by nucleophillic attack of methoxide (generated *in situ* by dissolving sodium metal in anhydrous methanol) to give the methyl ester. In the second step acid catalysed acetylation of the four remaining alcohol functional groups of **2.9** afforded the methyl tetra-acetylated glucopyranuronate ester **2.5** as white needles (29.5 g, 39%, mpt 175 – 177 °C, literature mpt 176.5 – 178 °C [131]). In the product forming step, bromine was incorporated at the anomeric centre (C1′) by reaction of the acetylated sugar **2.5** with hydrogen bromide (33%) in glacial acetic acid to afford methyl 1-bromo-1-deoxy-2,3,4-tri-*O*-acetyl-α-D-glucopyranuronate **2.6** as a white crystalline solid (5.19 g, 70%, mpt 104 – 106 °C, literature mpt 106 – 107 °C [131]).

Proton nmr of the tetracetylated sugar **2.5** confirmed that a β-configuration could be assigned to the anomeric centre on the carbohydrate ring. Because the anomeric carbon (C1′) is directly linked to two electron withdrawing oxygen atoms the anomeric proton (H1′) is strongly deshielded, thus it has a higher chemical shift value (5.72 ppm) than that of the 5-proton (H5′, 4.13 ppm) since C5′ is only linked directly to one oxygen atom. The H1′ coupling constant

($^3J_{H1',H2'}$ = 7.69 Hz) was also characteristic of an axial-axial coupling of H1′ and H2′, and is consistent with that of β-glucose where the OH group is in the equatorial configuration [134]. The coupling constant $^3J_{H1',H2'}$ expected for an axial-equatorial coupling in α-glucose is much smaller, typically 3.7 Hz [134].

The H1′ and H5′ protons of the α-bromosugar **2.6** can also be assigned unambiguously for the same reason. In the bromosugar the anomeric carbon (C1′) is directly linked to two electron withdrawing atoms (an oxygen and a bromine atom), while the C5′ carbon is directly linked to only one oxygen atom. As a result, the anomeric proton (H1′, 6.65 ppm) has a higher chemical shift value compared to the 5′-proton (H5′, 4.58 ppm). The H1′ and H5′ protons in the nmr of the bromosugar can also be distinguished from the 2′, 3′ and 4′ protons on the basis of their splitting patterns. Protons H1′ and H5′ both appear as doublets in the nmr due to splitting by a single neighbouring proton (H2′ for H1′, and H4′ for H5′), whereas protons 2′, 3′ and 4′ appear either as triplets or a doublet of doublets due to splitting from two neighbouring protons (H1′ and H3′ for H2′; H2′ and H4′ for H3′; H3′ and H5′ for H4′). The small coupling constant of the H1′ proton with H2′ in the bromosugar ($^3J_{H1',H2'}$ = 3.97 Hz) indicated an axial-equatorial relationship between protons H1′ and H2′, confirming an α-orientation of the bromine atom.

2.3.2 Koenigs-Knorr synthesis of testosterone glucuronide

Testosterone-17β-glucuronide **2.1** was synthesised using commercially available testosterone in a three step process under Koenigs-Knorr conditions using an overall molar ratio of testosterone:bromosugar:cadmium carbonate of 1:2.9:3.3 (see Scheme 2.3). The reaction was driven forward by the addition of excess bromosugar (2.9 molar equivalents) dissolved in anhydrous toluene to ensure that the majority of testosterone had reacted, thus simplifying the purification of the desired β-glucuronide conjugate from the reaction mixture. Any residual moisture from the glassware and water formed during the reaction was removed by azeotropic distillation before adding the α-bromosugar and by maintaining the distillation rate equal to the addition rate of the bromosugar solution.

In the next step of the synthesis, the acetyl and methyl groups located at C2′, 3′, 4′ and 6′ of the testosterone glucuronide protected ester were hydrolysed using sodium hydroxide (i.e. a 4:5 molar ratio of hydrolysable groups to NaOH). The pH of the solution was then titrated to pH 8 and rotary evaporated to dryness to afford the sodium salt **2.11** as a creamy white solid. Finally, the free acid form of the glucuronide was obtained by titrating an aqueous solution of the sodium salt to pH 2.5. Despite the glycosidic bond (an acetal link) being acid sensitive, the glycoside bond of the steroid glucuronide is resistant to hydrolysis at this pH (at least for a short period of time) [135].

The yield (35.6%) of testosterone glucuronide obtained in this chapter was disappointingly low compared to that reported by similar methods in the literature ~60 - 75% [132]. This was in part due to the persistence of the final product as an oil, which proved difficult to recrystallise.

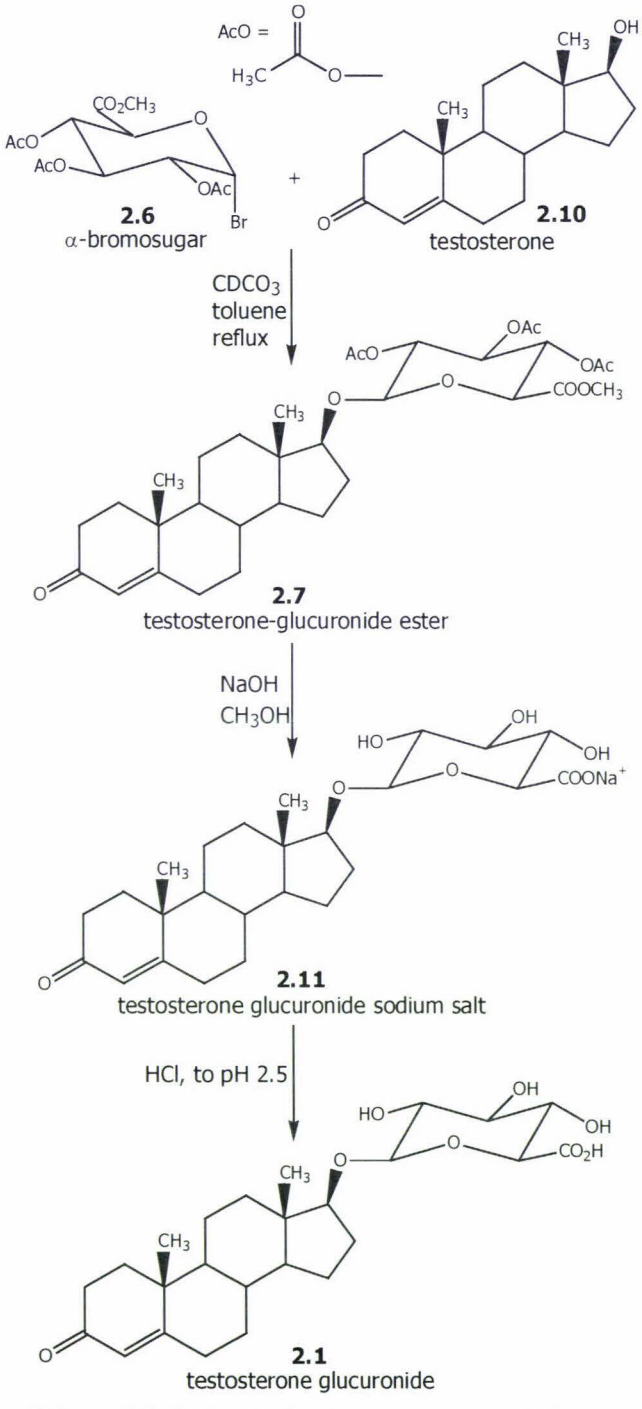

Scheme 2.3 Synthesis of testosterone glucuronide from α-bromosugar and testosterone

The batch of cadmium carbonate used may also have contributed to the reduced yield since the same batch gave variable yields during synthesis of estrone-glcuronide (E1G) conjugates during a parallel research project (K. Jayasundera personal communication). The yield of E1G was later found to improve when a second $CdCO_3$ batch was purchased, however due to the limited amount of testosterone available the testosterone glucuronide synthesis was not attempted here with the new $CdCO_3$. Similar problems with the efficacy of different $CdCO_3$ batches in Koenigs-Knorr condensations was noted as early as 1979 by Dick *et al.* [136] who observed large variation in the yield of phenol glycosides depending on the source and age of the $CdCO_3$. The authors also quantified the various by-products of the reaction (dehydrohalogenation and hydrolysis products) and found that product compositions could only be duplicated when the $CdCO_3$ was sieved to exclude particles larger than 100 mesh, thus confirming the earlier observation by Conrow and Berstein that the yields of glycosides are a function of the catalyst's surface area [137].

A simplified mechanism to account for the β-stereoselectivity of glycoside formation in the Koenigs-Knorr reaction is shown in Scheme 2.4. While the exact details of the mechanism are unclear [138,139] the fact that both the α- and β- stereoisomers of the bromosugar **2.6** give the same β-glycoside linkage suggests that both isomers react by a common pathway [140]. The initial rate-determining step is thought to involve heterolysis of the bromosugar carbon-bromide bond [139], which is assisted by the $CdCO_3$ (halide ion acceptor) and the driving force of the ring oxygen, to form a shielded carbocation **2.12**. This subsequently forms the 1,2-acyloxonium intermediate **2.13** by intramolecular reaction of the neighboring 2-*O*-acetyl group on C2' with the electron deficient C1' centre. Since the α-face is shielded by the acetoxonium group, nucleophillic attack of the hydroxyl group of the steroid with the acyloxonium ion is restricted to the β-face to give the desired β-isomer **2.14**.

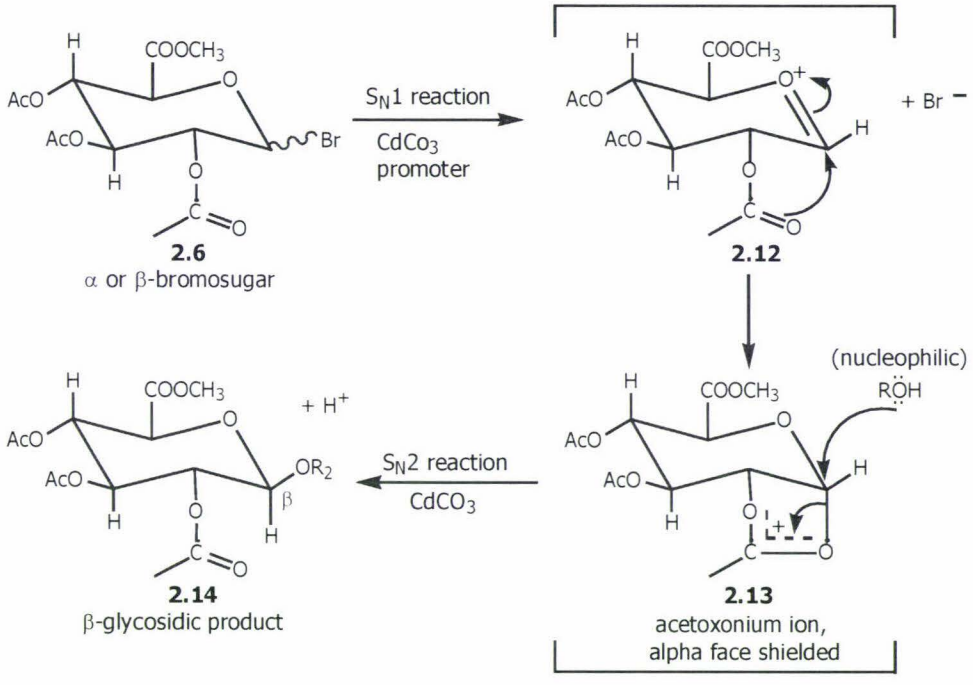

Scheme 2.4 Mechanism of the Koenigs-Knorr reaction [140].

Since the synthetic testosterone glucuronide prepared in section 2.2.3.4 was required for raising anti-testosterone antibodies, which would in turn specifically bind testosterone β-glucuronide excreted in urine, it was important to establish that the correct isomer had been synthesised. Although the melting point of the glucuronide was found to be approximately 12 °C lower than that reported in the literature [132], the 400 MHz ^{1}H NMR spectrum of the product (Figure 2.3) was consistent with that of commercially synthesised testosterone-17β-glucuronide (Sigma Chemical Co.). Hence this was considered to be adequate confirmation of the structural integrity of the final product.

In the steroid glucuronide the H1' and H5' protons of the glucuronide ring can also be assigned as described for the α-bromosugar. Since the anomeric carbon (C1') is linked directly to two oxygen atoms, whereas the C5' carbon is linked to only one oxygen atom, the anomeric proton

(H1', 4.27 ppm) has a higher chemical shift value than that of the 5'-proton (H5' 3.42 ppm). The large coupling constants for these two protons (H1' 7.80 Hz and H5' 9.01 Hz) were consistent with a *trans* configuration of the C1' and C2' protons, and hence by implication of the C4' and C5' protons of the glucoside ring, which confirmed that the sugar ring was in the chair conformation. The magnitude of the anomeric proton H1' coupling constant ($^3J_{H1',H2'}$ = 7.80 Hz) resulting from the axial-axial positioned hydrogens at C1' and C2' also confirms that the correct β-isomer (testosterone-17β-glucuronide) had been synthesised since the axial-axial arrangement of protons only permits an equatorial glycoside bond [141].

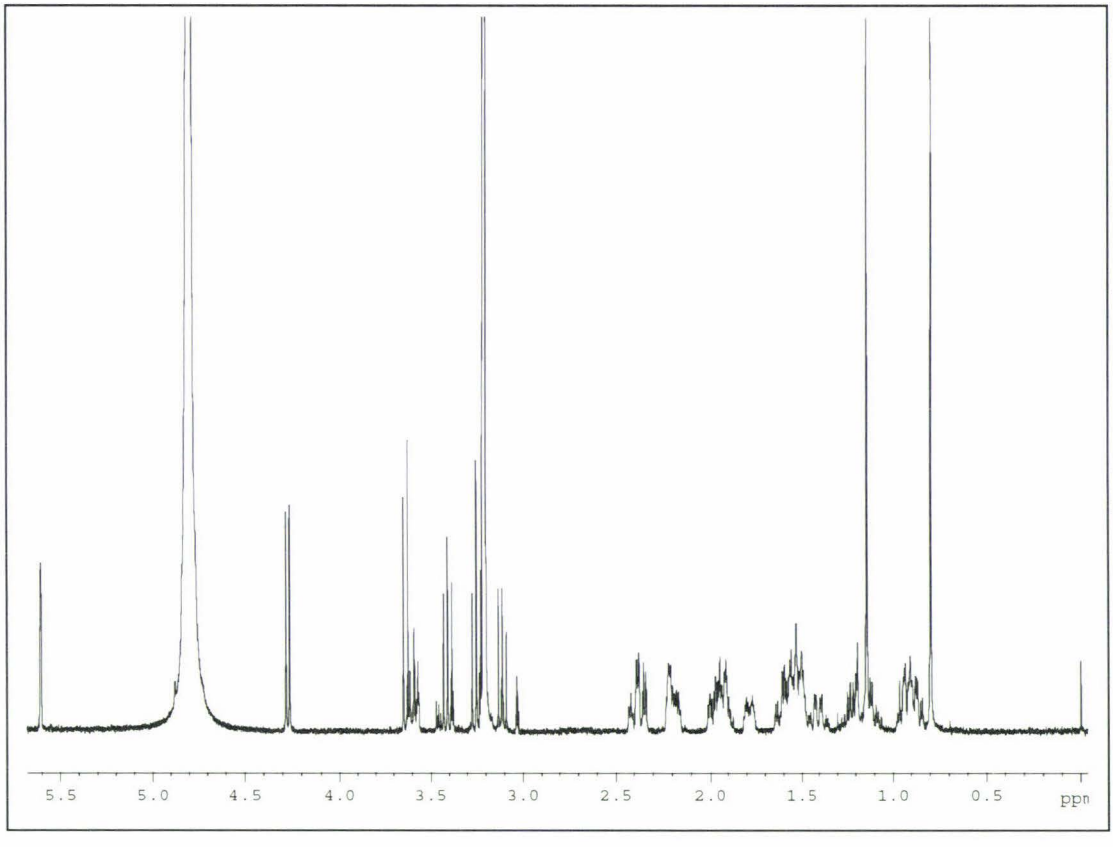

Figure 2.3 400 MHz ^{1}H nmr spectrum of testosterone-17β-glucuronide.

2.3.3 Alternatives to the Koenigs-Knorr reaction for the synthesis of aryl and alkyl glucuronides

The persistence of variable yields in the classical Koenigs-Knorr reaction and the requirement of at least equimolar amounts of bromosugar and $CdCO_3$ together with the problems associated with its disposal are major limiting factors for the large scale preparation of β-glucuronides. In addition, the strongly electron withdrawing character of the 6β-methoxycarbonyl group in acetyl protected glycosyl halides makes such species notoriously poor donors [142]. As a result, numerous other glycosyl donors and promoter systems have been evaluated and reviewed [3,143] for their effectiveness in glucuronidation reactions, a few examples of which are outlined below.

N-iodosuccinimide promoter systems for the glucuronidation of primary and secondary alcohols

Field and coworkers [144] employed the use of bromosugars in conjunction with iodine for the synthesis of simple alkyl glycosides as an alternative to the traditional Koenigs-Knorr method. Stachulski [143] recently evaluated this method for its use in the β-glucuronidation of primary and secondary alcohols. Using the bromosugar derivative **2.15** (see Scheme 2.5) in the presence of *N*-iodosuccinimide (NIS) as the promoter, the β-glucuronide isomer was produced exclusively in good yield (70 - 85%) where ROH was a primary alcohol, and in 50 - 65% yield from two secondary alcohols. By contrast, when IBr or ICl was used as a promoter for coupling of **2.15** with a primary alcohol the α-glucuronide was the main product [143].

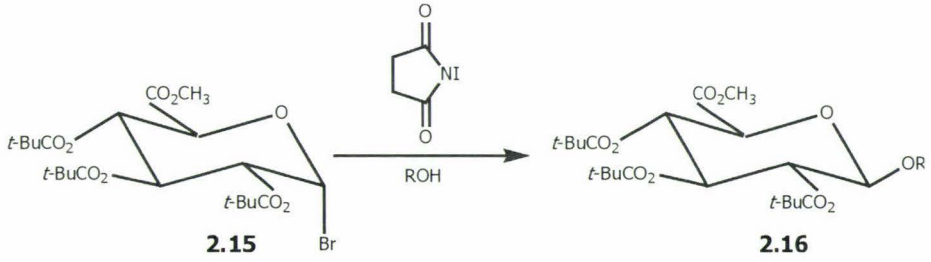

2.15 **2.16**

Scheme 2.5 Glucuronidation of primary and secondary alcohols using the α-bromosugar derivative in the presence of *N*-iodosuccinimide (NIS) promoter

Tricholoracetimidate glycosyl donors

Schmidt's pioneering studies on glycosylation reactions using trichloroacetimidates [145] has led to an increasing number of applications to glucuronidation in natural products synthesis. The thermally and chemically stable tricholoroacetimidate glycosyl donors may be prepared from the α-bromosugar **2.6** as outlined in Scheme 2.6. A major advantage of these intermediates lies in the relatively mild catalysis required, almost invariably $BF_3.Et_2O$ (occasionally TMSOTf) and high β-stereoselectivity. For example reaction of **2.17b** with *p*-nitrophenol using $BF_3.Et_2O$ catalysis, afforded the β-conjugate in 85% yield [146]. However, for *O*-alkyl glucuronide synthesis, the method may not be quite so reliable as the 3β-glucuronide ester of androstanediol was obtained

from **2.17b** in 40% yield, which was slightly superior to the Koenigs-Knorr method, but the 17β-glucuronide ester yield was only obtained in 8% yield [147].

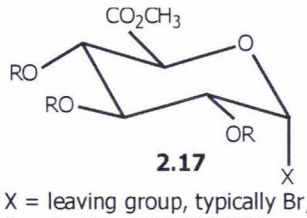

2.17

a X = leaving group, typically Br, Cl, F
b R = Ac, X = OC(=NH)CCl3
c R= Me_2HCCO, X= OC(=NH)CCl3

Figure 2.4 Examples of trichloroacetimate glycosyl donors

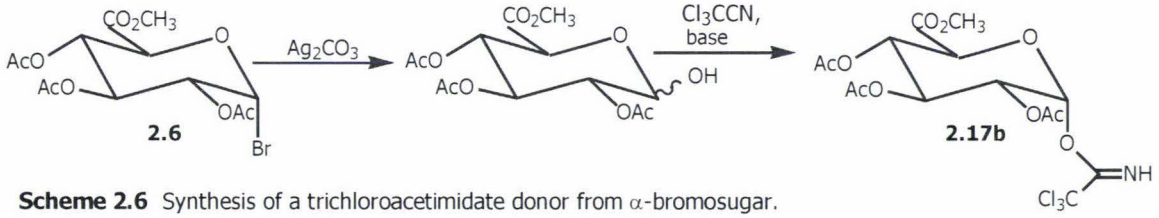

2.6 **2.17b**

Scheme 2.6 Synthesis of a trichloroacetimidate donor from α-bromosugar.

Compound **2.17c** in the presence of BF_3 was also recently used by Brown and co-workers [148] to synthesise gram quantities of a morphine metabolite, morphine-6-glucuronide (M6G) for its evaluation in clinical studies and radioimmunoassay analysis since it was discovered that M6G (Figure 2.5) has superior analgesic activity with reduced side effects (toxicity, nausea, respiratory depression and addiction) compared to the parent compound [149,150]. Although the classical Koenigs-Knorr reaction for the synthesis of M6G (i.e. heating methyl 2,3,4-triacetyl-1-α-bromoglucuronate and 3-acetylmorphine in benzene with Ag_2CO_3) used by Yoshimura [151] and others [131] was adequate for producing gram quantities of M6G, the yield was extremely variable (i.e. 0 - 70%). A further serious draw-back to the use of Koenigs-Knorr conditions in this case was the use of the heavy metal ion promoter, which must not be present in the final product to be used for the relief of severe pain in humans [3].

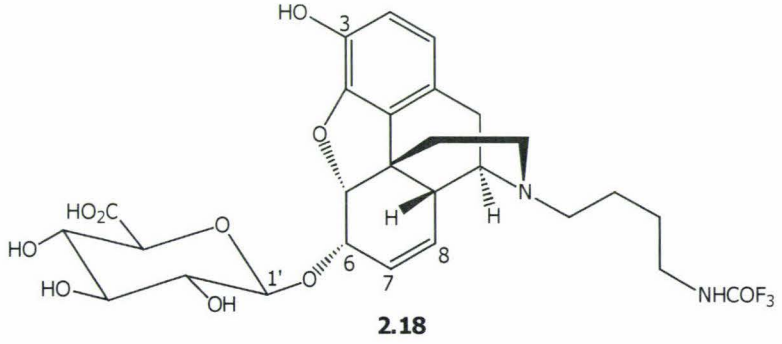

2.18

Figure 2.5 *N*-(4-aminobutyl)normorphine-6-glucuronide hapten used in the radioimmunoassay of morphine-6-glucuronide.

Phosphorous derivatives as glycosyl donors

The use of glycopyranosyl phosphates (Figure 2.6) as glycosyl donors for Koenigs-Knorr reactions in the presence of trimethylsilyl triflate (TMSOTF) was developed by Hashimoto *et al.* [152-155]. The reactions were extremely rapid, and highly specific for β-glycosidation, with or without neighboring group participation.

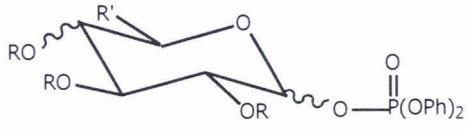

2.19

a R = $PhCH_2$, or PhCO,
b R′ = H, CO_2Me, CH_2OCH_2Ph or $CH_2COCOPh$

Figure 2.6 Examples of glycopyranosyl phosphate glycosyl donors in Koenigs-Knorr reactions

The above authors successfully used the glycopyranosyl phosphate **2.20** for the synthesis of estrone and testosterone glucuronide (Scheme 2.7). As well as being extremely rapid the reaction was highly β-specific and produced both glucuronides in excellent yield. The glycosidation reactions also showed that the anomeric configuration of the glycosyl donor was not crucial to either the stereochemical outcome or the final yield of the glycosylation reactions.

Glycosyl phosphates can be prepared easily by reacting the corresponding α-bromosugar with dibenzyl phosphate in a catalytic two-phase system using tetrabutylammonium hydrogen sulphate as a catalyst [156]. Since phosphorous compounds can be modified easily by several other kinds of atoms, numerous leaving groups with different properties may be designed.

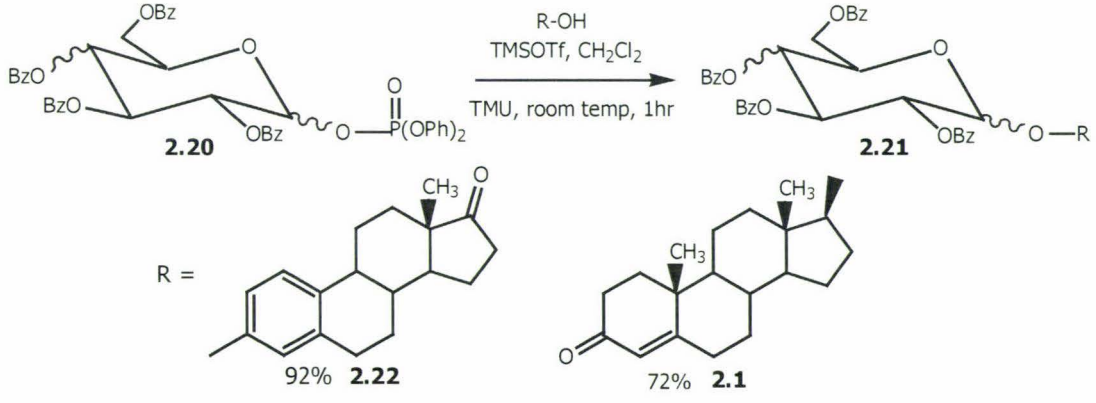

Scheme 2.7 Synthesis of testosterone glucuronide and estrone glucuronide using glycopyranosyl phosphate derivatives.

Glucopyranose derivatives as glycosyl donors

Among the known 1,2-*trans* glycosylations the traditional orthoester methods suffer from the disadvantage that unwanted by-products may be formed. Besides the desired glycoside **2.24a** obtained from the direct glycosylation of the starting orthoester **2.23a**, a second isomeric glycoside **2.24b** is also obtained by rearrangement (re-esterification) of the orthoester **2.23a** to form a second orthoester **2.23b** followed by glycosylation (Scheme 2.8) [157].

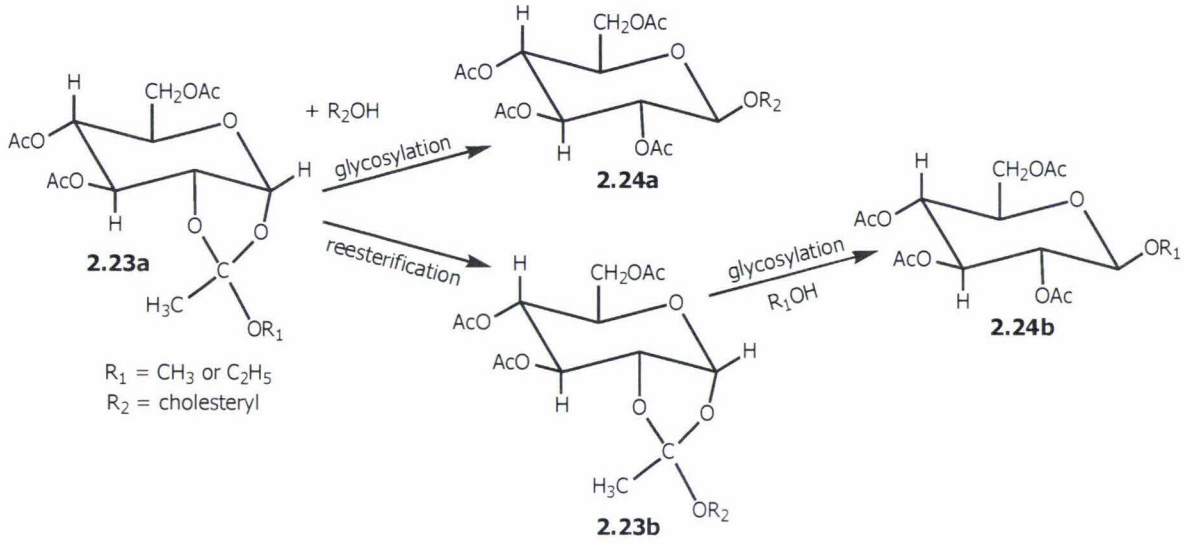

Scheme 2.8 Formation of unwanted byproducts in glycosylation reactions by re-esterification of orthoester intermediates

To overcome the re-esterification problem a new type of oximate orthoester of *O*-pivaloyl glucopyranose **2.25** was developed by Kunz *et al.* [157] and employed in the effective 1,2-*trans*-glycosylation of some complex alcohols and phenols including estrone and testosterone (Scheme 2.9). The oximate orthoester does not give rise to the unwanted side-products which are normally produced in orthoester glycosylations, and also allows the stereoselective β-glycosylation of both alcoholic (testosterone) and phenolic (estrone) groups under identical conditions.

Although some of the above discussed glycopyranose derivatives, phosphorous derivatives or tricholoroimidate glycosyl donors afford high chemical yield and good β-stereoselectivty in glycosidation reactions, and are typically more stable and less hydroscopic that the glycosyl bromides, these glycosyl donors usually require several extra steps starting from the glycosyl halides, and sometimes specialised reagents, to prepare. Hence their preparation is not as straightforward compared to that for the glycosyl bromides. Furthermore, the glycosyl bromides, in particular the acetate protected bromosugar used in this thesis, have been used as effective donors for β-coupling with drug and steroidal compounds for a number of years and are still used extensively in recent publications [158,159].

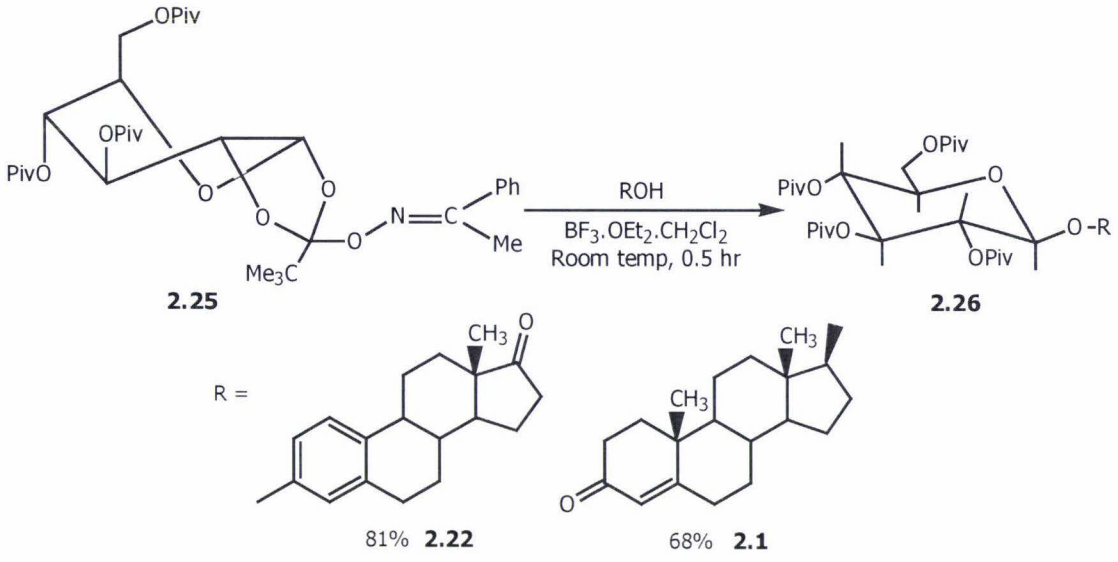

Scheme 2.9 Glycosylation of estrone and testosterone using the oximate orthoester of *O*-pivaloyl glucopyranose.

2.3.4 Preparation of testosterone glucuronide and tetrahydrocortisone glucuronide hen egg white lysozyme conjugates by the active ester method

TG and THEG conjugates of HEWL were prepared by the active ester *N*-hydroxysuccinimide (NHS) /*N,N'*-dicyclohexylcarbodiimide (DCC) coupling method [55] using a 1.5:1 molar ratio of steroid glucuronide to HEWL as shown in Scheme 2.10. Previously, the mixed anhydride method of Rubenstein *et al.* [51] and Leute *et al.* [54] has been used to prepare lysozyme conjugates used in the pre-coated Ovarian Monitor assay tubes for E1G and PdG analysis in urine. However, success with the mixed anhydride method is critically dependent on maintaining anhydrous reaction conditions and reliable temperature control, with different stages of the reaction being carried out at −10, 4, and 10 °C respectively. Because the standard active ester method (described in section 2.2.3.5) can be performed at room temperature and is less sensitive to moisture than the mixed anhydride method, it is quicker, less technically demanding and more reliable, particularly in the hands of a non-organic chemist or a biochemist. A further advantage of the active ester method is that since DCC **2.28** is insoluble in water, any unreacted DCC remaining after the first step does not react with the protein in aqueous solution to generate cross-linking between protein molecules which may cause some precipitation of the protein, as is the case with protein conjugates utilising water soluble carbodiimides [160].

In the first step, DCC was added to a solution of the steroid glucuronide dissolved in anhydrous DMF forming the DCC complex **2.29**. Although DCC is a good leaving group, **2.29** is insoluble in water hence will react only very slowly with HEWL in aqueous solution. Thus before the conjugation to HEWL, 1.3 molar equivalents of NHS **2.30** were added to the reaction mixture to displace DCC (as *N,N'*- dicyclohexylurea, DCU) and form the water soluble NHS-active ester **2.31**, which retains the good leaving group properties of DCC. The active ester is quite stable,

and its hydrolysis rate in aqueous buffer is slow compared with the rate of reaction with the ε-amino groups of HEWL at the reaction pH (pH 9) [161]. In all the active ester conjugation reactions, fine colourless needles of DCU could be seen after approximately one hour indicating that the active ester of the steroid glucuronide had formed successfully.

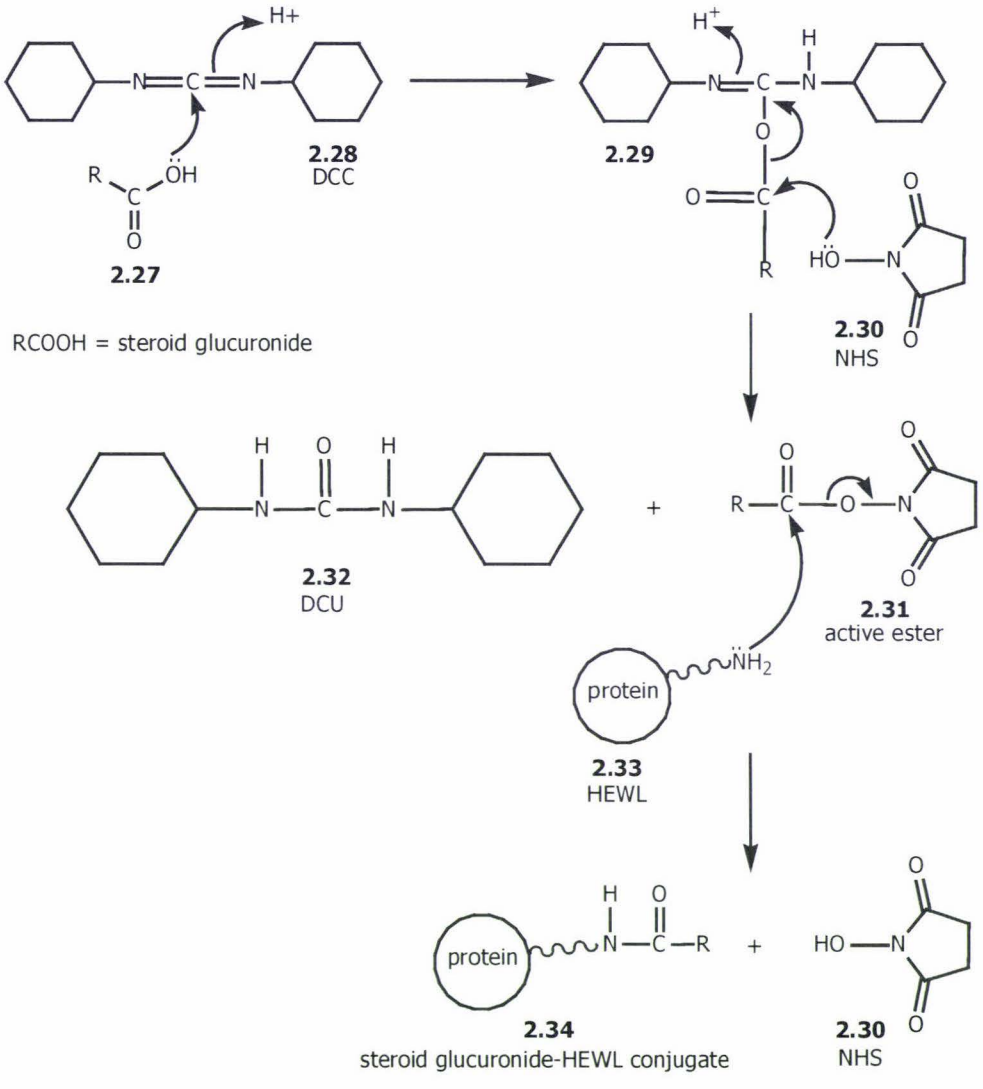

Scheme 2.10 Conjugation of steroid glucuronides via the carboxylic acid group of the sugar residue by activation with DCC and NHS

In the next step the peptide bond between the steroid glucuronide and HEWL was formed by adding the active ester solution slowly dropwise with continuous stirring to a solution of HEWL in a 1% aqueous sodium bicarbonate solution on ice (pH 9). After overnight stirring at 4 °C, the reaction mixture was dialysed to remove any free steroid, unreacted active ester reagent, DCU and sodium bicarbonate [162]. An aliquot was then set aside for analysis on the Mono-S cation exchange column and the remainder was stored at –20 °C.

2.3.4.1 Mono-S cation-exchange chromatography of the TG-HEWL and THEG-HEWL conjugates.

The success of each active ester coupling reaction was checked by cation exchange chromatography on a Mono-S HR 5/5 cation exchange column in 7 M urea buffers as described by Smales and Cooke *et al.* [113,115]. Dialysed supernatant from the active ester conjugation was diluted one part in nine with the equilibrating buffer and filtered through a 0.22 μm filter (Millipore) before injection onto the pre-equilibrated Mono-S column. Elution of each conjugate mixture was achieved by increasing the salt gradient from 0 to 50 mM NaCl over 50 minutes.

The Mono-S profile of the TG-HEWL conjugation mixture prepared using a 1.5:1 molar ratio of TG:HEWL gave seven chromatographically distinct peaks (Figure 2.7a), which was consistent with that observed for other steroid glucuronide active ester coupling reactions with lysozyme [113,115,162]. The largest peak (L) consisted of unreacted lysozyme (L), which was identified by its identical retention time with a sample of pure lysozyme (profile not shown). Since no other peaks were present in the chromatogram of the lysozyme control, the early eluting peaks in the reaction mixture trace must be due to TG-HEWL conjugates and were labeled TG1-TG6 accordingly, with the peak eluting closest to lysozyme designated TG1.

Overall, 71% of the initial amount of lysozyme was conjugated with testosterone glucuronide, as determined by normalising the area under peak L (peak area = height (h) x width at ½ h). The two largest conjugate fractions TG1 and TG2 comprised 41% and 16% of the total conjugated fraction respectively. The remaining 43% of the conjugated fraction consisted of TG3 (14%), TG4 (13%), TG5 (11%) and TG6 (5%).

The addition of the THEG active ester reagent (prepared from synthetic THEG as described in section 2.2.3.5) to HEWL using a THEG:HEWL molar ratio of 1.5:1, also resulted in seven distinct peaks but the relative ratios of each were different (Figure 2.7b). Once again the largest peak in the conjugate mixture consisted of unreacted free lysozyme (L), which represented 38% of the total sample, determined by normalising the peak area as described for the TG-HEWL mixture above. The largest conjugate peak (TH1), represented 40% of the total conjugate yield, similar to that observed for TG1 (41%). However, the distribution profile of the remaining peaks was different from that for TG-HEWL in that the largest conjugate peaks were TH3 (21%) and TH5 (15%), with much smaller amounts of TH2 (10%), TH4 (7%) and TH6 (7%).

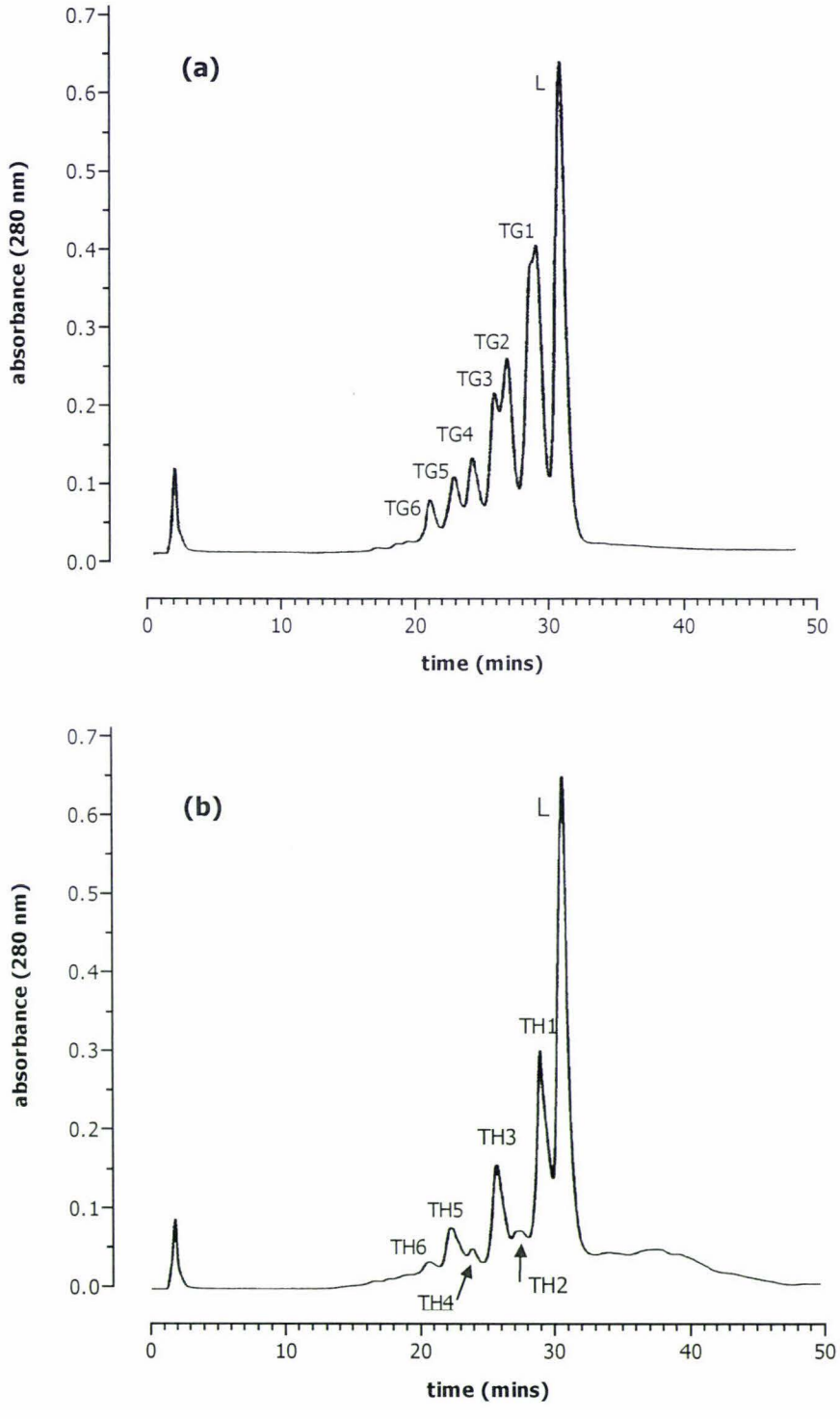

Figure 2.7 Mono-S cation-exchange profiles of (a) TG-HEWL and (b) THEG-HEWL active ester conjugation mixtures in 7 M urea. Conjugates were prepared using a hapten:HEWL molar ratio of 1.5:1. Conditions: buffer A, 7 M urea, 50 mM NaH_2PO_4 titrated to pH 6 with 1 M NaOH; buffer B, buffer A + 1 M NaCl titrated to pH 6. Gradient: 0% B for 5 min, 0-30% B in 40 min, 30-100% B in 5 min.

Based on the amount of unreacted HEWL present in the THEG-HEWL Mono-S profile (38%), conjugation of the THEG active ester with HEWL was less successful than for the TG active ester reaction in which 21% unreacted HEWL remained. The reason for this difference is unclear however previous studies with steroid glucuronide HEWL conjugates prepared by the mixed anhydride acylation method also gave different relative amounts of each conjugate and unreacted protein depending on the steroid used [55]. However, the relative retention time of each peak with respect to the lysozyme peak was similar between the two Mono-S separations.

In the active ester reaction between lysozyme and a steroid glucuronide, each conjugation event replaces a positively charged lysine residue with a neutral steroid moiety and hence reduces lysozyme's overall positive charge by one unit. Thus, if separation on the Mono-S cation exchange column were based solely on simple charge differences, then lysozyme and its conjugates would elute in order of their level of substitution. As mentioned earlier, at the near stoichiometric ratios of active ester to lysozyme (1.5:1) only three of lysozyme's six lysine residues (33, 97 and 116) are favoured for conjugation, thus producing a mixture of mono-, di- or tri-substituted conjugates. However, the fact that it is possible to get at least 6 large conjugate peaks suggests that at least some of the substitution levels are represented by more than one chromatographic peak.

For a separation based on cation exchange in 7 M urea [113,115], the most highly substituted conjugates should elute first, followed by the less highly substituted conjugates and finally by unreacted lysozyme. Comparison of the retention times of the active ester conjugate mixture with that of a lysozyme only control shows that unreacted lysozyme, which retains all of its positive charges, always elutes last as predicted. However, the elution order of the remaining conjugate peaks is not so simply defined and can only be determined by isolating and structurally characterising each conjugate.

For example both the PdG-HEWL and E1G-HEWL conjugate families obtained by the active ester method have been characterised in previous studies with respect to the number and position of the acylated steroids present by a combination of tryptic digestion, amino acid sequencing and electrospray mass spectrometry [162]. A summary of the results for each peak is given in Table 2.1, together with the specific activity of each conjugate (relative to lysozyme).

Table 2.1 A summary of the estrone glucuronide (E1G) and pregnanediol glucuronide (PdG) hen egg white lysozyme conjugates prepared by the active ester method [112,162].

Active ester conjugate	No of steroids per lysozyme molecule	Lysine residue acylated	Specific activity relative to lysozyme
Lysozyme	0		100
E1G			
E1	1	97/116	95
E2	2	97+116	88
E3	1	33	94
E4	2	33+116	61
E5	2	33+97	58
E6	3	33+97+116	42
PdG			
P1	1	97/116	92
P2	2	97+116	76
P3	1	33	88
P4	2	33+116	55
P5	2[‡]	33+97/33+116/ 97+116/33+97+116	61
P6	3	33+97+116	47

[‡]Although for the active ester conjugate family P5 there are only two PdG molecules per lysozyme molecule, there are three acylation positions because none of the three lysine positions are completely acylated in all of the lysozyme molecules. Consequently the three residues are only partially acylated and the sum of these gives an overall substitution ratio of two PdG molecules per lysozyme molecule.

As can be seen from the table, a decrease in specific activity of the conjugate families occurs as the level of substitution increases. The E1G and PdG peaks labeled E1, E3 and P1, P3 respectively were all mono-substituted conjugates and demonstrated the highest specific activity (mean 92%), whereas the E2 and P2 peaks were both di-substituted and showed moderately high specific activity (88 and 76% respectively). The E1G and PdG conjugate peaks labeled E4, E5, E6 and P4, P5, P6 eluted early and were either di- or tri-substituted (or mixtures of both in the case of P5) with much lower specific activities than lysozyme or the corresponding E1, E2, E3 and P1, P2 and P3 conjugate peaks. It is noteworthy that for both sets of conjugates the same lysozyme residues were acylated; lysine 33, 97 and 116, and all of the characterised conjugates were derived from all the possible combinations arising from acylation of these three lysine residues.

With the exception of the disubstituted E2 and P2 peaks which eluted later than the other disubstituted conjugates E4, E5, P4 and P5, and the mono-substituted conjugates E3 and P3, the conjugates eluted in order of their net positive charges based on their substitution levels. However, conjugates with the same level of substitution did not necessarily elute as a single peak. This suggests that although the separation of conjugates in ion exchange chromatography primarily depends upon the overall net charge of the protein for the general

separation of the mono-, di- and tri- substituted conjugates from each other, it is not the only factor influencing the separation as conjugates having the same net charge have different retention times. For example if the E1G and PdG conjugates eluted in strict order of their net charges (i.e. substitution level) on the Mono-S column the expected order of elution would have been: tri-substituted > disubstituted > mono-substituted > lysozyme.

The departure of the observed elution order from that expected based on the net charge (substitution level) of the conjugates may be explained by differences in charge density in the surface region of lysozyme in which the acylated lysine residues are found. Regions of high electrostatic potential on the surface of the protein can help orient its approach to the charged support, with the interaction between the resin and multiple sites (domains) on the protein depending on the relative positions of charges within the domains of interaction [163]. This means that the reduction in charge of a highly positive region of lysozyme by conjugation of a lysine residue with a steroid glucuronide will affect the binding more than the removal of a positive charge from a less concentrated area of charge [111]. Comparison of the relative orders of elution of the lysozyme mono-substituted conjugates with each other and the di-substituted conjugates with each other shows that conjugates substituted at lysine 116 always eluted later (closer to unconjugated HEWL), while those conjugates substituted at lysine 33 always eluted earlier. Thus the order of elution in 7 M urea of the conjugates according to the acylation position was lys 33>lys 97>lys 116.

The electrostatic charge distribution around the three most favoured lysine residues for conjugation has been previously characterised [111] and shows the charge microenvironment surrounding each of the three sites to be different. The crystal structure of lysozyme shows that lysine 116 is only partially exposed on the protein surface and thus produces the weakest electrostatic field of the three favoured residues. Lysozyme crystals grown in urea have also shown that urea can hydrogen bond to lysine 116 [164]. The presence of urea in solution is therefore expected to partially shield lysozyme 116 from interaction with the column matrix. lysine 33 is located close to several positively charged regions of the protein including several arginine residues, but is not close to any negatively charged residues. In contrast, lysine 97 lies close to a negatively charged region due to the carboxyl group of aspartic acid, which is thought to reduce the magnitude of the overall positive charge in the vicinity of lysine 97 and interact unfavourably with the negative charges on the cation exchange matrix. These two factors combined could account for the fact that lysine 33 has a greater contribution to the positive electrostatic field than lysine 97 at pH 6.0 and as a result the loss of the positively charge at lysine 33 on acylation causes the conjugate to be eluted more quickly from the cation exchange column. Thus the overall order of elution of the conjugates from the cation exchange column appears to be determined by a combination of the local differences in charge

distribution surrounding the lysine residues in the different conjugates as well as the overall net charge i.e. their level of substitution and not on the nature of the steroid glucuronide.

It has been shown that the nature of the acylating reagent influences the actual ratios of mono, di- and tri-substituted E1G and PdG conjugates but not the identity of the acylation positions [112,162]. Thus, it is likely that TG and THEG are also attached to the same lysine 33, 97 and 116 residues giving rise to a similar set of TG-HEWL and THEG-HEWL conjugates. Although these TG and THEG conjugates were not characterised, the levels of substitution and specific activity of the various conjugates was expected to show the same pattern observed for the PdG and E1G active ester conjugates. Thus the mono-substituted TG and THEG conjugates eluted at positions 1 and 3 with respect to lysozyme in the Mono-S profile were chosen for isolation in the next section on the basis that the E1 and E3 and P1 and P3 were the best signal generators [115].

2.3.4.2 Isolation and purification of individual TG-HEWL and THEG-HEWL conjugate families

After dialysis to remove the sodium bicarbonate salts the individual conjugate families were separated from each other and unreacted HEWL by large-scale chromatography on an S-Sepharose (fast flow) column using 7 M urea buffers as described by Cooke, Smales and Blackwell [113]. The sample was prepared for loading firstly by adding sufficient solid urea (0.42 g per mL sample, which increased the total volume by 44.9%), followed by solid sodium dihydrogen phosphate to the increased volume to give a 50 mM phosphate, 7 M urea solution. Separation of the conjugates was achieved using a long linear sodium chloride gradient (0 - 1 M NaCl in 810 minutes) as recorded on the S-Sepharose elution profiles for TG-HEWL and THEG-HEWL shown in Figures 2.8a and 2.8b respectively.

The S-Sepharose elution profile of the TG-HEWL active ester conjugation mixture consisted of seven well-defined peaks, consistent with the Mono-S profile shown in Figure 2.7a. The largest peak (lysozyme, L) eluted last, preceded by a second large broad peak with a shoulder on its tailing edge (TG1), two moderately sized peaks (TG2 and TG3) and three smaller peaks (TG4, TG5 and TG6). In addition, two very small peaks were eluted before the seven main peaks (TG1-6 and L), presumably due to families of more highly substituted conjugates. Previous work by Cooke [111] with E1G-HEWL conjugate mixtures separated using similar methods to those described in section 2.2.3.5 has established that the two sets of peaks on the S-Sepharose and Mono-S cation exchange columns are chromatographically equivalent, thus the peaks on the S-Sepharose profile were labeled TG1-TG6 accordingly.

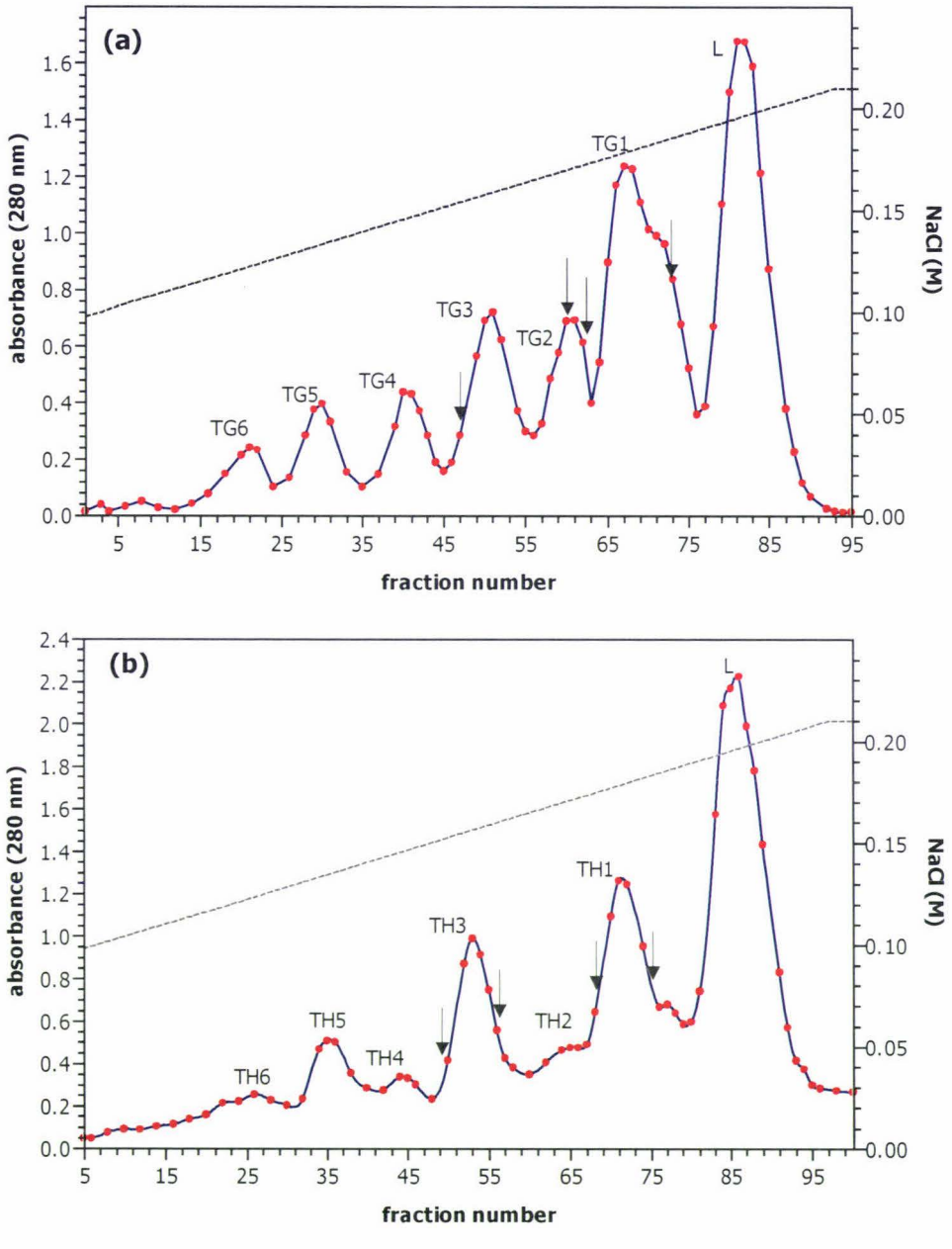

Figure 2.8 S-Sepharose fast-flow profile of (a) TG-HEWL and (b) THEG-HEWL active ester conjugation mixtures in 7 M urea. Conditions: Buffer A; 7 M urea, 50 mM NaH_2PO_4 adjusted to pH 6 with 1 M NaOH. Buffer B; buffer A + 1 M NaCl adjusted to pH 6 with 1 M NaOH. Gradient: 0-21% B in 693 min, 21% B for 90 min, 21-100% B in 27 min, 100% B for 90 min. 100-0% B in 20 min.

Compared to the TG-HEWL Mono-S profile obtained with an aliquot of the conjugated mixture before dialysis (Figure 2.7a), the scaled up S-Sepharose fast-flow profile successfully separated the overlapping peaks TG2 and TG3, and accentuated the shoulder on peak TG1, largely due to the long sodium chloride gradient used for the large scale S-Sepharose column. The peaks on the S-Sepharose trace were also broader than those seen on the Mono-S column, which was consistent with the larger column size and heavier sample loading.

As expected, the THEG-HEWL fast-flow S-Sepharose profile in Figure 2.8b was also similar to the corresponding Mono-S profile shown in Figure 2.7b, and the S-Sepharose peaks were again labeled accordingly. Once again the largest peak (L) was preceded by a series of smaller peaks, the largest of which was TH1, followed by peaks TH3 and TH5. The three smaller peaks TH2, TH4 and TH5 eluted between the larger peaks, and were less well resolved compared to the Mono-S profile due to the peak broadening associated with the long S-Sepharose gradient. The fractions from the S-Sepharose fast-flow columns were pooled as indicated by the arrows on the absorbance profiles, dialysed against Milli-Q water (5 x 2L changes at 4 °C) and stored at –20 °C.

Since the total volume of the dialysed THEG-HEWL active ester mixture adjusted to 7 M urea was too large (~20 mL) to be loaded onto the S-Sepharose column all at once, the sample was split into two 10 mL aliquots which were analysed separately on the S-Sepharose column. Because the resulting S-Sepharose profiles recorded by the chart recorder were essentially the same, the absorbance at 280 nm is shown for only one of the two aliquots of the THEG-HEWL conjugate mixture. The total volume of fractions corresponding to peaks TH1 and TH3 pooled from the two columns was therefore fairly large (84 mL). In contrast the volume of TG-HEWL conjugate mixture was small enough to load onto the column in a single run (~14 mL). The total volume of pooled fractions corresponding to peak TG1 in the S-Sepharose trace was also large (78 mL), however the total volume of fractions for peak TG3 was much smaller (42 mL). As a result, it was decided to combine the TG3 fractions with a proportion of peak TG2 prior to purification on the Butyl Sepharose column to retain as much of the conjugate as possible. The combined TG2 and TG3 fraction was thus renamed fraction TG2-3.

2.3.4.3 Butyl Sepharose chromatography of the pooled S-Sepharose TG-HEWL and THEG-HEWL fractions.

While cation-exchange chromatography in 7 M urea would appear to be an ideal method to separate the conjugate families from each other and unreacted HEWL, previous studies have shown that conjugates purified in this way show lower inhibition by anti-hapten antibodies (~70%) than required for homogenous enzyme immunoassays [113]. A possible reason to account for the less than optimal inhibition of purified S-Sepharose fractions is monocarbamylation of lysine residues of native HEWL by cyanate ions present in the urea solution. In 7M urea buffer an equilibrium exists between urea and ammonium cynanate, thus if the HEWL conjugate mixture is allowed to stand in urea for an extended period of time, carbamylation of free lysine residues may occur as depicted in Scheme 2.11

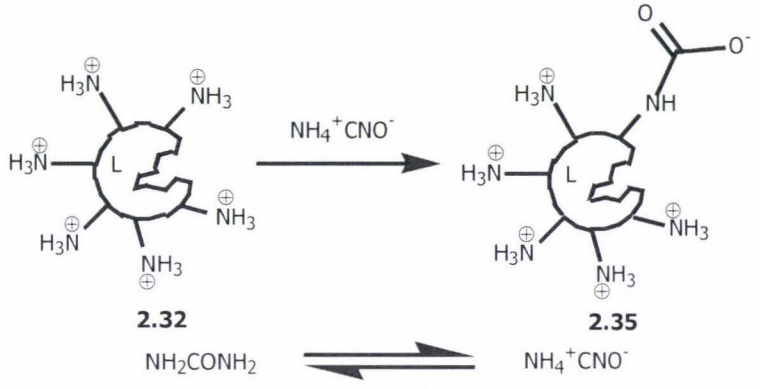

Scheme 2.11 Possible carbamylation of HEWL lysine residues in the presence of 7 M urea

Because each carbamylation event replaces a positive charge with a negative one, the net positive charge on the mono-carbamylated HEWL molecule will decrease by two. The presence of such a mono-carbamylated HEWL conjugate will not be detected in the S-Sepharose profile since it will elute at the same position as a disubstituted TG-HEWL or THEG-HEWL conjugate. Since carbamylation of a single lysine residue has little effect on the lytic activity of HEWL the S-Sepharose fractions contaminated with carbamylated HEWL would still show good specific activity (i.e. rate per unit of protein), but the apparent inhibition by anti-steroid antibodies would be reduced by the same percentage as the level of contamination.

Due to the difficulty in separating the carbamylated species from conjugates having the same net charge, the conjugate samples were processed by S-Sepharose chromatography as quickly as possible after the addition of solid urea to the sample. In addition, only freshly prepared urea buffers that were kept cool prior to use were used for the separation, followed by removal of the urea buffer by extensive dialysis immediately after elution.

A second possibility to account for the loss of conjugate inhibition is the well-known ability of urea to denature lysozyme by intercalating into the protein structure and disrupting hydrogen bonding [165]. The urea must be removed by dialysis before the conjugates can be used in the immunoassay, thus any incomplete or inaccurate refolding of HEWL during dialysis could explain the lower than expected conjugated inhibition after purification by ion exchange chromatography in 7 M urea. Whatever the reason, the low inhibition is readily reversed by a single passage of the conjugates through a Butyl Sepharose hydrophobic-interaction column in ammonium sulphate/sodium phosphate buffers. Although further work is required to elucidate the mechanism, it is possible that interactions between the hydrophobic regions of the protein generated by the addition of non-polar TG or THEG residues with the Butyl Sepharose hydrophobic-interaction column may help the protein to rearrange itself into its native conformation.

The Butyl Sepharose profiles of fractions TG1 and TG2-3 pooled from the S-Sepharose column are shown in Figure 2.9a and 2.9b respectively. The profile for fraction TG1 (Figure 2.9a) consisted of three peaks; a large broad peak with an early eluting shoulder, preceded by two smaller peaks. Fraction TG2-3 (Figure 2.9b) consisted of a large main peak and a much smaller earlier eluting peak. Figure 2.10a and 2.10b shows the Butyl Sepharose chromatograms corresponding to the S-Sepharose fractions TH1 and TH3 respectively. The profile for fractions TH1 (Figure 2.10a) consisted of a small broad peak followed by a much larger peak. In contrast, the profile for the TH3 fractions (Figure 2.10b) consisted of a large broad peak with a shoulder on its leading edge.

The fractions from the Butyl Sepharose separations were pooled as indicated by the arrows on the absorbance profiles, dialysed against Milli-Q water (6 x 1L changes at 4 °C) and concentrated by Macrosep centrifugal concentrators (10 K membrane). The concentrated conjugates were then diluted 1:1 with 0.7 M tris-maleate buffer (pH 7.0) to bring their final concentration to 0.35 M tris-maleate pH 7.0, since HEWL conjugates stored in this way retain their specific activity several years [111]. A small aliquot of each purified conjugate (~150 μL) was removed for Mono-S analysis and the remainder was stored at –20 °C

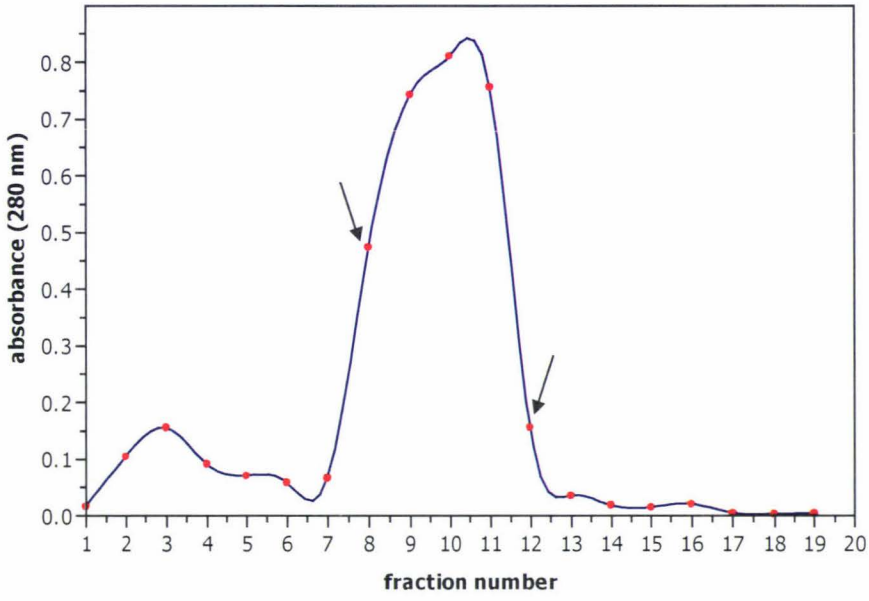

Figure 2.9a Butyl Sepharose elution profile for the TG1 (testosterone glucuronide-HEWL) fractions after initial purification by S-Sepharose cation-exchange fast-flow chromatography. Conditions: buffer A, 50 mM NaH_2PO_4 + 1.4 M $(NH_4)_2SO_4$ titrated to pH 6.6 with 1 M NaOH. Buffer B, 50 mM NaH_2PO_4 titrated to pH 6.6 with 1 M NaOH. Gradient: 0-10% B in 30 mins, 10% B for 20 mins, 10-100% B in 55 minutes, 100% B for 15 mins, 100-0% B in 5 mins.

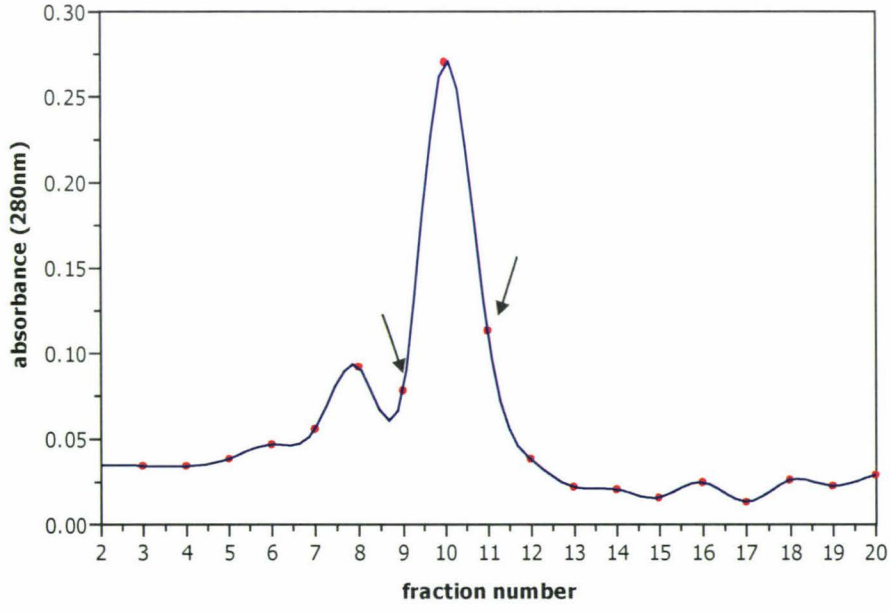

Figure 2.9b Butyl Sepharose elution profile for the TG2-3 (testosterone glucuronide-HEWL) fractions after initial purification by S-Sepharose fast-flow cation-exchange chromatography. Conditions are as described in Figure 2.9a. Gradient: 0-10% B in 30 mins, 10% B for 30 mins, 10-100% B in 35 mins, 100% B for 20 mins, 100-0% B in 5 mins.

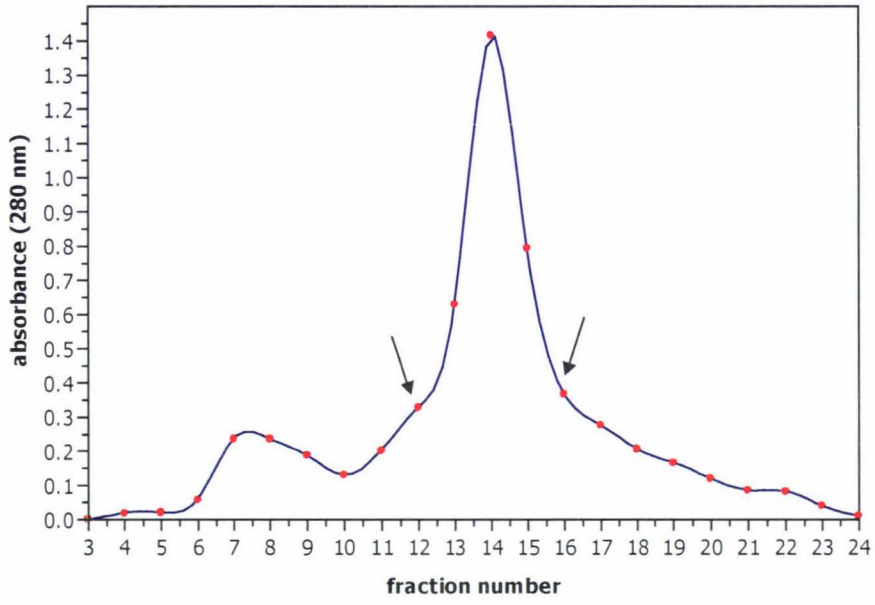

Figure 2.10a Butyl Sepharose elution profile for the TH1 (tetrahydrocortisone glucuronide-HEWL) peak fractions after initial purification by S-Sepharose fast-flow cation-exchange chromatography. Conditions are as described in Figure 2.9a. Gradient: 0-10% B in 30 mins, 10% B for 10 mins, 10-100% B in 80 mins, 100% B for 15 mins, 100-0% in 5 mins.

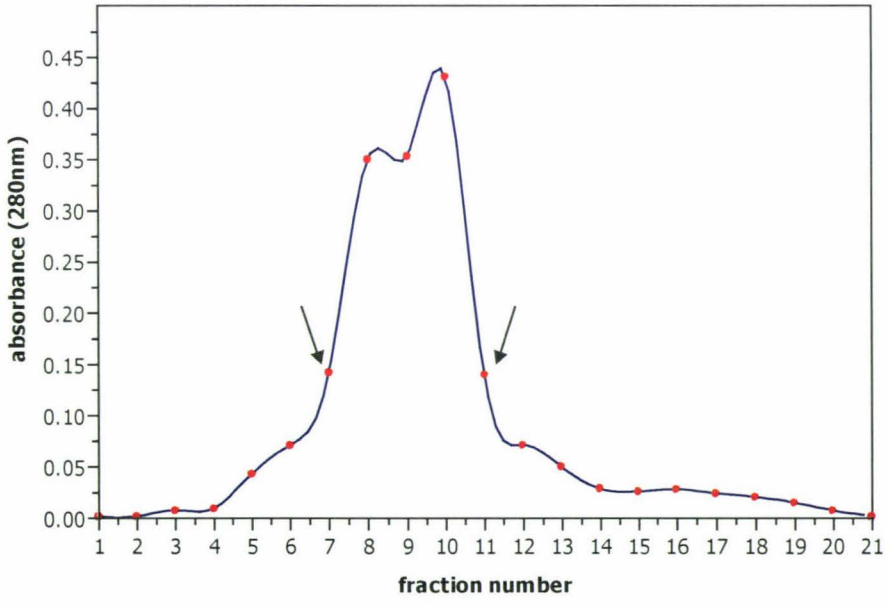

Figure 2.10b Butyl Sepharose elution profile for the TH3 (tetrahydrocortisone glucuronide-HEWL) peak fractions after initial purification by S-Sepharose fast-flow cation-exchange chromatography. Conditions are as described in Figure 2.9a. Gradient: 0-100% B in 105 mins, 100% B for 15 mins, 100-0% B in 5 mins.

2.3.4.4 Analysis of the purified TG-HEWL and THEG-HEWL conjugates by Mono–S cation-exchange chromatography in 7M urea.

The concentrated TG-HEWL and THEG-HEWL fractions purified on the Butyl Sepharose column were analysed on a Mono-S column using 7 M urea as described in section 2.2.3.6 to identify the conjugate and check for the presence of HEWL. The elution profiles for the pooled Butyl Sepharose fractions of each conjugate family are shown in Figure 2.11.

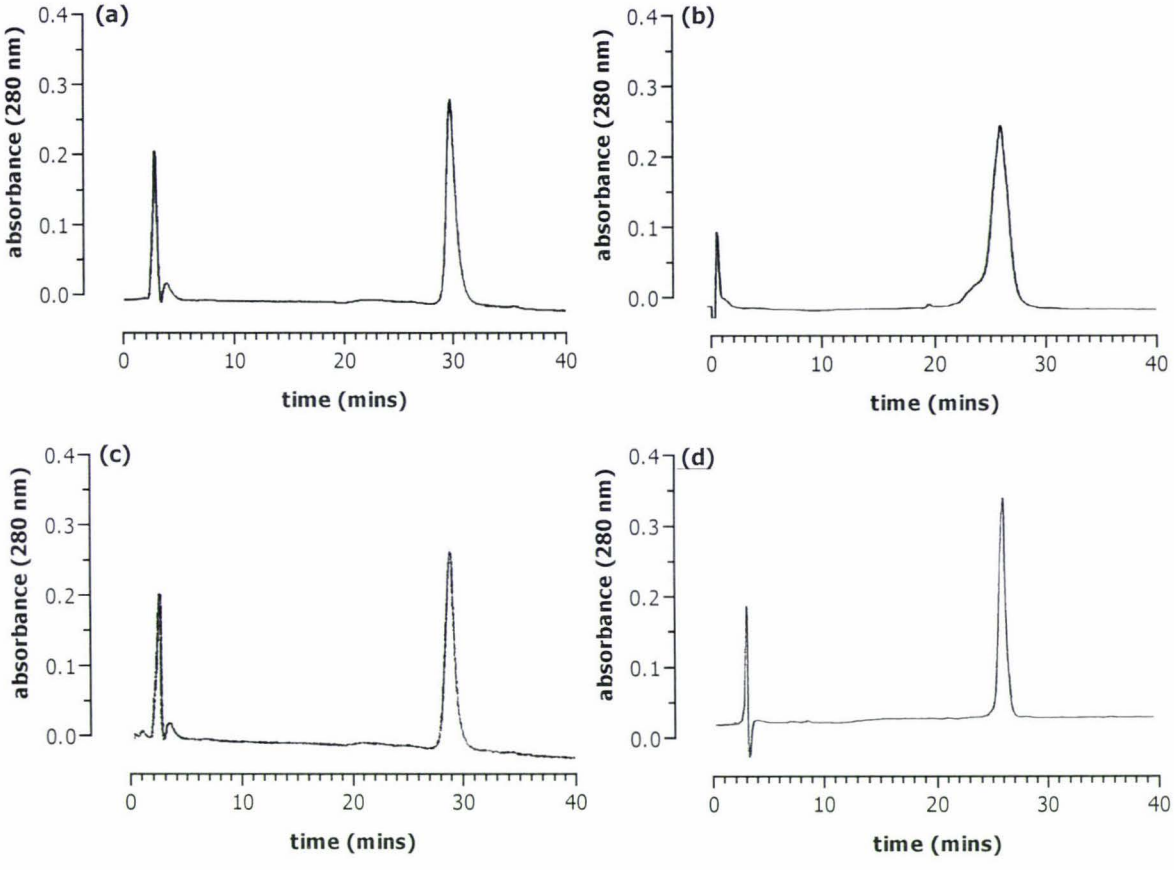

Figure 2.11 Mono-S cation-exchange profiles of HEWL conjugate fractions pooled after Butyl Sepharose purification (a) TG1 (b) TG2-3 (c) TH1 and (d) TH3. Conditions and gradient are as described in Figure 2.7.

Mono-S analysis of the TG1 conjugate Butyl Sepharose fractions (Figure 2.11a) showed a single peak whose retention time matched that of peak TG1 in the Mono-S profile of the original conjugate mixture before purification. Mono-S chromatography of the TG2-3 combined conjugate mixture (Figure 2.11b) from the Butyl Sepharose column on showed a much broader peak preceded by a small shoulder presumably due to the closely eluting TG2 and TG3 conjugates, however the retention time at the top of the main peak was approximately equal to that of the TG3 conjugate in the Mono-S profile of the conjugate mixture (Figure 2.7a). The Mono-S profiles of the Butyl Sepharose fractions TH1 and TH3 (shown in Figures 2.11c and 2.11d respectively) both showed a single peak whose retention time matched that of the TH1 and TH3 peaks respectively in the Mono-S trace for the original THEG-HEWL mixture (Figure 2.7b). Based on the absence of a peak in the Mono-S profiles at the characteristic retention

time for HEWL, all of the purified Butyl Sepharose fractions appeared to be free of unreacted lysozyme, and all were used in immunoassays without further purification.

2.3.4.5 Analysis of TG-HEWL and THEG-HEWL conjugates by matrix-assisted laser desorption and ionisation (MALDI) mass spectroscopy.

The purified conjugate fractions from the Butyl Sepharose column were then extensively dialysed against Milli-Q water and analysed by MALDI mass spectroscopy. In addition a sample of the same batch of lyophilised lysozyme used to prepare the conjugates was also dialysed for MALDI analysis. The major peak in the spectrum of native HEWL (m/z 14293.9), shown in Figure 2.12, was consistent with its molecular mass reported in the literature (14300 Da [108]) and was used to calculate the level of steroid glucuronide substitution in each conjugate.

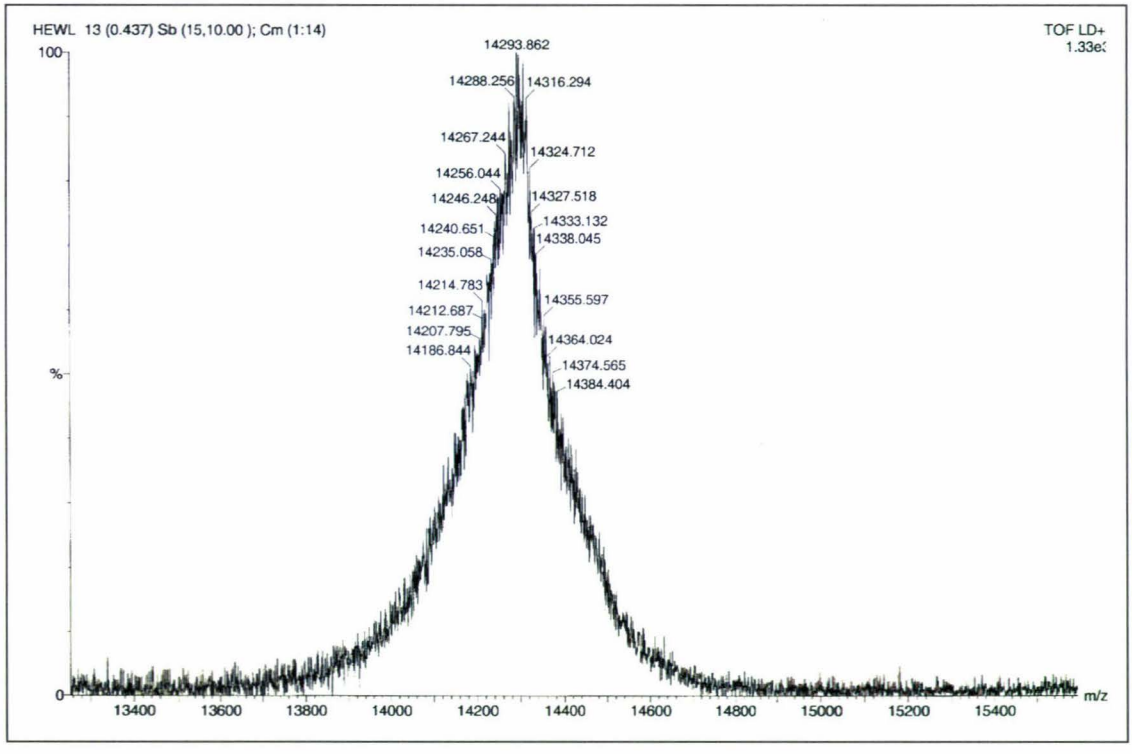

Figure 2.12 MALDI mass spectrum of hen egg white lysozyme (HEWL).

Figures 2.13 and 2.14 show the mass spectra obtained for the purified TH1, TH3, TG1 and TG2-3 conjugates. The major peak in both the TH1 and TH3 profiles (Figure 2.13a and 2.13b) corresponded to m/z 14819.3 and m/z 14810.0 respectively. Since acylation of HEWL (MW 14293.9) with THEG increases the mass by 540.6 mass units (less 18.0 mass units lost as H_20 when the peptide bond forms) these spectra provide conclusive evidence that the purified TH1 and TH3 conjugates were both mono-substituted lysozyme conjugates (calculated 14816.5 Da).

Although both conjugate fractions were mono-substituted the fact that they eluted in a different position on the cation-exchange column was consistent with previous work with estrone and

pregnanediol glucuronide conjugates and presumably again reflects differences in the distribution of charge in the microenvironment surrounding the acylated lysine residues. Figure 2.14a shows the major peak for conjugate fraction TG1 (m/z 14746.6) was also consistent with the mass of a mono-substituted TG-HEWL conjugate (calculated m/z 14740.4, molecular mass of TG 464.6). In contrast, the mass spectrum for conjugate TG2-3 (Figure 2.14b) consisted of two peaks; a major peak at m/z 14750.9 corresponding to mono-substituted TG-HEWL conjugate, and a second smaller peak (~50% relative intensity) of m/z 15186.9 which corresponded to the molecular mass of a di-substituted TG-HEWL conjugate (calculated m/z 15187.1). This was not unexpected since a portion of the TG2 peak was pooled with peak TG3 from the S-Sepharose column (shown in Figure 2.8a).

The mass spectra also confirmed that all conjugates were free of native lysozyme due to the absence of a peak at around 14293.9. The results also showed no evidence that the exposure of samples to urea caused any obvious carbamylation of lysine residues (as outlined in Scheme 2.11) since carbamylation adds 42 atomic units to the molecular weight of the protein and should be detectable by MALDI analysis.

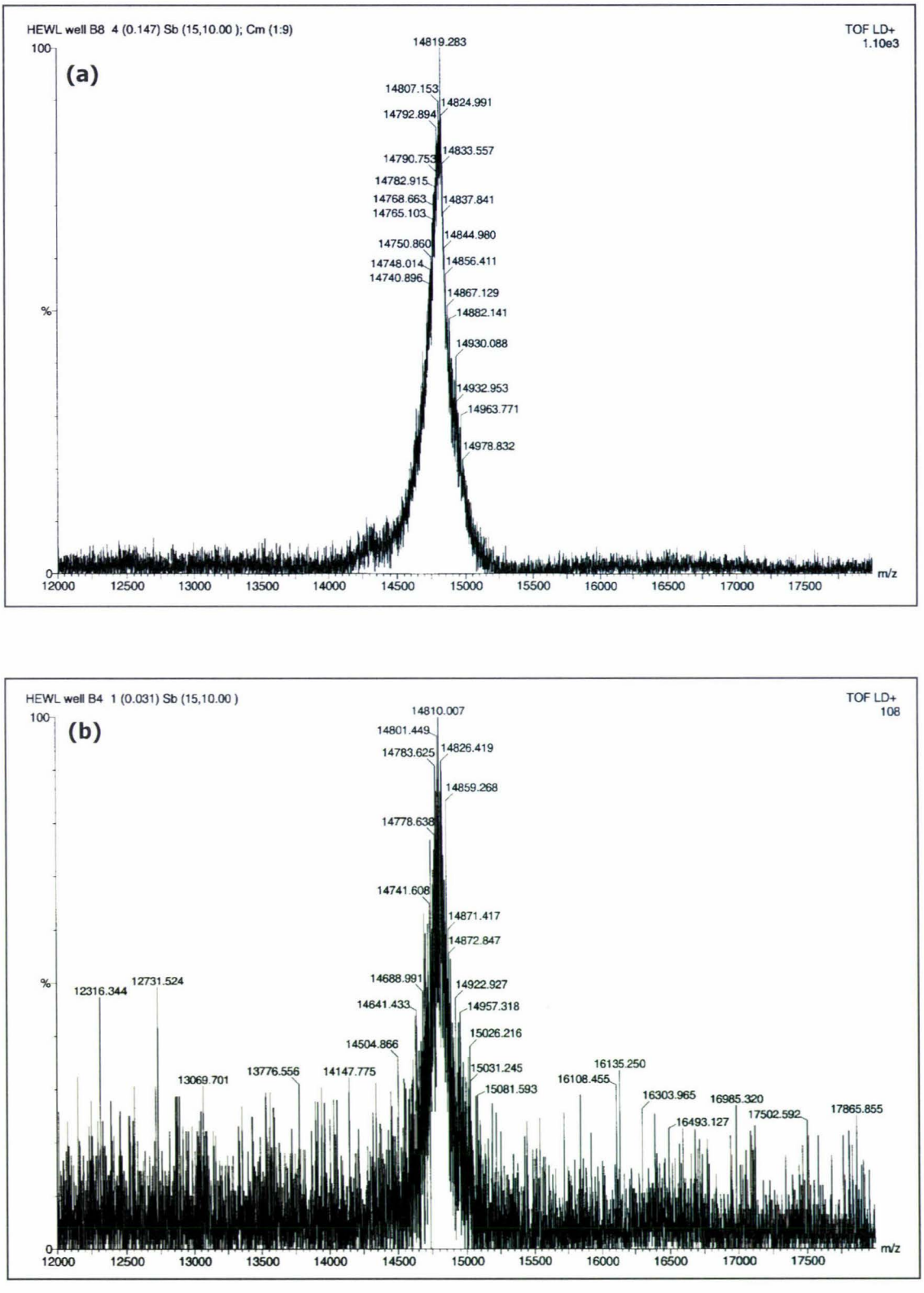

Figure 2.13 MALDI mass spectra of (a) TH1 and (b) TH3 tetrahydrocortisone glucuronide-hen egg white lysozyme conjugates.

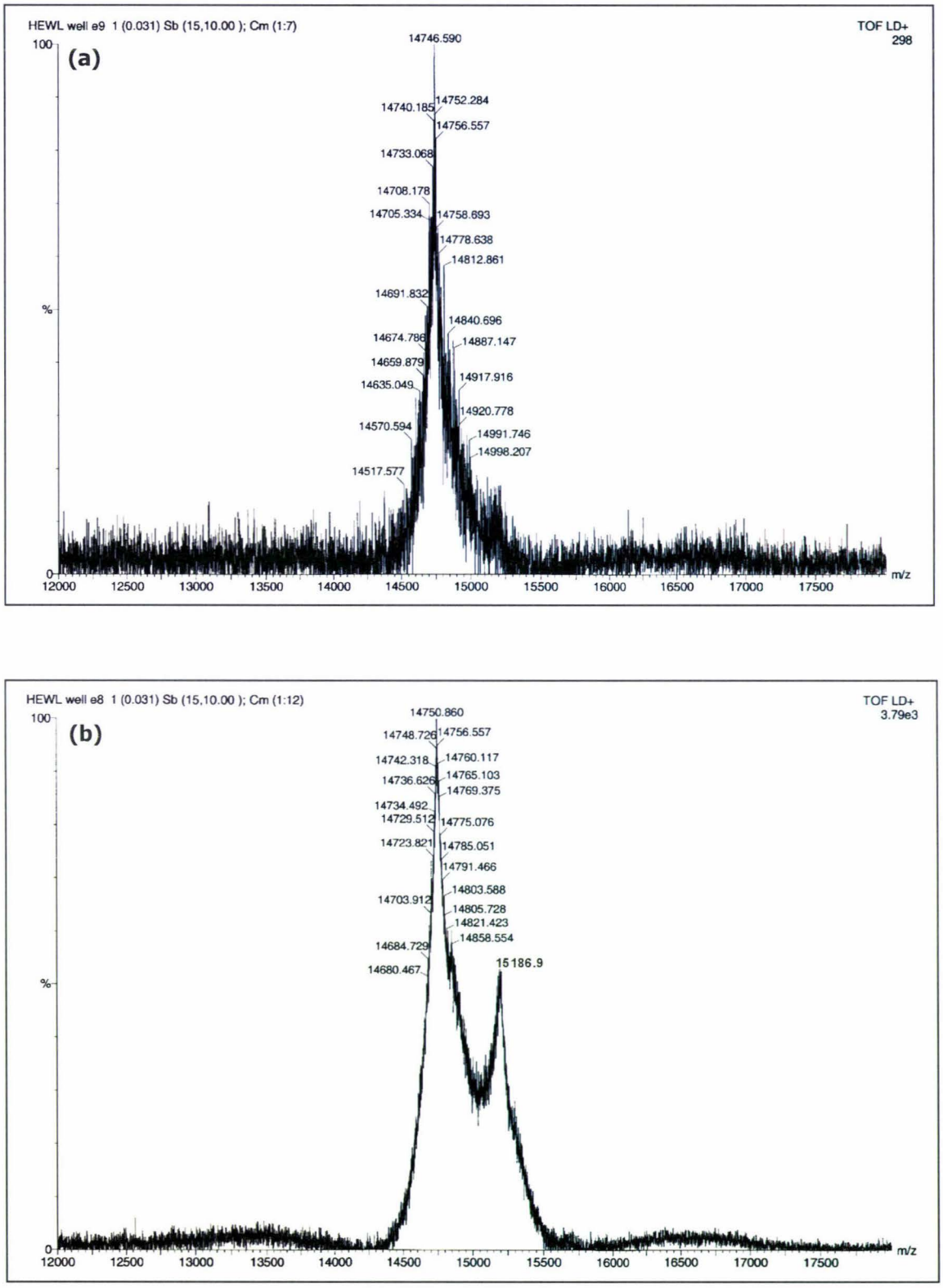

Figure 2.14 MALDI mass spectra of (a) TG1 and (b) TG2-3 testosterone glucuronide-hen egg white lysozyme conjugates.

2.3.5 Protein estimation of TG-HEWL and THEG-HEWL conjugate solutions

Aliquots of the dialysed HEWL conjugates used for MALDI analysis were also analysed for protein content by Coomassie assay [133]. The standard curve (absorbance versus μM lysozyme) used to estimate the protein concentration of the active ester conjugates is shown in Figure 2.15. The lysozyme content (μM) for each conjugate was read directly off the curve and corrected for any dilution factors to give an estimated lysozyme concentration of 91.9 μM for TG1, 70.8 μM for TG2-3, 121.6 μM for TH1 and 130.8 μM for TH3.

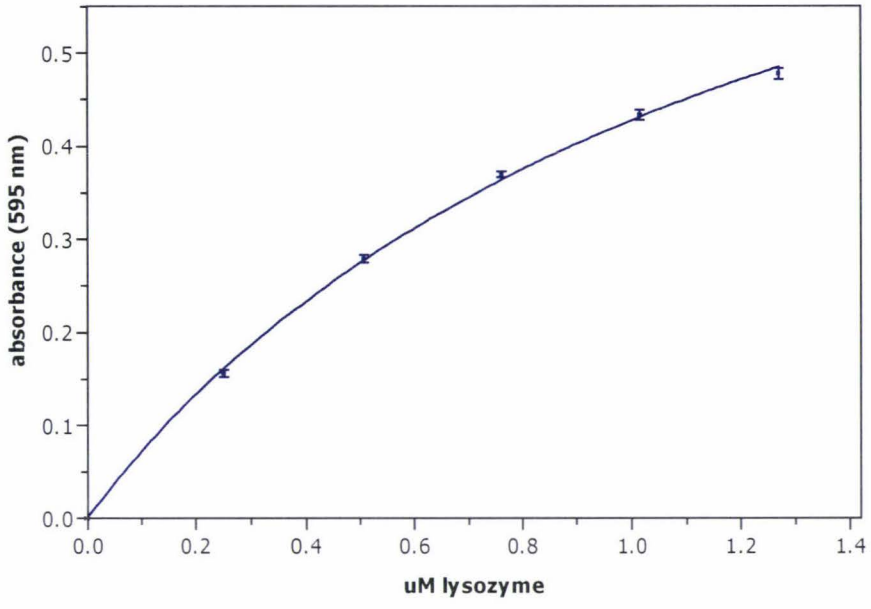

Figure 2.15 Coomassie standard curve for the determination of hen egg white lysozyme content of TG-HEWL and THEG-HEWL active ester conjugates.

2.3.6 Synthesis and characterisation of immunogens

As discussed earlier the steroid glucuronides TG and THEG are too small (MW 464.6 and 540.6 respectively) to act as immunogens. In order to generate anti-TG and anti-THEG antibodies required for the assay, the steroid glucuronides were covalently coupled to the lysine groups of a carrier protein (thyroglobulin, abbreviated as THY) according to the active ester method described in section 2.2.3.11 using a molar ratio of steroid glucuronide:thyroglobulin of 98:1.

2.3.6.1 Protein estimation of TG-THY and THEG-THY immunogen solutions

To determine the amount of steroid glucuronide-THY solution needed for immunisation the protein content of each active ester mixture was determined by Coomassie protein assay as described for the TG-HEWL and THEG-HEWL conjugates described in section 2.2.3.12.

The thyroglobulin content in each immunogen sample was read directly from the standard curve of absorbance versus μg of thyroglobulin (curve not shown) and corrected for the dilution factor to give an estimated concentration of 8.42 mg thyroglobulin mL^{-1} for the TG-THY

immunogen solution and 8.04 mg thyroglobulin mL^{-1} for THEG-THY immunogen solution. While it was not quantitated, the majority of thyroglobulin might have been lost in the precipitate that formed upon adding the steroid glucuronide active ester to the solution of thyroglobulin. Despite stirring the buffered solution of thyroglobulin (initially 40 mg mL^{-1}) and adding the active ester very slowly, the local concentration of active ester was sufficiently high to neutralise enough positively charged lysine residues to affect precipitation of the protein from solution. In addition protein precipitation may be affected by acylation of residues other than lysine which could also cause protein denaturation. Accumulated losses of small amounts of protein would also have occurred when transferring the solution out of the dialysis tubing and as a result of passing the solutions through the PD-10 column to remove unreacted reagents.

2.3.6.2 Estimation of the hapten:protein coupling ratio by TNBS titration

The average number of steroid glucuronide molecules covalently bound to the carrier was determined by two different methods (i) trinitrophenylation of the unacylated ε-amino groups with TNBS reagent using the free amino acids L-lysine and L-glutamic acid as reference standards, and (ii) differential ultraviolet absorption spectroscopy of the conjugated and native proteins. In Table 2.2 the results obtained for the two immunogen conjugates TG-THY and THEG-THY and free thyroglobulin are summarised. Also included in the table is the number of ε-amino groups in hen egg white lysozyme determined by the TNBS method. This protein was used as a control to optimise and test the experimental conditions before attempting to characterise the more complex immunogen conjugates by TNBS assay.

Table 2.2 Percentage hapten incorporation in TG-THY and THEG-THY immunogen conjugates by UV difference spectroscopy and TNBS assay.

Compound	no. of ε-amino groups	mole ratio hapten:protein		% conjugation	
	TNBS assay	UV difference	TNBS assay	UV[‡] difference	TNBS assay
TG-THY		44	39	25	22
THEG-THY		109	29	62	16
THY	265	-	-	-	-
HEWL	6	-	-	-	-

[‡]calculated assuming bovine thryoglobulin has 177 lysine residues per 660 000 molecular weight [120].

The trinitrophenylation method used in determination of the number of steroid residues coupled to thyroglobulin was essentially that of Shashidar *et al.* [126] with some modifications. Scheme 2.12 illustrates the principle reaction involved in treatment of the protein (or amino acid reference standard) with TNBS. Nucleophilic attack by unacylated ε-amino groups in the protein displaces sulphite from TNBS, resulting in a yellow ε-TNP-lysine derivative **2.37**. The number of TNP residues attached can therefore be estimated by their UV absorbance at 336 nm [166]. The reaction is essentially specific for ε-amino residues exposed on the surface of the

protein, however sulphite released during the reaction can associate reversibly with TNP-amino groups or TNP-thiol groups to form complexes that alter the absorption spectra. Furthermore, sulphite complexes of TNP-amino groups may interact with each other or with aromatic side chains in the protein and decrease the molar absorbance of these groups [125]. Thus to avoid errors associated with sulphite complexation, the solution was acidified at the end of the incubation period to dissociate the complexes before reading the absorbance.

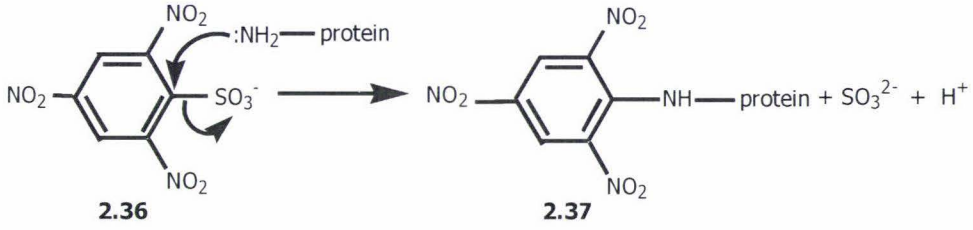

2.36 **2.37**

Scheme 2.12 Reaction of TNBS with unacylated lysine residues of the carrier protein.

TNBS reacts equally well with the α-amino group of L-glutamic acid and the α-amino and ε-amino groups present on L-lysine (Figure 2.16) [125]. Thus, the difference in absorbance at 336 nm of TNP-L-Lysine and TNP-L-glutamic solutions of equivalent concentration eliminates the contribution to the absorbance by the α-amino groups in lysine, leaving the absorbance due only to the number of free ε-amino groups in solution. The standard curve generated by the difference in absorbance observed with TNP-L-Lysine and TNP L-glutamic acid was used to calculate the concentration of ε-amino groups in free thyroglobulin (THY), the conjugates TG-THY, and THEG-THY and the percentage conjugation according to equation 2.1.

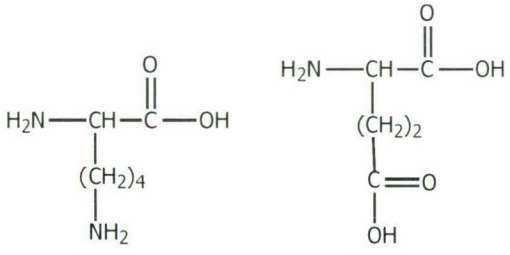

2.38 L-Lysine **2.39** L-glutamic acid

Figure 2.16 L-lysine and L-glutamic acid used as reference standards for ε-amino lysine estimation in thyroglobulin and thyroglobulin conjugates by the TNBS assay.

As expected, the TNP derivative of L-lysine showed twice the absorbance of the TNP derivative of L-glutamic acid when they were matched mole:mole (Figure 2.17). The relationship between absorbance and the concentration of ε-amino groups was found to be linear over the concentration range (0 - 8 μg), $R^2 = 0.9986$, $y = 0.0099x + 0.0029$.

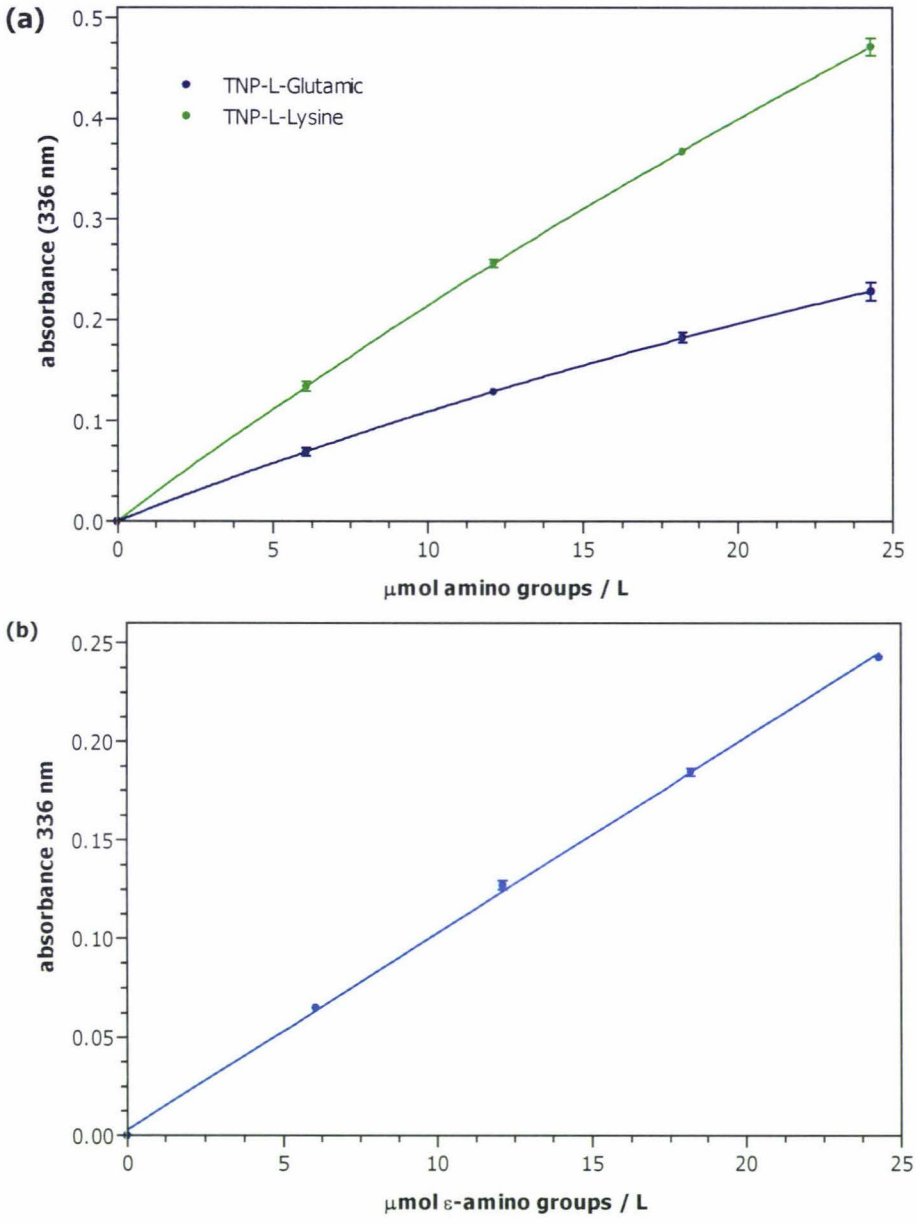

Figure 2.17 Standard curve for (a) estimation of ε- and α-amino groups in lysine, glutamic acid, and (b) ε-amino groups in lysine by TNBS assay. L-glutamic acid and L-lysine standard curves are fitted to non-linear regression curves (one-site binding hyperbola). The ε-amino standard curve was fitted to a linear regression line = difference in absorbance (336nm) for TNP-L-lysine and TNP- L-glutamic acid standards, $R^2 = 0.9986$, $y = 0.0044x + 0.0029$

The TNBS reaction conditions used here differed from that of Shashidar *et al.* [126] with respect to the incubation time (3 hrs versus 2 hrs) and TNBS concentration (0.1%, also used by Habeeb *et al.* [167] versus 0.01%) required to produce the ε-amino standard curve. The increased TNBS concentration and incubation time needed to achieve the required TNP-L-lysine:L-TNP-glutamic acid absorbance ratio of 2 was most likely caused by the incubation method (a thermostated water bath) and purity of the available TNBS being less than optimal. However the correct number of free lysine groups was found for lysozyme (~6) using the ε-amino standard curve after reaction of HEWL with TNBS reagent, confirming the accuracy of

the assay. Lysozyme has 7 free amino groups, including the N-terminal lysine residue, however the N-terminal group is involved in a salt bridge and does not react readily with TNBS [168].

Despite using the same reaction conditions as for HEWL, the number of ε-amino groups in native thyroglobulin (265) exceeded the literature value obtained by DNA sequencing (177) [120] by 88 residues. Possible reasons for the overestimation of ε-amino groups in unconjugated thyroglobulin may include an increased rate of reaction of TNBS with partly buried lysine or other nucleophillic residues [125] exposed during trinitrophenylation with 0.1% TNBS for 3 hours. Nucleophillic attack of TNBS by the thiol groups of cysteine residues may also occur at the pH of the reaction mixture (8.5) since the pka of the thiol group is 8.5 and half the residues would be in the more reactive thiolate form, although the TNP-cysteine product is thought to have a short half-life [125]. Formation of TNP residues with phenolic groups of tyrosine residues is also possible, however the resulting ester is fairly unstable. Extensive unfolding of the protein during trinitrophenylation may result from either the introduction of hydrophobic TNP groups, or via sulphite released during the reaction which is known to cleave disulfide bonds at high pH [125]. Whatever the explanation, because thyroglobulin is much bigger than HEWL, the potential for non-specific reactions contributing to the absorbance at 336 nm is greater. Incomplete trinitrophenylation due to steric interference by steroid residues on neighbouring ε-amino groups may also introduce errors in the estimation of the free lysine residues by TNBS assay. This possibility has not been examined here, but it is thought unlikely that the more than a few lysine residues would be involved [129].

Using equation 2.1 the percentage of acylated amino groups (those which did not react with TNBS) was calculated as 22% for TG-THY and 16% for THEG-THY. Assuming the effect that contributed to the increased absorbance in native THY occurred equally in the trinitrophenylated free protein and conjugates, the corresponding number of haptens present in TG-THY and THEG-THY was 39 and 29 respectively (calculated assuming thyroglobulin contained 177 ε-amino groups per mole, molecular weight 660 000).

2.3.6.3 Differential UV spectroscopy to estimate the protein:hapten ratio

The ultraviolet spectra of the conjugates together with the unconjugated steroid glucuronides and free thyroglobulin are shown in Figures 2.18a and 2.18b respectively.

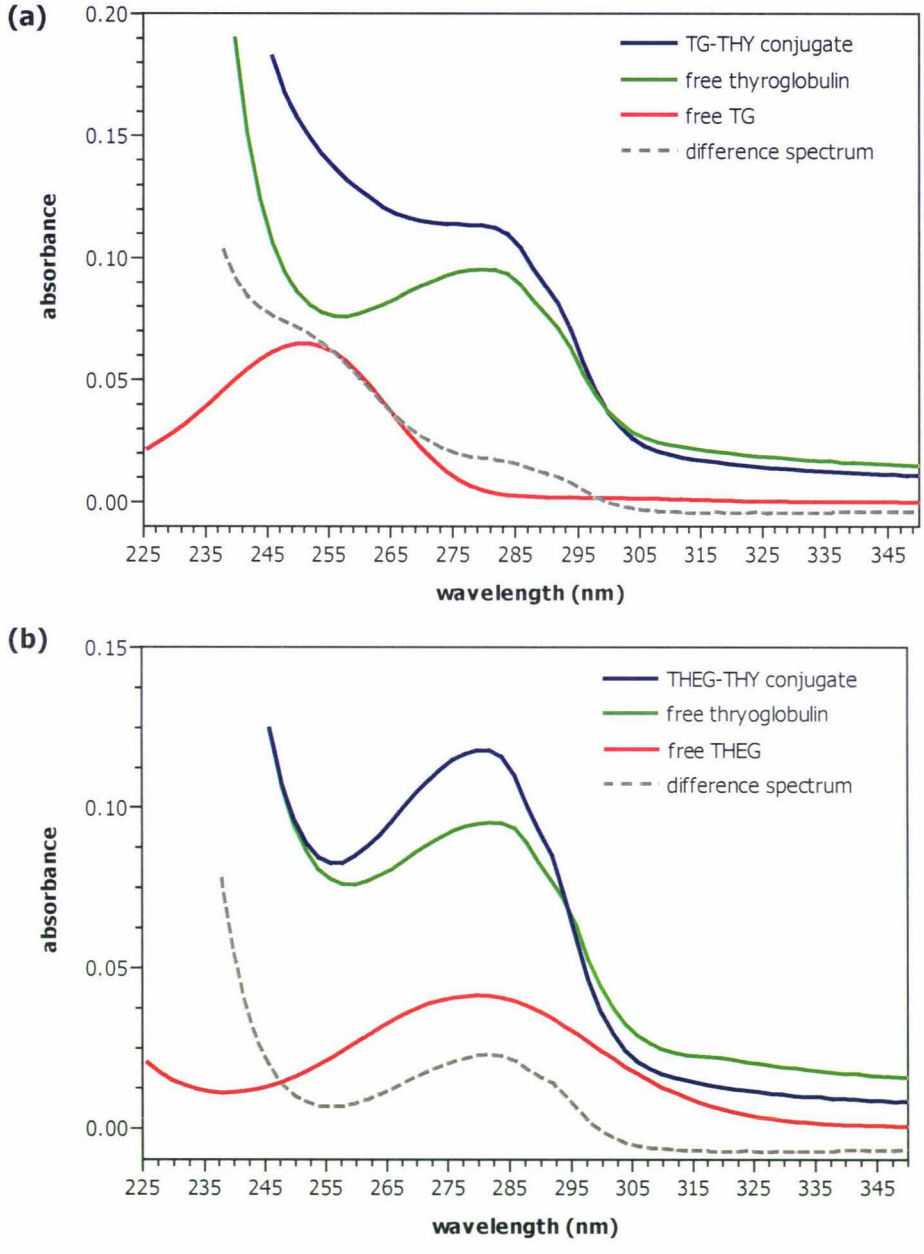

Figure 2.18 Ultraviolet spectra of (a) TG-THY and (b) THEG-THY conjugates and related substances. The curves composed of broken lines represent the contribution of the steroid moiety obtained by subtracting the absorption spectra of the conjugate from that of thyroglobulin, all having 123.5 nM protein). The UV spectra of TG (50.23 μM in 0.01 M NaCl, 1.7% MeOH) and THEG (197.31 μM in 0.01 M NaCl) were recorded and scaled to fit on each plot for visual comparison with the difference spectrum.

In each case the concentration of free thyroglobulin equaled that of the conjugate (123.5 nM as determined by Coomassie protein assay). The curves with broken lines represent the absorption values obtained by subtracting the absorption of free thyroglobulin from that of the conjugates. Since the molar extinction coefficient is dependant on pH and ionic strength [169], 0.01 M NaCl was used as the diluent for solutions of the free steroids, conjugates and carrier

protein, with the exception of the solution of TG, which contained a small amount of methanol added initially to dissolve the steroid. The final methanol concentration in this solution was 1.7%, which did not significantly change the pH or ionic strength compared to the other solutions.

Testosterone glucuronide possesses an α,β-unsaturated carbonyl functionality, and exhibited an absorption maximum in the region characteristic of this functional group, λ_{max} 252 nm [166] whereas λ_{max} for the carbonyl groups in THEG (280 nm) overlapped with the protein absorption. The hapten:protein molar ratio was calculated according to the method of Erlanger *et al.* [129]. For example, the calculation for TG-THY was as follows: free testosterone glucuronide exhibited an absorption maximum at 252 nm in 0.01 M NaCl, 1.7% methanol. Its molar extinction coefficient at this wavelength was calculated as 12,912 L mol^{-1} cm^{-1}. The absorbance of TG-THY at 252 nm and 123.5 nmol L^{-1} (82.62 mg L^{-1}) was 0.149, whereas the absorbance of free THY at the same concentration and wavelength was 0.0808. The difference between these two values (0.0686) was attributed to the conjugated TG residues. Hence the concentration of steroid residues is 0.0686/12912 L mol^{-1} cm^{-1}, or 5.31 μmol L^{-1}. The molecular weight of TG is 464.56 g mol^{-1}, hence its concentration is 5.31 μmol L^{-1} x 464.56 g mol^{-1} or 2.47 mg L^{-1}. By subtracting the concentration of the steroid residues from that of TG-THY, the concentration of the THY constituent is obtained 82.62 - 2.47 or 80.15 mg L^{-1}. If the MW of THY is 660 000, the number of moles L^{-1} THY in the sample is 80.15 mg L^{-1} / 660 000 or 121.44 nM. Therefore the number of moles of TG per mole of THY is 5.31 μM / 121.44 nM or 44. The corresponding calculation for THEG at λ_{max} = 280 nm (where ε_{280} = 1676 L mol^{-1} cm^{-1}) gave an estimated number of 109 moles of THEG per mole of THY.

The hapten:protein mole ratio for the TG-THY conjugate was in good agreement with the TNBS assay result, however the UV difference spectrum result estimated for THEG-THY was almost 4 fold higher than the TNBS estimate. The calculation for THEG-THY is thought to be unreliable in this case due to the substantial overlap in absorbance at 280 nm due to the protein. Such an overlap limits the accuracy of the hapten:carrier ratio because the optical density contribution by the THEG hapten is small compared to that of the protein [126].

The mole ratio calculations using this method also depend upon an assumption that may not be completely valid, i.e. that the extinction coefficient of the protein and steroid glucuronide is unaffected by the covalent linkage. The maximum absorbance of the hapten may also shift when conjugated to a protein, as observed by Erlanger *et al.* [129] and Westphal [170] in solutions of steroid-protein conjugates. Westphal also noted a corresponding decrease in the extinction coefficient by approximately 10%. Although it is difficult to determine in this case, if a shift in the λ_{max} observed with the steroid glucuronide conjugates was accompanied by a decrease in the absorbance, then the number of steroid residues would be underestimated.

This method also relies on the ability to prepare the solutions accurately at low concentrations. Because of the uncertainties inherent in both the TNBS assay and in the UV spectra, the exact number of steroid residues in either conjugate could not be precisely determined. However, the number of acylated residues in TG-THY is likely to be within the region of 33 - 44 residues. The result for THEG-THY was ~29 THEG moieties per THY molecule by trinitrophenylation, however this result was less certain since it could not be supported by the UV difference spectra.

2.3.7 Summary

In summary, THEG (purchased from Sigma Chemical Co.) and TG (synthesised in section 2.2.3.4) were effectively coupled to HEWL by the active ester coupling method resulting in the formation of a range of lysozyme conjugates, of which TH1, TH3 and TG1, TG2 and TG3, were the dominant forms, respectively. The two step isolation procedure used in this chapter was successful for the large-scale separation of these conjugates, and analysis of the thus purified conjugates by MALDI mass spectroscopy and 7 M urea Mono-S chromatography confirmed that the individual conjugates were free from lysozyme contamination. This allowed the main conjugates to be compared for their suitability as signal generators in the Ovarian Monitor Immunoassay system, which is addressed in Chapter 3.

CHAPTER THREE

Preliminary studies relating to the immunoassay of testosterone glucuronide and tetrahydrocortisone glucuronide with the Ovarian Monitor

3.1 Introduction

The success of an homogeneous immunoassay for testosterone glucuronide and tetrahydrocortisone glucuronide using the Ovarian Monitor format is critically dependant upon the characteristics of the steroid glucuronide–HEWL conjugates used as signal generators and the anti-steroid glucuronide antibodies used to inhibit their lytic activity. This chapter discusses the production and purification of the anti-TG and anti-THEG antibodies using the immunogens prepared in Chapter 2 and their potential to inhibit the corresponding steroid-HEWL conjugates, thus producing standard curves for testosterone glucuronide and tetrahydrocortisone glucuronide with the desired shape and sensitivity limits.

3.1.1 Substrate binding and measurement of enzyme activity

The Ovarian Monitor lytic assay is based on the hydrolytic activity of HEWL against its natural substrate, the cell wall of the gram-positive lyophilised bacterium *Micrococcus lysodeikticus*. More specifically the enzyme cleaves the β 1-4 glycosidic bond between C1 of the *N*-acetylmuramic (NAM) and C4 of the *N*-acetylglucosamine (NAG) repeating units of the polysaccharide component of the cell wall (Figure 3.1a). Crystallographic studies [108] have shown that lysozyme binds six sugar residues (A-F) in the active site cleft with lysis occurring only between residues D and E of the hexasaccharide unit.

The linear carbohydrate chains of alternating NAM-NAG residues are cross-linked into a three dimensional lattice by small negatively charged peptides covalently linked to the lactyl substituents on some (~50%) of the *N*-acetylmuramic acid residues [171,172]. The NAM residues may be linked through a dimer of cross-linked peptides or connected through one or more bridging peptides (see Figures 3.1c and 3.1d respectively).

At the pH of the assay buffer (pH 7) the cross-linked peptides and the free carboxylate groups of the NAM residues remain ionised. The high proportion of ionised carboxylate groups relative to protonated ε-amino lysine residues confers a high negative charge to the *Micrococcus* cell wall while the high proportion of basic residues on the surface of lysozyme makes the enzyme highly positively charged. The importance of the electrostatic interaction between the surface of the enzyme and the substrate cell wall to the lysis reaction is well illustrated by the loss in specific activity of lysozyme conjugates having ≥ 4 lysine residues acylated with neutral or negatively charged compounds [110].

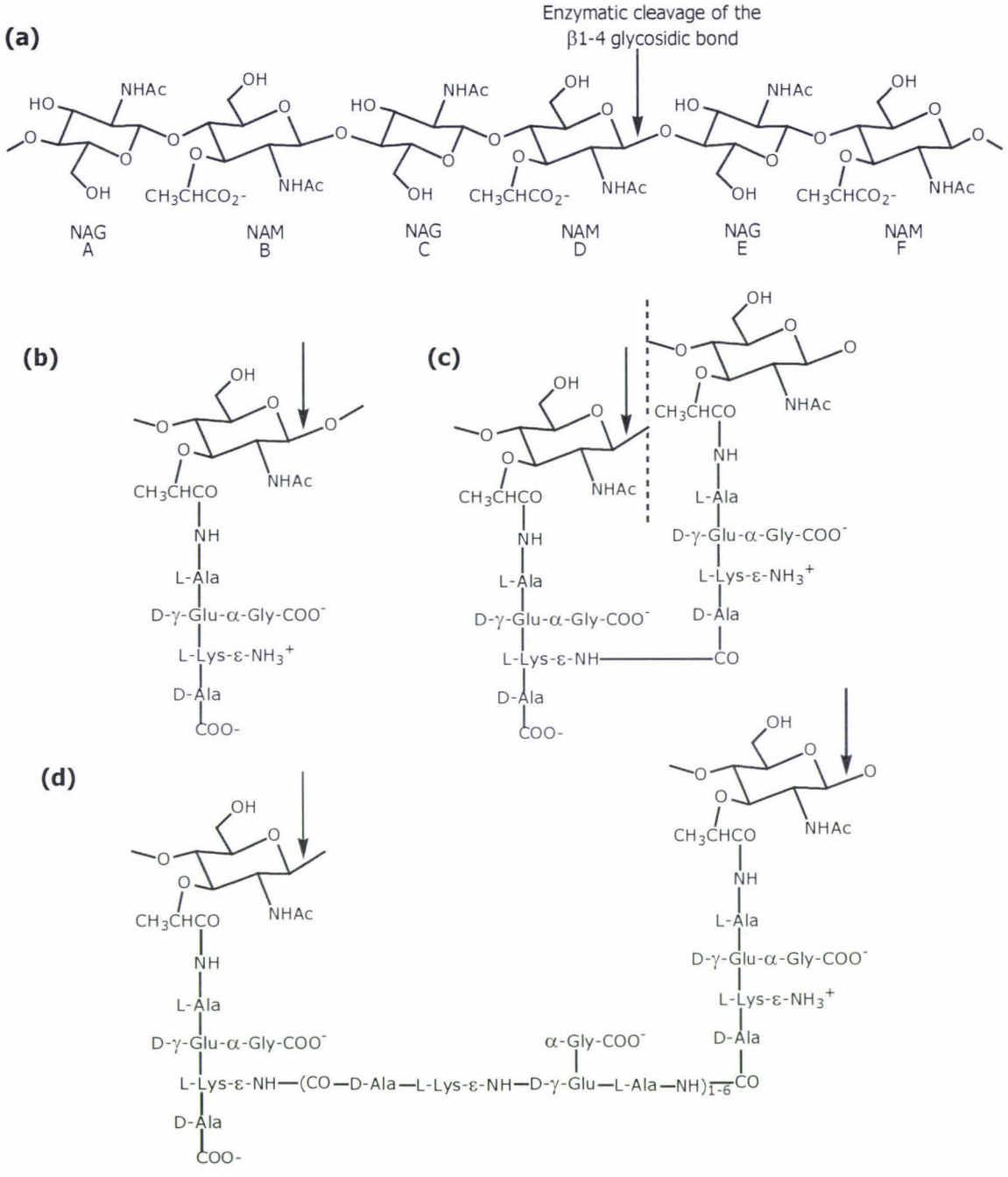

Figure 3.1 **(a)** The structure of the polysaccharide component of the *Micrococcus lysodeikticus* bacterial cell wall, the natural substrate of hen egg white lysozyme. The cell wall consists of polymers of alternating *N*-acetylglucosamine (NAG) and *N*-acetylmuramic acid (NAM) sugar residues cross-linked by small negatively charged peptides. Lysozyme cleaves the glycosidic bond between C1 of the NAM residue and C4 of the NAG residue as indicated by the arrows. NHAc refers to the *N*-acetyl or acetamido moiety found on both NAG and NAM sugars. **(b)** The lactyl group of the NAM residue bonds to the peptide unit via an amide bond. This unit may be either; **(c)** directly cross-linked to another NAM residue or **(d)** cross linked to another NAM residue via one or more "bridging" peptides [171].

When the direct catalytic activity of lysozyme (i.e. the lysis of glycosidic bonds) is compared with the catalytic activity of other enzymes it scores relatively poorly, being some three orders of magnitude lower than that of enzymes like catalase, urease or alcohol dehydrogenase [173]. However, when a suspension of whole *Micrococcus lysodeikticus* cells is used as the substrate

lysozyme generates a very large transmission change for a given concentration of enzyme and lytic activity. This is because the transmission of the cell suspension measured in the assay is due to physical obstruction and scattering of the light path by the intact cell wall and thus is only indirectly related to the lysozyme activity. As the lytic reaction proceeds the walls of the numerous bacterial cells are weakened and ultimately burst due to the high osmotic pressure inside the cell resulting in a large change in the transmission of the cell suspension for a relatively small number of catalytic events.

Despite the increased sensitivity of the assay based on the lysis of whole substrate cells, measuring lysozyme activity indirectly does have some added complications. Since lysozyme can attack the intact cell wall as well as the resulting cell wall fragments, cell lysis and collapse do not necessarily result in a decrease in the amount of substrate available to the enzyme [173]. Thus although the actual catalytic activity of lysozyme may not be affected with time by the removal of intact cells, because the number of intact cells remaining is decreasing with time, so too does the apparent rate of transmission change. The non-linear relationship between transmission and substrate concentration results in curvature of the transmission versus time plot for a given enzyme concentration as the assay proceeds. For example the clearing curve for an E1G conjugate (shown in Figure 3.2) at the concentration required for the assay of urinary estrone glucuronide is approximately second order [115] and thus can be fitted by the equation described by McKenzie and White [174]. The initial phase of the clearing curve is almost linear, but shows a smaller percentage change in rate as the assay proceeds towards the end point.

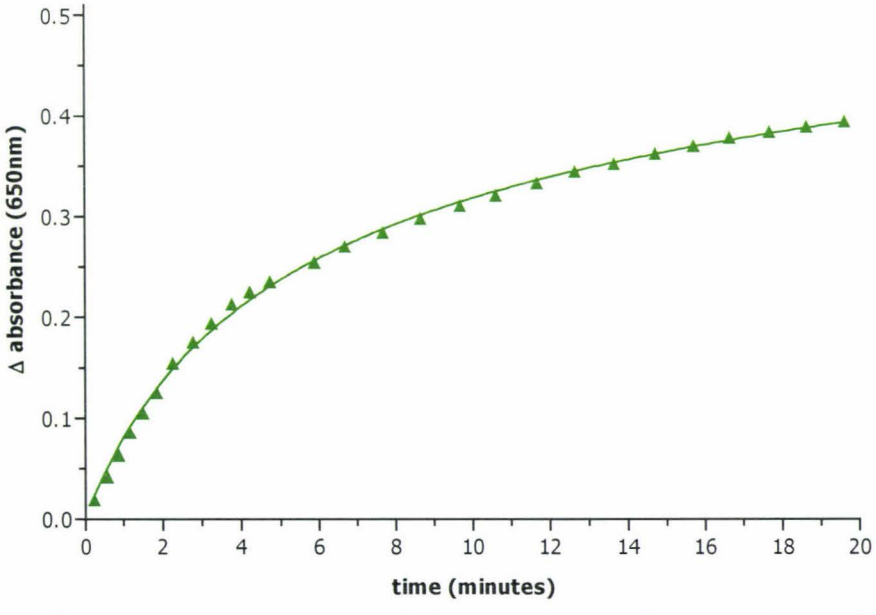

Figure 3.2 Clearing curve (change in transmission versus time plot) for estrone glucuronide [111].

3.1.2 Inhibition of steroid glucuronide-lysozyme conjugate activity by anti-steroid glucuronide antibodies.

The mode of lysis inhibition of steroid-lysozyme conjugates by anti-steroid antibody has recently been described by Smales [124]. The basic structure of an anti-steroid antibody (or immunoglobulin, IgG) glycoprotein consists of two identical heavy (H) polypeptide chains and two identical light (L) polypeptide chains forming a flexible "Y" shaped molecule as illustrated in Figure 3.3. Both H and L chains are subdivided into variable (V) and constant (C) domains consisting of approximately 110 amino acids each, giving a total molecular mass of approximately 150 kDa. The overall structure is stabilised by a variable number of disulphide bonds (-S-S-) between the L and H chains and the two H chains in the flexible "hinge" region.

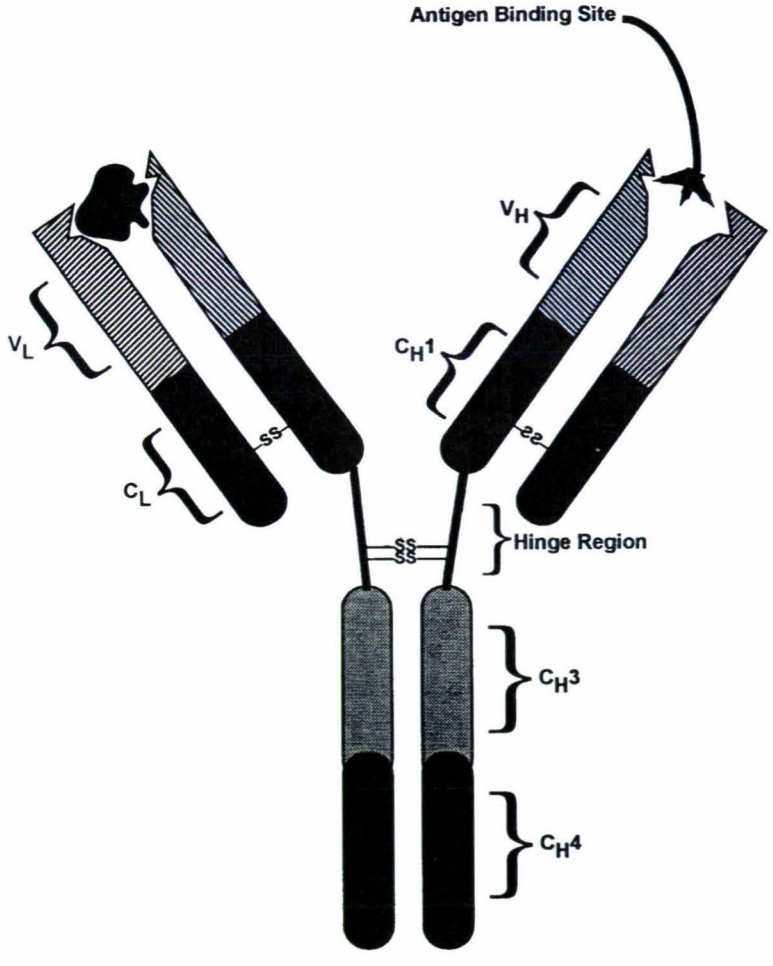

Figure 3.3 Basic four chain subunit common to immunoglobulin molecules illustrating a pair of identical heavy chains consisting of three constant domains (C_H1, C_H2, C_H3) and one variable domain (V_H) linked to a pair of identical light chains consisting of one constant domain (C_L) and one variable domain (V_L). The variable regions of heavy and light chains form the antigen binding sites. Heavy chains are held together by a variable number of disulphide bonds (–S-S-) in the flexible hinge region. Light chains are bound to the amino-terminus of the heavy chains by disulphide bonds [175].

The C_H and C_L domains of the heavy and light chains respectively are relatively constant in sequence with varying degrees of glycosylation, and are normally responsible for the effector functions of the antibody. i.e. its binding to the series of proteins (complement) and cells involved in mediation of immune reactions. The V_H and V_L domains however vary in amino acid sequence between antibodies of different specificity. Within the variable domains of each chain there are three areas of hypervariable sequence, known as complementarity determining regions (CDRs), each forming a loop structure joined by a framework of β-sheets. The six CDRs on each arm (i.e. H1, H2, H3 and L1, L2, L3) of the antibody "Y" together form the antigen binding sites.

There are five major classes of immunoglobulins, IgG, IgM, IgA, IgD and IgE, which differ on the basis of size, charge, amino acid composition and carbohydrate content. IgG is used almost exclusively in all types of steroid immunoassays since it is produced in the highest yield in response to immunisation and binds with high affinity to the hapten that stimulated its synthesis. It is this type of immunoglobulin that is specific for the steroid glucuronides being studied here. Treatment of IgG with the proteolytic enzyme papain results in cleavage of the molecule in the hinge region yielding three fragments (Figure 3.4).

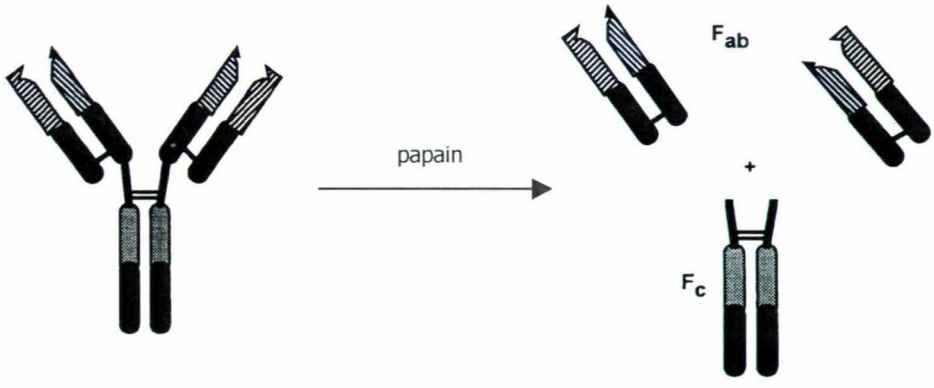

Figure 3.4 Pattern of protein fragments after enzymatic cleavage of IgG with papain [175].

Two of these fragments retain the antigen binding sites and are known as Fab fragments (Fragment, antigen binding). Each Fab fragment contains one combining site for the antigen or hapten, and has a similar binding affinity for the hapten as did the intact IgG molecule. The remaining fragment consists of the constant portion of two H chains, and is called Fc since it is readily crystallised, but has no affinity for the antigen.

The first X-ray crystal structure which demonstrated the way in which a steroid molecule binds to its corresponding antibody was solved in 1993 by Arevalo and co-workers [176] using a progesterone bound Fab immune complex. Binding of progesterone to the Fab fragment occurred via insertion of the relatively flat surface of the steroid B, C and D rings (shown in

Figure 3.5) into a narrow hydrophobic binding pocket formed by the H1, H2 and H3 hypervariable loops of the H chain and the L1 and L3 hypervariable loops of the L chain. When bound by the Fab fragment the steroid was almost completely buried (89%) by the binding site and specific recognition of the steroid was enforced by hydrogen bonding interactions between the binding domain on the protein and functional groups on the steroid [176].

Using the crystallographic data from the progesterone Fab complex, Smales [124] generated 3D models of the tertiary structures of pregnanediol glucuronide-HEWL-Fab immune complexes by overlapping the pregnanediol glucuronide (PdG) moiety of the lysozyme conjugates with the steroid co-ordinates from the progesterone-Fab immune complex. To ensure that the PdG-HEWL steroid moiety was oriented into the binding site in the same manner as the progesterone molecule, only those carbon atoms that were common to both steroids (marked with an asterix in Figure 3.5) were overlapped using a least squares fitting program.

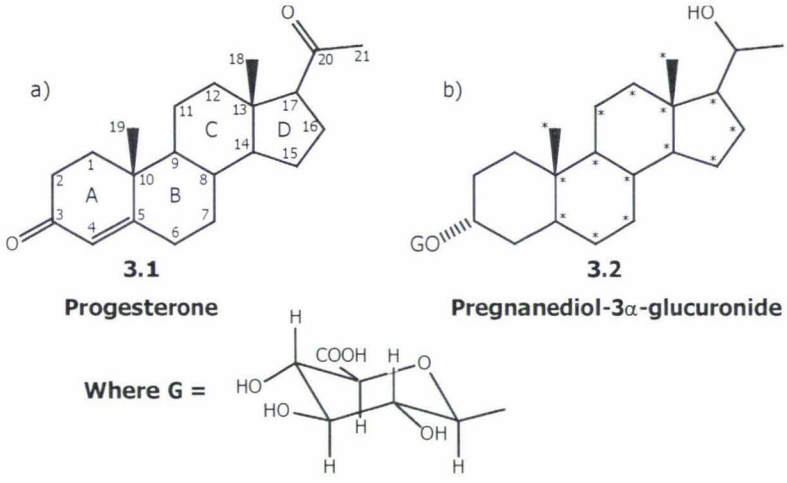

Figure 3.5 The structures of a) the progesterone steroid moiety from the progesterone-Fab complex and b) pregnanediol-3α-glucuronide. The carbon atoms of pregnanediol 3α-glucuronide overlapped with those of the progesterone structure using the least squares fit program are marked with an asterix (*).

Figure 3.6a depicts antibody binding to the steroid moiety of a PdG-HEWL conjugate mono-acylated at lysine 116. The model shows that when bound to a PdG moiety attached to lysine 116, the Fab fragment does not completely cover the enzymes active site which lies more or less directly below the PdG moiety. It does however protrude outwards from the lysozyme surface, thus preventing the approach of the giant *Micrococcus lysodeikticus* molecule close enough to the enzymes active site to allow binding and lysis of the cell wall polysaccharide. The steric hindrance by the antibody is more clearly observed in Figure 3.6b where the immune complex is viewed from the other side of the enzyme molecule, and the Fab moiety can be seen protruding outwards a considerable distance directly in front of the active site cleft [124].

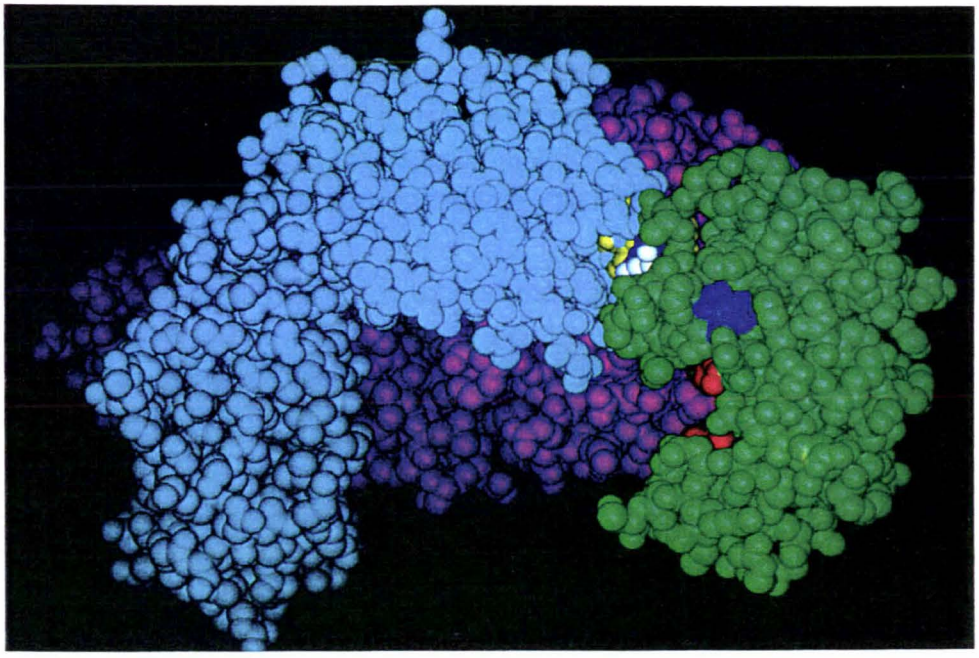

Figure 3.6a Computer generated space-filling representation of the PdG-HEWL anti-PdG antibody immune complex where the PdG moiety is acylated to lysine 116, and the active site cleft is oriented to the left hand side. The lysozyme molecule is shown in green, the PdG moiety is coloured yellow and the two catalytic residues of lysozyme are highlighted in red. The heavy chain of the Fab fragment is coloured purple and the light chain is coloured pastel green. Lysine 33 is highlighted in blue [124].

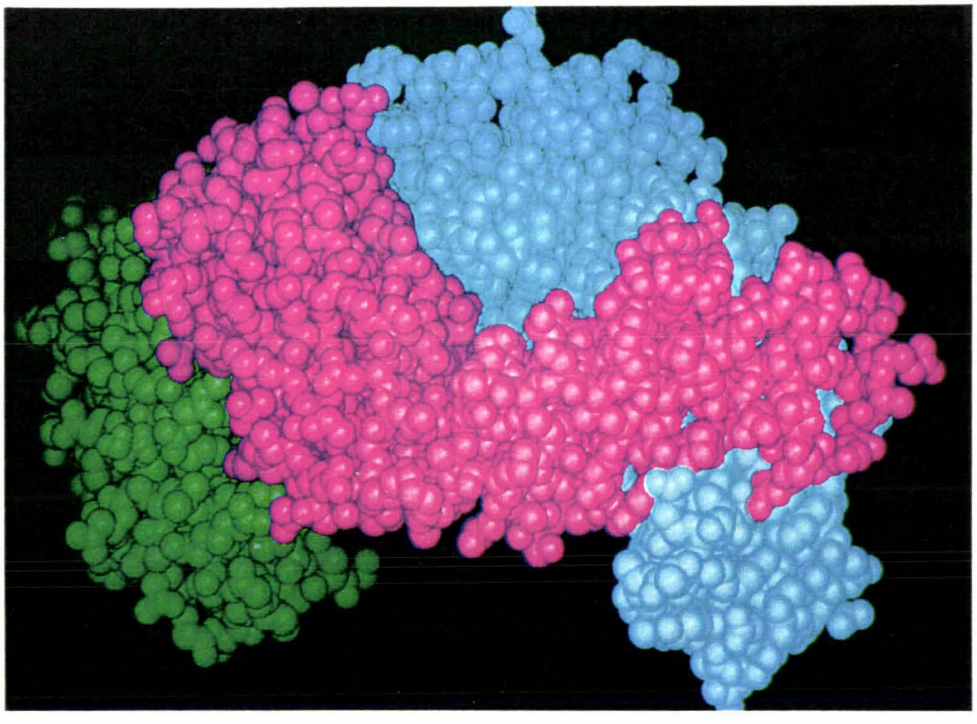

Figure 3.6b Computer generated space-filling representation of the PdG-HEWL anti-PdG antibody immune complex where the PdG moiety is acylated to lysine 116 and the active site cleft is orientated on the right hand side. The colours are coded as in Figure 3.6a [124].

A similar situation exists for the PdG-HEWL immune complex modelled by binding the Fab fragment to PdG attached to lysine 97 since the majority of the Fab structure lies orientated in a similar way to that seen when it is bound to a PdG molecule attached to lysine 116.

When the PdG moiety was acylated to lysine 33 of the lysozyme molecule, the bound Fab fragment lay in almost the same plane as the enzyme. In this orientation, the light chain of the Fab fragment may protrude slightly outwards and forward from the surface with respect to the active site. Several residues of the heavy chain also lay in close proximity to the enzyme active site and the catalytically active lysozyme residues. Thus the binding of the Fab structure to the lysine 33 PdG moiety is also expected to inactivate the lytic activity by preventing the substrate from approaching the active site close enough to allow productive binding and subsequent lysis of the cell wall.

Lysine residues 1 and 13 are not acylated by either the active ester or mixed anhydride coupling methods used to prepare PdG-HEWL (nor E1G-HEWL) conjugates for use in the Ovarian Monitor assay. The importance of this to the success of the assay can best be described by the computer generated 3D structure shown in Figure 3.7.

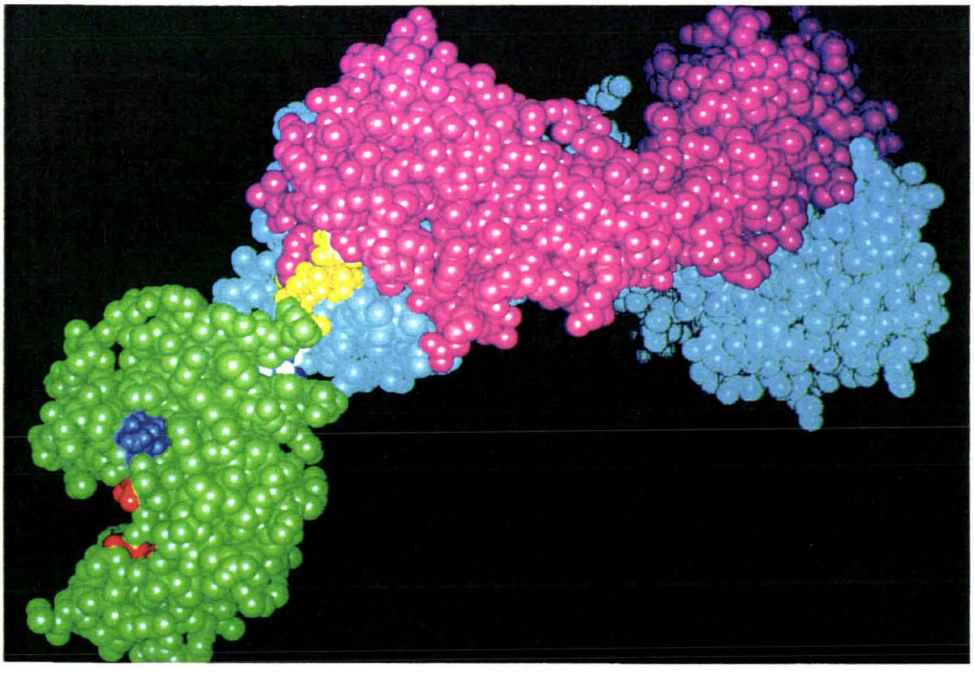

Figure 3.7 Computer generated space-filling representation of the PdG-HEWL anti-PdG antibody immune complex where the PdG moiety is acylated to lysine 13. The colour coding is as described in legend 3.6a [124].

In this model the PdG moiety is attached to the lysozyme molecule at lysine 13 and shows that the Fab fragment is bound on the opposite side of the molecule with respect to the active site. Similarly, lysine residue 1 (not shown in Figure 3.7) is also located on the opposite side of the molecule well away from the active site cleft. Thus it is expected that the lytic activity of lysozyme would be unaffected by the binding of the Fab fragment to either lysine 1 or lysine 13 since it cannot sterically inhibit the approach of the large bacterial substrate to the active site. If these lysine residues were acylated it would result in conjugates whose lytic activity could not be inhibited to any great extent upon binding of an anti-hapten antibody. Hence the coupling methods used to attach the steroid glucuronide to lysozyme by acylation of the lysine residues are ideal since only highly inhibitable conjugates are obtained.

3.1.3 The immune response *in vivo* and purification of the resulting antibodies

Classically, the immune response is described as occurring in two phases. Initial administration of the immunogen produces a primary phase (response) during which only small amounts of antibody molecules (typically the IgM class) are produced as the antibody-producing system is primed. Further administration of the immunogen results in the secondary phase (response) during which the production of IgM ceases and large amounts of IgG antibody molecules are produced by the large number of specifically programmed lymphocytes. In practice however the time scale and nature of the immunisation schedule often do not allow clear recognition of the two phases [177].

Immunisation with a hapten-protein conjugate generates three types of antibody specificity *in vivo*, as shown schematically in Figure 3.8; (i) specificity for the hapten (H), (ii) for the carrier protein (C) and (iii) for new antigenic determinants created by the conjugation of the steroid hapten to the carrier [121,178].

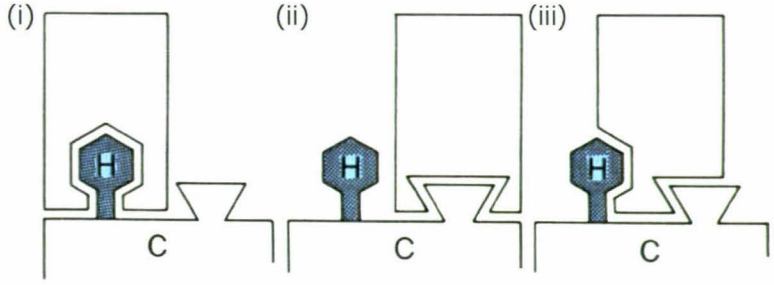

Figure 3.8 Epitopes of a hapten-carrier conjugate. Three types of epitopes may be distinguished by antibodies reacting with the hapten-carrier conjugate: (i) epitopes determined soley by the hapten, (ii) epitopes found only on the carrier, and (iii) new epitopes created by the coupling of hapten and carrier with contributions from both molecules. H represents the hapten of interest and C the carrier protein [178].

Of the total protein content in the serum (70 mg/mL), approximately 40 mg/mL exists as albumin, 12 mg/mL as IgG, and 5 - 6 mg/mL as IgA plus IgM. Only a small proportion of the total IgG content of the serum (1 - 10%) is thought to be specific for the hapten of interest

(Figure 3.8(i)), the remaining proportion is thought to reflect the animals previous exposure to various antigens. The remainder of the serum protein content consists of complement components and other transport proteins such as transferrin and lipoproteins [175].

For most homogenous immunoassays, including the Ovarian Monitor assay, the antisera can be used successfully without the need for purification. Where the antibody is to be labeled with detecting reagent (as is the case for radioimmunoassay), some form of prior purification is essential to avoid the high nonspecific binding caused by other labeled contaminating proteins [179]. In cases of a weak immune response, various purification steps can also be used to concentrate the antibodies to improve the titre and remove any non-specific serum proteins which may otherwise interfere with the assay.

There are four main techniques used to purify IgG from serum. The first, and undoubtedly the cheapest method uses a simple salting out procedure, usually with sodium or ammonium sulphate followed by extensive dialysis or gel filtration to remove the salt. The basis of salt precipitation is that as the salt concentration increases the IgG precipitates because its solubility decreases with increasing ionic strength. Purification results since at certain concentrations of ammonium sulphate (i.e. 1.2 – 1.8 M) immunoglobulins are precipitated, but other proteins such as albumin remain in solution. Caprylic (octanoic) acid precipitation may also be used prior to the ammonium sulphate step to precipitate non-IgG protein and improve the purity of the final product. Using the combined octanoic acid/ammonium sulphate precipitation method IgG can be obtained from antiserum with about 80 - 90% purity, which is sufficient for most purposes [179]. Some immunoglobulins will however always remain in solution; hence the yield is critically dependent upon the starting concentration of IgG. Care also needs to be taken to remove all the ammonium sulphate since this may interfere with the assay and ammonium ions may reversibly compete with many amino coupling reagents used for antibody labeling techniques. Precipitation methods can be used also as the preliminary step to the more expensive chromatography-based purification procedures where a high degree of purity is required.

The second method is based on gradient ion exchange techniques, which can give higher purity (>90%) than salt fractionation [180], but the method is more time consuming and considerably more expensive. The method is however widely used and works on the principle that IgG has a higher or more basic isoelectric point than most serum proteins. Therefore if the pH is kept below the isoelectric point of most antibodies, the immunoglobulins do not bind to an anion exchanger and are separated from the majority of the serum proteins bound to the column matrix. The yield is usually excellent, even with relatively low concentrations of antibody [179], and the high capacity of anion-exchange columns allows for large-scale purification of IgG from serum. Examples of anion exchange matrices include the reactive group diethyaminoethyl

(DEAE) covalently linked to Sepharose, which can be purchased pre-swollen and ready for packing. Other matrices (e.g. DEAE cellulose) are provided as solids, and thus require preparation and equilibration prior to use. Anion exchange can be carried out either using a laboratory prepared column that is washed and eluted under gravity, or by using high performance liquid chromatography (HPLC) and fast-performance liquid chromatography (FPLC) systems [181]. The latter method provides improved reproducibility (due to the automated pumps and timers), speed (because of the small, high capacity columns available) and increased resolution (due to the fine resins and quality control systems).

The third method takes advantage of the specific and reversible binding of the Fc region of antibodies to Protein A produced by some strains of *Staphylococcus aureus* or Protein G produced by some strains of *Streptococci* [182]. Crude antibody is passed through a column containing the protein immobilised on Sephadex or agarose beads. After washing the column, IgG is eluted using a low pH buffer to dissociate the complex. The technique is capable of producing antibody in high yield and purity, but is expensive and therefore may be out of reach of small laboratories. Protein A affinity chromatography however has substantial industrial applications in terms of the purification of high value antibodies for diagnostic or therapeutic use [183].

All of the above techniques isolate total IgG non-specifically. Immunoaffinity chromatography depends upon the immunological specificity of the antibodies, and thus can be used to purify only those IgG molecules in the serum specific for the antigen of interest (i.e. the steroid hapten). The antigen is covalently coupled to an inert support matrix (commonly Sepharose) and the crude antibody is passed through the column at a relatively low flow rate to allow the antibody to complex with the immobilised antigen. After extensive washing of the solid phase to remove everything which does not bind to the antigen, the specific antibody is eluted by disruption of immunological non-covalent binding by either an acidic buffer (pH 2.0), dilute ammonia or high concentrations of a chaotropic agent such as thiocyanate or pyrophosphate [184]. A variant of the method, immunoadsorption, can also be used to remove unwanted antibody. For example, antibodies to rabbit IgG can be purified by first using immunoaffinity chromatography with rabbit IgG, and then by passing down a column of immobilised human IgG to remove any antibody strongly cross reacting with human IgG [179]. While the inclusion of immunoaffinity/adsorption chromatography techniques to purify antibodies has been widely used on a laboratory and industrial scale [183] certain problems do exist. These include the denaturation of the antibody by the dissociating agents and the possibility that antibodies with very high affinity for the antigen may not be eluted readily from the immunoadsorbent. Many immunoaffinity columns also use monoclonal antibodies thus the success of the method relies on developing a method that produces large quantities of monospecific antiserum which can be immobilised onto the column. The generation and immobilisation of the monoclonal antibodies

is an expensive exercise, requiring a great deal of technical expertise. Despite such drawbacks, immunoaffinity is probably the most specific of all forms of biospecific chromatography available.

3.1.4 Features of an optimised Ovarian Monitor assay curve

An optimised standard curve (as shown in Figure 1.6 for E1G) is one which responds to low concentrations of free hormone by giving a clearly visible increase in the rate of lysis above the baseline (or zero standard) rate. This concentration, which determines the assay sensitivity, should be such that the steepest section of the curve which follows the baseline period lies within the physiological concentration range of hormone excreted in the urine. The general shape of the standard curve may be different for each of the different conjugate populations produced by the active ester method since this depends on the combined affinities of the antibodies for the conjugate, and thus must be optimised for every new combination of antibodies and conjugates.

To establish the optimal standard curve for a given TG-HEWL or THEG-HEWL conjugate involves firstly determining the concentration of conjugate required to give an optimal change in transmission over the assay period, which for the Ovarian Monitor is about 350 transmission units. Using this concentration the conjugates are then titrated against the various anti-TG and anti-THEG antisera to determine the lowest volume of antiserum which gives maximum inhibition (ideally > 95%) of the enzyme lytic activity. The optimal antibody and conjugate combination can then be used to generate a skeleton standard curve by measuring the change in transmission in the presence of a set of hormone standards of known concentration. Skeleton titration curves, i.e. standard curves constructed using only a few selected concentrations of hormone, can then be used to screen a range of antiserum concentrations at a given concentration of conjugate for their potential to produce a standard curve with the desired shape and sensitivity limits. If the standard curve constructed from these data demonstrates maximal sensitivity within the normal physiological range it can then be used for determination of the daily excretion rate (μmol 24 hr^{-1}) of hormone in the urine. It is then a candidate for incorporation into assay tubes (Figure 1.5b) and use in a multi-purpose Monitor system.

Thus the main aims of this chapter were to:

1. Compare the performance of the different conjugates for their relative potential as signal generators

2. Screen the anti-steroid rabbit antibodies collected over a number of months for their ability to inhibit lysis activity and thus select a suitable antiserum with which to establish a

standard curve. In the case of a weak antibody titre, and if the volume of serum obtained allows, use caprylic acid/ammonium sulphate precipitation to remove non-specific proteins and concentrate the IgG fraction.

3. Optimise the shape and working range of the TG and THEG standard curve to allow measurement of the physiological concentration of steroid glucuronide observed in the urine.

3.2 Experimental

3.2.1 Apparatus

Micrococcus lysodeikticus was homogenised in buffer using a two-piece glass homgoeniser and sonicated for 5 minutes using a Bandelin Sonorex RK-100 sonicator. Each assay was performed in plastic 1 mL cuvettes (Adindas Plastics, Melbourne, Australia) designed specifically for use in the Ovarian Monitor. The Ovarian Monitor and heating block were obtained from St Michael Natural Family Planning services Pty (Victoria, Australia). Glass syringes were manufactured either by the Hamilton Company (Reno, NV, USA) or Scientific Glass Engineering Pty Ltd (Melbourne, Australia). A 500 μL syringe fitted with a stepper apparatus (supplied by the Hamilton Company) was also used to allow repeated release of 10 μL aliquots of *Micrococcus lysodeikticus* substrate from a single 500 μL aliquot. Mixing of assay reagents in the assay tubes while performing the assay was achieved using a Chiltern bench-top vortex.

3.2.2 Reagents

Lyophilised *Micrococcus lysodeikticus* cells and testosterone-17β-glucuronide used for generation of the testosterone glucuronide standard curves were obtained from Sigma Chemical Co (St. Louis, MO, USA). Octanoic acid ($C_8H_{16}O_2$) was obtained from BDH (Poole, England). Saturated ammonium sulphate (4.05 M at 25 °C) was prepared by dissolving 761 g of ammonium sulphate (minimum assay 99.5%, Scharlau Chemie, Barcelona, Spain) in 1 L of Milli-Q water. Once the entire solid had dissolved, the solution was stirred for a further 24 hours, after which the pH was adjusted to 7.0 with ammonia or sulphuric acid as required.

Dialysis tubing, centrifuges and tris-maleate buffer used in the following chapter are as described in section 2.2.1 and 2.2.2.

3.2.3 Animals

Four New Zealand white rabbits (two males and two females) were obtained for the study by Debbie Chesterfield, Manager, Massey University Small Animal Production Unit (SAPU).

3.2.4 Methodology

3.2.4.1 Production of polyclonal anti-TG and anti-THEG antibodies in New Zealand white rabbits

All polyclonal testosterone glucuronide and tetrahydrocortisone glucuronide antisera were raised in NZ white rabbits by Debbie Chesterfield (Manager, Small Animal Unit (SAPU), Massey University) according to Massey University Animal Care guidelines using hapten-thyroglobulin conjugates synthesised in section 2.2.3.11 by the active ester method [55]. Ethical permission for the trial was obtained from the Massey University Animal Ethics Committee.

In total, four (two male and two female) adult New Zealand white rabbits were included in the study. One male (code named B52, body weight (BW) 4.9 Kg) and one female (B41, 4.7 Kg) were immunized with the TG-THY immunogen conjugates. The other male (L57, 3.7 Kg) and female (B42, 5.6 Kg) rabbits in the group were immunised with THEG-THY immunogen conjugates.

The primary immunisation consisted of 3.5 mg protein equivalent (or approximately 0.43 mL) of hapten-THY conjugate in 0.01 M NaCl thoroughly emulsified in an equivalent volume of Freund's complete adjuvent (CFA). The emulsion was injected subcutaneously at multiple (2 - 3) sites on the neck of each rabbit and dispersed by gentle rubbing. Three weeks after the primary immunisation, the first booster immunisation was given, followed by five more boosts at approximately 4 week intervals. The first two booster injections consisted of 2.0 mg protein equivalent (or 0.25 mL) of the hapten-THY immunogen emulsified with 0.25 mL incomplete Freund's adjuvent (IFA). On the 10^{th} day after each booster injection, 3 - 5 mL of blood was drawn from the marginal ear vein into a glass centrifuge tube to monitor polyclonal antibody production. Because of the relatively poor immunogenic response from the test bleed following the second booster immunisation, the booster dose was increased to 4 mg protein equivalent (or 0.5 mL) of hapten-THY immunogen solution emulsified with an equivalent volume of IFA for the last three booster shots. The final bleed was collected by heart puncture. At the time of exsanguination, all the rabbits were in good health, with the exception of rabbit L57 (immunised with THEG-THY), which had lost its appetite due to the formation of an abscess and localised swelling at the injection site. Despite treating the abscess, the rabbits' health failed to improve. As a result rabbit L57 was exsanguinated two weeks earlier than the other rabbits. The antisera collected 10 days after each booster injection were numbered consecutively from B1 (first antiserum collected after the primary immunisation) to B6 (final antiserum collected at the end of the study by heart puncture). For example, B52-B3 refers to the third test serum (B3) collected from rabbit B52.

To remove the red blood cells from each test sample the blood was allowed to coagulate for one hour at 37 °C. The clot was then separated from the walls of the tube using a glass Pasteur pipette and left to stand overnight at 4 °C to allow the clot to contract. The serum was then decanted and centrifuged (13,000 rpm for 25 mins at 4 °C), and stored as conveniently sized aliquots (0.3 - 0.5 mL) at –20 °C until required.

3.2.4.2 Antibody purification by octanoic acid and ammonium sulphate precipitation

(a) Octanoic acid precipitation

Rabbit serum collected at exsanguination by heart puncture (typically 40 - 70 mL after removal of red blood cells) was gently stirred with two volumes of 60 mM acetate buffer (pH 4). After adjusting the pH of the solution to 4.8 using 1 M NaOH, octanoic acid (0.75 mL per 10 mL of original serum volume) was added slowly dropwise while vigorously stirring the solution at room temperature (taking care to avoid bubbles and frothing) to afford a milky white precipitate. The solution was stirred for a further 30 minutes and centrifuged at 5000 rpm for 30 mins at 10 °C. The supernatant was then decanted, adjusted to pH 5.7 with 1 M NaOH and dialysed (6 x 2 L) against 10 mM tris-maleate buffer (pH 7.0) at 4 °C.

(b) Ammonium sulphate precipitation

Saturated ammonium sulphate (4.05 M, 0.5 volume) was added slowly to a stirred solution of dialysed serum cooled on ice, followed by overnight stirring at 4 °C to afford a small amount of white precipitate. After centrifuging the solution at 3000 rpm for 30 mins, the supernatant was carefully decanted and stirred gently with additional saturated ammonium sulphate (0.5 x the original volume of dialysed serum) and stirred overnight at 4 °C to precipitate the IgG fraction. The precipitate was collected by centrifuging at 3000 rpm for 30 minutes, re-suspended in a minimum amount of Milli-Q water and dialysed extensively (8 x 1 L) against 10 mM tris-maleate buffer (pH 7.0). After centrifuging (5000 rpm for 30 mins) to remove any undissolved precipitate, the IgG solution was stored at –20 °C in conveniently sized aliquots until required.

3.2.4.3 Standard lytic assay protocol

a) Preparation of Substrate

The suspension of *Micrococcus lysodeikticus* (*M. lysodeikticus)* cells was prepared fresh daily by manually homogenising lyophilised *M. lysodeikticus* (30 mg) in 75 mM tris-maleate buffer (4 mL, pH 7.0) in a two piece glass homogeniser. When a pale yellow, visually uniform suspension was observed the solution was transferred into a scintillation vial and sonicated for 5 minutes to completely homogenise the solution. The *M. lysodeikticus* solution was kept on ice throughout the day and resonicated every few hours.

(b) Lytic activity assay protocol

In the first step, aliquots (0 - 45 μL) of HEWL conjugate (diluted between 1:50 and 1:200 with 0.35 M tris-maleate buffer, pH 7.0) were dispensed into an empty Ovarian Monitor assay tube and diluted to 340 μL total volume with 40 mM tris-maleate buffer (pH 7.0). The tubes containing the diluted enzyme sample were then incubated in a custom-made stainless steel incubation block at 40 °C for 5 minutes. To initiate the assay 10 μL of the bacterial substrate

(*Micrococcus lysodeikticus)* was added via a stepper syringe. Immediately after addition of the substrate, the reaction mixture was vortexed for 2 - 3 seconds using a bench top vortex mixer and placed in the Ovarian Monitor cell holder. The initial transmission ($T_{0\ min}$) was recorded (at 650 nm) after shutting the cell holder lid followed by the final transmission five minutes later ($T_{5\ min}$). The rate of reaction was reported as the difference ($T_{5\ min}$ - $T_{0\ min}$) in transmission over the 5 minute assay period ($\Delta T\ 5\ min^{-1}$) and plotted as a function of HEWL concentration (nM). The data were fitted after non-linear regression analysis (one site binding hyperbola) using GraphPad prism (version 2.00) software. All assays were performed in duplicate.

When assaying multiple samples (for example multiple dilutions of a particular conjugate), the assay tube was transferred from the Ovarian Monitor cell holder after recording $T_{0\ min}$ and incubated for 5 minutes in a heating block. This freed up the Ovarian Monitor to be used for reading $T_{0\ min}$ of the next assay tube. In this instance, a separate timer and recording sheet were used to determine when the 5 minute incubation period for each sample tube had ended.

3.2.4.4 Inhibition studies

In order to standardise the volume of conjugate which was added to the assay tube each steroid glucuronide-HEWL conjugate was diluted such that a 10 μL aliquot gave a change in transmission of approximately 350 units over 5 minutes in the standard lytic activity assay.

Studies to determine the inhibition of conjugate activity by antibodies raised in section 3.2.4.1 were carried out as follows: A HEWL-conjugate solution (10 μL of the appropriate dilution) and antiserum (between 2 and 90 μL of neat antiserum depending on the titre) were placed in opposite corners of an Ovarian Monitor assay tube. The total volume was made up to 100 μL with 40 mM tris-maleate buffer (pH 7.0) and the resulting solution was briefly mixed using a bench top vortex mixer. The tube was then warmed for 5 minutes at 40 °C in an incubation block to allow the antibody to bind to the conjugate. At the end of the initial incubation period the total volume was increased to 340 μL with 40 mM tris-maleate buffer (pH 7.0) and incubated for a further 5 minutes at 40 °C. The remainder of the assay procedure was performed as described in section 3.2.4.3. All assays were performed either in triplicate or duplicate and the results were expressed as a percentage inhibition of the control rate (i.e. rate of substrate lysis in the absence of antiserum). GraphPad Prism software (version 2.00) was used to plot the data and obtain the best-fit curve using non-linear regression analysis (one-site binding hyperbola).

3.2.4.5 Clearing curves

The change in transmission versus time plot for each conjugate at the concentration giving a ΔT 5 min^{-1} of approximately 350 was recorded using the standard lytic assay protocol, with the exception that after the addition of substrate the transmission reading was recorded at 5 second intervals throughout the entire 5 minute incubation period.

3.2.4.6 Standard curves for the determination of urinary testosterone glucuronide

Testosterone glucuronide stock solution (1493.89 μM) was prepared by dissolving commercially available TG (3.47 mg, 7.47 μmol, initially dissolved in 100 μL of methanol) with 10 mM tris-maleate buffer (pH 7.0). Aliquots of the stock TG solution were then diluted with 10 mM tris-maleate buffer (pH 7.0) to give a series of standards ranging from 0.00028 – 1111.11 μmol TG L^{-1} which is equivalent to 0.001 – 4000 μmol TG 24 hr^{-1} since the mean urine volume passed in 24 hours is 3.6 L.

Lytic assays to generate standard curves for TG were performed essentially as described in section 3.2.4.4 with the following exceptions. In the first step 50 μL of TG standard (0.001 to 4000 μmol 24 hr^{-1}) and 5 - 10 μL of antiserum were added to each tube with vortex mixing and incubated for 5 minutes at 40 °C. At the end of the incubation period the total volume was made up to 330 μL with 40 mM tris-maleate buffer (pH 7.0). An aliquot (10 μL of the appropriate dilution) of TG-HEWL conjugate was added to each tube with vortex mixing, followed by incubation for 10 minutes at 40 °C. The remainder of the assay was performed as described in section 3.2.4.4.

3.2.4.7 Effect of the urinary matrix on the working range of the testosterone glucuronide standard curve

To determine the effect of a urinary matrix on the working range of the testosterone glucuronide standard curve, 50 μL of female urine (diluted to the standard 150 mL hr^{-1} of collection) was incubated for 5 minutes at 40 °C with 50 μL of TG standard and 5 μL of antiserum. The remainder of the assay was performed as for the TG standard curve described in section 3.2.4.6.

3.2.4.8 Standard curves for the determination of urinary tetrahydrocortisone glucuronide

A tetrahydrocortisone glucuronide stock solution (6587.08 μM) was prepared by dissolving commercially available THEG (3.65 mg, 6.75 μmol, initially dissolved in 50 μL of methanol) with 10 mM tris-maleate buffer (pH 7.0). Aliquots of the stock THEG solution were then diluted with 10 mM tris-maleate buffer (pH 7.0) to give a series of standards ranging from 0.084 – 841.67 μmol THEG L^{-1} (0.303 – 3030 μmol 24 hr^{-1}).

Lytic assays to generate the standard curves for tetrahyrocortisone glucuronide were performed essentially as described in section 3.2.4.4 with the following exceptions. In the first step 50 μL of THEG standard (0.303 to 3030 μmol THEG 24 hr^{-1}) and between 2 and 100 μL of neat antiserum depending on the titre were added to each assay tube and gently vortex mixed followed by incubating for 5 minutes at 40 °C. At the end of the incubation period, the total volume was made up to 330 μL with 40 mM tris-maleate buffer (pH 7.0). A 10 μL aliquot of appropriately diluted THEG-HEWL conjugate was then added to each tube with vortex mixing followed by incubation for 10 minutes at 40 °C. The remainder of the assay was performed as described in section 3.2.4.4.

3.2.4.9 Fitting of the testosterone glucuronide and tetrahydrocortisone glucuronide standard curves

The standard curve was generated for each combination of antiserum and conjugate by plotting the change in transmission (ΔT 5 min^{-1}) versus the logarithm of the analyte concentration. Using GraphPad Prism (version 2.00) software, the curves were fitted to a Boltzman sigmoidal dose response curve with a variable slope which can be expressed by the following four parameter logistic equation:

$$Y = \text{Bottom} + \frac{(\text{Top} - \text{Bottom})}{1 + 10^{(\log EC_{50} - X).\text{Hill slope}}}$$

Equation 3.1

where Y represents the assay rate, measured by the change in transmission in five minutes (ΔT 5 min^{-1}) and X represents the time diluted urinary TG concentration, expressed as μmol 24 hr^{-1}. Top and Bottom refer to the Y values at the top and bottom plateaus of the standard curve respectively and EC_{50} refers to the steroid concentration halfway between the maximum and minimum rates (i.e. halfway between the top and bottom plateau). The Hill slope variable is unitless and represents the slope of the curve. When the Hill slope = 1, the equation generates a standard dose response curve for which the response shifts from 10% to 90% of the maximum rate (ΔT_{max}) over approximately two log units. Thus when the Hill slope is less than 1.0 the curve is more shallow, and a Hill slope greater than one results in a steeper standard curve.

3.3 Results and Discussion

3.3.1 Polyclonal antibody production

Polyclonal antibodies against TG and THEG were raised in New Zealand White rabbits by Debbie Chesterfield at the Small Animal Production Unit (SAPU) Massey University using the thyroglobulin-steroid glucuronide conjugates prepared in section 2.2.3.11. Typically the volume of antiserum collected from the marginal ear vein ten days after each booster was ~5 mL, and this was reduced to ~2.5 mL of serum after clotting and centrifuging to remove the red blood cells. At the time of exsanguination between 80 - 140 mL of serum was obtained from each rabbit, which was reduced to 40 - 70 mL after removal of the red blood cells. As described in section 3.2.4.1 the antisera collected 10 days after each booster injection were numbered consecutively from B1 (first antiserum collected) to B6 (final antiserum collected at exsanguination).

3.3.2 Lytic activity of the TG-HEWL and THEG-HEWL conjugates

As discussed in Chapter One, the Ovarian Monitor assay system relies on the accurate measurement of the total change in transmission (at 650 nm) over a fixed time period (for example $\Delta T\ 5\ min^{-1}$) of a turbid suspension of *M. lysodeikticus* substrate cells (214 mg L^{-1} in the assay tube). The parameter $\Delta T\ 5\ min^{-1}$ is calculated by subtracting the change in transmission recorded by the monitor at time zero ($T_{0\ min}$) from the change in transmission recorded at five minutes ($T_{5\ min}$) or any other convenient time period. In the present work 5 minutes was chosen as a convenient and practical measurement time. Because previous studies [185] show that the greatest photometric accuracy of the Ovarian Monitor readings occurs between 200 and 600 transmission units, the concentration of substrate added to initiate the reaction was chosen to give an initial transmission ($T_{0\ min}$) value of between 200 - 220. To determine the optimal conjugate concentration to lyse this level of substrate sufficiently, the concentration of TG-HEWL or THEG-HEWL in the assay tube was gradually increased until the final transmission reading ($T_{5\ min}$) reached ~550 units. Thus the final change in transmission (ΔT) was within the range of 300 - 350 units over the five minute assay period. This change in transmission is considered optimal for standard curve production since it gives the greatest difference between the zero standard and the maximum steroid concentration while remaining within the accuracy limits of the monitor.

The dependence of the lysis rate ($\Delta T\ 5\ min^{-1}$) for a constant concentration of *M. lysodeikticus* substrate solution on the concentration of TG-HEWL and THEG-HEWL conjugates is shown in Figures 3.9 and 3.10 respectively. The fact that each lytic curve fitted equally well to a one-site binding hyperbolic equation (R^2 for TG1 and TG2-3 was 0.997; for TH1, R^2= 0.992; and for TH3, R^2 = 0.996) showed the relationship between the observed lysis rate and the enzyme

concentration as measured under the above conditions was essentially the same for all four conjugates.

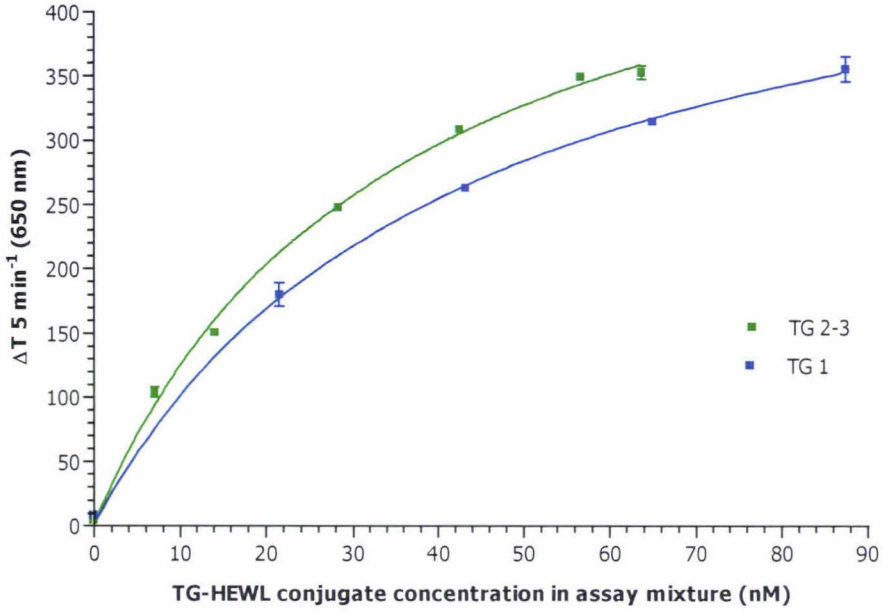

Figure 3.9 Relationship between lysis rate (ΔT 5 min^{-1} at 650 nm) and concentration of testosterone glucuronide-hen egg white lysozyme conjugates TG1 and TG2-3 using a 5 minute end point assay.

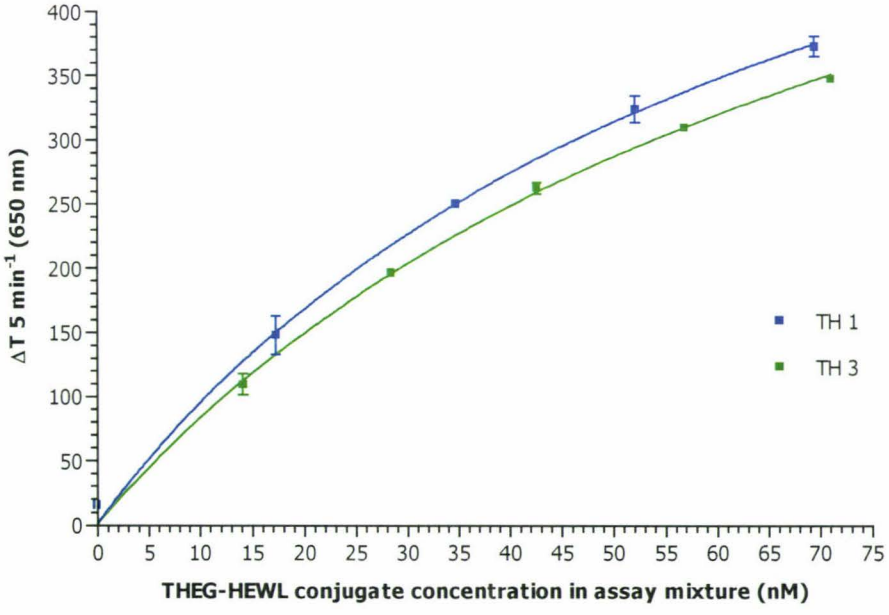

Figure 3.10 Relationship between lysis rate (ΔT 5 min^{-1} at 650 nm) and concentration of tetrahydrocortisone glucuronide-hen egg white lysozyme conjugates TH1 and TH3 using a 5 minute end point assay.

Although the concentration versus transmission profiles were of similar shape, the magnitude of the specific activity (in units per mg of protein) of the TH1 and TG2-3 conjugates was significantly elevated compared to the TG1 and TH3 conjugates respectively and the relative difference increased with increasing enzyme concentration. The final enzyme concentration in the assay tube required to reach the optimal ΔT 5 min^{-1} of 350 units was 85.5 nM of TG1 compared to 59.5 nM of TG2-3, thus the TG2-3 conjugate had a much higher specific activity. In comparison the THEG conjugates had relatively similar specific activities since 61.0 nM of TH1 and 71.1 nM of TH3 were required to reach the desired lysis rate. The extra TG1 and TH3 conjugate required to increase the lysis rate to the optimal value means that more antiserum will be required to maximally inhibit their lytic activity, thus making them potentially less sensitive and hence less suitable for use in the homogenous immunoassay. This is because a higher concentration of free steroid would be required to bind to the extra antiserum before a significant increase in the free conjugate concentration, and hence an increase in the lysis rate above the baseline value could be observed.

It is well known that the electrostatic attraction between the normally highly basic lysozyme surface and the negatively charged bacterial cell wall is important for binding and subsequent lytic activity of the conjugates [186]. Previous studies with pregnanediol glucuronide (PdG) and estrone glucuronide (E1G) HEWL conjugates have shown that monosubstituted conjugates have specific activities close to that of native HEWL, whereas higher substituted conjugates have progressively lower specific activities as the degree of substitution increases [112]. Evidence that charge effects are responsible for the differences in relative specific activity is provided by Habeeb and Atassi [110]. These authors showed that that substitution of four or more lysine residues with neutral or negatively charged moieties removes all enzyme activity. On the other hand when the lysine residues were acylated with a positively charged guanidine molecule the specific activity was much less affected. Furthermore the magnitude of the reduced activity is thought to be dependant not only on the total number of acylated residues but also on the site of conjugation, with conjugation of those lysine residues closest to the binding site cleft having the greatest potential to reduce the enzymes activity.

The MALDI mass spectra (described in section 2.3.4.5) suggested that conjugates TH1 and TH3 were homogenous and both acylated at a level of one steroid glucuronide molecule per lysozyme molecule. This was consistent with previous acylation studies with estrone glucuronide (E1 and E3) and pregnanediol glucuronide (P1 and P3) lysozyme conjugates. It is not known which lysine residue is acylated in TH3, but it is likely to be lysine 33 based on its order of elution with respect to lysozyme by cation-exchange chromatography as found previously by Smales [112,162]. Thus, the location of the THEG residue is unlikely to be the major cause of the lower specific activity for TH3. It is more reasonable therefore to propose

that the reduced specific activity is due to the presence of some denatured conjugate resulting from the isolation and purification procedure.

The MALDI spectrum for the TG2-3 conjugate (Figure 2.14b) showed that it contained a small amount of disubstituted conjugate as expected on the basis of the S-Sepharose fractions pooled in section 2.3.4.2. Given that the disubstituted TG-HEWL conjugate mixture would have a lower overall positive charge, the TG2-3 conjugate mixture was expected to show reduced activity compared to the monosubstituted TG1 conjugate. However the opposite was observed, the specific activity of the conjugate TG2-3 conjugate being ~32% higher than the TG1 conjugate, suggesting that in the present case at least, there was no extra loss in enzymic activity by neutralisation of two positively charged lysine residues. Without further information on the site and orientation of the steroid moieties from tryptic digest experiments and a crystal structure of each conjugate, it is not possible to explain fully the reduced specific activity of TG1 compared to TG2-3. It is possible that more denatured enzyme is also present in the TG1 conjugate preparation compared to the TG2-3 preparation. The presence of more denatured enzyme would effectively increase the protein concentration of the conjugate solution determined by the Coomassie assay and because the denatured enzyme is inactive the change in transmission per mg of protein will be lower.

Overall, the active ester testosterone glucuronide conjugates showed 30% (for TG1) and 14% (for TG2-3) lower specific activities than the corresponding THEG conjugates TH1 and TH3. Smales *et al.* [112,162] also noted a difference between the lytic ability of the estrone glucuronide (E1G) and pregnanediol glucuronide (PdG) HEWL active ester conjugates when there were two steroid moieties attached. Disubstituted PdG conjugates had a specific activity only 75% of unreacted lysozyme compared to the E1G conjugates whose specific activity was 88% that of the unreacted lysozyme. It was thought that the reduced activity of the PdG conjugate (compared to the E1G conjugate) was due to the greater increase in the enzymes hydrophobic character associated with the attachment of the PdG moieties. A similar argument could (at least in part) also explain the reduced activity of the TG conjugates synthesised in Chapter 2 since a monoacylated TG-HEWL conjugate would be expected to have more hydrophobic character than the corresponding THEG-HEWL conjugate due to the extra hydroxyl groups on the THEG moiety. However, a mechanism to explain such an effect is not obvious since the precise structural nature of the substrate surface is not yet known. Whatever the reason, attachment of a TG molecule to the enzyme surface must have resulted in greater disruption (than a THEG molecule) to the process of binding and association between the net positively charged surface of HEWL and the negatively charged cell wall of the *Micrococcus lysodeikticus.*

Using the empirically determined optimal conjugate concentration from the hyperbolic plots in Figures 3.9 and 3.10, assay mixtures were prepared by dilution of each conjugate such that a 10 μL aliquot gave a $\Delta T\ 5\ min^{-1}$ of ~350 units. This allowed the bulk of the reaction mixture to be stored frozen and standardised the volume of conjugate and assay buffer that was added to each assay tube, thus simplifying the processing of multiple samples. To follow the reaction progress for each conjugate mixture, transmission readings were recorded every 5 seconds over the five minute assay period, thus generating the clearing curves shown in Figure 3.11 and 3.12.

As the non-linear fit of the assay data in Figures 3.9 to 3.12 indicates the rate of clearing of the turbid suspension of *M. lysodeikticus* cells is not constant with respect to time and the degree of curvature increases with increasing enzyme concentration. Each clearing curve produced by conjugate-catalysed lysis of a suspension of *M. lysodeikticus* is a single second order process for over 90% of the reaction [115,174]. However as the lytic assay proceeds the transmission of the cell suspension approaches that of a blank sample (i.e. without substrate) hence an apparent saturation of the rate occurs. This is because over the assay period the proportion of substrate available to the enzyme as intact cells diminishes and the enzymes activity becomes increasingly directed towards reducing the remnants of the lysed cell walls into smaller fragments, a process which cannot be detected by the spectrophotometer. Hence the results are inherently more accurate at lower conjugate concentration and it becomes necessary during sample measurement to dilute the sample into the working range of the standard curve (from about 50 - 350 units).

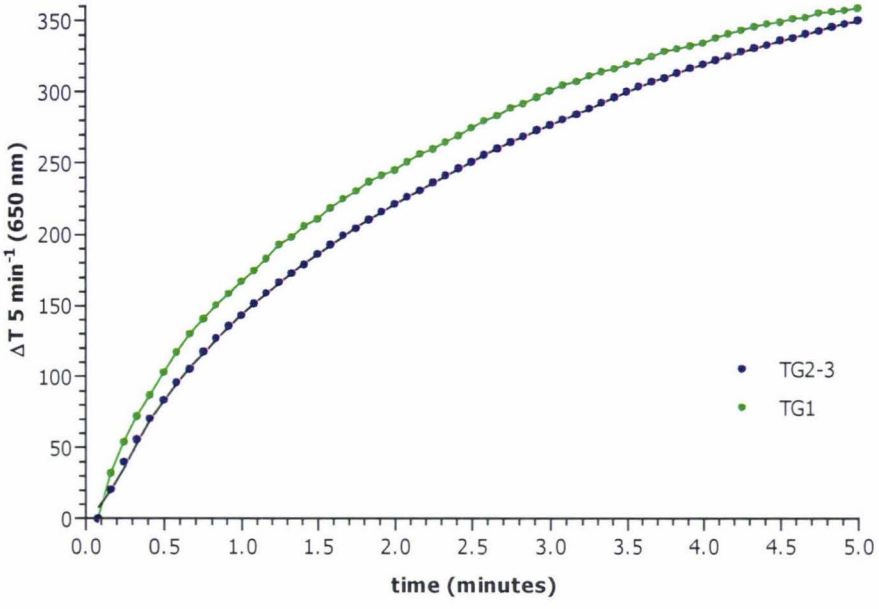

Figure 3.11 Clearing curves for testosterone glucuronide-hen egg white lysozyme conjugates TG1 and TG2-3.

Assay conditions: TG1, 85.5 nM; TG2-3, 59.5 nM.

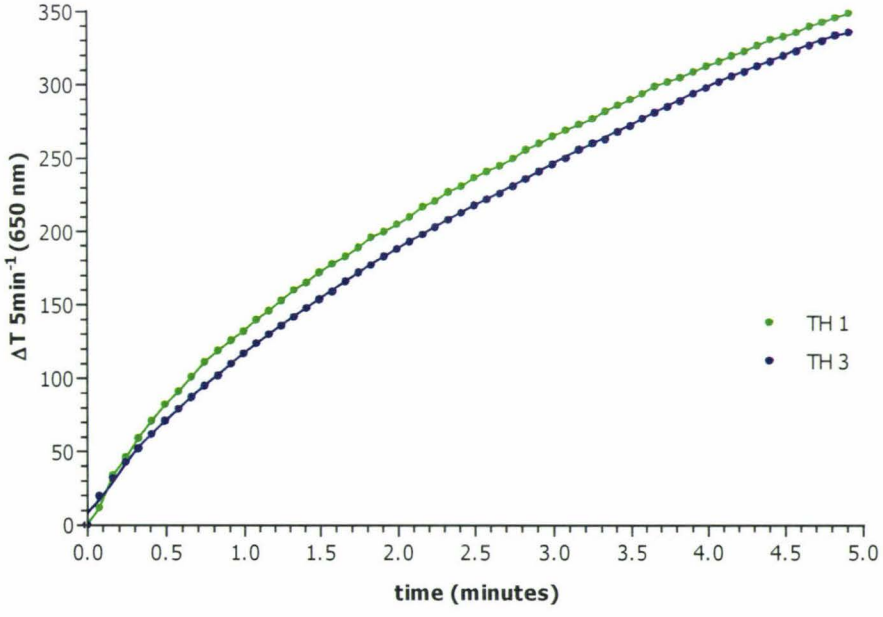

Figure 3.12 Clearing curves for tetrahydrocortisone glucuronide-hen egg white lysozyme conjugates TH1 and TH3.

Assay conditions: TH1, 61.0 nM; TH3, 71.1 nM.

3.3.3 Comparison of TG-HEWL and THEG-HEWL conjugates as signal generators in the presence of antiserum

To compare the two pairs of structurally isomeric TG and THEG conjugates for their relative potential as signal generators in the Ovarian Monitor assay, each conjugate was titrated against increasing volumes of the corresponding anti-TG or anti-THEG antiserum. The concentration of conjugate used in each case was chosen to give a control rate (i.e. conjugate only or zero standard rate) of 350 transmission units in the absence of antiserum.

3.3.3.1 Titration of TG-HEWL conjugates TG1 and TG2-3 with bleed four anti-TG antiserum B52.

Since the concentration of conjugate required to reach the required change in transmission was significantly different for the two conjugates, the antiserum titration curves for the fourth bleed of antiserum B52 with TG1 and TG2-3 were compared by plotting the ratio of antiserum volume (μL):conjugate concentration (nM) conjugates as shown in Figure 3.13.

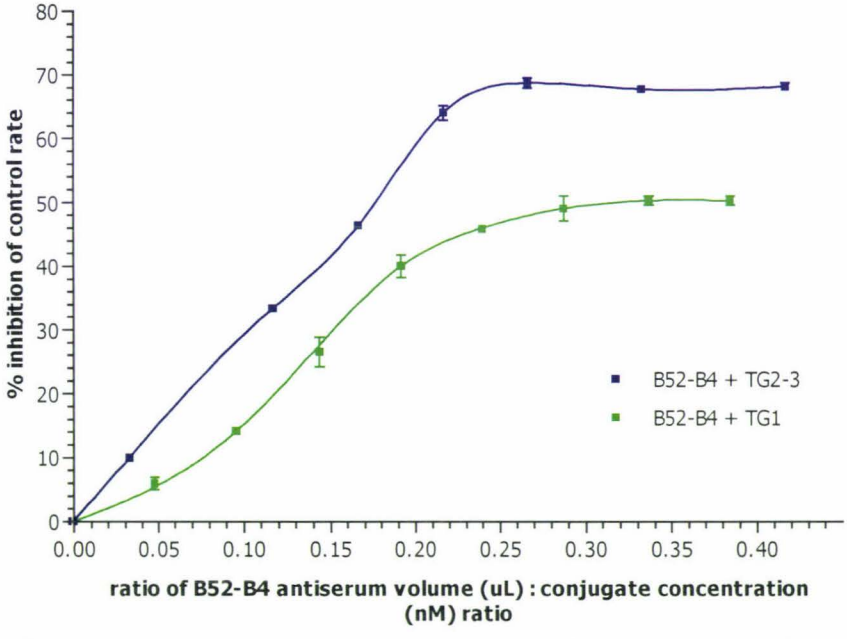

Figure 3.13 Titration curves for the fourth bleed of anti-TG antiserum B52 with testosterone glucuronide-hen egg white lysozyme conjugates TG1 and TG2-3 expressed as a ratio of antiserum volume (μL):conjugate concentration (nM).

Assay conditions: Assay conditions; TG1, 85.5 nM; TG2-3, 59.5 nM

Despite the two conjugates having a similar control rate the gradient of the TG1 conjugate titration curve was shallower and reached only 50% maximum inhibition (using 30 μL of antiserum) compared to the TG2-3 titration curve which reached 68% inhibition using 15 μL of antiserum. Since both conjugates were titrated against the same antiserum the differences in the shape of the titration curves cannot be attributed to the concentration of antibody binding sites and must be due to the different affinities of each conjugate for the anti-TG antibodies in the serum.

Given that the TG2-3 conjugate preparation contained a small amount of disubstituted conjugate it was expected to require more antiserum than the monosubstituted TG1 conjugate to achieve the same level of inhibition due to the fraction of enzyme molecules having two antibody binding sites. However, the fact that a much higher volume of neat antiserum was required to reach the end point of the titration for TG1 than TG2-3 indicates that the TG1 conjugate has a much lower binding affinity than the TG2-3 conjugate mixture. This effect may be due to different electrostatic and hydrophobic microenvironments on the lysozyme surface surrounding the presumed acylation sites in TG2-3 and TG1 and is similar to the behaviour reported for the estrone glucuronide (E1G) conjugate [115]. In this study, the E1G conjugate (E3) acylated at lysine 33 had a higher binding affinity with an anti-E1G antiserum than did E1 monoacylated at either lysine 97 or 116. If the TG2-3 conjugate consists largely of a monoacylated lysine 33 conjugate (i.e. TG3) then a similar pattern of behaviour is being observed.

Whatever the correct explanation for the difference in binding affinity of the two conjugates, the antiserum titration curves in Figure 3.13 suggest that a more sensitive assay would result using TG2-3 as the signal generator. This is because much less antiserum will be required to maximally inhibit TG2-3 compared to TG1 in the absence of any testosterone glucuronide. Since the standard TG is added first in the assay protocol, less of it will be required to bind to the antibody binding sites before the subsequent binding of the antibody to the TG2-3 is affected. This results in an earlier rate of lysis, and hence a more sensitive assay.

3.3.3.2 Titration of THEG-HEWL conjugates TH1 and TH3 with bleed five anti-THEG antiserum L57.

Comparison of the titration curves for the THEG conjugates TH1 (61.0 nM) and TH3 (71.1 nM) with the fifth bleed of antiserum L57, expressed as the ratio of antiserum volume (μL):conjugate concentration (nM) is shown in Figure 3.14.

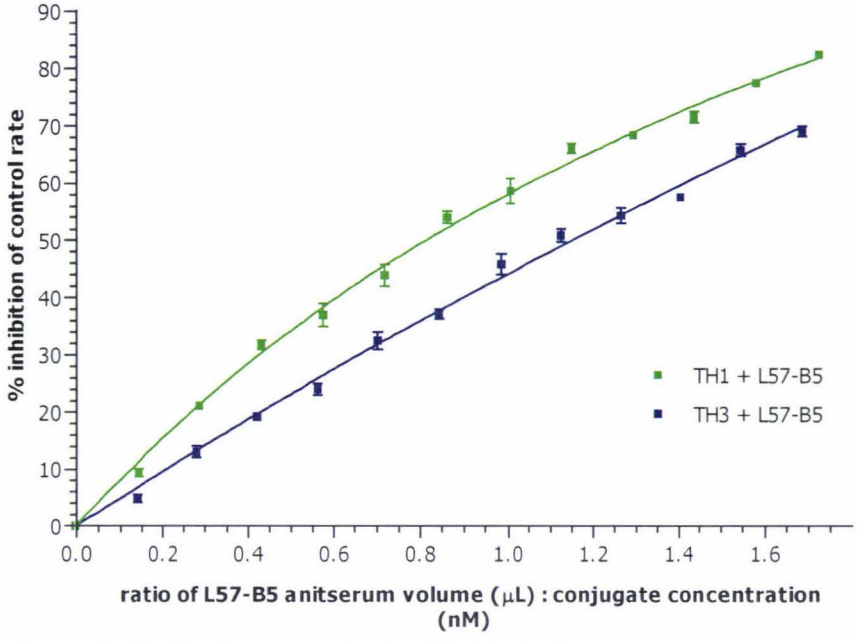

Figure 3.14 Titration curves for the fifth bleed of anti-THEG antiserum L57 with tetrahydrocortisone glucuronide-hen egg white lysozyme conjugates TH1 and TH3 expressed as a ratio of antiserum volume (μL):conjugate concentration (nM).

Assay conditions: TH1, 61.0 nM; TH3, 71.1 nM.

Both conjugates had a control rate (i.e. conjugate only rate) of approximately 350 units in 5 minutes. Although each curve could be fitted using the equation for a one site binding hyperbolic curve (for TH1, R^2= 0.994; for TH3, R^2= 0.993), the TH3 conjugate curve was more linear than the TH1 conjugate curve. The level of inhibition of both conjugates increased in parallel over the range of antiserum concentrations tested, however the TH3 conjugate required on average ~13% more antiserum to reach the same level of inhibition per nM of conjugate as did the TH1 conjugate. This effect was also noted by Cooke [115] with mono-substituted estrone glucuronide HEWL conjugates where the E3 conjugate acylated at lysine 33 resulted in much tighter binding with the anti-E1G antibody than did binding to the E3 conjugate acylated at either lysine 97 or 116. The significantly higher inhibition by antiserum L57-B5 of the TH1 conjugate mixture than for TH3 suggests that a more sensitive immunoassay might result using TH1 as the signal generator. In this case however, due to the commercial interest in developing the THEG assay and the fact that preliminary results showed the THEG antiserum to be of poor quality, it was decided to reserve the TH1 conjugate for experiments with higher titre antisera once they became available. As a result the TH3 conjugate was used in this thesis to screen the low titre antisera from rabbits L57 and B42.

According to the 3D structure of the anti E1G-glucuronide Fab antibody fragment solved by Trinh *et al.* [187], the binding site for the hapten lies in a cleft in the centre of the antibody binding site with the glucuronide carboxyl group exposed to the solvent [188]. Because of the 1,6-linkage between the steroid moiety and the ε-amino lysine residue of the lysozyme conjugates, the steroid-glucuronide structure lies virtually at right angles to the lysozyme surface. In the immune complex this allows the antibody binding surface and the lysozyme surface in the region of the acylated lysine residue to come into close contact. The acylation site will therefore determine not only the distance of the TG or THEG moiety to the antibody-binding cleft (since not all the lysine residues are equally exposed on the enzymes surface [115]), but also the distance of the bound antibody from the enzymes active site. The hydrophobic and electrostatic character of the lysozyme surface surrounding the acylated steroid residue may also impair or promote antibody binding. However, since the orientation of the TG and THEG moiety relative to the surface of the lysozyme molecule and the actual area of protein-protein interaction in the immune complex is unknown a detailed explanation for the apparent differences in affinity and inhibition of the various conjugates cannot be given at present.

3.3.3.3 Clearing curves for TH1 tetrahydrocortisone glucuronide-HEWL and TG2-3 testosterone glucuronide-HEWL conjugates in the presence of antiserum

Figures 3.15 and 3.16 show the effect on the lysis activity during the five minute assay period of premixing the TH1 and TG2-3 conjugates with a predetermined volume of antiserum L57-B5 and B52-B4 respectively. The curves outlined with solid grey markers represent the percentage inhibition of lysis activity in the presence of antiserum relative to the control rate i.e. $\Delta T\ 5\ min^{-1}$ in the presence of antiserum / $\Delta T\ 5\ min^{-1}$ in the control x 100 %.

The relatively high level of conjugate inhibition in both cases after one minute means that both antisera are blocking access of the *Micrococcus lysodeikticus* substrate to the active site of the enzyme conjugate to a large extent. For the clearing curve catalysed by the TH1 conjugate (Figure 3.15) the maximum inhibition of conjugate activity (79% using 120 μL of L57-B5 antiserum) was reached after ~2.4 minutes of incubation. Thereafter it stayed relatively constant; dropping only slightly to 78% inhibition after 5 minutes suggesting that the dissociation rate of the conjugate from the immune complex was not a contributing factor to the relatively low degree of inhibition. In contrast, the clearing curve for the TG2-3 conjugate (Figure 3.16) reached maximum inhibition (80%) using 16 μL of antiserum B52-B4 after only ~1.2 minutes and declined steady to 69% inhibition at 5 minutes.

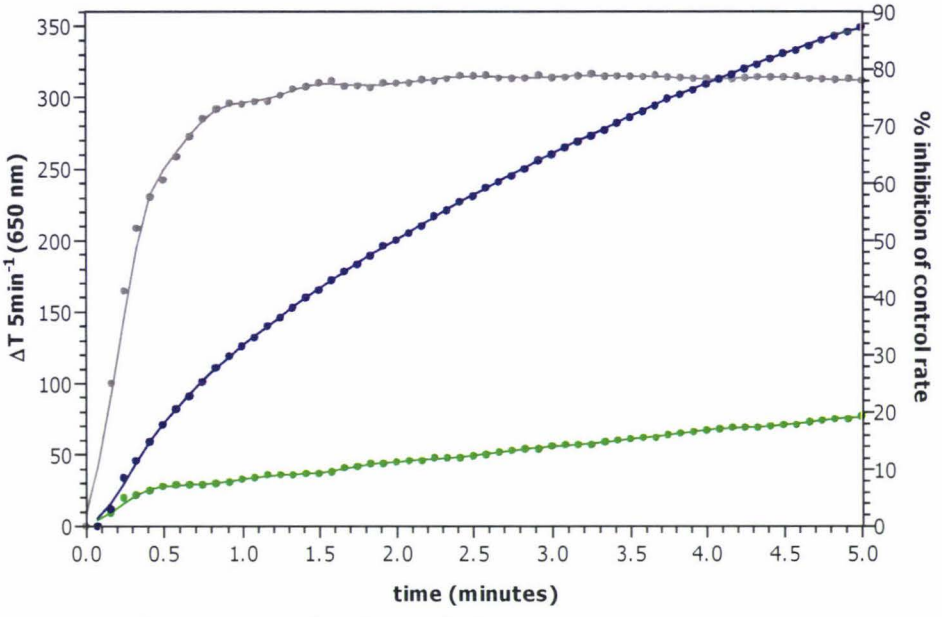

Figure 3.15 Clearing curves for the tetrahydrocortisone glucuronide-hen egg white lysozyme conjugate TH1 in the presence and absence of the L57-B5 antiserum. ● TH1 clearing curve in the presence of the L57-B5 antiserum, ● TH1 clearing curve in the absence of the antiserum, ● Percentage inhibition of conjugate TH1 activity (relative to the control curve in the absence of the antiserum) in the presence of the L57-B5 antiserum

Assay conditions: volume of L57-B5 antiserum, 120 μL; TH1, 61.0 nM.

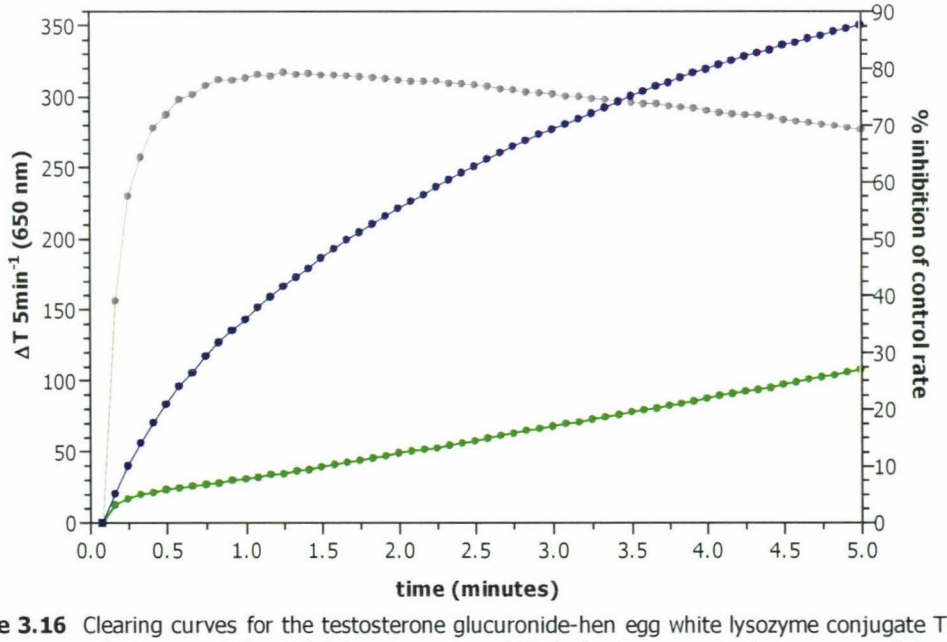

Figure 3.16 Clearing curves for the testosterone glucuronide-hen egg white lysozyme conjugate TG2-3 in the presence and absence of the B52-B4 antiserum. ● TG2-3 clearing curve in the presence of the B52-B4 antiserum, ● TG2-3 clearing curve in the absence of the antiserum, ● Percentage inhibition of conjugate TG2-3 activity (relative to the control curve in the absence of the antiserum) in presence of the B52-B4 antiserum.

Assay conditions: volume of B52-B4 antiserum, 16 μL; TG2-3, 59.5 nM

This fall off in inhibition for the TG2-3 conjugate as the assay proceeds is a methodological artefact of the assay due to a small lag phase observed between ~0.5 and 2.4 minutes in the clearing curve (outlined by the solid green markers) in the presence of the antiserum. This can be explained by considering the relative affinity of the conjugate for binding to the substrate and antiserum as outlined in Scheme 3.1. For any given combination of conjugate (Cj) and antibody (Ab), the rate of conjugate-antibody binding (to form the immune complex Ab.Cj) is determined by the association rate constant (k_{on}) and the relative concentration of free antibody and conjugate. Conversely, the rate of dissociation of the immune complex (Ab.Cj) is determined by its concentration and the dissociation rate constant (k_{off}). The immune complex

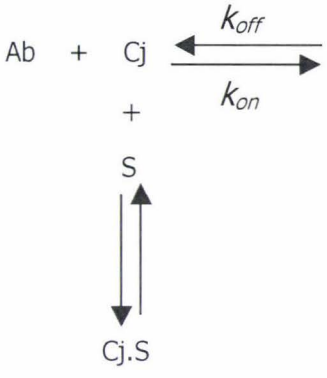

Equation. 3.1

Equation 3.2

Scheme 3.1 Competing reactions involved in the Ovarian Monitor homogenous immunoassay

reaction (Equation 3.1) is reversible and the dissociation step (characterised by the dissociation rate constant, k_{off}) is usually slow over the time scale of the reaction (LF Blackwell unpublished results). Since the binding of the large bacterial substrate (S) and the antibody to the conjugate are likely to be competitive, as the dissociation reaction proceeds there may be a shift in the overall equilibrium towards the Cj.S complex. Thus, depending on the relative rates of the various reactions and the relative concentrations of the antiserum and the substrate there may or may not be an increase in the inhibited rate with time. Clearly there is a small increase in the lysis rate in the presence of antiserum B52-B4 which follows the lag phase suggesting that the dissociation rate for the testosterone glucuronide conjugate (TG2-3) is fast enough to affect the observed degree of inhibition over the five minute assay time scale.

3.3.4 Inhibition studies with the different anti-TG and anti-THEG antisera

The amount of polyclonal rabbit antiserum required to bind and inhibit a particular hapten-HEWL conjugate population must be experimentally determined since it depends upon such characteristics as the antiserum titre, the affinity of the antibody for binding the hapten-HEWL conjugate and the location of the hapten on the surface of the lysozyme. Ideally > 90% inhibition of conjugate activity is required to maximise the sensitivity of the Ovarian Monitor assay. The antisera collected from the four rabbits inoculated with either TG (rabbit B52 and B41) or THEG-thyroglobulin (rabbits L57 and B42) immunogens were titrated against the optimal conjugate concentration (established in section 3.3.2) of the conjugates TG2-3 and TH3 respectively. This procedure was used to screen the antisera to determine the best antiserum and conjugate combination for use in the standard curve format.

3.3.4.1 Inhibition of TG-HEWL conjugates by the different anti-TG antisera

(a) Anti-testosterone glucuronide antiserum B41.

Figure 3.17 shows the titration curves for the anti-TG antisera obtained from rabbit B41 after the 4th, 5th and 6th bleeds using the Ovarian Monitor end point assay.

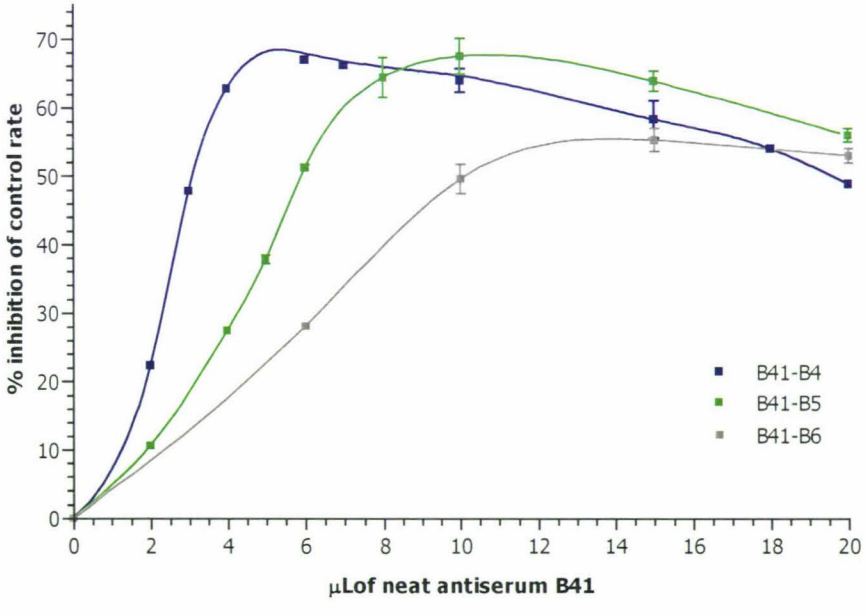

Figure 3.17 Titration curves for the fourth, fifth and sixth bleeds of B41 anti-testosterone glucuronide antiserum with the TG2-3 testosterone glucuronide-hen egg white lysozyme conjugate.

Assay conditions: TG2-3 59.5 nM.

All B41 antisera were titrated against a constant concentration of TG2-3 (59.5 nM) and substrate (214 mg L^{-1} in the assay tube). Although no significant difference was observed in the maximum degree of inhibition (~68%) of conjugate TG2-3 which was reached by the B41-B4 and B41-B5 antisera, the volume of B41-B4 (6 µL) required to achieve this level of inhibition was almost half that of the B41-B5 antisera (10 µL) taken four weeks later. The inhibition

midpoint (I_{50}) i.e. the antiserum volume corresponding to halfway between the conjugate only (control) rate and the maximally inhibited rate was estimated as 2.5 μL of neat antiserum for B41-B4 and 4.7 μL of neat antiserum for B41-B5. These volumes corresponded to titres (defined as the ratio of midpoint volume of antiserum to the total volume of assay mixture) of 1:140 and 1:74 respectively. The maximal degree of inhibition of the TG2-3 conjugate achieved using antiserum B41-B6 was ~15% lower (57%) than the maximum inhibition seen for the previous two bleeds and required more antiserum (14.4 μL) to reach the maximal rate. Thus the quality of the antiserum was decreasing with time, and with the benefit of hindsight it would have been better to exsanguinate the rabbit at the time test bleed four was taken, ~3.5 months after the primary injection.

Ideally if sufficiently tight binding between the antibody and conjugate population is achieved the titration curve should consist of two almost linear regions. An initial steep region corresponding to rapid binding and inactivation of the TG-HEWL conjugate followed by a shallow line when all the TG-HEWL is bound by the antiserum and no further change in the lysis rate is observed. The point where the slope changes for a particular combination of antiserum and conjugates represents the minimum volume of antiserum for which maximum inhibition of the conjugates is achieved. From visual examination of the titration curves in Figure 3.17 it can be seen that at very low antiserum concentrations the curve is non-linear and shows an apparent lag phase. This may be an artefact of the Ovarian Monitor system due to flattening of the change in transmission versus conjugate concentration curve. Because the antibody has only a low affinity for the conjugate, the first additions of antiserum do not reduce the concentration of free conjugate very much hence there is initially little change in $\Delta T\ 5\ min^{-1}$. As the titration proceeds bigger changes in $\Delta T\ 5\ min^{-1}$ occur as the concentration of free conjugate is reduced below about 40 nM (see Figures 3.9 and 3.10).

(b) Anti-testosterone glucuronide antiserum B52

Figure 3.18 shows the inhibition of lysis rates for the test antisera collected 10 days after each booster injection from rabbit B52 titrated against a constant concentration of conjugate TG2-3 (59.5 nM).

In contrast to the pattern observed for the B41 rabbit, the maximum inhibition of the lysis rates increased between the fourth and fifth bleeds from 71% (using 19 μL, titre 1:50) to 82% (using 15 μL, titre 1:79) respectively. Despite the encouraging increase in titre the serum obtained at exsanguination (B52-B6) gave only 67% maximum inhibition (titre 1:36) using ~25 μL of neat antiserum, 15% lower than the previous bleed. Since the inhibition of TG2-3 by the B52-B6 antiserum obtained at exsanguination was higher than that for B41-B6 it was decided to purify the IgG from B52-B6 using octanoic acid and ammonium sulphate precipitation in an attempt to improve the level of TG2-3 conjugate inhibition.

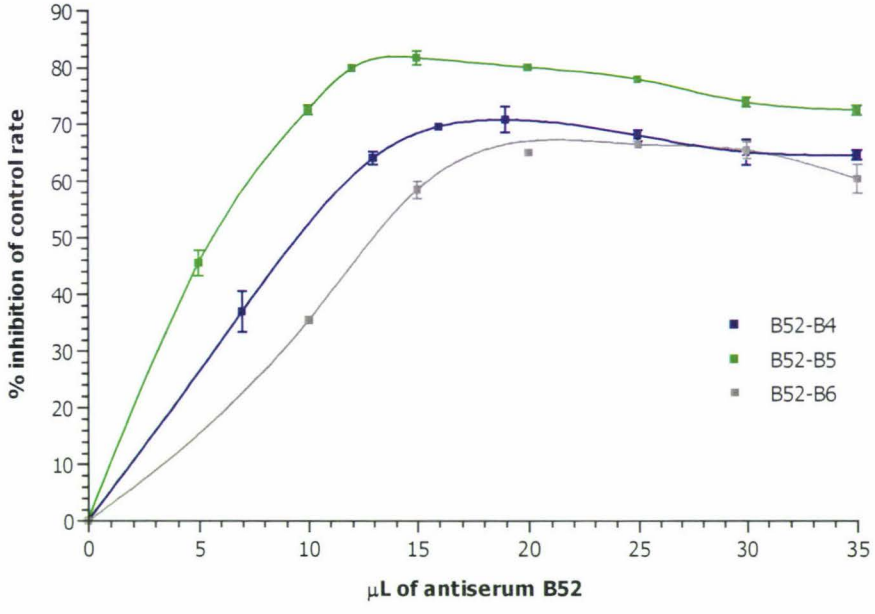

Figure 3.18 Titration curves for the fourth, fifth and sixth bleeds of B52 anti-testosterone glucuronide antiserum (before and after purification) with the TG2-3 testosterone glucuronide-hen egg white lysozyme conjugate.

Assay conditions: TG2-3 59.5 nM.

Figure 3.19 shows the inhibition curves obtained by titration of crude and purified antiserum B52-B6 against the same concentration of TG2-3 conjugate (59.5 nM). The maximum inhibition observed with undiluted B52-B6 antiserum before purification was 67% using 25 μL of undiluted antiserum. When an equivalent volume of purified B52-B6 antiserum was used, the inhibition was increased to 83%, and reached 90% using 35 μL of the purified antiserum indicating that the IgG fraction had been successfully isolated and concentrated by the purification procedure.

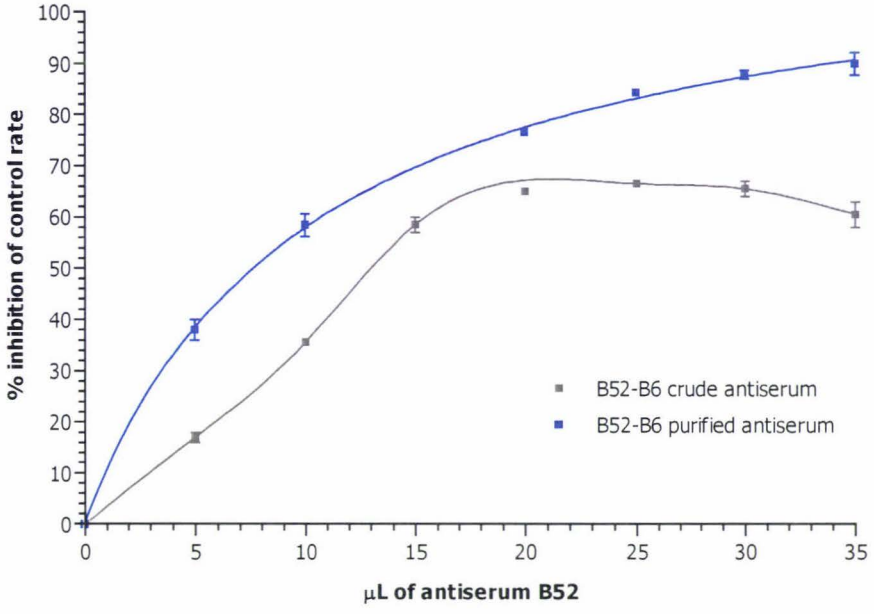

Figure 3.19 Titration curves of the sixth bleed of B52 anti-testosterone glucuronide antiserum (before and after purification) with TG2-3 testosterone glucuronide-hen egg white lysozyme conjugate.

Assay conditions: TG2-3, 59.5 nM

Comparison of the fourth bleed titration curves for rabbit B52 with that of rabbit B41 shows the maximum percentage inhibition of the conjugate lytic activity was approximately the same (68 - 71%). However the titre for antiserum B41-B4 was much higher (1:140) than that for B52-B4 (1:50) indicating that it contained either antibodies at a higher concentration or with higher affinity for the conjugate than the B52-B4 antiserum. Despite the drop-off in titre, because the B52-B5 antiserum inhibition (82% using 15 µL of undiluted antiserum per assay tube) clearly exceeded that of the optimal antiserum from rabbit B41 the B52-B4 antiserum was chosen as the most suitable antiserum for the production of the standard curve. This level of inhibition was below the ideal inhibition level of 90 - 95% required to maximise the sensitivity of the assay, but can still be used for production of a viable standard curve for urinary TG measurement. Antiserum B52-B5 was also preferred over the purified B52-B6 antiserum since a smaller volume (15 µL compared to ~25 µL of purified antiserum) could be used to achieve close to the desired level of inhibition.

3.3.4.2 Inhibition of THEG-HEWL conjugates by different anti-THEG antisera

(a) Anti-tetrahydrocortisone glucuronide antiserum L57

Figure 3.20 shows the corresponding antiserum titration curves obtained when antiserum from rabbit L57 was titrated against a constant concentration of TH3 (71.1 nM) and *Micrococcus lysodeikticus* as substrate (214 mg L^{-1} in the assay tube).

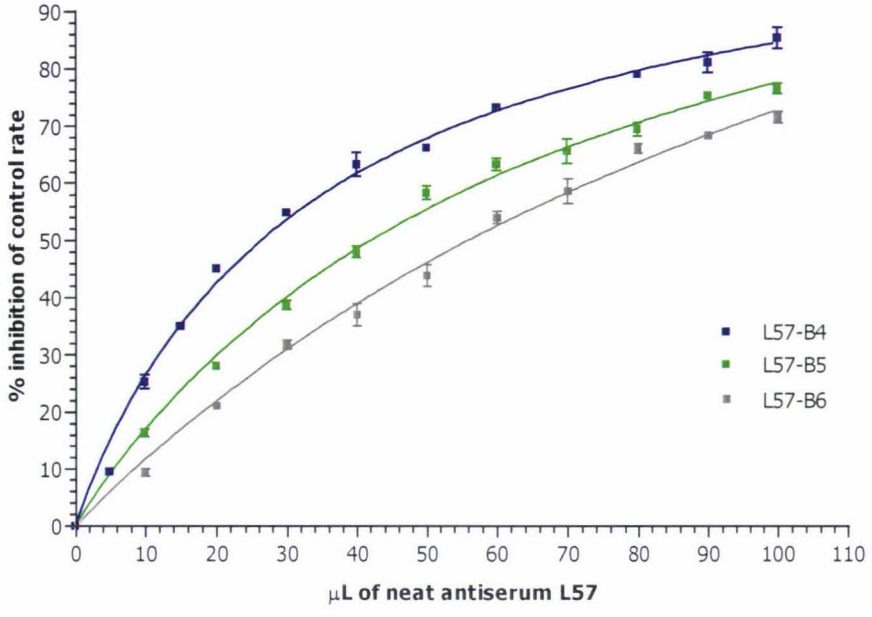

Figure 3.20 Titration curves for the fourth, fifth and sixth bleeds of L57 anti-tetrahydrocortisone glucuronide antiserum with the TH3 tetrahydrocortisone glucuronide-hen egg white lysozyme conjugate.

Assay conditions: TH3, 71.1 nM.

Unlike the previous rabbits used for the production of the anti-TG antisera, the inhibition of conjugate activity as a function of increasing volume of L57 antiserum could be fitted using a one-site binding hyperbolic equation. Over the range of antiserum volumes tested, the maximum inhibition of conjugate activity was observed using 100 µL of undiluted L57-B4 antiserum. Thereafter the maximum inhibition of the subsequent bleeds L57-B5 and L57-B6 diminished to reach only 77 and 71% conjugate inhibition respectively using 100 µL of undiluted antiserum, again suggesting that the titres were decreasing with time.

As for the anti-TG antiserum B52-B6, antiserum L57-B6 was collected by cardiac puncture at the end of the study. Because a large volume of L57-B6 was obtained it was decided also to purify L57-B6 in an attempt to increase the inhibition of the TH3 conjugate catalysed lysis reaction. As shown in Figure 3.21 purification of antiserum L57-B6 did increase the inhibition of the TH3 lytic activity compared to the crude sample (on a v/v basis) but only for volumes of antisera within the range 10 - 50 µL.

When greater than 50 μL of the purified antiserum was added to the assay tube the improvement in inhibition declined to approximately the same level as seen for 80 μL of the crude antiserum. The exact cause of the severe hook effect in the purified L57 antiserum compared to the unpurified serum is unknown. It may be an interfering substance was concentrated along with the IgG molecules or that the ammonium sulphate buffer was not completely removed by dialysis. Because any ammonium salts remaining in the precipitate of IgG would be present in increasing amounts with increased volume of the purified antiserum these may have inhibited the formation of the Ab.Cj immune complex by associating with charged residues important to antibody recognition and binding. While the presence of excess salt was not completely ruled out, it was thought unlikely since an equivalent loss in inhibition was not observed for the B52-B6 antiserum after purification using the same procedure.

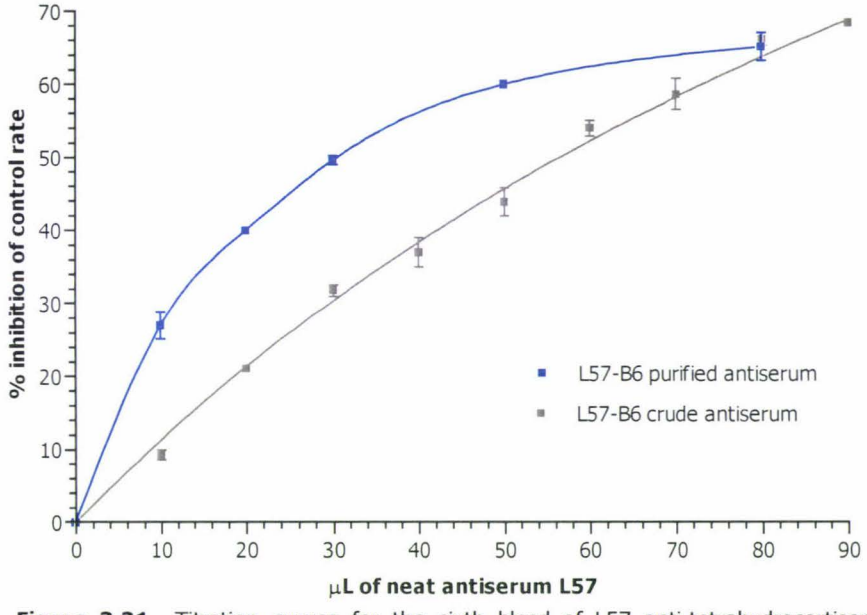

Figure 3.21 Titration curves for the sixth bleed of L57 anti-tetrahydrocortisone glucuronide antiserum (before and after purification) with the TH3 tetrahydrocortisone glucuronide-hen egg white lysozyme conjugate.

Assay conditions: TH3, 71.1 nM.

(b) Anti-tetrahydrocortisone glucuronide antiserum B42

Figure 3.22 shows the titration curves for the antisera collected from rabbit B42 titrated against a constant concentration of conjugate TH3 (71.1 nM). The maximum inhibition of conjugate TH3 with the fourth bleed from rabbit B42 was ~30% using 20 μL of neat antiserum. Thereafter, further increases in the volume of antiserum (up to 50 μL) had no significant effect on the overall inhibition. Subsequent bleeds five and six showed an improvement in maximum inhibition with 20 μL of neat antisera to 39% and 48% respectively, indicating the quality of the antisera had improved as a result of the booster injections.

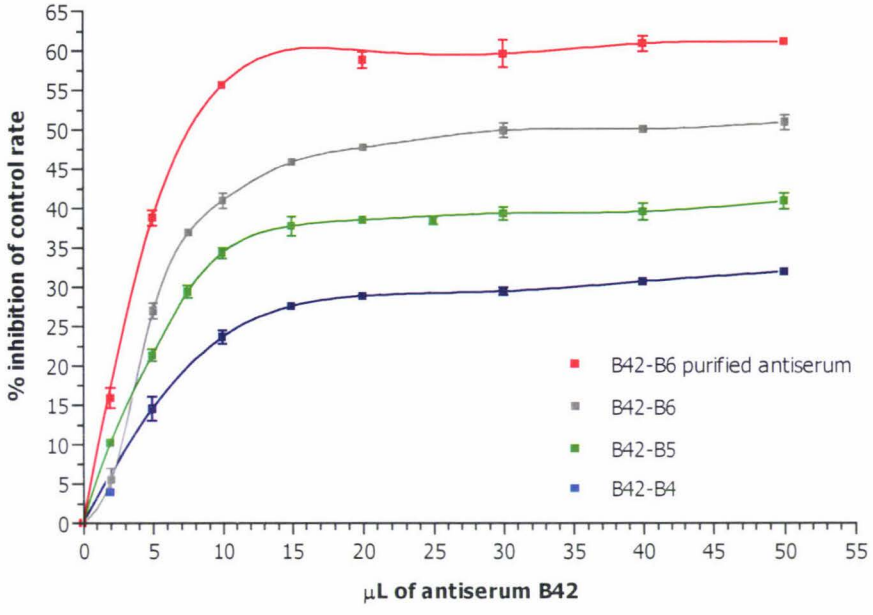

Figure 3.22 Titration curves for the fourth, fifth and sixth (before and after purification) bleeds of B42 anti-tetrahydrocortisone glucuronide antiserum with the TH3 tetrahydrocortisone glucuronide-hen egg white lysozyme conjugate.

Assay conditions: TH3, 71.1 nM.

Despite the improvement in antiserum quality, the shape of each titration curve remained relatively unchanged with no significant increase in inhibition with volumes of antisera greater than 15 - 20 μL. Since the inhibition for the B42-B6 antiserum obtained at exsanguination was relatively good at low volume (~41% with 10 μL), this antiserum was also purified as described for antiserum L57-B6. Although the inhibition achieved using 10 μL increased to ~56% as a result of purification, only a small increase in inhibition was observed when volumes of antiserum > 10 μL were used. The higher inhibition at lower volume of the fourth bleed antiserum from rabbit L57 (higher titre) indicated that this antiserum either contained antibodies at a higher concentration, or with lower k_{off} values than the antiserum produced by rabbit B42. Thus, the L57-B4 antiserum was chosen for further study towards the immunoassay for THEG using the Ovarian Monitor immunoassay.

3.3.5 Factors affecting the titre of anti-TG and anti-THEG antibodies

The antiserum titration curves for each rabbit (Figures 3.17 - 3.22) showed that all test bleeds demonstrated some level of inhibition of conjugate activity, but that the maximum percentage inhibition achieved varied substantially between the antisera produced by the different rabbits. The maximum inhibition for each antiserum titration curve is summarised for each rabbit in Figure 3.23.

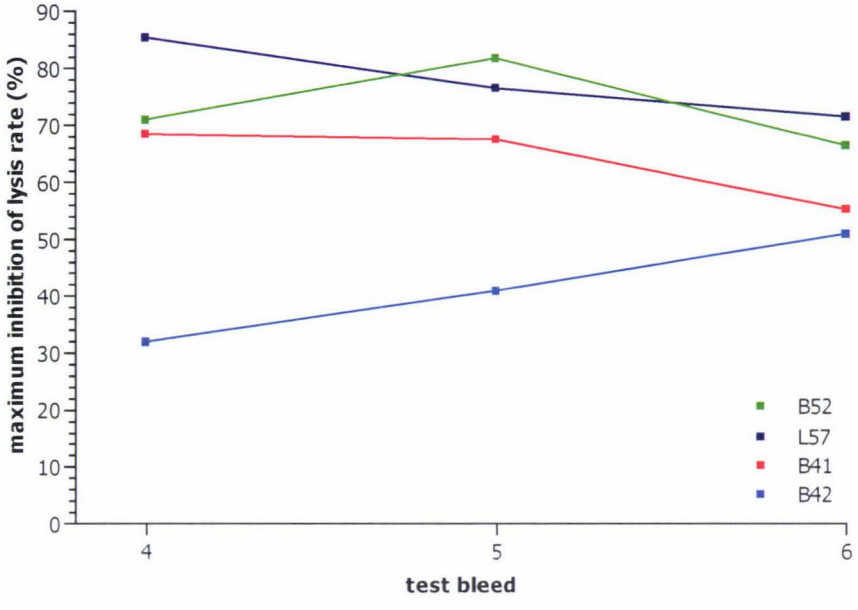

Figure 3.23 Summary of maximum inhibition obtained with test bleed antisera from rabbits immunised with either testosterone glucuronide-thyroglobulin immunogens (B52 and B41) or tetrahydrocortisone glucuronide-thyroglobulin immunogens (L57 and B42).

For a given conjugate the shape of the titration curve and thus the antiserum titre, is determined by such characteristics of the antibody as its affinity for the conjugate and concentration of the antibody in the antiserum. The present results are consistent with the general finding of immunoassay studies that the concentration and binding affinity of polyclonal antibodies differs between animals injected with the same immunogen and after different times of immunisation within the same animal [189,190]. Much of the underlying variation in the immune response of individual rabbits to a particular antigen lies in differences at specific loci in the immune response (Ir) genes. The Ir genes form part of the major histocompatibility complex (MHC), a large group of closely linked highly polymorphic genes, the protein products of which are crucial for the generation and execution of the immune response [191]. For further detail on the antibody structure and generation of diversity refer to Roitt (1997) [192] and Male *et al.* (1996) [193].

For rabbits B52, B41 and B42 the decrease in conjugate inhibition associated with increasing volumes of antisera, referred to as the hook effect, represented a major set-back towards achieving the greater than 90% inhibition of lysis activity required for optimising the standard

curve. A possible explanation cited by Cooke [111] is that the antibody molecules form complexes with either other antibody molecules or other antiserum components at high concentration, thus preventing their inhibition of the enzyme conjugates. Although the explanation for this apparently inhibitory effect is only speculative it could account for the observation that the hook effect occurred at a lower volume of antiserum for test bleeds in which the titre (i.e. antibody concentration) was high, than for antiserum samples in which the titre was low. Presumably as the concentration of antibodies in the assay tube increases, so too does the potential for complex formation, thus the volume at which the drop in inhibition is observed decreases.

The hook effect has important practical ramifications for the selection of antisera for generation of a standard curve. Obviously, using a single high volume of a test antiserum to estimate its maximum inhibitory action of a conjugate solution will almost certainly result in underestimating the inhibition and possible rejection of a highly inhibiting antiserum or highly inhibitable lysozyme conjugate. Thus each antiserum must always be titrated over a range of volumes to find the minimum volume that gives maximal inhibition of lysis activity.

Although close to the desired level of TG and THEG-HEWL conjugate inhibition was achieved, the volume of B52-B5 (15 μL) anti-TG antiserum and L57-B4 (100 μL) anti-THEG antiserum required was several orders of magnitude higher than that obtained in previous E1G studies by Cooke [115] using antisera raised against E1G-thyroglobulin conjugates in sheep. The fact that the maximum degree of inhibition in the present study did not reach > 90% implies that the mechanism of antibody inhibition of the conjugate-catalysed lytic rate may be subtle. It would be anticipated that for a small enzyme molecule such as lysozyme, once the conjugate was bound to the appropriate anti-steroid glucuronide antibody, the same high level of inhibition (> 90%) would be obtained irrespective of the identity of the steroid glucuronide. This was clearly not the case. It may be that with the low affinity antibodies obtained in the present work the operation of the hook effect, observed when high levels of antiserum are present, is the cause of the low levels of inhibition. Production of high titre, high affinity antibodies is therefore expected to alleviate this problem. It is likely that a combination of numerous factors, including the hapten density on the immunogen, the quality of the immunogen/Freund's adjuvant emulsion and the immunisation schedule were responsible to a greater or lesser degree for the low immune response. Unfortunately, due to a limited budget and time constraints, it was not possible to attempt further experiments to improve the antiserum quality. However, the discussion below outlines some variations in protocol that could be adopted for future studies.

3.3.5.1 Immunogen hapten density

Both the nature (size, charge and polarity) of the hapten, and its spacing and density on the surface of a given carrier protein have an important effect on the antibody response. Since there are also no set rules for the preparation of an antigenic immunogen, it may be necessary to prepare active ester conjugates with several carriers and with a range of hapten-carrier coupling ratios for immunisation to find the best constructed immunogen. Estimates of the ideal coupling ratio range from one to three haptenic groups per 10,000 Da of carrier protein. Aside from thyroglobulin, numerous other proteins including keyhole limpet haemocyanin (KLH), and bovine serum albumin (BSA) which have been widely used to produce antigenic steroid glucuronide immunogens could be used as carriers. Choosing the appropriate dose and frequency of the booster immunisations will depend on the inherent antigenicity of the immunogen. Since the binding constants of antibodies can also be affected by the amount of antigen administered the most promising immunogens should ideally be tried at different dosage levels.

3.3.5.2 Adjuvant

Prior to the primary inoculation, the immunogen was emulsified in Freund's complete adjuvant (CFA). This consists of a mineral oil base containing a suspension of killed *Mycobacteria tuberculosis* or *M. butyricum*. Booster doses were emulsified in incomplete Freund's adjuvant (IFA) prior to injection, which consists of CFA without the killed mycobacterium. When emulsified with immunogen, CFA allows slow but continuous release of the immunogen and stimulates certain subpopulations of lymphocytes (T-cells) and macrophages. First reported over fifty years ago, CFA is still the adjuvant of choice for immunisations. However, adverse side effects may be associated with its use in some animals [194]. During the study, a common adverse reaction of CFA was seen in rabbit L57, which developed a small lesion and localised swelling at an injection site at the back of its neck, coupled with weight loss due to loss of appetite. Despite treating the lesion, the rabbit failed to regain weight and was sacrificed earlier than the other rabbits. Besides Freund's adjuvant, several other commercially available adjuvant systems could be used to avoid loss of animals in future trials. These include Ribi, Adjuvax, TiterMax, Quil A and synthetic lipopeptides some of which are claimed to elicit at least as strong and long-lasting an immunoresponse as CFA for several types of immunogens [195]. Recently CSIRO scientists from the Australian Animal Health Laboratories in Geelong, Australia have developed an adjuvant formulation based on Quil A (a saponin), DEAE dextran and Montanide 888 [194]. The new adjuvant was directly compared to the adjuvant activity of CFA in sheep, cattle, rabbits and poultry with a number of different antigens. Their results showed that the adjuvant was able to induce antibody responses equivalent to those induced by CFA, and showed excellent adjuvant activity in sheep, but with considerably less inflammation at the injection sites [194]. Thus, the CSIRO formulation is of great interest for use in further antibody production trials, possibly in sheep, which will allow a larger volume of serum to be

obtained and reduce the likelihood of having to sacrifice animals early due to side effects resulting from the use of adjuvant.

3.3.5.3 Immunisation schedule

Many different methods have been reported for the production of polyclonal antibodies which recognise steroid molecules in rabbits, varying in the amount of immunogen required, the route of injection and the frequency and number of immunisations. In general, booster doses (of between 2 and 3.5 mg of immunogen conjugate are emulsified in incomplete Freund's adjuvant (IFA) and injected subcutaneously at one month intervals [117,196]. Other common dosage protocols include multiple (3 - 5) booster injections emulsified in IFA given at one or two week intervals [197,198], followed by monthly injections. A Less common approach is the use of both incomplete Freund's adjuvant and complete Freund's adjuvant (normally used only for the primary inoculation) emulsified immunogens injected alternately at one month intervals [199]. Practical immunology texts may also recommend intervals of ten days [200], six weeks [201], and even up to several months or "as long as possible" between booster injections [202]. In practice, because each immunogen is different, the best immunisation protocol for a particular immunogen and animal species can only be established by trial and error. Hence it is difficult to decide on a suitable schedule without the wisdom of experience. Following the poor immune response to monthly immunisations in this case, a more successful schedule may involve combining closely spaced booster immunisations, for example 4 - 5 booster shots at ten day intervals (the recommended minimum [200]) with increased resting periods of 4 to 6 weeks between later boosts. If time permits, allowing animals resting periods of several months between booster injections may also be advantageous [202].

3.3.6 Production of standard curves for testosterone glucuronide and tetrahydrocortisone glucuronide.

The final step in establishing an assay for TG and THEG was to construct standard curves using the optimised conjugate concentration and antiserum volume determined in sections 3.3.4.1 and 3.3.4.2 respectively. The concentration range of steroid glucuronide standards used was established to include the daily excretion rate of each steroid glucuronide observed for male and female adults reported in the literature. i.e. for testosterone glucuronide in males 0.38 μmol 24 hr^{-1}, range 0.21 - 0.74 μmol 24 hr^{-1} [203] and females 0.05 μmol 24 hr^{-1}, range 0.02 - 0.08 μmol 24 hr^{-1} [204]; for tetrahydrocortisone glucuronide in males 4.24 μmol 24 hr^{-1}, range 3.91 - 5.02 μmol 24 hr^{-1}, and females 2.75 μmol 24 hr^{-1}, range 2.11 - 3.68 μmol 24 hr^{-1} [102].

3.3.6.1 Comparison of TG1 and TG2-3 testosterone glucuronide-hen egg white lysozyme conjugate standard curves with antiserum B52-B5.

Figure 3.24 compares the standard curves obtained by titration of conjugates TG1 and TG2-3 respectively with antiserum B52-B5 (15 μL) in the presence of free testosterone glucuronide standards ranging from 0.0028 - 111.11 μmol L^{-1} (0.010 - 400 μmol 24 hr^{-1}). The volume of diluted conjugate used in each case was sufficient to give a control rate (i.e. conjugate only rate) of 350 transmission units in 5 minutes in the absence of antiserum (as determined in section 3.3.2).

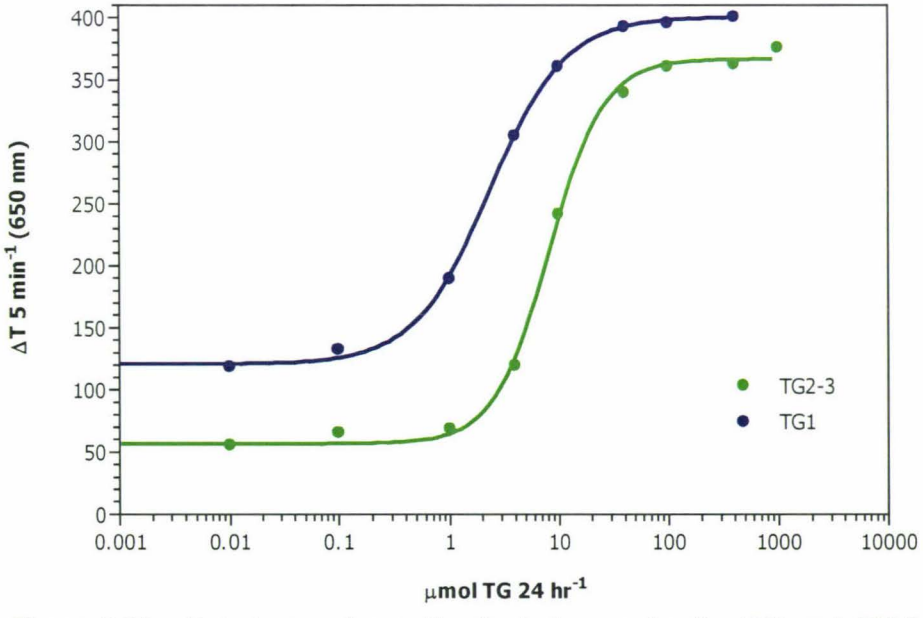

Figure 3.24 Testosterone glucuronide standard curve for the TG1 and TG2-3 testosterone glucuronide-hen egg white lysozyme conjugates as signal generators with the B52-B5 anti-testosterone glucuronide antiserum.

Assay conditions: volume of B52-B5 antiserum, 15 μL; TG1, 85.5 nM; TG2-3, 59.5 nM.

The shape of the standard curve for each conjugate was characteristic of a sigmoidal dose response curve typical of a competitive binding assay. In the presence of high levels of free steroid (high excretion rates), a large proportion of the antibody sites become occupied with free TG and are hence unavailable for binding and inhibiting the activity of the TG-HEWL conjugates. Thus, a high level of steroid is associated with higher rates of substrate lysis (larger ΔT 5 min^{-1}). The reverse is shown at low concentrations, where a low level of free steroid glucuronide means a large amount of the antibody remains unbound and hence is available to bind to the conjugate forming an inactive immune complex resulting in a low rate of lysis. The lower plateau represents the sensitivity of the assay. Below about 1 μmol TG 24 hr^{-1} there is not enough TG to affect the binding of the anti-TG antiserum to the conjugate. At the higher plateau all the anti-TG antibody is neutralised, thus the change in transmission at the plateau corresponds to the maximum rate of lysis activity, i.e. all the enzyme conjugate present is free. The working range (the range of excretion rates over which the curve is steepest) for the TG1 conjugate was 0.1 - 40 μmol TG 24 hr^{-1} compared to 1 - 100 μmol 24 hr^{-1} for the TG2-3 conjugate and the midpoint (or point of inflection, EC_{50}) of each curve corresponded to 2.51 and 8.71 μmol TG 24 hr^{-1} respectively. The left shift along the concentration axis for the TG1 standard curve is consistent with the TG1 conjugate having a lower affinity for the B52 antibodies than the TG2-3 conjugate (higher k_{off}), hence much less free steroid glucuronide is required to bind the antibody hapten binding sites before the rate of lysis (ΔT 5 min^{-1}) subsequently increases. Although the TG1 assay curve appeared to be the most sensitive, the shape of the TG2-3 curve was superior having a lower baseline and a more rapid increase in lysis rate with increasing TG excretion rates, resulting in a steeper curve (TG2-3 Hill slope, 1.719; compared to 1.247 for TG1). The discrimination of the TG2-3 curve, measured by the difference between the maximum and minimum response rates (ΔT_{max} - ΔT_{min}) was also greater for conjugate TG2-3 (311) compared to TG1 (280). This enables the TG2-3 curve to better distinguish between samples having similar hormone concentrations.

3.3.6.2 Effect of antiserum concentration on the TG2-3 testosterone glucuronide-hen egg white lysozyme conjugate standard curve.

It has been shown previously [115] that the standard curves generated by two signal generators with different affinities for the same antiserum can be made to superimpose by increasing the amount of antiserum for the lowest affinity signal generator. It follows therefore that the higher affinity TG2-3 conjugate curve could be made to shift to a more sensitive working range (i.e. towards the lower affinity TG1 conjugate curve) by decreasing the concentration of antiserum. Figure 3.25 shows the effect on the standard curve performed with antiserum B52-B5 and the TG2-3 conjugate of decreasing the antiserum volume in each assay tube from 15 to 10 μL.

Both standard curves were obtained on the same day and thus were produced using the same dilution of TG2-3 conjugate and substrate. Decreasing the volume of undiluted antiserum in the assay tube from 15 to 10 μL caused the midpoint of the curve to shift from 7.6 μmol TG 24 hr^{-1} (working range 0.75 - 100 μmol TG 24 hr^{-1}) to 4 μmol TG 24 hr^{-1} (working range 0.20 - 50 μmol 24 hr^{-1}). However, the improved sensitivity was offset by an increase in the baseline with the rate of lysis for the zero standard increasing from approximately 48 ΔT 5 min^{-1} to 62 ΔT 5 min^{-1}, and a subsequent slight decrease in assay discrimination. The left shift in the standard curve along the concentration axis caused by reducing the antiserum concentration stems from the fact that since less antiserum binding sites are available, less free testosterone glucuronide is required to occupy the available binding sites before the concentration of free conjugate and hence the rate of enzyme lysis is increased. This effect highlights one of the problems with choosing the optimal antibody:conjugate ratio as well as maintaining the assay sensitivity, since there is likely to be only a narrow range of antibody concentrations that can be used to maintain the maximum difference between ΔT_{max} and ΔT_{min}. The antiserum volume must be chosen such that it is high enough to maintain a low baseline lysis rate, while at the same time ensuring that the antibody concentration is kept low enough to give an early increase in lysis rate above the baseline value with increasing steroid concentration.

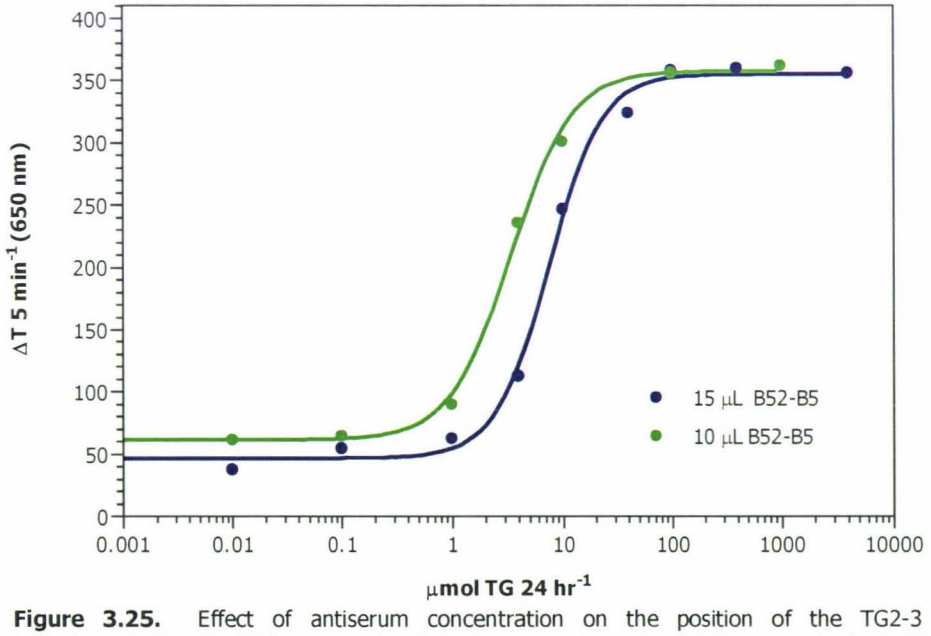

Figure 3.25. Effect of antiserum concentration on the position of the TG2-3 testosterone glucuronide-hen egg white lysozyme conjugate standard curve with the B52 anti-testosterone glucuronide antiserum B52-B5.

Assay conditions: antiserum volume B52-B5, 15 and 10 μL; TG2-3, 59.5 nM.

Despite the increased sensitivity of the standard curve associated with reducing the volume of antiserum, both the TG1 and TG2-3 signal generators showed an optimal sensitivity which was above the expected normal physiological urinary concentration for males (0.38 μmol 24 hr^{-1}

[203]) and females (0.05 μmol 24 hr^{-1} [204]) aged 25 to 35 years as indicated on Figure 3.26 by the dotted lines and legends. Thus the best signal generator TG2-3 has an optimum measurement range about 10 times higher than required for a 5 minute assay. By lowering the concentration of the signal generator and increasing the assay time to 20 minutes as is done with the E1G assay [60] it should be possible to measure the physiological levels of TG for males and also possibly for females with a home Monitor assay.

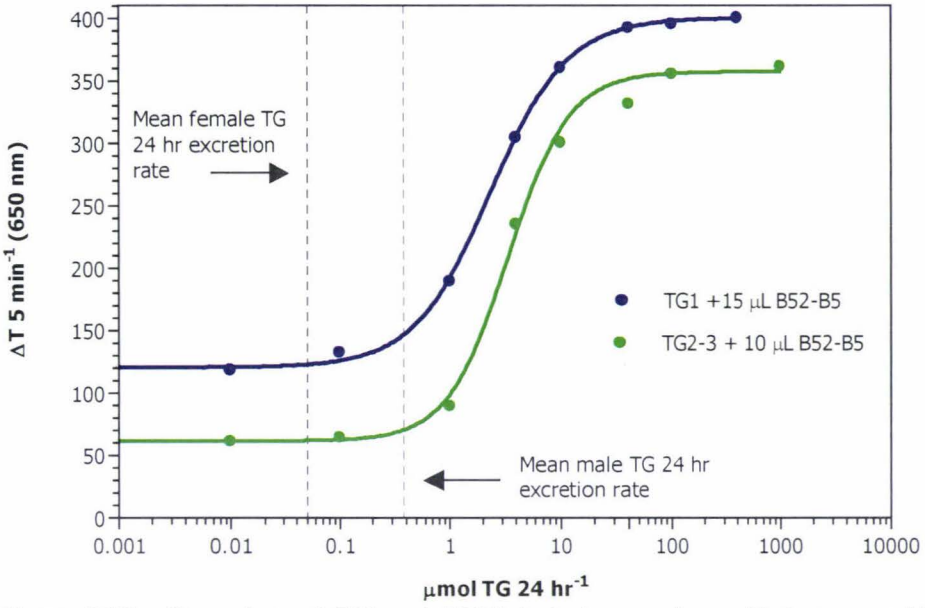

Figure 3.26 Comparison of TG1 and TG2-3 testosterone glucuronide-hen egg white lysozyme conjugates with B52-B5 anti-testosterone glucuronide antiserum

Assay conditions: antiserum volume B52-B5, 15 and 10 μL; TG2-3, 59.5 nM.

3.3.6.3 Determination of the effect of a urine matrix on the TG2-3 testosterone glucuronide-hen egg white lysozyme conjugate standard curve

The addition of blank urine to the assay tube was investigated to determine the effect on the standard curve of any non-specific urinary matrix effects which are not due to the presence of urinary testosterone glucuronide, but which may nevertheless affect the assay. Figure 3.27 demonstrates the effect of the addition of a urine sample from an adult female on the shape and position of the standard curve obtained with the TG2-3 conjugate and the B52-B5 antiserum.

Both standard curves were generated on the same day and thus were produced using the same batch of *M. lysodeikticus* substrate and the same dilution of TG2-3 conjugate. The urine sample was obtained from a 28-year-old female in good health, and diluted to an excretion rate equivalent to 150 mL hr^{-1} prior to addition to each assay tube. While not confirmed in this study, the testosterone glucuronide level of the female sample is expected to be within the range of 0.02 - 0.08 μmol TG 24 hr^{-1} as reported in the literature [204]. This sample therefore was used to test the effect of a urinary matrix on the position of the standard curve since a completely testosterone glucuronide free sample, for example one in which only the testosterone glucuronide had been removed or from an androgen deficient male, was unavailable.

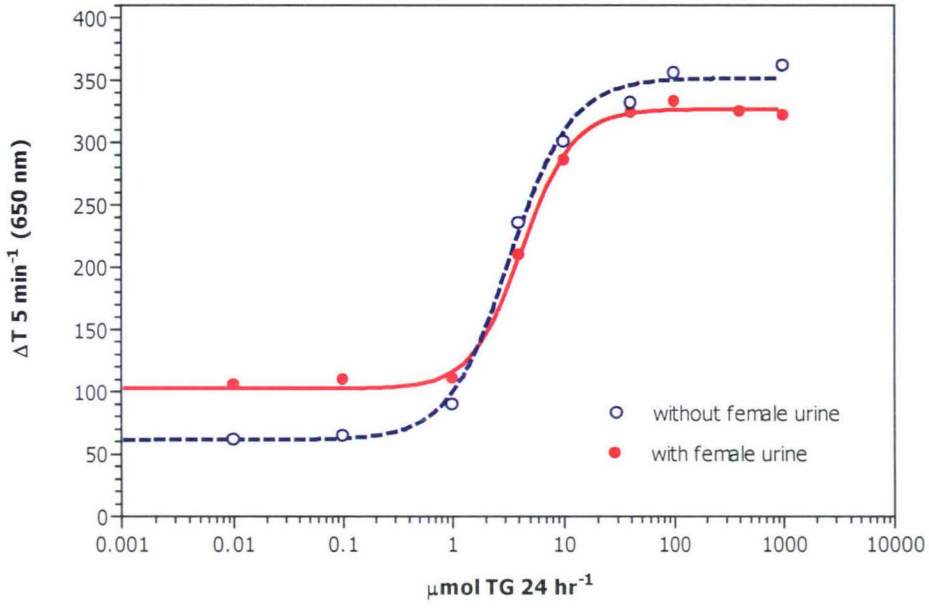

Figure 3.27 Testosterone glucuronide standard curve for the TG2-3 conjugate with anti-testosterone glucuronide antiserum B52-B5 in the presence and absence of a sample of female urine.

Assay conditions: volume of B52-B5 antiserum, 10 μL; TG2-3, 59.5 nM.

Compared to the control curve, the added urine increased the baseline lysis rate from the relatively low level of 62 ΔT 5 min^{-1} to 105 ΔT 5 min^{-1} and reduced the maximum rate from 350 ΔT 5 min^{-1} down to 325 ΔT 5 min^{-1}. By decreasing the difference between ΔT_{max} and ΔT_{min} the urine matrix effectively reduced the discrimination of the standard curve. Although the urine affected the shape of the curve its position on the concentration axis appeared to be stable since each standard curve had a midpoint equivalent to ~4 μmol of TG per 24 hr^{-1}. The reason for the reduction in the maximum lysis rate of the urine added curve compared to the control is unknown. The increase in ΔT 5 min^{-1} values can be however be explained by endogenous testosterone glucuronide or other cross-reacting glucuronides present in the urine binding to the anti-TG antibodies, thus causing a greater proportion of the enzyme conjugate to remain unbound and subsequently increase the baseline lysis rate. The presence of extra steroid in the

urine would also be expected to shift the midpoint of the curve (EC_{50}) to a lower concentration since the actual level of TG present (endogenous + standard) would have been higher than that indicated by the log scale on the X-axis (synthetic TG alone). The fact that EC_{50} and the concentration at which the lysis rate first increased remained relatively unchanged suggests the endogenous TG level in the female urine sample was too low to effectively compete with increasing amounts of standard TG for the antibody binding sites.

An elevated baseline result is also consistent with non-specific interactions between the antibody and small organic molecules in the urine competing with the specific analyte-antibody reaction [205]. The most likely candidates for such non-specific binding would be other steroid glucuronides or possibly other glucuronide conjugates structurally similar to steroid glucuronides (such as urinary phytoestrogens) or testosterone based sulphate conjugates [111] of which there are relatively large amounts excreted in urine. It may also be that ionic salt species present in the urine can shield charged residues important to antibody binding in the vicinity of the acylated lysine residue, and in this way increase the baseline lysis rate by inhibiting the formation of the TG2-3.Ab immune complex. The volume of urine that can be added before the system is swamped by non-specific interference will thus greatly affect the assay sensitivity. For example, in the analysis of urinary cannabinoids by chemiluminescent assay, Sharma *et al.* [45] found that not more than 10 μL of urine could be used for quantitative analysis since larger volumes adversely affected the binding of labeled Δ^9-THC antigens.

The level of urinary based interference is expected to vary between individuals, in particular male urine contains a greater amount of cross-reacting steroidal substances than female urine and the excretion profile of various steroids differs with age in both genders [102]. Thus to avoid matrix interference affecting the accuracy of the standard curve readings, the standard curve would need to be further optimised in the presence of both male and female urine from which the TG has been removed. The difficulty in obtaining such a sample however is that the removal of TG or THEG (for example by solid phase extraction) would also be expected to result in the removal of other cross-reacting steroid molecules. Because of the urine dependant bias, preparation of standard curves to be programmed into the Monitor requires that the data be obtained from assays with blank urine added in an amount equivalent to the volume of urine being assayed. A suitable blank urine must be selected on the basis that it contains undetectable levels of hormone measured by a reference chromatography or immunoassay method.

3.3.6.4 Studies towards optimising the TH3 tetrahydrocortisone glucuronide hen egg white lysozyme standard curve

Based on the estimated optimal TH3 and L57-B4 combined conditions determined in section 3.3.4.2 (71.1 nM of conjugate and 100 μL undiluted antiserum per assay mixture), a full standard curve was generated using THEG standards containing 8.42 - 841.68 μmol L^{-1} THEG (0.303 - 3030.06 μmol THEG 24 hr^{-1}). Figure 3.28 shows that the TH3 standard curve obtained under the optimised conditions had an EC_{50} of 9.2 μmol THEG 24 hr^{-1} and working range between 0.7 - 100 μmol THEG 24 hr^{-1}.

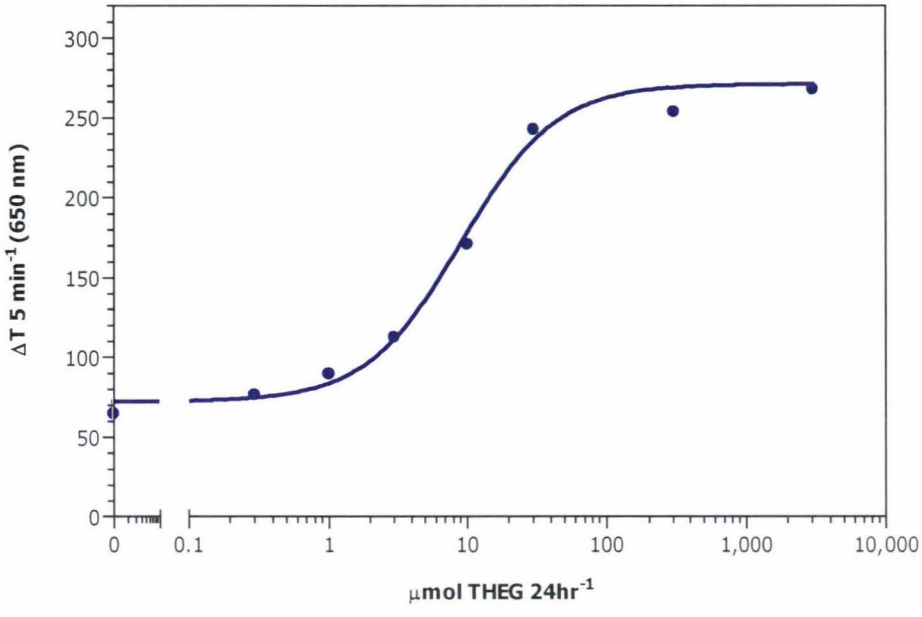

Figure 3.28 Standard curve for the TH3 tetrahydrocortisone glucuronide-hen egg white lysozyme conjugate with L57-B4 anti-tetrahydrocortisone glucuronide antiserum.

Assay conditions: volume of L57-B4 antiserum, 100 μL; TH3, 71.1 nM.

Although the less than optimal inhibition of the conjugate meant the baseline lysis rate was relatively high, the working range of the curve included the mean 24 hr THEG excretion rate expected for both males (4.24 μmol THEG 24 hr^{-1}) and females (2.75 μmol THEG 24 hr^{-1}) reported in the literature [102]. By extending the assay time or using a lower concentration of anti-THEG antiserum it may be possible to shift the curve to a lower concentration range, ideally so that the midpoint corresponded to the excretion rate between the mean male and female values (i.e. ~3.5 μmol THEG 24 hr^{-1}). However as was noted with the TG standard curve in Figure 3.25, decreasing the volume of antiserum in the above conditions is likely to be at the expense of the assay discrimination. Unfortunately, despite the promising results no further study towards optimising the TH3 conjugate standard curve was possible due to the low volume of L57-B4 (a test bleed) remaining.

Since the TH1 conjugate was shown to bind more tightly to the L57 antiserum than did the TH3 conjugate (see section 3.3.3.2) it was postulated that by using the TH1 conjugate and antiserum L57-B4 a standard curve with a lower baseline lysis rate could be obtained. However, because of the lack of availability of the L57-B4 antiserum the TH1 conjugate was instead titrated with L57-B5, the next best anti-THEG antiserum available. Figure 3.29 shows the standard curves obtained with the TH1 conjugate (61.0 nM) and 100 μL of antiserum L57-B5 compared to the TH3 conjugate with 100 μL of antiserum L57-B4 (outlined by the broken line). The lysis rate for the zero standard shows the maximum inhibition of each conjugate was relatively similar (TH1, 78.9%; TH3, 81.4%). Despite this the TH1 standard curve was significantly elevated at low THEG concentrations and much shallower than the TH3 curve.

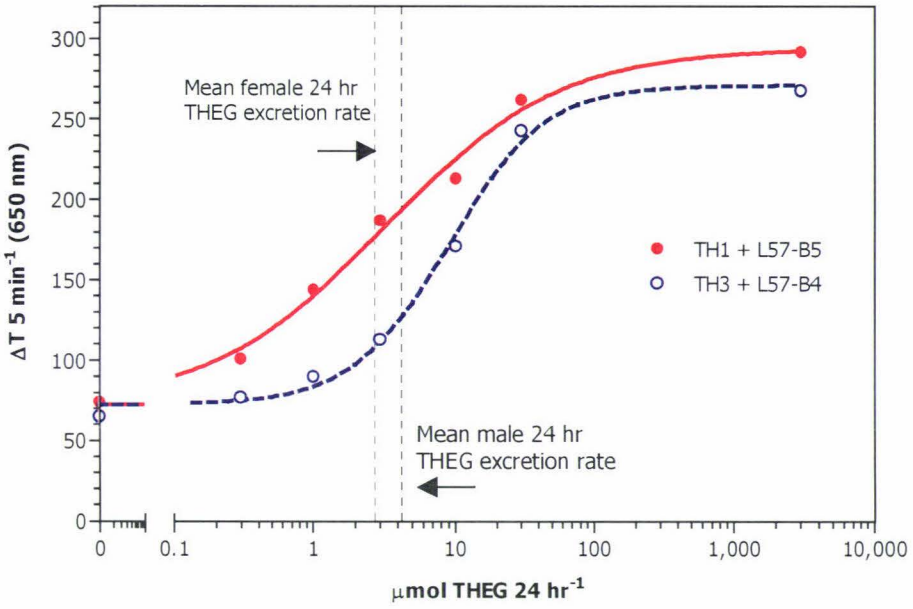

Figure 3.29 Comparison of standard curves for TH1 and TH3 tetrahydrocortisone glucuronide-hen egg white lysozyme conjugates with L57-B5 and L57-B4 anti-tetrahydrocortisone glucuronide antiserum.

Assay conditions: volume of L57-B5 antiserum, 100 μL; TH1, 61.0 nM; volume of L57-B4 antiserum, 100 μL; TH3, 71.1 nM.

Interestingly the region of maximum sensitivity for the TH1 standard curve lay almost in the middle of the critical physiological range ~2.75 - 4.24 μmol THEG 24 hr^{-1} observed in adult male and female urine. This represented a significant improvement in the sensitivity compared to the TH3 curve and is ideal for the measurement of urinary levels of THEG.

3.3.7 Summary and future work

The main aims of this chapter were to determine whether or not the new biomaterials could be used to prepare a 5 minute assay sensitive enough for the measurement of TG and THEG in urine, thus in the main these aims have been achieved. Any attempt to adapt the current Ovarian Monitor assay to measure alternative steroid metabolites in urine requires each component of the assay to be prepared and optimised. In the work presented in this chapter, the new biomaterials enabled workable TG and THEG standard curves to be generated that gave responses within or close to the expected physiological range of the steroid glucuronide in urine. Despite the limited sensitivity, the study demonstrates that there are no fundamental obstacles to prevent either assay from working, provided a steady supply of high affinity antibodies can be found with which to optimise each system. Thus the concept of a multi-purpose Monitor assay has been established.

Much more interesting and challenging work is yet to be done however, particularly in the area of optimising the home assay to measure TG and THEG in a range of human urine samples as markers of hormonal status.

3.3.7.1 Optimising the shape of the standard curve

The shape of the standard curve and its position on the concentration axis (i.e. the assay sensitivity) is determined by several factors. The critical parameters that can be relatively easily controlled and optimised include the concentration of antiserum, the hapten-HEWL conjugate used in the assay and their relative concentrations. An optimal antibody concentration is chosen as a compromise based on the best EC_{50} value obtainable and the maximum difference between the maximum and minimum change in transmission value for the sigmoidal standard curves (ΔT_{max} - ΔT_{min}). To produce a highly sensitive assay, a low EC_{50} and high value for ΔT_{max} - ΔT_{min} is desirable. Other important determinants affecting the shape and position of the standard curve that are less easily controlled include the structure and specific activity of the conjugate, the nature of the antibody and any antibody related matrix effects, and the dissociation constants for the antibody.hapten and the antibody.hapten-conjugate immune complexes [114]. In addition the accuracy of the data produced by the immunoassay depends, in part, on the specificity of the anti-steroid glucuronide antisera and the similarity of the urine matrix to the medium used to generate the standard curve.

The characteristics of the TG and THEG antisera in this study were the main uncertain variables in the establishment of a reproducible home assay for TG and THEG. The finite volume of low titre antisera available also limited the number of points which could be obtained on each titration curve, such that the lowest antiserum concentration required for maximum inhibition could not be determined precisely. The number of assays that could be carried out to produce

standard curves with the desired shape and sensitivity limits was also reduced due to the high volume of antiserum required to achieve good inhibition. Thus further antibody production is necessary to complete the optimisation of both the TG and THEG assay systems.

The detailed specificity of the antisera used to generate the TG and THEG standard curves could not be examined as part of this thesis due to time and material constraints. Since the accuracy of the data produced by any immunoassay depends largely on the specificity of the antibodies for the analyte these studies will need to be carried out once a more ready supply of high titre anti-TG and anti-THEG antibodies becomes available. Further work in this area would require titration of the antisera in the presence of different amounts of free testosterone and other related androgen metabolites such as testosterone sulphate, 5α-dihydrotestosterone, androstenedione, androsterone and etiocholanolone. The major urinary glucocorticoids capable of non-specific binding include free cortisol, allo-tetrahydrocortisone, tetrahydrocortisol and allo-tetrahydrocortisol. Steroids present in urine from other classes including the estrogens and mineralocorticoids should also be included in cross-reactivity studies with both anti-TG and anti-THEG antibodies. If the assay will be used to measure TG or THEG in the urine of patients who may be receiving synthetic steroids, such as contraceptive steroids and synthetic glucocorticoids, the cross-reactivity of these substances should also be characterised. In addition before any combination of antibody and signal generator can be used to construct assay tubes for home use, the quality of the data must be validated using a range of clinical samples and the results compared with those of an established chromatographic technique such as HPLC-MS to confirm the concentration and identity of the analytes.

The structure of the various conjugates also needs to be investigated further before their immunoassay properties can be related to their structural differences. Preliminary experiments by Cooke [111] showed a more sensitive estrone glucuronide (E1G) standard curve could be obtained using a 2:1 molar ratio of E1:E3 than with either of the pure conjugates used alone as signal generators. Thus, future studies may also include the testing of various molar ratios of the TG1:TG3 and TH1:TH3 conjugates for their effect on the standard curve sensitivity.

3.3.7.2 Development of a lateral flow membrane assay format

In recent years there has been a steady increase in the development and use of diagnostic reagents in immobilised form. Enzymes immobilised on reagent strips are used for selected diagnostic purposes in clinical labs (such as blood glucose, drug monitoring and pregnancy testing), directly by doctors or indeed the patients themselves [206]. The main disadvantage of such assays lies in the fact that very few quantitative assays have been developed so far.

With the multi-purpose Monitor kit, the patient needs to acquire some simple laboratory skills, such as the accurate measurement of small volumes of water. Since some patients may lack

the ability or feel uncomfortable about their ability to use the Monitor the development of a strip test, in which the strip is simply dipped into a sample of the undiluted patients' urine, would offer a major advantage. Other advantages of the strip type assay are the favourable cost implications for the home user and the fact that no additional reagents or equipment are required to take measurements. The strip assays are also potentially highly portable for use away from the home, and may be used more easily and rapidly.

Preliminary experiments towards the synthesis of a capture material for the conversion of the assay to a lateral flow membrane format were carried out using the antiserum produced in section 3.2.4.1 however numerous problems arose associated with the capture of the signal generator (a gold antibody conjugate) on the strip. It also proved notoriously difficult, as noted in the literature to produce uniformly sized gold particles required for good colour development. Due to time constraints all further studies towards solving these problems had to be abandoned. Since that time however, lateral flow membrane tests have been produced for other analytes using commercially available gold particles and high titre antisera that can produce a reliable standard curve similar to that obtained with the Ovarian Monitor. Thus it is only a matter of time before a working strip type assay for THEG and TG becomes available.

Bibliography

[1] Timbrell JA (1998). Biomarkers in Toxicology. *Toxicology.* **129**(1):1-12.

[2] Poon GK, Chui YC, Mccague R, Lønning PE, Feng R, Rowlands MG and Jarman M (1993). Analysis of phase I and phase II metabolites of tamoxifen in breast cancer patients. *Drug Metabolism and Disposition* **21**(6):1119-1124.

[3] Stachulski AV and Jenkins GN (1998). The synthesis of *O*-glucuronides. *Natural Product Reports* **15**(2):173-186.

[4] Grattarola R (1973). Androgens in breast cancer. I. Atypical endometrial hyperplasia and breast cancer in married premenopausal women. *American Journal of Obstetrics and Gynecology* **116**(3):423-428.

[5] Secreto G, Toniolo P, Pisani P, Recchione C, Cavalleri A, Fariselli G, Totis A, Di Pietro S and Berrino F (1989). Androgens and breast cancer in premenopausal women. *Cancer Research* **49**(2):471-476.

[6] Ballerini P, Oriana S, Duca P, Martinetti A, Venturelli E, Ferrari L, Dolci S and Secreto G (1993). Urinary testosterone as a marker of risk of recurrence in operable breast cancer. *Breast Cancer Research and Treatment* **26**(1):1-6.

[7] Schaeffer MA and Baum A (1984). Adrenal cortical response to stress at three mile island. *Psychosomatic Medicine* **46**(3):227-237.

[8] Möstl E and Palme R (2002). Hormones as indicators of stress. *Domestic Animal Endocrinology* **23**(1-2):67-74.

[9] Joyce PR, Donald RA and Elder PA (1987). Individual differences in plasma cortisol changes during mania and depression. *Journal of Affective Disorders* **12**(1):1-5.

[10] Vierhapper H and Nowotny P (2000). The stress of being a doctor: steroid excretion rates in internal medicine residents on and off duty. *The American Journal of Medicine* **109**(6):492-494.

[11] Stead SK, Meltzer DGA and Palme R (2000). The measurement of glucocorticoid concentrations in the serum and faeces of captive African elephants *(Loxodonta africana)* after ACTH stimulation. *Journal of the South African Veterinary Association* **71**(3):192-196.

[12] Morrow CJ, Klover ES, Verkerk GA and Mathews LR (2002). Fecal glucocorticoid metabolites as a measure of adrenal activity in dairy cattle. *General and Comparative Endocrinology* **126**(2):229-241.

[13] Andrew R (2001). Clinical measurement of steroid metabolism. *Best Practice and Research Clinical Endocrinology and Metabolism* **15**(1):1-16

[14] Farrow SM (editor) (1997) *Molecular endocrinology - genetic analysis of hormones and their receptors*. BIOS Scientific Publishers, Oxford, England.

[15] Lingappa VR and Mellon SH (2001) Hormone synthesis and release. In: Greenspan FS and Gardner DG (editors). *Basic and Clinical Endocrinology.* Lange Medical Books/McGraw-Hill, New York. 6th edition, p38-58.

[16] Stocco DM and Clark BJ (1996). Regulation of the acute production of steroids in steroidogenic cells. *Endocrine Reviews* **17**(3):221-244.

[17] Griffin JE and Wilson JD (2003). Disorders of the testes and the male reproductive tract. In: Larsen R, Kronenberg HM, Melmed S and Polonsky KS (editors). *Williams Textbook of Endocrinology*. Elsevier Science, Philadelphia, USA. 10th edition, p709-769

[18] Venturelli E, Cavalleri A and Secreto G (1995). Methods for urinary testosterone analysis. *Journal of chromatography B* **671**(1-2):363-380.

[19] White PC (2001). Synthesis and metabolism of corticosteroids. In: Becker KL (editor). *Principles and Practice of Endocrinology and Metabolism.* Lippincott Williams and Wilkins, Philadelphia, USA. 3rd edition, p704-714.

[20] Stryer L (1988). Biosynthesis of membrane lipids and steroid hormones. In: *Biochemistry.* WH Freeman, New York. 3rd edition, p547-574.

[21] Hillier SG (1994). Current concepts of the roles of follicle stimulating hormone and luteinising hormone in folliculogenesis. *Human Reproduction* **9**(2):188-191.

[22] Gross BA (1989). Clinical indicators of the fertile period. *Supplement to International Journal of Gynaecology and Obstetrics* **1**:45-51.

[23] Serra GB (editor) (1983). *Comprehensive endocrinology*. Raven Press, New York. p432.

[24] Goldfien A (2001). Ovaries. In: Greenspan FS and Gardner DG (editors). *Basic and Clinical Endocrinology*. Lange Medical Books/McGraw-Hill, New York. 6th edition, p453-508.

[25] Blackwell LF, Brown JB and Cooke D (1998). Definition of the potentially fertile period from urinary steroid excretion rates. Part II. A threshold value for pregnanediol glucuronide as a marker for the end of the potentially fertile period in the human menstrual cycle. *Steroids* **63**(1):5-13.

[26] Wallace AM (1995). Analytical support for the detection and treatment of congenital adrenal hyperplasia. *Annals of Clinical Biochemistry* **32**(Pt. 1):9-27.

[27] Honour JW (2001). Urinary steroid profile analysis. *Clinica Chimica Acta* **313**(1-2):45-50.

[28] Ulick S, Chan CK and Rao KN (1989). A new form of the syndrome of apparent mineralocorticoid excess. *Journal of Steroid Biochemistry* **32**(1B):209-212.

[29] Yaku K and Morishita F (2000). Separation of drugs by packed-column supercritical fluid chromatography. *Biochemical and Biophysical Methods* **43**(1-3):59-76.

[30] Honour JW (1997). Steroid profiling. *Annals of Clinical Biochemistry* **34**(Pt 1):32-44.

[31] Brown JB, MacLeod SC, Macnaughton C and Smyth BA (1968). Rapid method for estimating estrogens in urine using a semi-automatic extractor. *Journal of Endocrinology* **42**:5-15.

[32] Bowers LD (2000). Direct measurement of steroid sulphate and glucuronide conjugates with high-performance liquid chromatography-mass spectrometry. *Journal of Chromatography B* **687**(1):61-68.

[33] Park S-J, Kim Y-J, Pyo H-S and Park J (1990). Analysis of corticosteroids in urine by HPLC and thermospray LC/MS. *Journal of Analytical Toxicology* **14**(2):102-108.

[34] Behrman HR (1988). The history of hormone assays. *Progress in Clinical and Biological Research* **285**:1-14.

[35] Gosling JP (1990). A decade of development in immunoassay methodology. *Clinical Chemistry* **36**(8):1480-1427.

[36] Hage DS (1993). Immunoassays. *Analytical Chemistry* **67**(12):455R-462R.

[37] Yalow RS and Berson SA (1960). Immunoassay of endogenous plasma insulin in man. *Journal of Clinical Investigation* **39**:1157-1175.

[38] Nowak M, Swietochowska E, Jochan K and Buntner B (2000). Hormonal changes in male patients with primary open angle glaucoma. *Klinika Oczna* **102**(2):103-108.

[39] Jaffre C, Lac G, Benhamou CL and Courteix D (2002). Effects of chronic intensive training on androgenic and cortisol profiles in premenarchal female gymnasts. *European Journal of Applied Physiology* **87**(1):85-89.

[40] Shirtcliff EA, Granger DA and Likos A (2002). Gender differences in the validity of testosterone measured in saliva by immunoassay. *Hormones and Behaviour* **42**(1):62-69.

[41] Bandelow B, Wedekind D, Pauls J, Broocks A, Hajak G and Rüther E (2000). Salivary cortisol in panic attacks. *American Journal of Psychiatry* **157**(3):454-456.

[42] Falk RT, Gail MH, Fears TR, Rossi SC, Stanczyk F, Adlercreutz H, Kiura P, Wahala K, Donaldson JL, Vaught JB, Fillmore C, Hoover RN and Ziegler RG (1999). Reproducibility and validity of radioimmunoassays for urinary hormones and metabolites in pre- and postmenopausal women. *Cancer Epidemiology, Biomarkers & Prevention* **8**(6):567-577.

[43] Karg H and Rapp M (1988). The development of radioimmunoassays for the determination of anabolic sexual hormones (literature summary). *Archiv fuer Lebensmittelhygiene* **39**(5):111-114.

[44] Presser SC, Stanczyk FZ and Lobo RA (1991). Simultaneous measurements of prostacyclin and thromboxane metabolites during the menstrual cycle. *American Journal of Obstetrics and Gynecology* **165**(3):647-651.

[45] Sharma JD, Aherne GW and Marks V (1989). Enhanced chemiluminescent enzyme immunoassay for cannabinoids in urine. *Analyst* **114**(10):1279-1282.

[46] Messeri G, Caldini AL, Bolelli GF, Pazzagli M, Tommasi A, Vannucchi PL and Serio M (1984). Homogenous luminescence immunoassay for total estrogens in urine. *Clinical Chemistry* **30**(5):653-657.

[47] Adamczyk M, Chen Y, Johnson DD and Reddy RE (1997). A stereoselective synthesis of 1α-(3'-Carboxypropyl)-4-androsten-17β-ol-3-one: Preparation of immunoreagents for quantification of testosterone by fluorescence polarization immunoassay. *Tetrahedron* **53**(38):12855-12866.

[48] Exley D (1980). Steroid immunoassay in clinical chemistry. *Pure and Applied Chemistry* **52**(1):33-44.

[49] Munro CJ and Lasley BL (1988). Non-radiometric methods for immunoassay of steroid hormones. *Progress in Clinical and Biological Research* **285**:289-329.

[50] Van Weemen BK, Bosch AM, Dawson EC and Schuurs AH (1979). Enzyme-immunoassay of steroids: possibilities and pitfalls. *Journal of Steroid Biochemistry* **11**(1A):147-151.

[51] Rubenstein KE, Schneider RS and Ullman EF (1972). Homogenous enzyme immunoassay. A new immunological technique. *Biochemical and Biophysical Research Communications* **47**(4):846-851.

[52] Santoro N, Crawford SL, Allsworth JE, Gold EB, Greendale GA, Korenman S, Lasley BL, McConnell D, McGaffigan P, Midgely R, Schocken M, Sowers M, and Weiss G (2003). Assessing menstrual cycles with urinary hormone assays. *American Journal of Physiology Endocrinology and Metabolism* **284**(3):E521-530.

[53] Barnard G and Kohen F (1998). Monitoring ovarian function by the simultaneous time-resolved fluorescence immunoassay of two urinary steroid metabolites. *Clinical Chemistry* **44**(7):1520-1528.

[54] Leute RK, Ullman EF, Goldstein A and Herzenberg LA (1972). Spin immunoassay technique for determination of morphine. *Nature – New Biology* **236**(64):93-94.

[55] Rajkowski KM and Cittanova N (1981). The efficiency of different coupling procedures for the linkage of oestriol-16α-glucuronide, oestrone-3-glucuronide and pregnanediol-3α-glucuronide to four different enzymes. *Journal of Steroid Biochemistry* **14**(9):861-6.

[56] Brown JB, Blackwell LF, Cox RI, Holmes JM and Smith MA (1988). Chemical and homogenous enzyme immunoassay methods for the measurement of estrogens and pregnanediol and their glucuronides in urine. *Progress in Clinical and Biological Research* **285**:119-38.

[57] Smales CM and Blackwell LF (2003). Lysozyme conjugate immune complex formation and the effects on substrate hydrolysis. *Biochemical and Biophysical Research Communications* **304**(4):818-824.

[58] Blackwell LF and Brown JB (1992). Application of time-series analysis for the recognition of increases in urinary estrogens as markers for the beginning of the potentially fertile period. *Steroids* **57**(11):554-62.

[59] Blackwell LF, Brown JB, Vigil P, Gross BA, Sufi S and d'Arcangues C (2003). Hormonal monitoring of ovarian activity using the Ovarian Monitor, Part I. Validation of home and laboratory results obtained during ovulatory cycles by comparison with radioimmunoassay. *Steroids* **69**(5):465-477.

[60] Brown JB, Blackwell LF, Holmes J and Smyth K (1989). New assays for identifying the fertile period. *Supplement to International Journal of Gynecology and Obstetrics* **1**:111-122.

[61] Plymate SR (2001). Male hypogonadism. In: Becker KL (editor). *Principles and Practice of Endocrinology and Metabolism.* Lippincott Williams and Wilkins, Philadelphia, USA. 3rd edition, p1125-1150.

[62] Baker HW (2001). Testicular dysfunction in systemic disease. In: Becker KL (editor). *Principles and Practice of Endocrinology and Metabolism.* Lippincott Williams and Wilkins, Philadelphia, USA. 3rd edition, p1150-1158.

[63] Gary A, Feldman HA, McKinley JB and Longcope C (1991). Age, disease and changing sex hormone levels in middle-aged men: results of the Massachusetts male ageing study. *Journal of Clinical Endrocrinology and Metabolism* **73**(5):1016-1025.

[64] Stewart PM, Shackleton CHL, Beastall GH and Edwards CR (1990). 5α-reductase activity in polycystic ovary syndrome. *Lancet* **335**(8687):431-433.

[65] Rodin A, Thakkar H, Taylor N and Clayton R (1994). Hyperandrogenism in polycystic ovary syndrome. Evidence of dysregularion of 11 beta-hydroxysteroid dehydrogenase. *New England Journal of Medicine* **330**(7):460-465.

[66] Lacayo R (2000). Are you man enough? *TIME New Zealand Magazine Limited.* Auckland, New Zealand. No.16, p44-53.

[67] Matsumoto AM (2001). Clinical use and abuse of androgens and antiandrogens. In: Becker KL (editor). *Principles and Practice of Endocrinology and Metabolism.* Lippincott Williams and Wilkins, Philadelphia, USA. 3rd edition, p1181-1200.

[68] http://www.androgel.com

[69] Braunstein GD (2001). Testes. In: Greenspan FS and Gardner DG (editors). *Basic and Clinical Endocrinology.* Lange Medical Books/McGraw-Hill, New York. 6th edition, p422-452.

[70] Neal JM (2000). *Basic Endocrinology – an interactive approach.* Blackwell Science Inc., Massachusetts USA. p198-233.

[71] Morse HC, Horike N, Rowley MJ and Heller CG (1973). Testosterone concentrations in testes of normal men: effects of propionate administration. *Journal of Clinical Endocrinology and Metabolism* **37**(6):882-886.

[72] Hall R, Anderson J, Smart GA and Besser M (1974). *Fundamentals of Clinical Endocrinology.* Pitman Medical, London. 2nd edition, p248.

[73] Dunn JF, Nisula BC and Rodbard D (1981). Transport of steroid hormones: binding of 21 endogenous steroids to both testosterone-binding globulin and corticosteroid-binding globulin in human plasma. *Journal of Clinical Endocrinology & Metabolism* **53**(1):58-68.

[74] Pardridge WM (1986). Serum bioavailability of sex steroid hormones. *Journal of Clinical Endocrinology and Metabolism* **15**(2):259-278.

[75] Cumming DC and Wall SR (1985). Non-sex hormone-binding globulin-bound testosterone as a marker for hyperandrogenism. *Journal of Clinical Endocrinology and Metabolism* **61**(5):873-876.

[76] Spratt DI, O'Dea LS, Schoenfeld D, Butler J, Rao PN, and Crowley WF Jr (1988). Neuroendocrine-gonadal axis in men: frequent sampling of LH, FSH, and testosterone. *American Journal of Physiology* **254**(5 Pt 1):E658-666.

[77] Bremner WJ, Vitiello MV and Prinz PN (1983). Loss of circadian rhythmicity in blood testosterone levels with ageing in normal men. *Journal of Clinical Endocrinology and Metabolism* **56**(6):1278-1281.

[78] King SL and Hegadoren KM (2002). Stress hormones: how do they measure up? *Biological Research for Nursing* **4**(2):92-103.

[79] Cohen S, Kessler RC and Gordon LU (1997). Strategies for measuring stress in studies of psychiatric and physical disorders. In: Cohen S, Kessler RC and, Gordon LU (editors). *Measuring stress: a guide for health and social scientists.* New York, Oxford University Press. p3-26.

[80] Vanderhaeghe L (2001). Stress, ageing and total cortisol. *Total Health* **23**(1):34-35.

[81] Evans DL, Leserman J, Perkins DO, Stern RA and Murphy C (1997). Severe life stress as a predictor of early disease progression in HIV infection. *American Journal of Psychiatry* **154**(5):630-634.

[82] Leserman J, Petitto JM, Golden RN, Gaynes BN, Gu H, Perkins DO, Silva SG, Folds JD and Evans DL (2000). Impact of stressful life events, depression, social support, coping, and cortisol on progression to AIDS. *American Journal of Psychiatry* **157**(8):1221-8.

[83] Sapse AT (1997). Cortisol, high cortisol diseases and anti-cortisol therapy. *Psychoneuroendocrinology* **22**(Suppl. 1):S3-S10.

[84] Castro, M, Elias PC, Quidute AR, Halah FP and Moreira AC (1999). Out-patient screening for Cushing's syndrome: the sensitivity of the combination of circadian rhythm and overnight dexamethasone suppression salivary cortisol tests. *Journal of Clinical Endocrinology and Metabolism* **84**(3):878-882.

[85] Iki K, Miyamori I, Hatakeyama H, Yoneda T, Takeda Y, Takeda R and Dai QL (1994). The activities of 5β-reductase and 11β-hydroxysteroid dehydrogenase in essential hypertension. *Steroids* **59**(11):656-60.

[86] Gibson EL, Checkley S, Papadopoulos A, Poon L, Daley S and Wardle J (1999). Increased salivary cortisol reliably induced by a protein-rich midday meal. *Psychosomatic Medicine* **61**(5):214-224.

[87] Clerici M, Traboattoni D, Piconi S, Fusi ML, Ruzzante S, Clerici C and Villa ML (1997). A possible role for cortisol/anticortisols imbalance in the progression of human immunodeficiency virus. *Psychoneuroendocrinology* **22**(Suppl. 1):S27-S31.

[88] Sapse AT (1984). Stress, cortisol, interferon and "stress" diseases. I. Cortisol as the cause of "stress" diseases. *Medical Hypotheses* **13**(1):31-44.

[89] Loucks AB, Mortola JF, Girton L and Yen SS (1989). Alterations in the hypothalamic-pituitary-ovarian and the hypothalamic-adrenal axes in athletic women. *Journal of Endocrinology and Metabolism* **68**(2):402-411.

[90] Milgrom E (1990). Steroid hormones. In: Baulieu E and Kelly PA (editors). *Hormones: from molecules to disease.* Hermann Publishers, Paris, France. p387-442.

[91] Aron DC, Findling JW and Tyrrell JB (2001). Glucocorticoids and adrenal androgens. In: Greenspan FS and Gardner DG (editors). *Basic and Clinical Endocrinology.* Lange Medical Books/McGraw-Hill, New York. 6th edition, p334-376.

[92] Baum A and Grunberg N (1997). Measurement of stress hormones. In: Cohen S, Kessler RC and Gordon LU (editors). *Measuring stress: a guide for health and social scientists.* New York, Oxford University Press. p175-92.

[93] Kirschbaum C and Hellhammer DH (2000). Salivary cortisol. *Encyc Stress* **3**:379-83.

[94] Schimmer BP and Parker KL (1996). Adrenocorticotropic hormone; andrenocortical steroids and their analogues; inhibitors of the synthesis and actions of adrenocortical hormones. In: Hardman JG, Limberg LE, Molinoff PB, Ruddon RW and Gliman AG (editors*). Goodman and Gilman's: the pharmacological basis of therapeutics*. McGraw-Hill, New York. 9th edition, p1459-1485.

[95] Sapolsky RM (2000). Why zebras don't get ulcers: an updated guide to stress, stress related diseases and coping. NewYork, WH Freeman.

[96] Brown RW, Chapman KE, Kotelevtsev Y, Yau JL, Lindsay RS, Brett L, Leckie C, Murad P and Lyons V (1996). Cloning and production of antisera to human placental 11β-hydroxysteroid dehydrogenase type 2. *Biochemical Journal* **313**(3):1007-1017.

[97] Edwards CR, Stewart PM, Burt D, Brett L, McIntyre MA, Sutanto WS, De Kloet ER and Monder C (1988). Localization of 11β-hydroxy steroid dehydrogenase - tissue specific protector of the mineralocorticoid receptor. *Lancet* **2**(8618):986-989.

[98] Finken MJ, Andrews RC, Andrew Ruth and Walker BR (1999). Cortisol metabolism in healthy young adults: sexual dimorphism in activities of A-ring reductases, but not 11β-hydroxysteroid dehydrogenases. *Journal of Clinical Endocrinology and Metabolism* **84**(9):3316-3321.

[99] Jamieson PM, Chapman KE, Edwards CRW and Seckl JR (1995). 11β-HSD is an exclusive 11β-reductase in primary cultures of rat hepatocytes: effect of the physiochemical and hormonal manipulations. *Endocrinology* **136**(11):4754-4761.

[100] Fukushima DK, Bradlow HL, Hellman L, Zumoff B and Gallagher TF (1960). Metabolic transformation of hydrocortisone-4-C14 in normal men. *Journal of Biological Chemistry* **235**:2246-2252.

[101] Shackleton CH (1993). Mass spectrometry in the diagnosis of steroid-related disorders and in hypertension research. *Journal of Steroid Biochemistry and Molecular Biology* **45**(1-3):127-140.

[102] Shamim W, Yousufuddin M, Bakhai A, Coats AJ and Honour JW (2000). Gender differences in the urinary excretion rates of cortisol and androgen metabolites. *Annals of Clinical Biochemistry* **37**(Pt. 6):770-774.

[103] Yergey AL, Teffera Y, Esteban NV and Abramson FP (1995). Direct determination of human urinary cortisol metabolites by HPLC/CRIMS. *Steroids* **60**(3):295-298.

[104] Garegg PJ, Konradsson P, Kvarnstroem I, Norberg T, Svensson SC and Wigilius B (1985). Studies on Koenigs-Knorr glycosidations. *Acta Chemica Scandinavica B* **39**(7):569-577.

[105] Koenigs W and Knorr E (1901). *Ber.* **34**:957-981.

[106] Igarashi K (1977). The Koenigs-Knorr reaction. *Advances in Carbohydrate Chemistry and Biochemistry* **34**:243-83.

[107] Phillips DC (1967). The hen-egg white lysozyme molecule. *Proceedings of the National Academy of Science* **57**(3):484-495.

[108] Stryer L (1988). Mechanisms of enzyme action. In: *Biochemistry.* WH Freeman, New York. 3rd edition, p201-232.

[109] Verhamme IMA, Van Dedem GW and Lauwers AR (1988). Ionic-strength-dependent substrate inhibition of the lysis of *Micrococcus luteus* by hen egg-white lysozyme. *European Journal of Biochemistry* **172**(3):615-620.

[110] Habeeb AF and Atassi MZ (1971). Enzymic and immunochemical properties of lysozyme V. Derivatives modified at lysine residues by guanidination, acetylation, succinylation or maleylation. *Immunochemistry* **8**(11):1047-1059.

[111] Cooke DG (2000). Homogenous and heterogeneous enzyme immunoassays for the home detection of fertility. PhD Thesis, Massey University, Palmerston North, New Zealand.

[112] Smales CM and Blackwell LF (2002). Purification and characterization of lysozyme-pregnanediol glucuronide conjugates: the effect of the hapten and coupling reagent on the substitution level, sites of acylation and the consequences for the development of future immunoassays. *Biotechnology and Applied Biochemistry* **36**(2):101-110.

[113] Smales CM, Cooke D and Blackwell LF (1994). Use of ion-exchange and hydrophobic-interaction chromatography for the rapid purification of lysozyme-estrone glucuronide conjugates. *Journal of Chromatography B* **662**(1):3-14.

[114] Daunert S, Payne BR and Bachas LG (1989). Pyruvate carboxylase as a model for oligosubstituted enzyme-ligand conjugates in homogenous enzyme immunoassays. *Analytical Chemistry* **61**(19):2160-2164.

[115] Cooke DG, Flight S, Smales CM and Blackwell LF (2003). Use of defined estrone glucuronide-hen egg white lysozyme conjugates as signal generators in homogeneous enzyme immunoassays for urinary estrone glucuronide. *Journal of Immunoassay and Immunochemistry* **24**(2):147-172.

[116] Henderson KM, Camberis M, Simmons MH, Starrs WJ and Hardie AH (1994). Application of enzymeimmunoassay to measure oestrone sulphate concentrations in cow's milk during pregnancy. *Journal of Steroid Biochemistry and Molecular Biology* **50**(3-4):189-196.

[117] Elder PA and Lewis JG (1985). An enzyme-linked immunosorbent assay (ELISA) for plasma testosterone. *Journal of Steroid Biochemistry* **22**(5):635-638.

[118] Tateishi K, Hamaoka T, Takatsu K and Hayashi C (1980). A novel immunization procedure for production of antitestosterone and anti-5α-dihydrotestosterone antiserums of low crossreactivity. *Journal of Steroid Biochemistry* **13**(8):951-959.

[119] Erlanger BF (1980). The preparation of antigenic hapten-carrier conjugates: a survey. *Methods In Enzymology* **70**(Pt A):85-104.

[120] Spiro MJ (1970). Studies on the protein portion of thyroglobulin. Amino acid composition and terminal amino acids of several thyroglobulins. *Journal of Biological Chemistry* **245**(21):5820-5826.

[121] Gabor F, Pittner F and Spiegl P (1995). Drug-Protein conjugates: Preparation of Triamcinolone-acetonide containing bovine serum albumin/Keyhole limpet hemocyanin-conjugates and polyclonal antibodies. *Archiv der Pharmazie* **328**(11-12):775-780.

[122] Swerdlow RD, Ebert RF, Lee P, Bonaventura C and Miller KI (1996). Keyhole limpet hemocyanin: structural and functional characterization of two different subunits and multimers. *Comparative Biochemistry and Physiology, B: Biochemistry and Molecular Biology* **113B**(3):537-548.

[123] Fréche JP (1993). Characterization of immunogens. *Methods of Immunological Analysis: samples and reagents* **2**:64-69.

[124] Smales CM (1992). Preparation and characterisation of conjugates in the urinary assay of estrogen and pregnanediol. PhD Thesis, Massey University, Palmerston North, New Zealand.

[125] Fields R (1972). The rapid determination of amino groups with TNBS [2,4,6-trinitrobenzenesulfonic acid]. *Methods in Enzymology* **25**(Pt. B):464-468.

[126] Sashidhar RB, Capoor AK, Ramana (1994). Quantitation of ε-amino group using amino acids as reference standards by trinitrobenzene sulfonic acid: a simple spectrophotometric method for the estimation of hapten to carrier protein ratio. *Journal of Immunological Methods* **167**(1-2):121-127.

[127] Shuler KR, Dunham RG and Kanda P (1992). A simplified method for determination of peptide-protein molar ratios using amino acid analysis. *Journal of Immunological Methods* **156**(2):137-149.

[128] Makela O and Seppala IJT (1986). Haptens and Carriers. In: Weir DM (editor). *Handbook of experimental immunology: Immunochemistry.* Blackwell Scientific Publications, London. Vol. 1, p31.

[129] Erlanger BF, Borek F, Beiser SM, Lieberman S (1957). Steroid-protein conjugates I. Preparation and characterisation of conjugates of bovine serum albumin with testosterone and with cortisone. *Journal of Biological Chemistry* **228**(2):713-727.

[130] Manesis NJ and Goodman M (1987). Synthesis of a novel class of peptides: dilactam-bridged tetrapeptides. *Journal of Organic Chemistry* **52**(24):5331-5341.

[131] Bollenback GN, Long JW, Benjamin DG and Lindquist JA (1955). The synthesis of aryl-D-glucopyranosiduronic acids. *Journal of the American Chemical Society* **77**:3310-3315.

[132] Wotiz HH, Smakula E, Lichtin NN and Leftin JH (1959). D-Glucopyranosiduronates. I. Steroidyl-β-D-glucopyranosides. *Journal of the American Chemical Society* **81**:1704-1708.

[133] Kruger NJ (1996). The Bradford method for protein quantitation. The protein protocols handbook. In: Walker JM (editor). *The protein protocols handbook*. Humana Press, New Jersey. p15-20

[134] Friebolin H (1991). *Basic one- and two-dimensional NMR spectroscopy*. Weinheim, Germany. p80.

[135] Wu Y (1996). Syntheses and characterisation of steroid glucuronides for the preparation of horseradish peroxidase conjugates *via* hemin modification. PhD Thesis, Massey University, Palmerston North, New Zealand.

[136] Dick WE (1979). Efficiency of cadmium carbonate as an aryl glycosidation catalyst: effects of lot variations on product compositions. *Carbohydrate Research* **70**(2):313-318.

[137] Conrow RB and Bernstein S (1971). Steroid conjugates. VI. An improved Koenigs-Knorr synthesis of aryl glucuronides using cadmium carbonate, a new and effective catalyst. *Journal of Organic Chemistry* **36**(7):863-70.

[138] Lemieux RU, Hendriks KB, Stick RV and James K (1975). Halide ion catalyzed glycosidation reactions. Syntheses of α-linked disaccharides. *Journal of the American Chemical Society* **97**(14):4056-4062.

[139] Wallace JE and Schroeder LR (1977). Koenigs-Knorr reactions. Part 3. Mechanistic study of mercury(II) cyanide promoted reactions of 2-*O*-acetyl-3,4,6-tri-*O*-methyl-α-D-glucopyranosyl bromide with cyclohexanol in benzene-nitromethane. *Journal of the Chemical Society, Perkin Transactions* **II**(6):795-802.

[140] McMurry J (1988). *Organic Chemistry*. Brooks/Cole Publishing Company, Pacific Grove, California. 2nd edition, p870-871.

[141] Thevis M, Opfermann G, Schmickler H and Schänzer W (2001). Mass spectrometry of steroid glucuronide conjugates. II-Electron impact fragmentation of 3-keto-4-en- and 3-keto-5α-steroid-17-*O*-β glucuronides and 5α-steroid-3α,17β-diol 3- and 17-glucuronides. *Journal of Mass Spectrometry* **36**(9):998-1012.

[142] Muller T, Schneider R and Schmidt RR (1994). Utility of glycosyl phosphites as glycosyl donors-fructofuranosyl and 2-deoxyhexopyranosyl phosphites in glycoside bond formation. *Tetrahedron Letters* **35**(27):4763-4766.

[143] Stachulski AV (2001). Glucuronidation of alcohols using the bromosugar-iodonium reagent method. *Tetrahedron letters* **42**(37):6611-6613

[144] Ravindranathan KK, Aloui M and Field RA (1996). Iodine: a versatile reagent in carbohydrate chemistry. III. Efficient activation of glycosyl halides in combination with DDQ. *Tetrahedron Letters* **37**(48):8807-8810.

[145] Schmidt RR and Kinzy W (1994). Anomeric-oxygen activation for glycoside synthesis: the trichloroacetimidate method. *Advances in Carbohydrate Chemistry and Biochemistry* **50**:21-23.

[146] Fischer B, Nudelman AR, Margareta H, Jacob G, Hugo E, and Keinan E (1984). A novel method for stereoselective glucuronidation. *Journal of Organic Chemistry* **49**(25):4988-4993.

[147] Rao PN, Rodriguez AM and Miller DW (1986). Synthesis of 5α-androstane-3α,17β-diol 3- and 17-glucuronides. *Journal of Steroid Biochemistry* **25**(3):417-421.

[148] Brown RT, Carter NE, Lumbard KW and Scheinmann F (1995). Synthesis of a morphine-6-glucuronide hapten, N-(4-aminobutyl)normophine-6-glucuronide, and related haptens. *Tetrahedron Letters* **36**(47):8661-8664.

[149] Osborne R, Joel SP, Trew D and Slevin ML (1988). Analgesic activity of morphine-6-glucuronide. [Letter] *The Lancet* **1**(8589):828.

[150] Thompson PI, Joel SP, John L, Wedzicha JA, MacLean M, Slevin ML (1995). Respiratory depression following morphine and morphine-6-glucuronide in normal subjects. *British Journal of Clinical Pharmacology* **40**(2):145-152.

[151] Yoshimura H, Oguri K and Tsukamoto H (1968). Metabolism of drugs. LX. The synthesis of codeine and morphine glucuronides. *Chemical And Pharmaceutical Bulletin* **16**(11):2114-2119.

[152] Hashimoto S, Honda T and Ikegami S (1989). A rapid and efficient synthesis of 1,2-*trans*-β-linked glycosides *via* benzyl- or benzoyl-protected glycopyranosyl phosphates. *Journal of the Chemical Society, Chemical Communications* **11**:685-687.

[153] Hashimoto S, Honda T and Ikegami S (1990). A mild and rapid 1,2-trans-glycosidation method *via* benzoyl-protected glycopyranosyl P,P-diphenyl-N-(p-toluenesulfonyl)phosphinimidates. *Heterocycles* (1990), **30**(2, Spec. Issue):775-778.

[154] Hashimoto S, Yanagiya Y, Honda T, Harada H and Ikegami S (1992). An efficient construction of 1,2-trans-β-glycosidic linkages capitalizing on glycopyranosyl *N,N,N',N'*-tetramethylphosphoroamidates as shelf-stable glycosyl donors. *Tetrahedron Letters* **33**(24):3523-3526.

[155] Hashimoto S, Honda T and Ikegami S (1991). A new and general glycosidation method for podophyllum lignan glycosides. *Tetrahedron Letters* **32**(13):1653-1654.

[156] Roy R, Tropper FD and Grand-Maitre C (1991). Syntheses of glycosyl phosphates by phase transfer catalysis. *Canadian Journal of Chemistry* **69**(9):1462-1467.

[157] Kunz H and Pfrengle W (1986). Effective 1,2-*trans*-glycosylation of complex alcohols and phenols using the oximate orthoester of *O*-pivaloyl glucopyranose. *Journal of the Chemical Society, Chemical Communications* **9**:713-714.

[158] Cerny I, Pouzar V, Drasar P and Havel M (1992). On steroids. Part CCCLXII. Glucosylation of some steroidal 17-hydroxy derivatives. *Collection of Czechoslovak Chemical Communications* **57**(2):362-74.

[159] Borowiecka J and Stanczak A (2001). Glycosyl derivatives of 2-bromosugar of selected non-steroidal anti-inflammatory drugs. Synthesis and QSAR data. *FARMACO* **56**(4):257-62.

[160] Mattox VR, Litwiller RD and Nelson AN (1979). A comparison of procedures for attaching steroidal glucosiduronic acids to bovine serum albumin. *Journal of Steroid Biochemistry* **10**(2):167-172.

[161] Sehgal D and Vijay IK (1994). A method for the high efficiency of water-soluble carbodiimide-mediated amidation. *Analytical Biochemistry* **218**(1):87-91.

[162] Smales CM, Moore CH and Blackwell LF (1999). Characterization of lysozyme-estrone glucuronide conjugates. The effect of the coupling reagent on the substitution level and sites of acylation. *Bioconjugate Chemistry* **10**(4):693-700.

[163] Kopaciewicz W, Rounds MA, Fausnaugh J and Regnier FE (1983). Retention model for high-performance ion-exchange chromatography. *Journal of Chromatography* **266**:3-21.

[164] Pike AC and Acharya KR (1994). A structural basis for the interaction of urea with lysozyme. *Protein Science* **3**(4):706-10.

[165] Hennig M, Bermel W, Spencer A, Dobson CM, Smith LJ, and Schwalbe H (1999). Side-chain conformations in an unfolded protein: $\chi 1$ distributions in denatured hen lysozyme determined by heteronuclear 13C, 15N NMR spectroscopy. *Journal of Molecular Biology* **288**(4):705-723.

[166] Lieberman S, Erlanger BF, Beiser SM and Agate FJ (1960). Steroid-protein conjugates: their chemical, immunochemical, and endocrinological properties. *Recent Progress in Hormone Research* **15**:165-200.

[167] Habeeb AFSA (1966). Determination of free amino groups in protein by trinitrobenzene sulfonic acid. *Analytical Biochemistry* **14**:328.

[168] Gerken TA, Jentoft JE, Jentoft N and Dearborn DG (1982). Intramolecular interactions of amino groups in ^{13}C reductively methylated hen egg-white lysozyme. *Journal of Biological Chemistry* **257**(6):2894-2900.

[169] Stoscheck CM (1990). Quantitation of protein. *Methods in Enzymology* **182**:50-68.

[170] Westphal U (1957). Steroid-protein interactions. III. Spectrophotometric demonstration of interaction between proteins and progesterone, deoxycorticosterone, and cortisol. *Archives of Biochemistry and Biophysics* **66**:71-90.

[171] Matsumura I and Kirsch JF (1996). Is aspartate 52 essential for catalysis by chicken egg white lysozyme? The role of natural substrate-assisted hydrolysis. *Biochemistry* **35**(6):1881-1889.

[172] Ghuysen J, Bricas E, Lache M and Leyh-Bouille M (1968). Structure of the cell walls of *Micrococcus lysodeikticus* III. Isolation of a new peptide dimer, N^{ϵ}-[L-alanyl-γ-(α-D-glutamyl-glycine)]-L-lysyl-D-alanyl-N^{ϵ}-[L-alanyl-γ-(α-D-glutamyl-glycine)]-L-lysyl-D-alanine. *Biochemistry* **7**(4):1450-1460.

[173] Gorin G, Wang SF and Papapavlou L (1971). Assay of lysozyme by its lytic action on *M. lysodeikticus* cells. *Analytical Biochemistry* **39**(1):113-127.

[174] McKenzie HA and White FH Jr. (1986). Determination of lysozyme activity at low levels with emphasis on the milk enzyme. *Analytical Biochemistry* **157**(2):367-74.

[175] Feldkamp CS and Karey JL (1996). Immune function and antibody structure. In: Christopoulos TK and Diamandis EP (editors). *Immunoassay*. Academic Press, San Diego. p5-24.

[176] Arevalo JH, Stura EA, Taussig MJ and Wilson IA (1993). Three-dimensional structure of an anti-steroid Fab' and progesterone-Fab' complex. *Journal of Molecular Biology* **231**(1):103-118.

[177] Bailey GS (1996). Part VII Immunochemical techniques: raising of polyclonal antisera. In: Walker JM (editor). *The Protein Protocols Handbook*. Humana Press, Towota, New Jersey. p695-698.

[178] Bona CA and Bonilla FA (1996). Antigens. In: *Textbook of Immunology*. Harwood Academic publishers, The Netherlands. 2nd edition, p43-59.

[179] Liddell E (2001). Antibodies. In: Wild D (editor). *The Immunoassay Handbook*. Nature Publishing Group, London. p118-139

[180] Page M and Thorpe R (1996). Purification of IgG using DEAE-Sepharose chromatography. In: Walker JM (editor). *The Protein Protocols Handbook* Humana Press, New Jersey. p725-726.

[181] Page M and Thorpe R (1996). Purification of IgG using ion-exchange HPLC/FPLC. In: Walker JM (editor). *The Protein Protocols Handbook.* Humana Press, New Jersey. p727-729.

[182] Bona CA and Bonilla FA (1996). Immunoglobulins. In: *Textbook of Immunology.* Harwood Academic publishers, The Netherlands. 2nd edition, p61-99.

[183] Walsh G (2002). Therapeutic proteins: blood products and vaccines. In: *Proteins: Biochemistry and Biotechnology.* John Wiley and Sons Ltd, West Sussex, England. p213-249.

[184] Steward MW (1984). *Antibodies their structure and function.* Chapman and Hall, London. p12-20

[185] Cooke DG (1993). Studies relating to the Ovarian Monitor. MSc Thesis, Massey University, Palmerston North, New Zealand.

[186] Price JAR and Pethig R (1986). Surface charge measurements on *Micrococcus lysodeikticus* and the catalytic implications for lysozyme. *Biochimica et Biophysica Acta* **889**(2):128-135.

[187] Trinh CH, Hemmington SD, Verhoeyen ME and Phillips SE (1997). Antibody fragment Fv4155 bound to two closely related steroid hormones: the structural basis of fine specificity. *Structure* **5**(7):937-948.

[188] Vargas-Madrazo E, Lara-Ochoa F and Almagro JC (1995). Canonical structure repertoire of the antigen-binding site of immunoglobulins suggests strong geometrical restrictions associated to the mechanism of immune recognition. *Journal of Molecular Biology* **254**(3):497-504.

[189] Fránek M (1987). Structural aspects of steroid-antibody specificity. *Journal of Steroid Biochemistry* **28**(1):95-108.

[190] Zimmering PE, Beiser SM and Elanger BF (1965). Purification and some properties of anti-testosterone antibodies. *The Journal of Immunology* **95**(2):262-272.

[191] Bona CA and Bonilla FA (1996). The major histocompatibility complex. In: *Textbook of Immunology*. Harwood Academic publishers, The Netherlands. 2nd edition, p221-254.

[192] Roitt IM (1997). *Roitt's Essential Immunology.* Blackwell, Oxford. 9th edition.

[193] Male D, Cooke A, Owen M, Trowsdale J and Champion B (1996). *Advanced Immunology*. Mosby, Oxford. 3rd edition.

[194] Prowse S (2000). A new adjuvant. *ANZCCART news* **13**(3):7.

[195] Szurdoki F, Bekheit HK, Marco MP, Goodrow MH and Hammock BD (1995). Important factors in hapten design and enzyme-linked immunosorbent assay development. *New Frontiers in Agrochemical Immunoassay* **4**:39-63.

[196] Kellie AE (1975). The radioimmunoassay of steroid conjugates. *Journal of Steroid Biochemistry* **6**(3-4):277-281.

[197] Bermúdez JA, Coronado V, Mijares A, León C, Velázquez A, Noble P and Mateos JL (1975). Stereochemical approach to increase the specificity of steroid antibodies. *Journal of Steroid Biochemistry* **6**(3-4):283-290.

[198] Kellie AE, Samuel VK, Riley WJ and Robertson DM (1972). Steroid glucuronoside-BSA complexes as antigens: the radioimmunoassay of steroid conjugates. *Journal of Steroid Biochemistry* **3**(3):275-288.

[199] Tateishi K, Hamaoka T and Hayashi C (1980). Non-chromatographic radioimmunoassays for testosterone and 5α-dihydrotestosterone in adult female serum using antisera with low cross-reactivities. *Journal of Steroid Biochemistry* **13**(8):869-872.

[200] Johnstone A and Thorpe R (1987). *Immunochemistry in practice.* Blackwell Scientific Publications, Chigago, Illinois. p214

[201] Harlow E and Lane D (1988). *Antibodies: A laboratory manual.* Cold Spring Harbour laboratory Publications, New York.

[202] Catty D and Raykundalia C (1988). Production and quality control of polyclonal antibodies. In: Catty D (editor). *Antibodies Volume I: a practical approach.* IRL Press, Oxford. p19-79.

[203] Tresguerres JAF, Lisboa BP and Tamm J (1976). A simple radioimmunoassay for the measurement of testosterone glucosiduronate in unextracted urine. *Steroids* **28**(1):13-23.

[204] Vannucchi PL, Messeri G, Bolelli GF, Pazzagli M, Masala A and Serio M (1983). A solid phase chemiluminescent immunoassay (LIA) for testosterone glucuronide in diluted urines. *Journal of Steroid Biochemistry* **18**(5):625-629.

[205] Manclús JJ and Montoya A (1996). Development of enzyme-linked immunosorbent assays for the insecticide chlorpyrifos. 2. Assay optimization and application to environmental waters. *Journal of Agricultural and Food Chemistry* **44**(12):4063-4070.

[206] Walsh G (2002). Proteins used for analytical purposes. In: *Proteins: Biochemistry and biotechnology.* John Wiley and Sons Ltd, West Sussex, England. p350-391.